



UNIVERSITY OF
LIVERPOOL

Developing novel iron catalysts for the asymmetric hydrogenation of C=O bonds

Thesis submitted in accordance with the requirements of the
University of Liverpool for the degree of Doctor in Philosophy
by

Naomi Ritchie

September 2019

Supervisors: Prof. Jianliang Xiao and Dr Jonathan Iggo

Industrial supervisor: Dr Matthew Ball (AstraZeneca)



PGR Declaration of Academic Honesty

Name: Naomi Ritchie

Student Number: 200816385

School/Institute: School of Physical Sciences, Department of Chemistry

Title of work: Developing novel iron catalysts for the asymmetric hydrogenation of C=O bonds

Student Declaration

I confirm that:

- I have read and understood the University's PGR Policy on Plagiarism and Dishonest Use of Data.
- I have acted honestly, ethically and professionally in conduct leading to assessment for the programme of study.
- I have not copied material from another source nor committed plagiarism nor fabricated, falsified or embellished data when completing the attached material.
- I have not copied material from another source, nor colluded with any other student in the preparation and production of this material.
- If an allegation of suspected academic malpractice is made, I give permission to the University to use source-matching software to ensure that the submitted material is all my own work.

Signature.....

Date.....

Acknowledgements

I would very much like to thank my supervisors Professor Jianliang Xiao and Dr Jon Iggo. Their help, support and guidance have been invaluable. I would also like to thank my industrial supervisor at AstraZeneca, Dr Matt Ball, and Kev Leslie for looking after me in the lab at AstraZeneca and making me feel very welcome. Also, funding from EPSRC and AstraZeneca was greatly appreciated.

I am thankful to Professor Nick Greeves for always being helpful and answering all my random questions, and for believing in me, that I could do a PhD. I would like to acknowledge the work of the following MChem students: Daniel Latham for working with me towards the synthesis of macrocyclic ligand **37c**, Liam Williams for making macrocycle **37a** and Zac Ellis for making macrocycle **63**. I am grateful to the X-ray Diffraction Department at the University of Liverpool for the crystal structure of **62**, and the Analytical Services Team for mass spectra of all compounds. I would like to thank Dr Elliot Bennett for being friendly and helping me in the lab, George Cheng for working out the conditions for cyclisation, Dr Ahmed Aboo and everyone else in the Xiao group.

I have appreciated all the love and support from my family - Madre, Padre, Hermano, Perro, Abuela and everyone else. Especially my dog Max, who patiently listened to me practice my presentations and sat next to me when I started to write my thesis, for always smiling and being happy and giving me cuddles! I would like to thank Sarah for being my friend, and finally, I would like to thank God for everything.



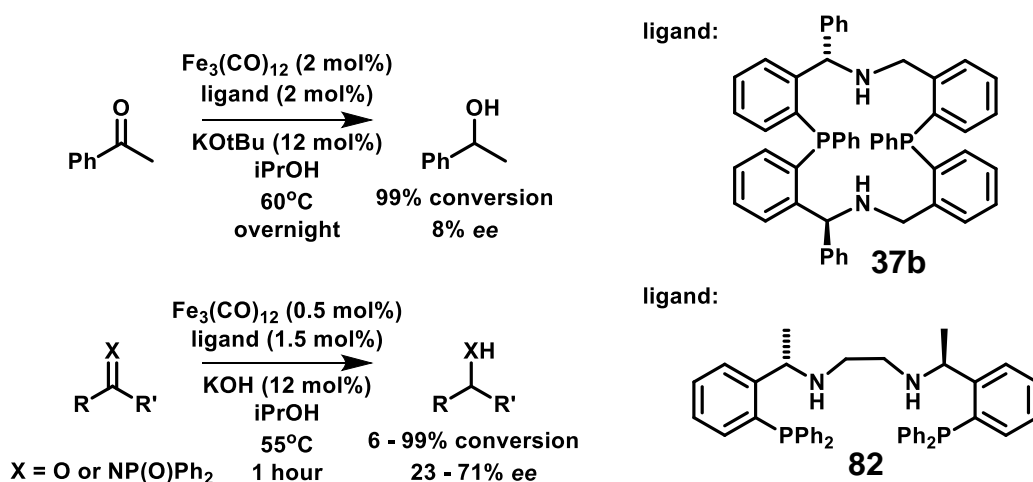
Abstract

Developing novel iron catalysts for the asymmetric hydrogenation of C=O bonds - Naomi Ritchie

Enantiomerically pure compounds are important in the pharmaceutical and agrochemical industries because opposite enantiomers can have considerably different effects in a chiral environment. Asymmetric hydrogenation (AH) is an effective method for the synthesis of chiral alcohols and amines; however, this method has mainly used expensive and toxic metal catalysts such as ruthenium, rhodium and iridium. This work focuses on the replacement of these metals with iron.

Inspired by the reports of Gao and our group,^{1, 2} the type of ligand that this project focuses on is macrocyclic ligands. A library of eight new chiral macrocyclic ligands with nitrogen and phosphorus donor atoms have been synthesised by the condensation of a variety of chiral diamines with dialdehydes under high dilution conditions. The library of macrocycles displays a range of ring sizes, denticity, and chiral groups. A second library, comprising eight acyclic ligands of varying size, denticity and chiral groups has also been prepared.

All of the ligands have been tested for the iron catalysed asymmetric hydrogenation (AH) and asymmetric transfer hydrogenation (ATH) of acetophenone in order to gain an understanding of ligand and macrocyclic effects and so direct the design of more active catalyst systems with increased substrate scope. Although none of the ligands proved to be effective in the AH of acetophenone under the conditions examined, several of the ligands prepared were successfully used for the ATH of acetophenone. A comparison of the ligands tested suggests that the phosphorus donor atoms are important for activity. The best ligands in terms of conversion were the macrocyclic ligand **37b** and the PNNP acyclic ligand **82**.



Reaction conditions including reaction time, temperature, base, mol% of base, and ligand/iron ratios were optimised for the ATH of acetophenone using PNNP ligand **82**, and these optimized conditions were subsequently used in the ATH of a variety of acetophenone type substrates and one imine substrate to demonstrate the substrate scope of the reaction.

Abbreviations

°C	degrees Celsius
AH	asymmetric hydrogenation
aq.	aqueous
ATH	asymmetric transfer hydrogenation
AZ	AstraZeneca
BuLi	butyllithium
CAS	Chemical Abstracts Service
COD	1,5-cyclooctadiene
Cy	cyclohexane
d	doublet
DCM	dichloromethane
<i>dr</i>	diastereomeric ratio
<i>ee</i>	enantiomeric excess
EPSRC	Engineering and Physical Sciences Research Council
eq.	equivalents
HOMO	highest occupied molecular orbital
HPLC	high performance liquid chromatography
Hz	hertz
iPr	isopropyl
IR	infrared
M	molar (mol/L)
m	multiplet
mg	milligrams
min	minutes
MPV	Meerwein-Ponndorf-Verley
nm	nanometres
NMR	nuclear magnetic resonance
Ph	phenyl
ppm	parts per million
q	quartet
r.t.	room temperature
R_f	retention factor - the ratio of the distance travelled by the centre of a spot to the distance travelled by the solvent front.
s	singlet
SFC	supercritical fluid chromatography
SPS	solvent purification system
t	triplet
THF	tetrahydrofuran
TLC	thin layer chromatography
TMS	trimethylsilyl
TOF	turn over frequency
UV	ultraviolet

Contents

	page
Acknowledgements	iii
Abstract	iv
Abbreviations	v
Chapter 1. Introduction	1
1.1 The importance of enantiomers	1
1.2 The synthesis of enantiomers	3
1.3 Asymmetric catalysis	4
1.4 Asymmetric hydrogenation (AH) and asymmetric transfer hydrogenation	6
1.4.1 Hydrogenation mechanisms	6
1.5 AH and ATH of ketones with noble metals	8
1.6 AH and ATH of ketones with iron	11
1.6.1 Transfer hydrogenation	12
1.6.2 Hydrogenation using H ₂	22
1.7 Aims of the project	27
Chapter 2. Synthesis of Macrocyclic ligands	29
2.1 Introduction	29
2.2 Route 1	32
2.3 Route 2	38
2.2.1 Synthesis of dialdehyde	39
2.2.2 Synthesis of chiral diimine 46	44
2.2.3 Diastereoselective Grignard addition to diimine 46	45
2.2.4 Removal of the sulfoxide groups	49
2.2.5 Cyclisation	50
2.2.6 Reduction of imine macrocycles	54
2.4 Other macrocycles	58
2.4.1 Synthesis of macrocycle 63	58
2.4.2 Synthesis of macrocycle 64	61
2.4.2 Synthesis of macrocycle 65	63
2.5 Attempted formation of metal complexes	63
2.6 Summary	65
Chapter 3. Synthesis of Acyclic ligands	67
3.1 Synthesis of bidentate PN ligands	69
3.1.1 Synthesis of PN ligand 81	69
3.1.2 Synthesis of PN ligand 85	70

3.2 Synthesis of tetradentate PNNP ligands	72
3.2.1 Synthesis of PNNP ligand 82	72
3.2.2 Synthesis of racemic PNNP ligand 83	74
3.2.3 Synthesis of PNNP ligand 86	75
3.3 Synthesis of tridentate NPN ligands	76
3.4 Synthesis of pentadentate ligand 87	76
3.5 Complex formation	77
3.6 Summary	84
Chapter 4. Catalysis	87
4.1 Asymmetric Hydrogenation (AH)	89
4.2 ATH under Schlenk conditions	90
4.3 ATH in a glovebox	92
4.4 Optimisation of PNNP ligand 82	95
4.5 Substrate scope of PNNP ligand 82	99
4.6 Summary	102
Chapter 5. Conclusions and suggestions for future work	105
Chapter 6. Experimental	109
6.1 Synthesis of (S)-1,1,1-trimethyl-N-(1-phenylethyl)silamine 38	109
6.2 Synthesis of (S)-2,2,5,5-tetramethyl-1-(1-phenylethyl)-1,2,5-azadisilolidine 41 ⁷²	110
6.3 Synthesis of (S)-N,N-dimethyl-1-phenylethan-1-amine 43 ⁷⁶	110
6.4 Synthesis of (1S,1'S)-1,1'-((phenylphosphanediyl)bis(2,1-phenylene))bis(N,N-dimethylethan-1-amine) 44 ⁷³	111
6.5 Synthesis of 2-(2-bromophenyl)-1,3-dioxolane 49 ⁸³	111
6.6 Synthesis of bis(2-(1,3-dioxolan-2-yl)phenyl)-(phenyl)phosphane 50 ⁸²	112
6.7 Synthesis of 2,2'-(phenylphosphanediyl)-dibenzaldehyde 45 ⁸²	113
6.8 Synthesis of N,N'-((1E,1'E)-((phenylphosphanediyl)-bis(2,1-phenylene))bis(methanylylidene))bis(2-methylpropane-2-sulfinamide) 46	113
6.9 General method for Grignard addition to diimine 46	114
6.10 Synthesis of (1S,1'S)-((phenylphosphanediyl)bis(2,1-phenylene))bis(phenylmethanamine) 36b	118
6.11 Synthesis of (1S,1'S)-((phenylphosphanediyl)bis(2,1-phenylene))bis(p-tolylmethanamine) 36c	119
6.12 Synthesis of (1S,1'S)-((phenylphosphanediyl)bis(2,1-phenylene))bis((3,5-dimethylphenyl)methanamine) 36d	120
6.13 General method for cyclisation	120
6.14 General procedure for the reduction of the imine macrocycles	124
6.15 Synthesis of [1,1'-biphenyl]-3,3'-dicarbaldehyde 59	130

6.16 Synthesis of (R,R)-N,N'-((1E,1'E)-[1,1'-biphenyl]-3,3'-diylbis(methaneylylidene))bis(2-methylpropane-2-sulfinamide) 68	130
6.17 Synthesis of (R,R)-N,N'-((1S,1'S)-[1,1'-biphenyl]-3,3'-diylbis(phenylmethylene))bis(2-methylpropane-2-sulfinamide) 69	131
6.18 Synthesis of (1S,1'S)-[1,1'-biphenyl]-3,3'-diylbis(phenylmethanamine) 70	131
6.19 Synthesis of (R,R)-N,N'-((1E,1'E)-(azanediylbis(2,1-phenylene))-bis(methaneylylidene))bis(2-methylpropane-2-sulfinamide) 76	132
6.20 Synthesis of (R,R)-N,N'-((1S,1'S)-(azanediylbis(2,1-phenylene))-bis(ethane-1,1-diyl))bis(2-methylpropane-2-sulfinamide) 77	133
6.21 Synthesis of bis(2-((S)-1-aminoethyl)phenyl)amine 78	133
6.22 Synthesis of (S)-1-[2-(diphenylphosphino)phenyl]-ethylamine 81	134
6.23 Synthesis of (R)-N-(2-(diphenylphosphaneyl)-benzylidene)-2-methylpropane-2-sulfinamide 89	135
6.24 Synthesis of (R)-N-((S)-1-(2-(diphenylphosphaneyl)-phenyl)-2-methylpropyl)-2-methylpropane-2-sulfinamide 90	135
6.25 Synthesis of (R)-2-methyl-N-(2-methylpropylidene)-propane-2-sulfinamide 92⁹⁷	136
6.26 Synthesis of (R)-2-methyl-N-((R)-2-methyl-1-phenylpropyl)propane-2-sulfinamide 93⁹⁷	137
6.27 Synthesis of (R)-2-methyl-1-phenylpropan-1-amine 94⁹⁷	137
6.28 Synthesis of (R)-1-(2-(diphenylphosphaneyl)phenyl)-2-methylpropan-1-amine 85	138
6.29 Synthesis of N1,N2-bis((S)-1-(2-(diphenylphosphanyl)phenyl)ethyl)ethane-1,2-diamine 82	139
6.30 Synthesis of N1,N2-bis((R)-1-(2-(diphenylphosphaneyl)phenyl)-2-methylpropyl)ethane-1,2-diamine 86	140
6.31 Synthesis of (1E,1'E)-N,N'-((1S,1'S)-((phenylphosphanediy)bis(2,1-phenylene))bis(phenylmethylene))-bis(1-phenylmethanimine) 99	141
6.32 Synthesis of (1S,1'S)-1,1'-((phenylphosphane-diyl)bis(2,1-phenylene))bis(N-benzyl-1-phenylmethanamine) 84	141
6.33 Synthesis of 1,1'-((phenylphosphanediy)bis(2,1-phenylene))bis(N-((S)-1-(2-(diphenylphosphaneyl)-phenyl)ethyl)methanimine) 100	142
6.34 Synthesis of (1S,1'S)-N,N'-(((phenylphosphanediy)-bis(2,1-phenylene))bis(methylene))bis(1-(2-(diphenylphosphaneyl)phenyl)ethan-1-amine) 87	143
6.35 Synthesis of 1-phenylethan-1-one oxime ¹²³	144
6.36 Synthesis of P,P-diphenyl-N-(1-phenylethylidene)phosphinic amide ¹²⁴	144
6.37 Synthesis of P,P-diphenyl-N-(1-phenylethyl)-phosphinic amide ⁵⁴	145
6.38 Synthesis of N-benzyl-1-phenylethan-1-imine ¹²⁵	145
6.39 Synthesis of N-benzyl-1-phenylethan-1-amine	146

6.40 General procedure for the synthesis of racemic alcohols	146
6.41 General procedure for AH at AZ	147
6.42 General procedure for ATH at AZ	148
6.43 General procedure for ATH at University of Liverpool	149
Chapter 7. References	153
Chapter 8. Appendix	157
8.1 NMR spectra of ligands	157
8.1.1 Macrocyclic ligand 37b	157
8.1.2 Macrocyclic ligand 37c	157
8.1.3 Macrocyclic ligand 37d	158
8.1.4 Macrocyclic ligand 37e	159
8.1.5 Macrocyclic ligand 64	159
8.1.6 Macrocyclic ligand 63	160
8.1.7 Macrocyclic ligand 37a	161
8.1.8 Macrocyclic ligand 65	161
8.1.9 PN ligand 81	162
8.1.10 PN ligand 85	163
8.1.11 PNNP ligand 82	163
8.1.12 PNNP ligand 86	164
8.1.13 PNP ligand 44	165
8.1.14 PNP ligand 84	165
8.1.15 Pentadentate ligand 87	166
8.2 Crystal structure data for 62	167

Chapter 1. Introduction

This chapter introduces enantiomers and discusses the importance of being able to synthesise single enantiomers. Various ways to make enantiomers are discussed, followed by a detailed introduction to asymmetric catalysis, particularly asymmetric hydrogenation (AH) and asymmetric transfer hydrogenation (ATH). Examples of AH and ATH using ruthenium and iron are given. An introduction to the synthesis of the ligands will be given at the beginning of Chapter 2 (Synthesis of Macrocyclic Ligands, p 29) and Chapter 3 (Synthesis of Acyclic Ligands, p 67).

1.1. The importance of enantiomers

Chirality is the geometric property of an object of being non-superimposable on its mirror image.³ The word chiral is derived from the Greek word for 'hand', which is the most familiar chiral object. Many man-made objects are chiral and are designed to be operated using one hand, for example, scissors. Other things have a chiral set up to favour a dominant hand, such as a drum kit (**Figure 1**, left). Nature is chiral, although it is often only seen on a molecular level. An example of chirality which can easily be seen in nature is a snail's shell (**Figure 1**, right).



Figure 1 – left: The chiral set up of a drum kit for a right-handed drummer.
right: A snail showing its chiral shell.

Enantiomers are molecules which are chiral.³ When carbon is sp^3 hybridised it has a tetrahedral shape, so when four different groups are attached to it, its mirror image is non-superimposable (**Figure 2**).

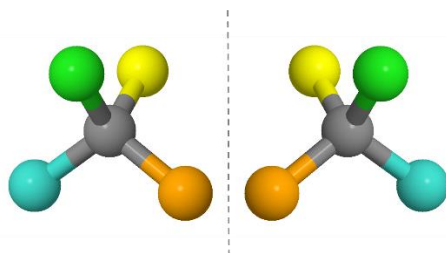


Figure 2 – A tetrahedral carbon atom (grey) bonded to 4 different groups showing its non-superimposable mirror image.

In an achiral environment, enantiomers have exactly the same physical and chemical properties, apart from the rotation of plane-polarized light, but in a chiral environment they have diastereomeric interactions with the enantiomerically pure natural products and can have considerably different effects.

There are many examples of compounds where the enantiomers have different effects (**Figure 3**). One of the most famous examples is thalidomide,⁴ where the *R* enantiomer acts as a sedative but the *S* enantiomer is teratogenic.⁴

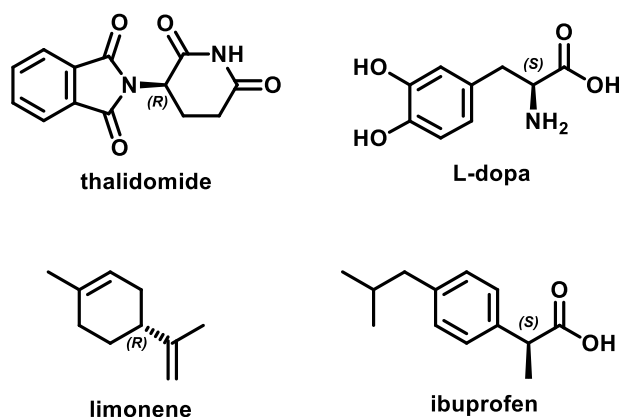


Figure 3 – Examples of compounds of which the enantiomers have different effects.

Other examples include dopa, limonene and ibuprofen. The *S* enantiomer of the amino acid dopa is used to treat Parkinson's disease, but the *R* enantiomer is ineffective and toxic.⁵ (*R*)-Limonene smells of oranges and is used in food and cosmetics, whereas (*S*)-limonene has a turpentine smell.⁶ (*S*)-Ibuprofen is an anti-inflammatory drug but its *R* enantiomer is inactive.⁷ Therefore, the synthesis of enantiomerically pure compounds is extremely important in the synthesis of pharmaceuticals, agrichemicals, flavours and fragrances.

1.2. The synthesis of enantiomers

There are various ways to synthesise enantiomerically pure compounds, but all of the methods must involve an enantiomerically pure source at some stage, which must initially be taken from nature.

One way is chiral pool synthesis which uses naturally occurring chiral compounds which are then modified to make the desired product. Commonly used chiral compounds from nature include amino acids and carbohydrates. Disadvantages with this method include the difficulty in extracting the products from the natural sources, the limitation of products available and that usually only one enantiomer of a compound is available.⁸

Another method is resolution, which is the separation of the enantiomers of a racemic mixture by use of an enantiomerically pure resolving agent. One way this can be achieved is by reacting the racemic mixture with an enantiomerically pure compound to form diastereoisomers which are then separable by crystallisation or column chromatography, for example. An advantage of this method is that both enantiomers are available. However, the disadvantage is that if only one enantiomer is needed, the yield is limited to 50% and the other enantiomer is waste.⁸

Another form of resolution is dynamic kinetic resolution (DKR) which allows up to 100% yield of a single enantiomer. It works by continually racemising the starting material whilst a chiral catalyst selectively reacts with only one of the enantiomers (**Figure 4**). Another advantage over standard kinetic resolution is that the ee of the product does not depend on the extent of conversion, since the ratio of enantiomers in the starting material remains the same throughout the reaction. An important requisite of this method is that the product must not be racemised under the same conditions as the starting material.⁹

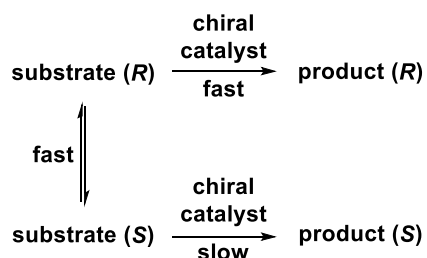


Figure 4 – Dynamic kinetic resolution.

Another method is asymmetric synthesis using chiral auxiliaries. A chiral auxiliary is an enantiomerically pure compound which is temporarily attached to another molecule to allow a diastereoselective reaction to occur, producing a new chiral centre. The auxiliary is then removed, for example by hydrolysis, leaving a single enantiomer of product. Disadvantages of this method is that a stoichiometric quantity of auxiliary is needed (although some auxiliaries can be recovered and reused) and extra steps are needed to add and remove the auxiliary.⁸

The method used in this project is asymmetric catalysis.

1.3. Asymmetric catalysis

Asymmetric catalysis uses a chiral catalyst to selectively produce one enantiomer from a prochiral substrate. A prochiral substrate is a compound which can be made chiral by the addition of a new atom or group.³ An advantage of asymmetric catalysis is that only a very small amount of chiral source is needed to produce a large amount of chiral product.^{10, 11} Ideal catalyst systems should have a broad substrate scope and should be able to operate with low levels of catalyst.¹²

The catalysis can be divided into three groups: heterogeneous catalysis, homogeneous catalysis or catalysis with nanoparticles. Catalysts for homogeneous catalysis typically consist of a transition metal complex with one or more organic ligands coordinated.¹³ Advantages of homogeneous catalysis are that the catalyst and the substrate are in the same phase so it is not hindered by diffusion problems, the catalyst can be tuned by changing the metal, ligand or counter ion, and the molecular nature of the catalyst makes

mechanistic studies easier (e.g. by NMR). Disadvantages of homogeneous catalysis are the separation of the catalyst from the product and the instability of the catalyst.¹³

Heterogeneous catalysis typically involves a metal which is deposited onto a support such as silica, aluminium oxide or carbon. Advantages of heterogeneous catalysis are that the catalysts are usually very robust and are not easily deactivated, which means they can be used at high temperatures and for extended periods of time, and they are easily separated from the product. Disadvantages include the fact that only the metal atoms on the surface are active and it is more difficult to tune the activity and selectivity.¹³

Nanoparticles are a collection of metal atoms, between 1 and 100 nm, stabilised by ligands which form a steric or charge barrier which prevents them from growing into larger particles. Nanoparticles can be prepared by the reduction of a metal salt in the presence of a stabiliser, or they can sometimes be formed accidentally during catalysis. Advantages are that the stabilising ligands are often cheaper than commonly used ligands in homogeneous catalysis, and the ligands are usually not very strongly bound so can be easily displaced by substrate. Disadvantages are the instability of the nanoparticles at higher temperatures and they can sometimes precipitate from the reaction mixture.¹³

Distinguishing between these three types of catalysis is often not easy. Also, sometimes a mixture of types may be present due to, for example, leaching from a heterogeneous catalyst, or decomposition of a homogeneous metal complex into nanoparticles. Various tests to distinguish which type of catalysis is occurring include poisoning studies (e.g. PPh_3 or mercury) and kinetic evidence (e.g. the observance of an induction period).¹³

1.4. Asymmetric hydrogenation (AH) and asymmetric transfer hydrogenation (ATH)

One of the most commonly used asymmetric catalysis reactions is asymmetric hydrogenation (AH) (**Figure 5**). Hydrogen is added selectively to one of the enantiotopic faces of a prochiral substrate, such as ketones, imines or alkenes.

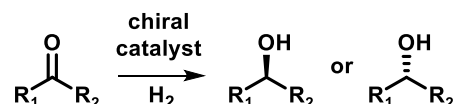


Figure 5 – Asymmetric hydrogenation of ketones (AH).

Asymmetric transfer hydrogenation (ATH) is the transfer of hydrogen from a source other than molecular H_2 (**Figure 6**). The most commonly used hydrogen sources for transfer hydrogenation are isopropanol and formic acid.¹⁴

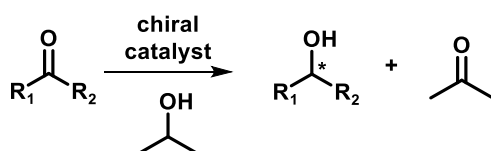


Figure 6 – Asymmetric transfer hydrogenation (ATH) of ketones using isopropanol as the hydrogen source.

There are advantages and disadvantages for each method. The use of molecular H_2 is atom economical as all of the atoms in the starting materials end up in the product. The disadvantages of using molecular H_2 are the extra safety precautions needed for the handling of highly flammable gas and the specialist equipment needed for high pressure reactions. The advantages of transfer hydrogenation are that no specialist equipment or safety precautions are needed. The disadvantages include the production of waste products (e.g. acetone from isopropanol) and often the reactions are reversible because the product can act as a hydrogen source.¹⁴

1.4.1. Hydrogenation mechanisms

An example of heterogeneous hydrogenation is the hydrogenation of alkenes using Pd/C. The hydrogen adsorbs to the metal surface which results in the

breakage of the H-H bond and then the alkene coordinates to the metal surface which can then react with the hydrogen.⁸

There are two main pathways for homogeneous hydrogenation: direct hydrogen transfer or a hydridic route.^{11, 15-17} Direct hydrogen transfer is thought to be the main pathway for main group metals, whereas the hydridic route operates when transition metals are used. The hydridic route is further split into two routes: monohydride and dihydride.

Direct hydrogen transfer, also known as the MPV mechanism, is when the hydrogen donor and the substrate both coordinate to the metal, and then hydrogen is transferred directly from the hydrogen donor to the substrate via a six-membered ring transition state (**Figure 7**). The hydridic mechanisms involve the reaction of the hydrogen donor with the metal to form an intermediate metal hydride species which then transfers the hydrogen to the substrate in a subsequent step (**Figure 8**).

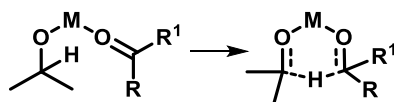


Figure 7 – Direct hydrogen transfer mechanism.

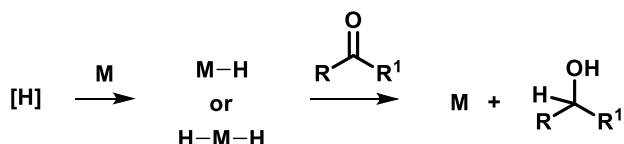


Figure 8 – The hydridic route.

The two hydridic routes can be distinguished by deuterium labelling of the hydrogen source. The monohydride mechanism results in the exclusive transfer of hydride from donor carbon to substrate carbon. The dihydride mechanism results in hydride transfer from donor carbon to both substrate carbon as well as substrate oxygen.

The monohydride mechanism can go by an inner sphere pathway where the substrate coordinates to the metal, or an outer sphere pathway where the substrate does not coordinate to the metal (**Figure 9**). The outer sphere pathway is also known as metal ligand bifunctional catalysis.¹⁷

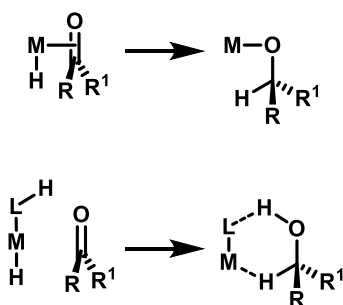


Figure 9 – Inner sphere (top) and outer sphere (bottom) mechanisms.
M = metal, L = ligand.

1.5. AH and ATH of ketones with noble metals

The AH of functionalised ketones was achieved by the use of ruthenium BINAP dihalide complexes **1** (**Figure 10**).¹⁰ The nitrogen, oxygen or halogen atoms near the ketone coordinate to the metal and direct the reactivity and stereochemical outcome. A wide variety of functionalised ketones can be hydrogenated to the corresponding chiral alcohols in 90-100% ee. However, these catalysts are unable to hydrogenate simple, unfunctionalized ketones.

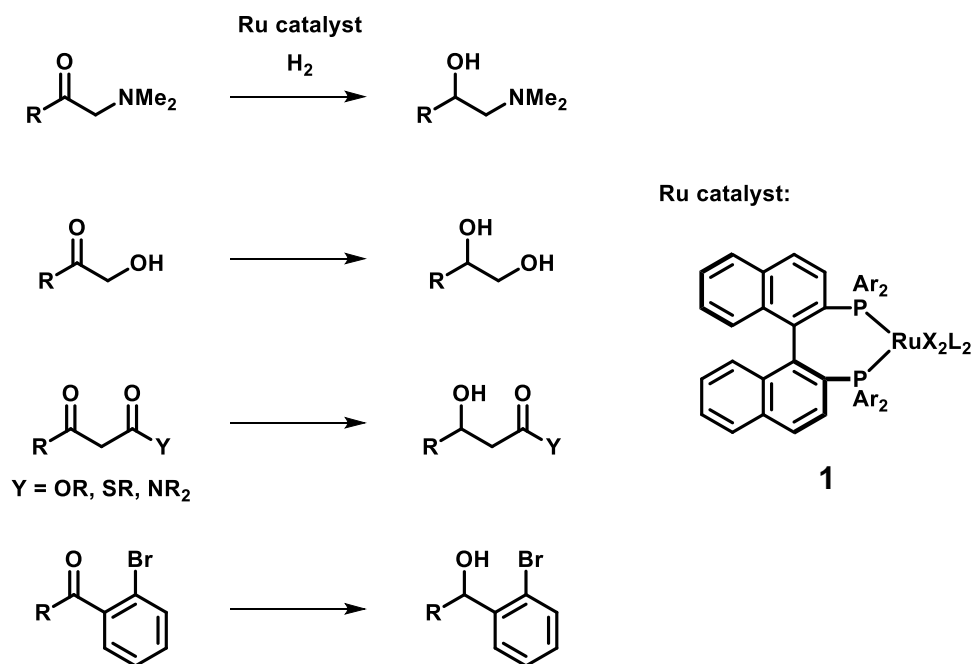


Figure 10 – AH of functionalised ketones using ruthenium BINAP complexes **1**.¹⁰

In 1995, the AH of simple ketones was accomplished using ruthenium BINAP/diamine complexes **2** (**Figure 11**).¹⁰ This efficient catalyst system is highly enantioselective and is able to hydrogenate aromatic, heteroaromatic

and olefinic ketones. The steric and electronic properties of the ligands can be varied to enhance the reactivity and enantioselectivity. The hydrogenation goes by a metal-ligand bifunctional mechanism where the ketone does not coordinate to ruthenium. The hydride on ruthenium and a proton from the nitrogen ligand are simultaneously transferred to the C=O via a six-membered ring transition state (**Figure 12**).¹⁸

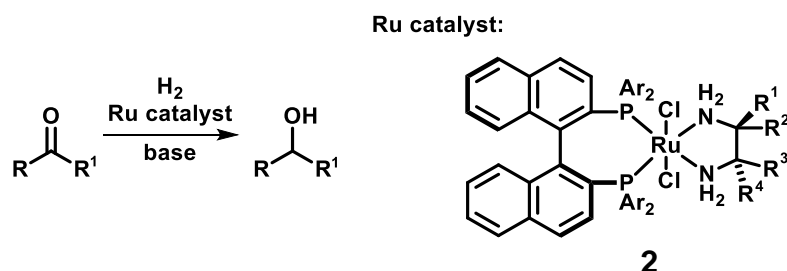


Figure 11 – AH of ketones by ruthenium BINAP/diamine complexes **2**.¹⁰

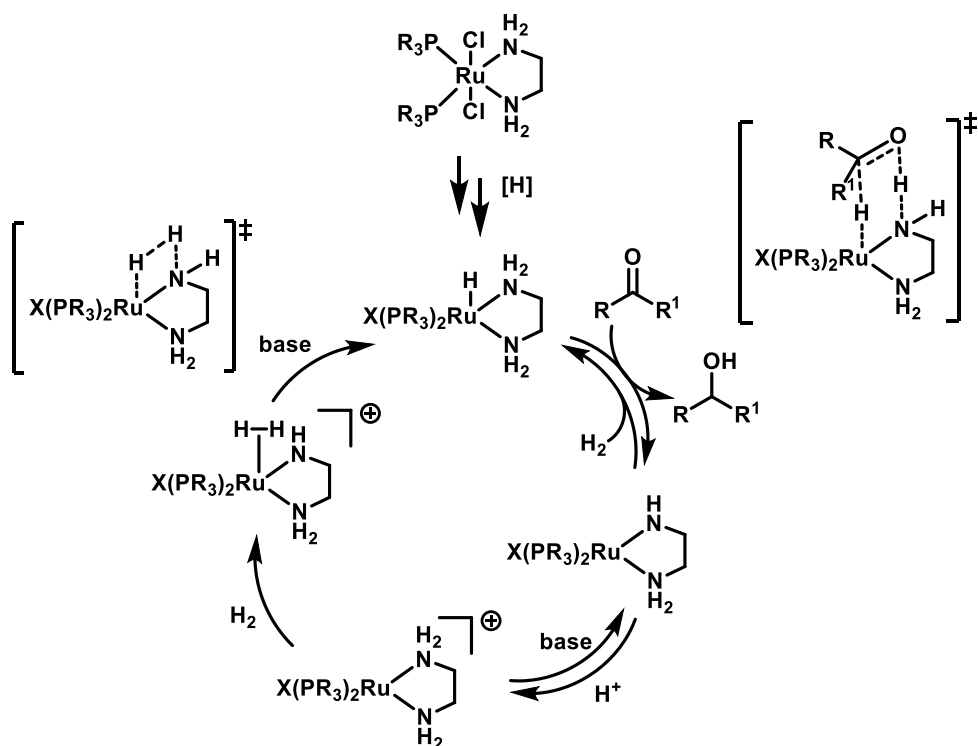


Figure 12 – The mechanism of AH of ketones by ruthenium BINAP/diamine complexes **2**.¹⁸

There have been some variations on the ruthenium catalyst **2** such as the ruthenabicyclic complex **3** which has excellent activity (**Figure 13**). This achieves >99% conversion of acetophenone in just one minute to give the product in >99% ee, compared to catalyst **2** which takes 4 hours to achieve a similar result (>99% conversion, 98% ee).¹⁹ Catalyst **4** allows for the base-

free AH of base-sensitive ketones with excellent yields and ee.²⁰ Complex **5** allows for the reduction of sterically congested t-alkyl ketones, giving the products in high ee.²¹

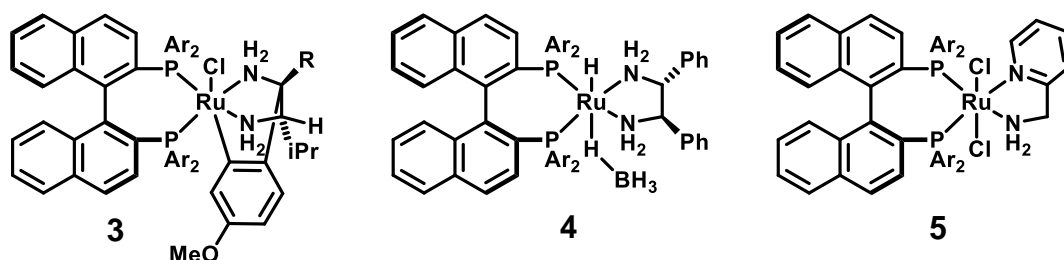


Figure 13 – Variations of the ruthenium catalyst **2**.

An example of ATH using noble metals is the ATH of carbonyl compounds and imines catalysed by chiral ruthenium complexes **6** (**Figure 14**), giving the products in high ee.¹⁰ Isopropanol or a mixture of formic acid/triethylamine can be used as the hydrogen source. This involves a metal-ligand bifunctional mechanism via a 6-membered ring transition state (**Figure 16**).²²

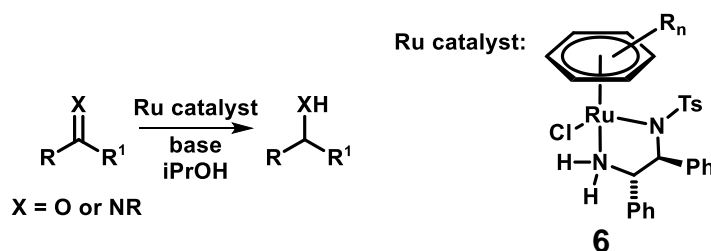


Figure 14 – ATH of carbonyl compounds and imines catalysed by chiral ruthenium complexes **6**.¹⁰

Various ligands have been tested as alternatives of the *N*-(*p*-toluenesulfonyl)-1,2-diamine ligand in complex **6** (**Figure 15**). For example, the use of the rigid amino alcohol ligand **7** does better than complex **6** in some cases; however, it does not work with a formic acid/triethylamine system and longer reaction times can result in a lower ee.²³ The conformationally rigid, sterically bulky ligand **8** is an excellent catalyst for ATH of aryl ketones, including sterically bulky ketones, showing high activity and ee.²⁴

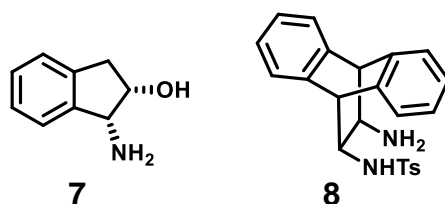


Figure 15 – Alternative ligands used for the ATH catalyst **6**.

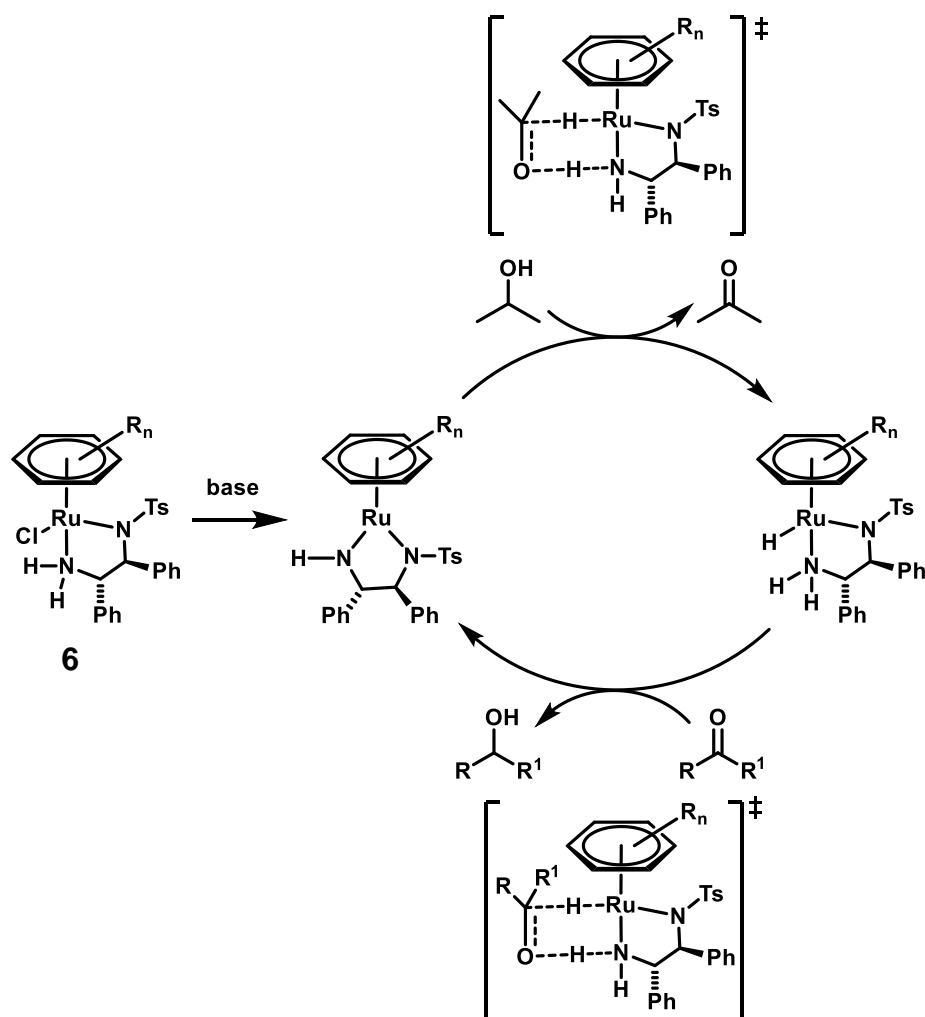


Figure 16 – The mechanism of ATH of carbonyl compounds using chiral ruthenium complexes **6**.²²

1.6. AH and ATH of ketones with iron

Up until recently, AH and ATH have mainly used rhodium, ruthenium and iridium metal catalysts.^{10, 11, 14} In recent years a considerable amount of research has gone into asymmetric catalysis reactions which use base metals such as iron, cobalt and nickel instead of precious metals.²⁵⁻³³ Iron is the most abundant metal in the earth's crust and is also an essential element in nature as it is found in haemoglobin in the blood and in many other metalloproteins.³⁴ This makes it a lot cheaper and less toxic than the precious metals.

1.6.1. Transfer hydrogenation

In 2004, a chiral diaminodiphosphine ligand **9**,³⁵ was combined with $[\text{Et}_3\text{NH}][\text{HFe}_3(\text{CO})_{11}]$ for the ATH of aromatic ketones using KOH as the base and isopropanol as solvent (**Figure 17**).³⁶ Ten different ketones were reduced giving moderate to high yields in most cases, although a chlorine atom in the ortho position resulted in a very low yield (5%). Moderate to good ees were obtained except with some very sterically hindered ketones which gave excellent ee. Monitoring the reaction by infrared spectroscopy indicated that the iron carbonyl cluster remained intact during the reaction.

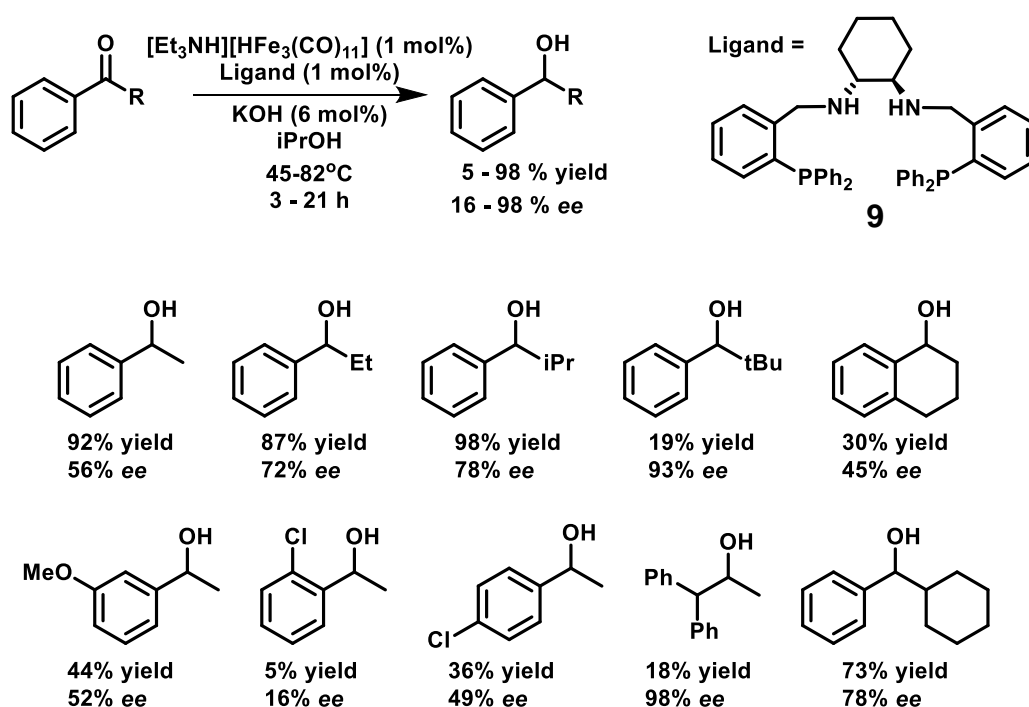


Figure 17 – ATH of aromatic ketones using chiral diaminodiphosphine ligands.³⁶

In 2006, a three-component catalyst system consisting of an iron source, terpy **10** and PPh_3 was used for the transfer hydrogenation of aliphatic and aromatic ketones (**Figure 18**).¹⁵ A small amount of product (23%) is obtained without the use of any ligands, but the yield was improved to 78% with a 1:1 mixture of terpy **10** and PPh_3 . Various iron sources and bases were examined and the best results were obtained with the iron carbonyls $\text{Fe}_2(\text{CO})_9$ and $\text{Fe}_3(\text{CO})_{12}$, and with iPrONa as the base. Ten different ketones were reduced to give the alcohol products in good to excellent yield. However, a chlorine atom adjacent to the carbonyl group gave very low yield (5%). Mechanistic studies suggested

that the reaction was homogeneous and went via a monohydride reaction pathway.

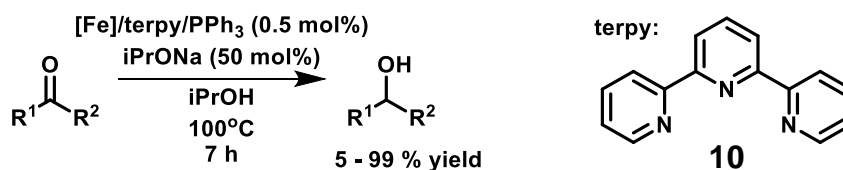


Figure 18 – Transfer hydrogenation of ketones using a $[\text{Fe}]/\text{terpy}/\text{PPH}_3$.¹⁵

In a subsequent paper,³⁷ iron porphyrin catalysts were also used for the transfer hydrogenation of ketones (**Figure 19**). Different temperatures, bases, iron sources, ligands and metal-ligand ratios were investigated. The products were generally obtained in good to excellent yield. Low yields were obtained for ketones substituted adjacent to the carbonyl group. The reaction also worked without any ligand to give around 50% yield of 1-phenylethanol. α -Substituted ketones were added to the substrate scope in a later paper, using FeCl_2 as the iron source.³⁸

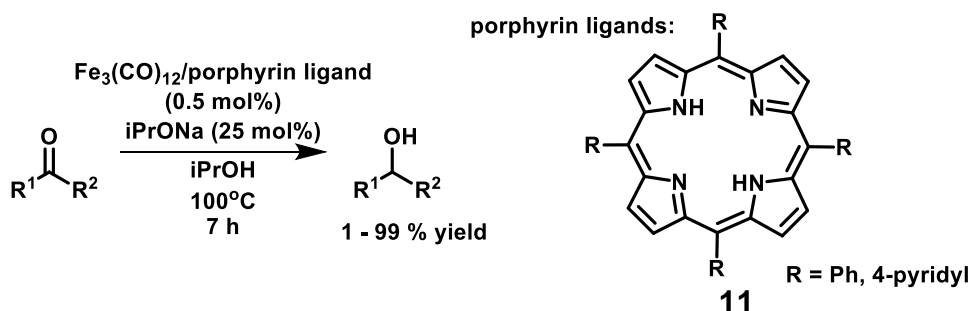


Figure 19 – Transfer hydrogenation of ketones using iron porphyrin catalysts.³⁷

The transfer hydrogenation of acetophenone was carried out using Knölker's iron complex **12**³⁹ in isopropanol to give 1-phenylethanol in 87% yield (**Figure 20**).⁴⁰ The iron complex **12** has a hydridic hydrogen on the iron and an acidic hydrogen on the oxygen which can be transferred to the ketone. This complex **12** also catalyses the hydrogenation of ketones with H_2 (see p 23).

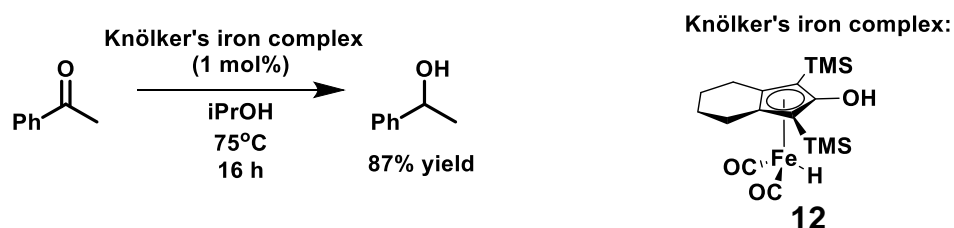


Figure 20 – Transfer hydrogenation of acetophenone using Knölker's iron complex.⁴⁰

Morris's group have done a lot of work with iron complexes with PNNP ligands. In 2008, iron complexes **13** with a diiminodiphosphine PNNP ligand analogous to **9** were used for the ATH of polar bonds, including ketones, aldehydes and imines (**Figure 21**).⁴¹

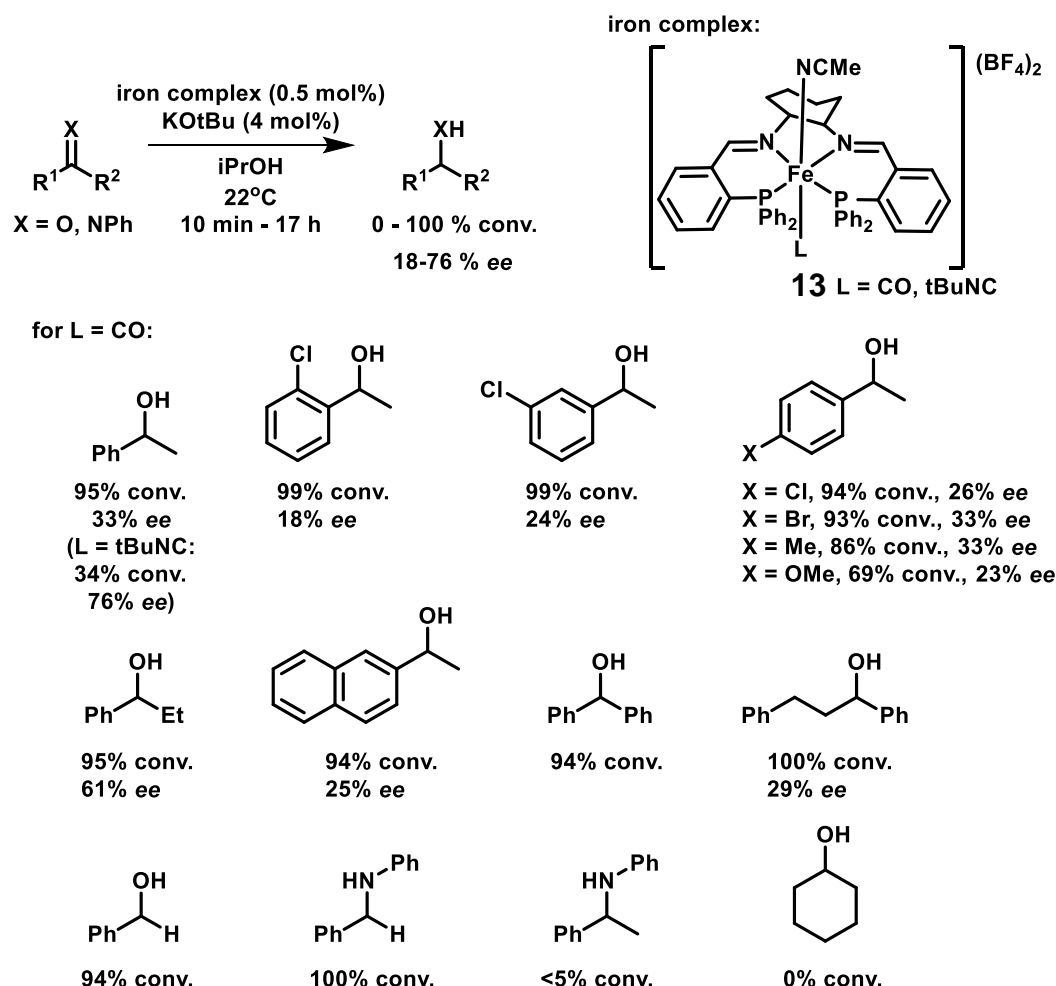


Figure 21 – Asymmetric transfer hydrogenation of polar bonds using an iron complex with a PNNP ligand.⁴¹

This gave generally good conversions above 70%, but a couple of substrates including cyclohexanone and the ketimine derived from acetophenone did not work. The ees were poor, with only two substrates achieving above 60% ee. Reduction of an α,β -unsaturated ketone resulted in some reduction of the C=C bond. The mechanism of catalysis was uncertain.

In 2009, a similar iron complex **14** was reported to catalyse the ATH of aromatic and aliphatic ketones using KOtBu as base in isopropanol at room temperature (**Figure 22**).⁴² Good catalytic activities were observed and excellent ees were obtained for bulky substrates. A later paper suggests that

the active catalyst species are iron(0) nanoparticles functionalised with PNNP ligands.⁴³

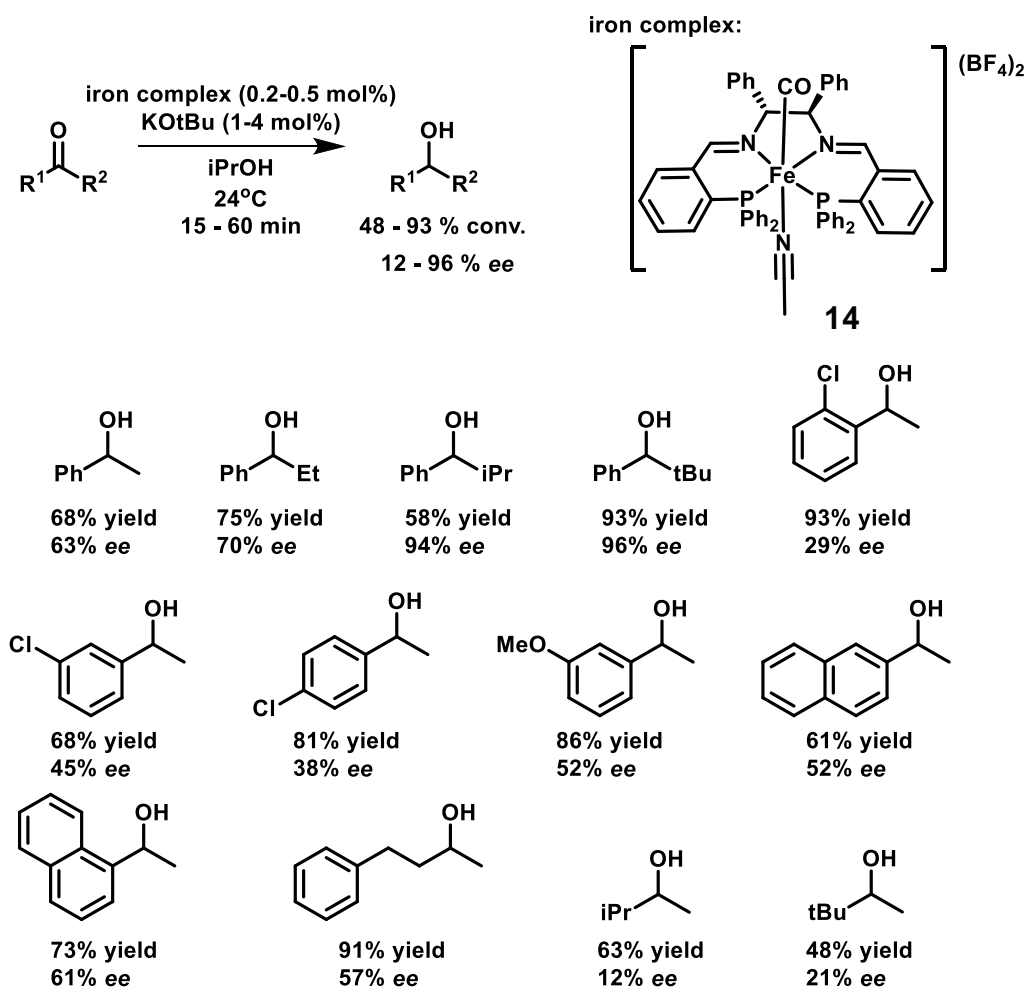


Figure 22 – ATH of aromatic and aliphatic ketones by a PNNP iron complex.⁴²

A paper in 2012 performed spectroscopic and DFT studies on transfer hydrogenation using a related PNNP iron complex **15**. An unusual ferraaziridinido complex **16** was detected during the catalytic reaction, where one of the imine bonds in the ligand is reduced and the benzylic carbon is coordinated to iron (**Figure 23**). Complex **16** was not catalytically active, however it was suggested that this could be a route towards nanoparticles.⁴⁴

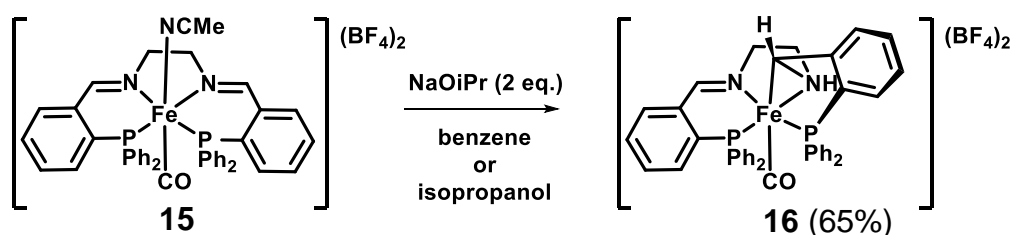


Figure 23 – PNNP iron complex forms unusual ferraaziridinido complex.

Another PNNP iron complex **17** was synthesised in 2009 (**Figure 24**),⁴⁵ which has higher activity and selectivity compared to the previous complex **13**. Reduction of acetophenone produced the alcohol product with 75% conversion and 83% ee after 8 minutes, but a longer reaction time (30 min) resulted in racemisation giving 90% conversion but only 12% ee. The best enantioselectivity (99%) was obtained with a bulky tertiary butyl group substituent. An outer sphere mechanism involving an H-Fe-N-H motif is suggested.

Variations of the ligand in complex **17** were made by changing the phenyl groups on phosphorus to alkyl substituents.⁴⁶ It was found that bulky substituents (Cy and iPr) rendered the complex inactive, whereas ethyl groups on phosphorus produced an active catalyst, but was less active and enantioselective than **17**. Another paper added substituents to the phenyl rings on phosphorus to vary the electronic and steric properties.⁴⁷ Electron donating methyl groups in the para- and 3,5- positions worked well, whereas a methyl group in the ortho- position was completely inactive. Electron withdrawing CF₃ groups also rendered the complexes completely inactive. These variations show that there is a fine balance between sterics and electronics.

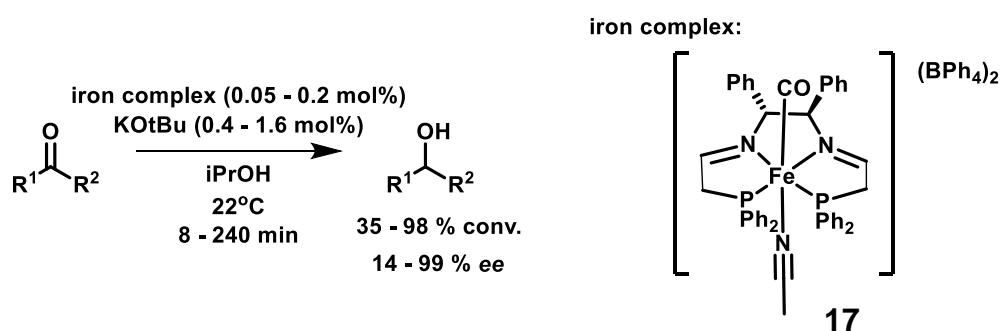


Figure 24 – ATH of ketones catalysed by PNNP iron complex.⁴⁵

Another paper investigated the incorporation of different diamines into the backbone of the PNNP ligand in complex **17**.⁴⁸ There did not seem to be any good correlation between the basicity of the nitrogen ligands and catalytic activity, but increased steric bulk of the groups in the backbone increased the activity. Towards the end of the reaction, the rate decreased due to

competition between acetone and acetophenone for the active site on the catalyst.

In 2011, another paper found that the role of the base is to doubly deprotonate the PNNP ligand in complex **18** at the carbons α to phosphorus to produce the 5-coordinate iron(II) complex **19** (**Figure 25**).⁴⁹ Complex **19** was tested for the ATH of acetophenone without the addition of base which gave similar results to the use of **18** with base. This suggests that both complexes lead to the same active catalyst species and that the base plays no further role in the catalysis.

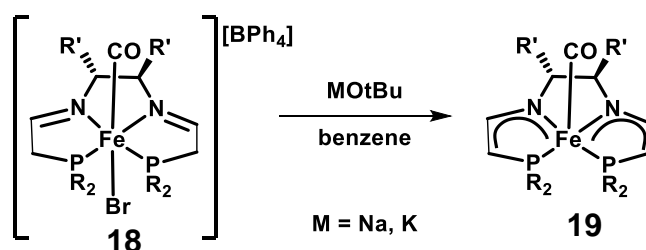


Figure 25 – Double deprotonation of the tetradentate PNNP ligands **18**.⁴⁹

Further mechanistic studies suggest that one of the imine groups is reduced to produce the active catalyst species (**Figure 26**).⁵⁰

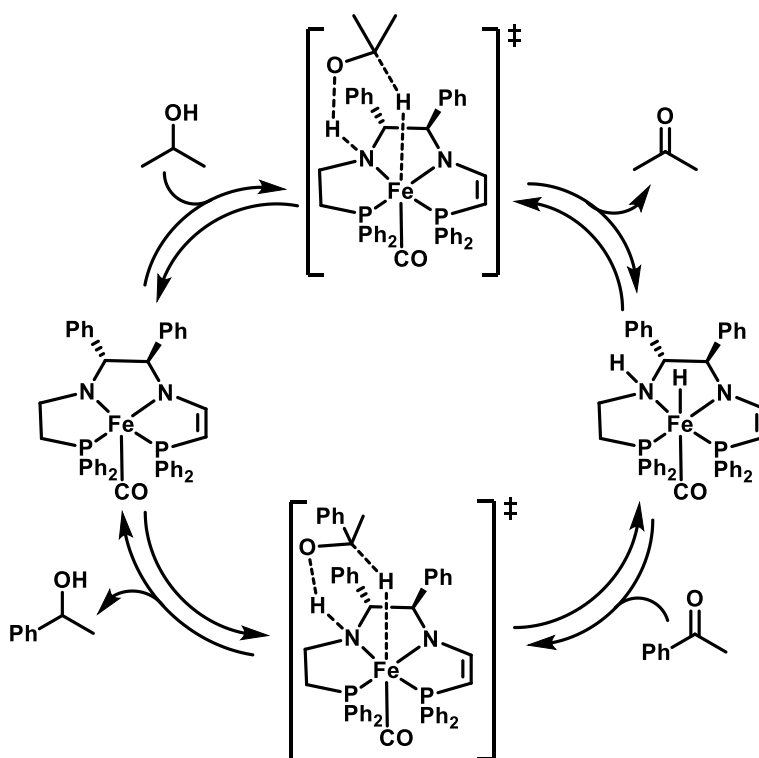


Figure 26 – Proposed mechanism for the transfer hydrogenation of acetophenone.⁵⁰

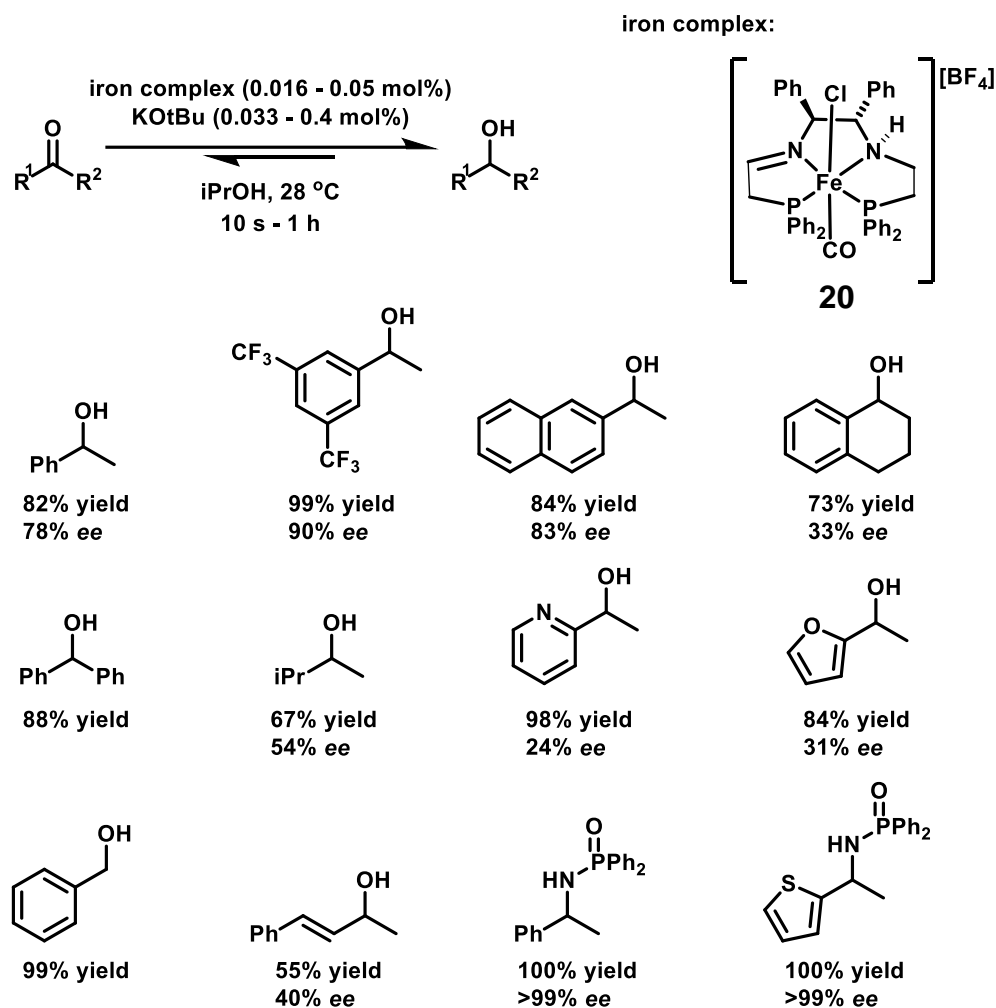


Figure 27 – ATH of ketones, aldehydes and imines using an amine(imine)diphosphine iron complex.⁵¹

In 2013, iron catalysts **20** with partially saturated amine(imine)diphosphine ligands (**Figure 27**) were synthesised and were used for the ATH of ketones and imines with isopropanol as the hydrogen source.⁵¹ TOF as high as 200 s⁻¹ (720,000 h⁻¹) at 28 °C and high yields and enantioselectivities were reported. A chemoselectivity for the polar C=O versus the nonpolar C=C indicated an outer-sphere mechanism of proton and hydride transfer (**Figure 28**).

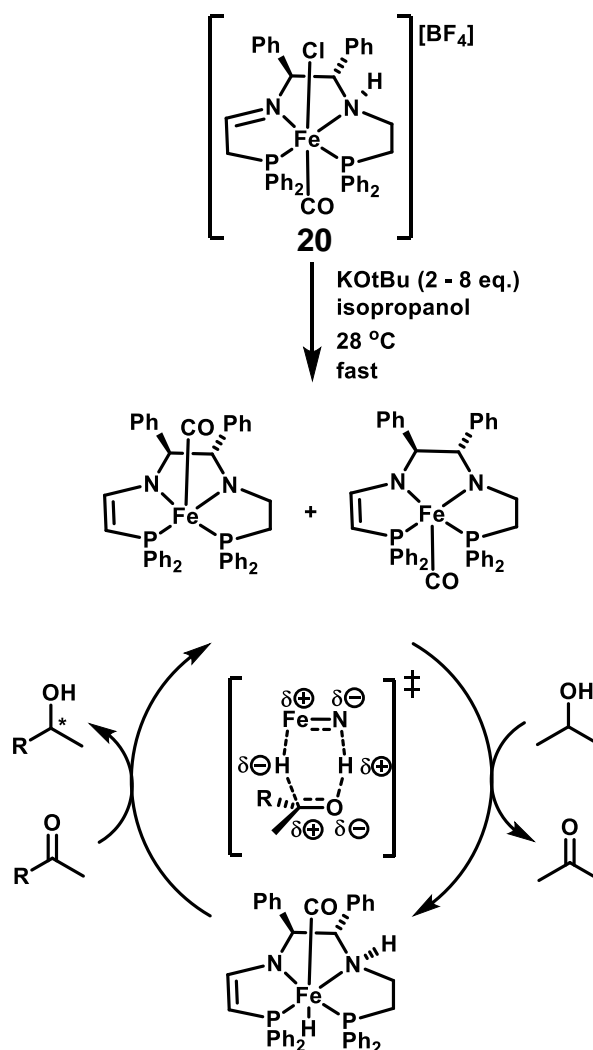
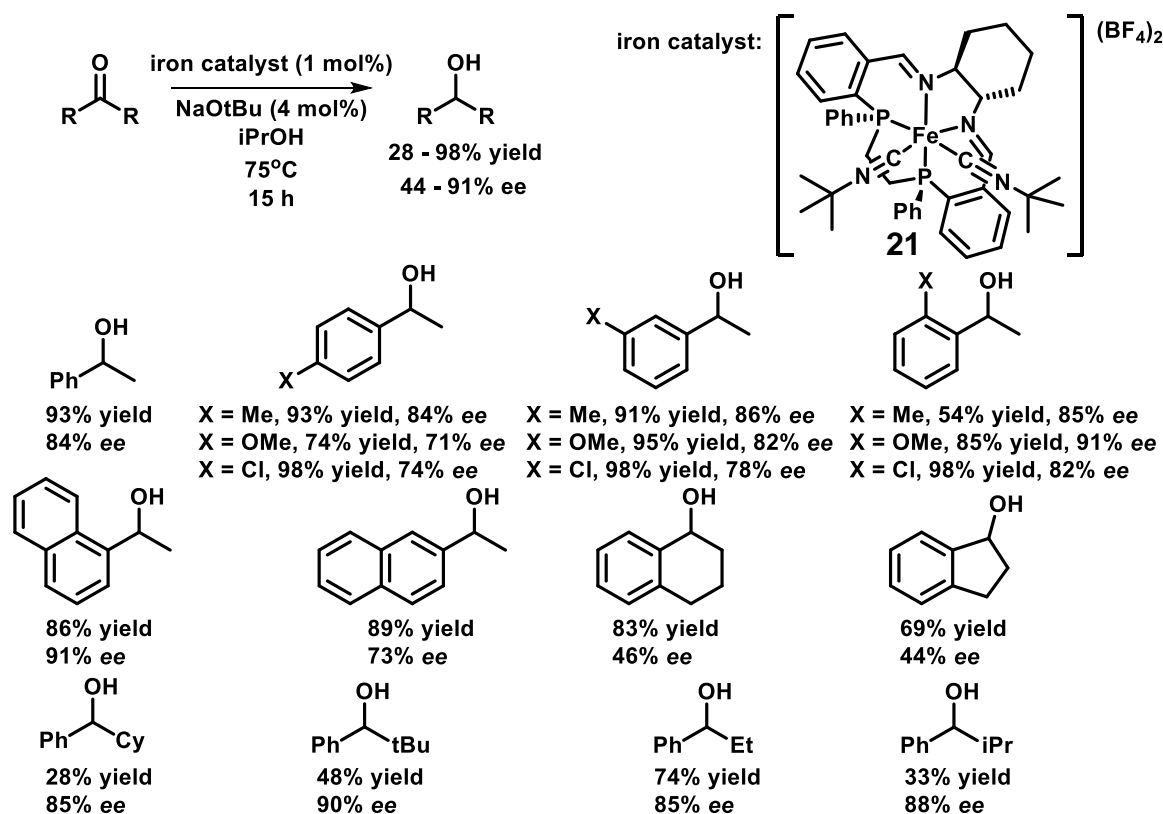
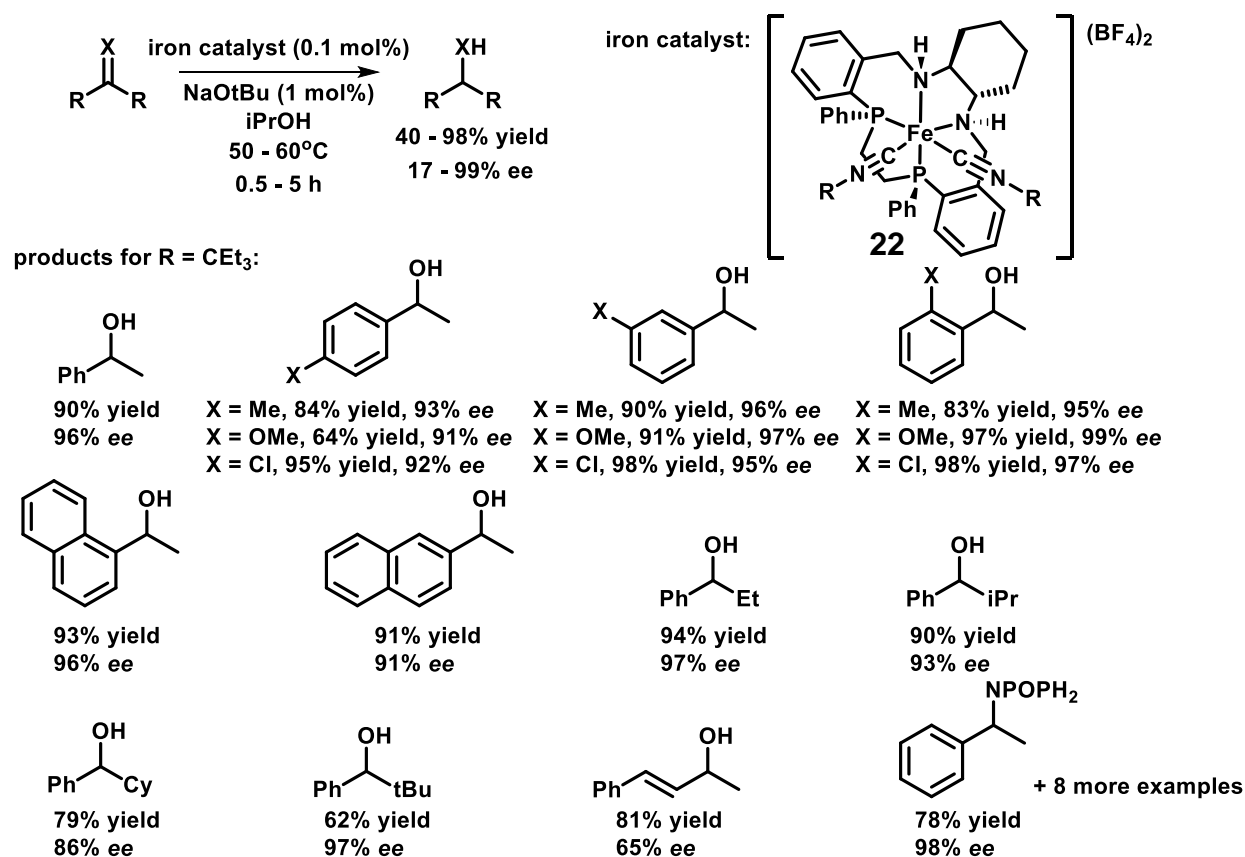


Figure 28 – Proposed mechanism for ATH of ketones using the amine(imine)diphosphine complex **20**.⁵¹

In 2014, iron complexes **21** with 14-membered N_2P_2 macrocyclic ligands were synthesised (**Figure 29**),⁵² and were used for the ATH of a broad scope of aromatic ketones giving excellent yields (up to 98%) and high ee (up to 91%).⁵³ Reduction of the ligand to give the diamino analogue **22** increases the activity substantially, allowing the catalyst loading, temperature and reaction time to be reduced (**Figure 30**). This catalyst was also able to reduce a phosphoryl imine and an α,β -unsaturated ketone. Both the activity and enantioselectivity are strongly influenced by varying the isonitrile ligands.⁵⁴

Figure 29 – ATH using iron complexes with a N₂P₂ macrocyclic imine ligand.⁵³Figure 30 - ATH using iron complexes with a N₂P₂ macrocyclic amine ligand.⁵⁴

In 2012, a 22-membered macrocyclic ligand **23** (**Figure 40**) was made which has 6 potentially coordinating nitrogen and phosphorus donor atoms and a crystal structure was obtained which confirmed its C_2 symmetry.¹ In combination with $Fe_3(CO)_{12}$, **23** catalysed the ATH of aromatic ketones, showing high activity (TOF up to 1940 h^{-1}) and giving excellent enantioselectivities (90 - 99%) and generally good conversions (**Figure 31**).¹

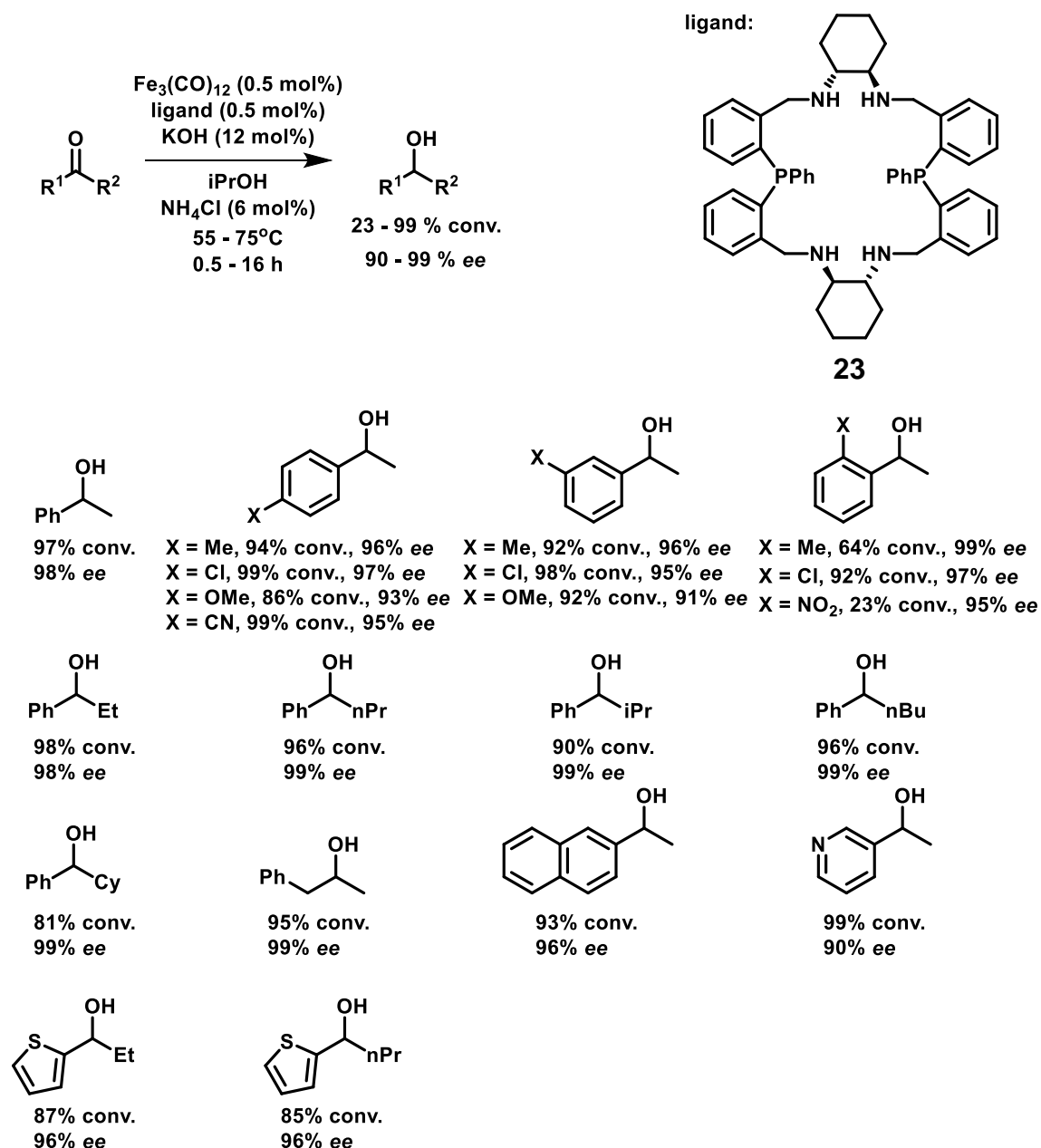


Figure 31 – ATH of ketones using macrocyclic ligand **23**.¹

An iron complex **24** was made by reacting $Fe_3(CO)_{12}$ with **23** in acetonitrile (**Figure 32**).⁵⁵ This complex **24** was tested for the ATH of ketones and was

found to give lower activity and enantioselectivity compared to the catalyst formed in situ from $\text{Fe}_3(\text{CO})_{12}$ and **23**. Therefore, it was speculated that **24** was not the active catalyst. However, a mixture of toluene and isopropanol was used as solvent because the complex **24** was insoluble in isopropanol, so these results are not directly comparable.

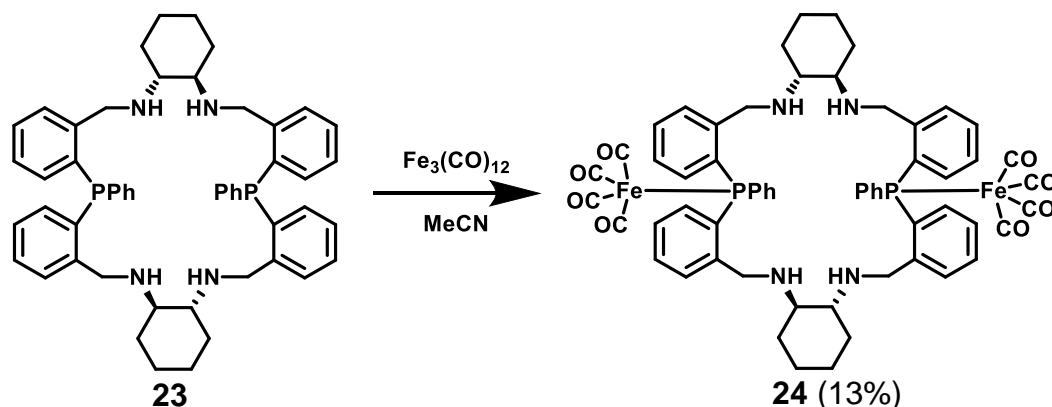


Figure 32 – Formation of an iron complex using the 22-membered macrocycle.⁵⁵

1.6.2. Hydrogenation using H_2

In 2007, Knölker's iron complex **12**³⁹ was used for the hydrogenation of aldehydes and ketones (**Figure 33**).⁴⁰ The reaction was performed using low hydrogen pressure (3 atm) at room temperature to produce the alcohol products in moderate to high yield. Epoxides, esters and isolated alkenes and alkynes were not reduced, and functional groups including halide bonds, nitro groups, benzyl ethers and cyclopropyl rings were tolerated. An imine substrate was also reduced to the corresponding amine in 50% yield.

The mechanism was investigated in a subsequent paper.⁵⁶ Firstly, alcohol complexes were synthesised by the stoichiometric reduction of aldehydes by Knölker's iron complex **12**. Then intramolecular trapping experiments and a study of the kinetic and thermodynamic stability of the formed complexes towards substitution reactions led them to suggest an outer-sphere mechanism of reduction, with concerted transfer of a proton from the OH and hydride from the iron (**Figure 34**).

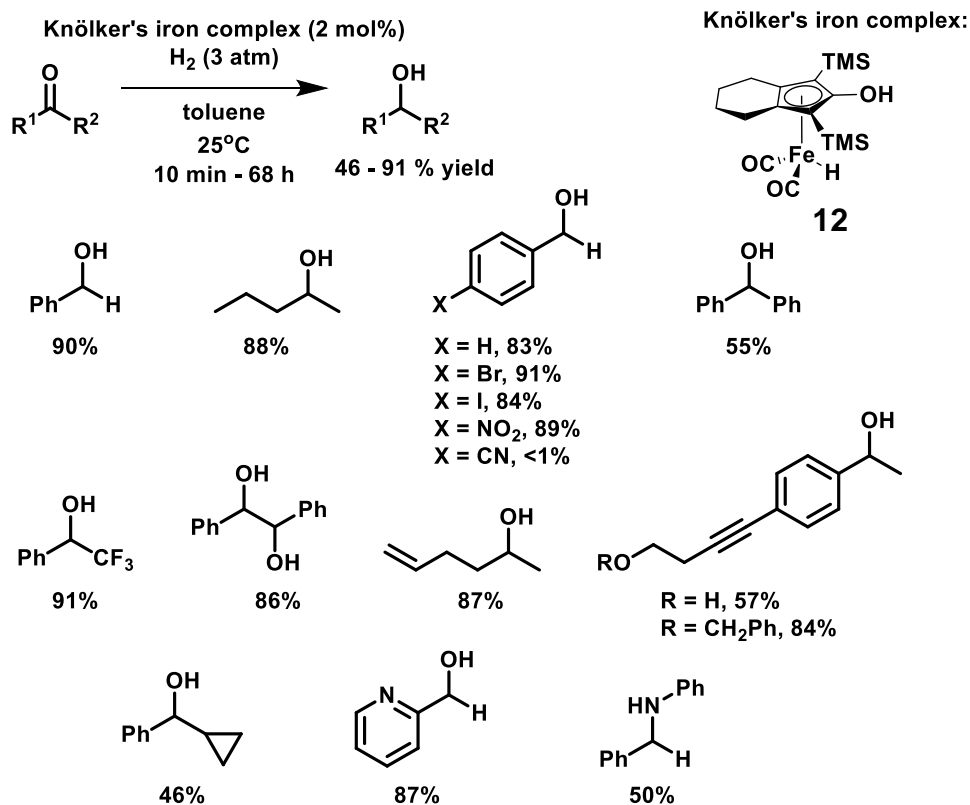


Figure 33 – Hydrogenation of aldehydes and ketones using Knölker's iron complex.⁴⁰

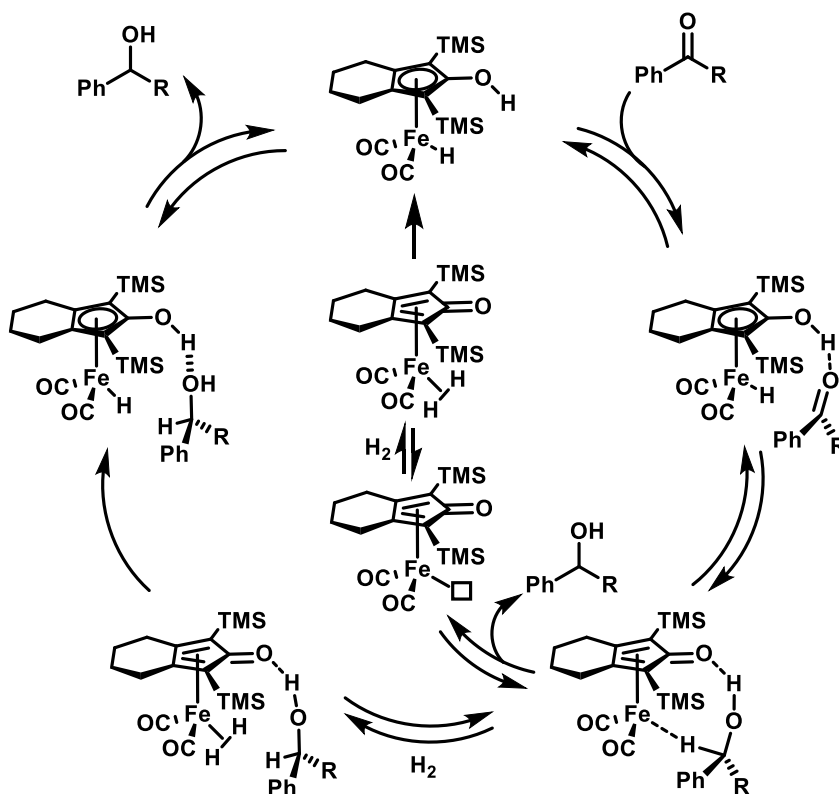


Figure 34 – Mechanism of hydrogenation of aldehydes and ketones using Knölker's iron complex.⁵⁶

The catalyst **12** was modified by adding chiral phosphoramidite ligands **25** (**Figure 35**), which replace one of the CO ligands on iron, to produce acetophenone with up to 31% ee.⁵⁷

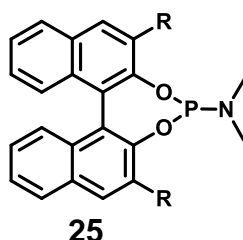


Figure 35 – Chiral phosphoramidite ligands.⁵⁷

In 2009, six different PNNP iron complexes **26** were synthesised and used for the AH of acetophenone (**Figure 36**).⁵⁸ Comparison of the activity of complexes **26a** and **b** suggested that the diimine ligand is reduced to the diamine before becoming an active catalyst. Complexes **26a**, **b** and **c** have moderate activity whereas complexes **26d** and **e** have very low activity. Complex **26d** gave essentially racemic product but **26e** gave 61% ee. DFT studies indicated that the reaction may go via an H-Fe-N-H outer sphere mechanism (**Figure 37**).

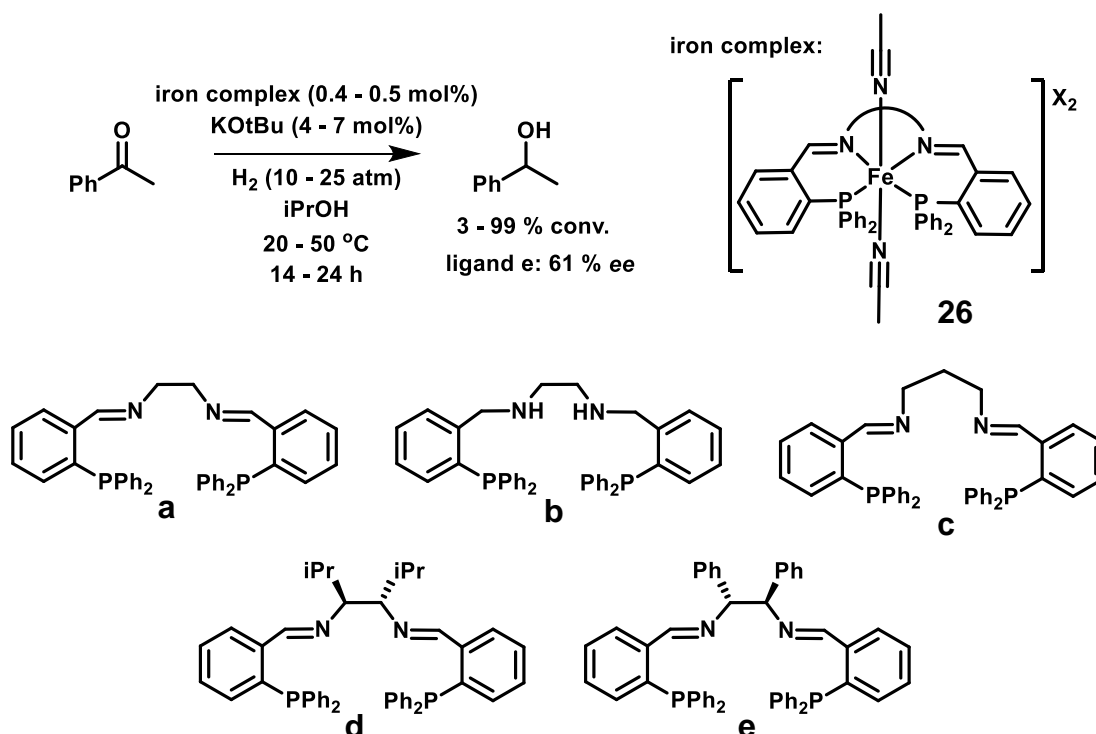


Figure 36 – Various PNNP ligands used to make iron complexes for AH of acetophenone.⁵⁸

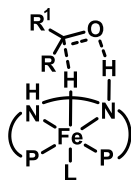


Figure 37 – H-Fe-N-H outer sphere mechanism.

In 2011, an iron pincer complex **27** (**Figure 38**) was developed for the hydrogenation of ketones.⁵⁹ The reaction takes place under mild conditions (4.1 atm H₂, room temperature) and gives the alcohol products in high yield. NMR studies suggested that the reaction proceeds through a dearomatized intermediate (**Figure 39**).

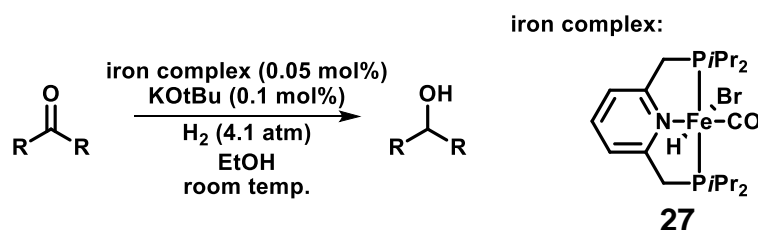


Figure 38 – Hydrogenation of ketones using an iron pincer complex.⁵⁹

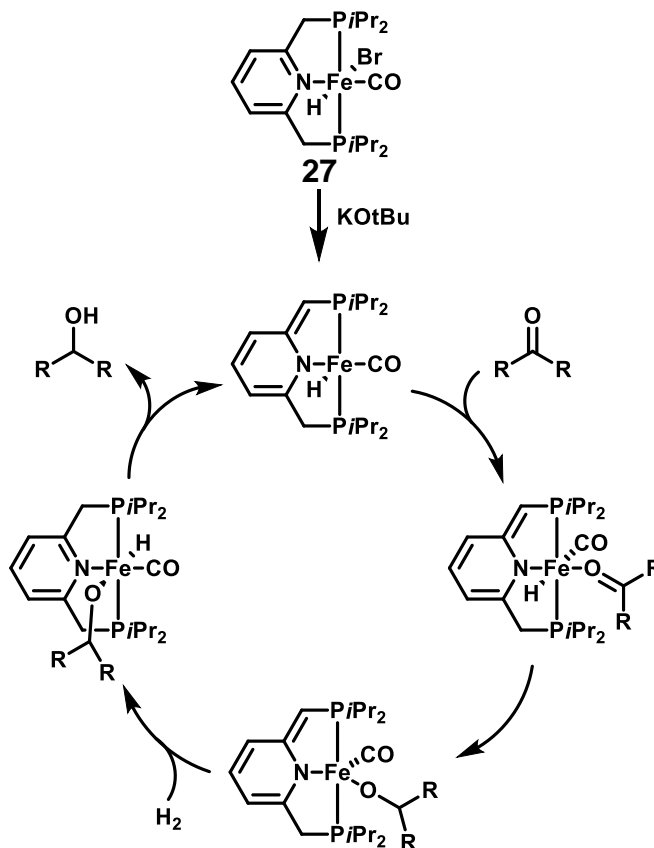


Figure 39 – Proposed mechanism of hydrogenation of ketones catalysed by **27** via a dearomatized intermediate.⁵⁹

In 2014, the 22-membered macrocyclic ligand **23** was shown by the group of Gao and our group to catalyse the hydrogenation of a wide variety of ketones using molecular H₂ (**Figure 40**),² giving the corresponding alcohols with ees near or better than those obtained with noble metal catalysts. The hydrogenation appears to be heterogeneous involving iron particles as the active catalytic species. Observations to support this include the cloudiness of the reaction mixture throughout the reaction and dynamic light scattering confirmed the existence of iron particles. Also, the catalyst needs an induction period in order to form the catalytically active species and a significant poisoning effect occurred upon addition of PPh₃ or Hg(0).

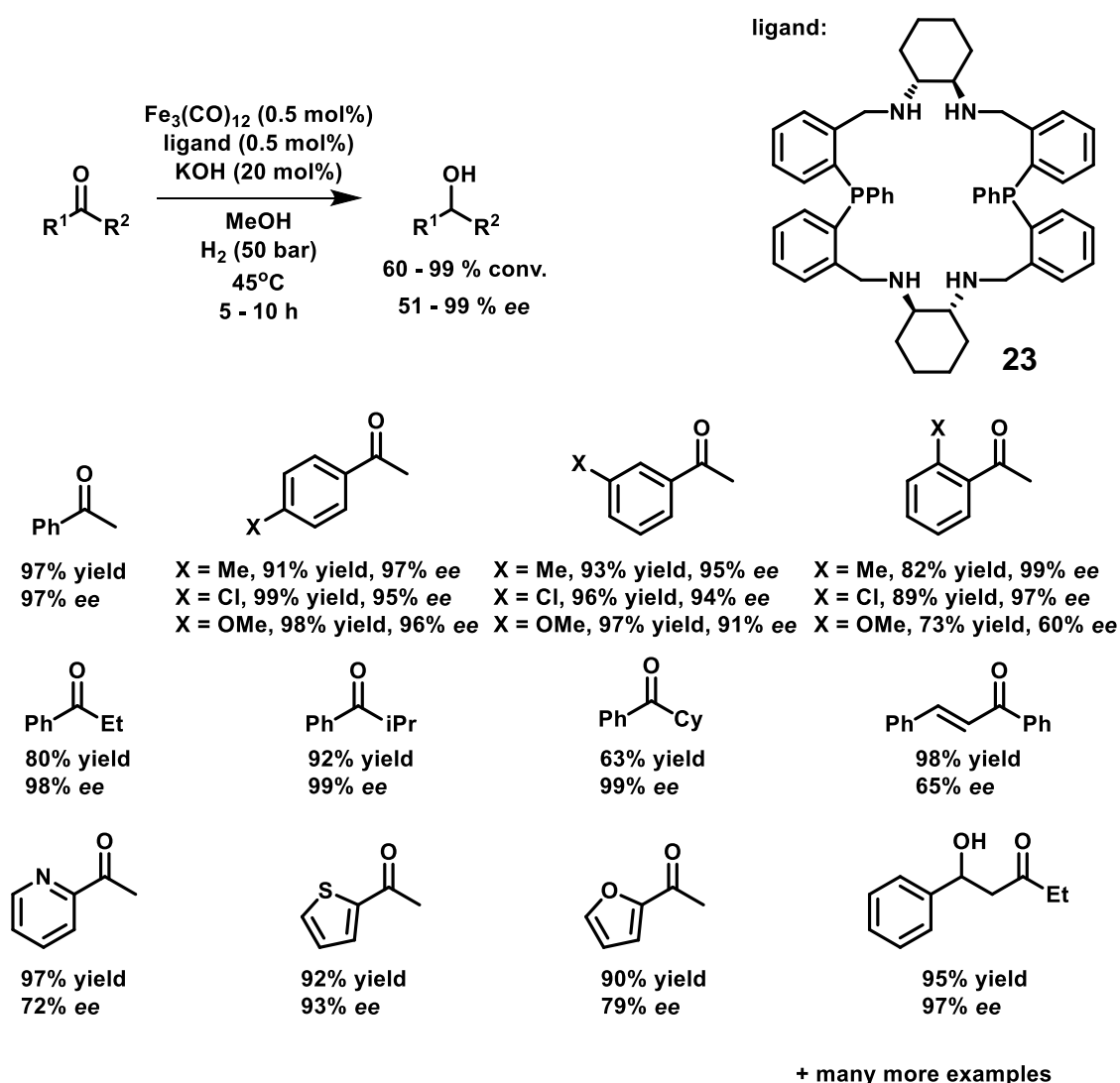


Figure 40 – Iron catalysed ATH and AH of ketones using a 22-membered macrocyclic ligand.²

The macrocyclic ligand **23** is the most enantioselective ligand for iron catalysed AH of ketones so far. The cyclic structure of the ligand may be responsible for the high ee due to its restricted flexibility.⁵⁵ However, there are some disadvantages including the low TOF, the high H₂ pressure needed (50 bar), and its inability to hydrogenate other substrates such as imines.

1.7. Aims of the project

Most of the examples of iron catalysed reactions found in the literature use multidentate ligands, which reflects the lower stability of iron complexes in comparison with those made with noble metals.² Following the success of the macrocyclic ligand **23** (**Figure 40**), the aim of this project is to synthesise a variety of macrocyclic ligands with nitrogen and phosphorus donor atoms, and test them for iron catalysed AH and ATH of ketones and imines, with the hope of obtaining an iron catalyst with increased activity and substrate scope. Some acyclic ligands will also be synthesised for comparison. Comparison of the various ligands will enable the optimisation and understanding of the catalyst with regards to the activity and ee. The first ligands to be synthesised will be based on (*S*)-phenylethylamine and phenyl phosphines (**Figure 41**), since these incorporate features similar to those ligands which have previously been shown to have some success, such as the macrocyclic ligand **23**.

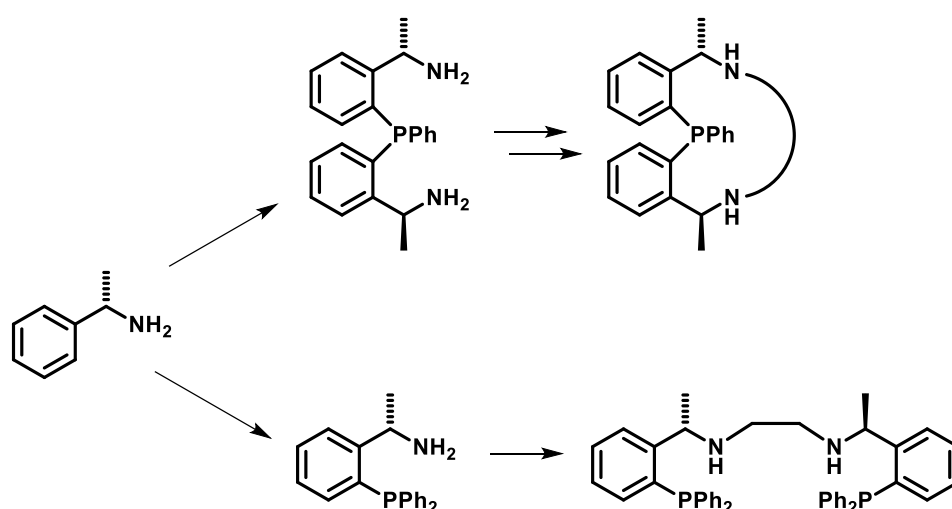


Figure 41 – Ligands to be synthesised.

The ligands will then be tested for the iron catalysed AH and ATH of ketones and imines. If the ee is not satisfactory, the ligands may be modified by changing the phenyl groups on phosphorus,^{46, 47} or the methyl group on the chiral centre next to the amine.⁴⁸ Greater steric bulk may lead to improved ee, but too much may decrease the activity. The electronic properties of the ligands will affect the stability of the complexes. Strongly σ donating ligands would be expected to form more stable complexes, however, ligands bearing electron withdrawing substituents are expected to facilitate heterolytic H₂ activation. Ligands with alkyl spacers instead of aryl spacers could be investigated,⁴⁵ as these will be more flexible so may be able to coordinate more easily to the iron centre. This may result in more stable complexes and higher ees. To enhance the stability of the complex, the phosphine unit may be replaced by a pyridine unit to make the complex more stable in air. Another alternative would be to replace the phosphine unit with an N-heterocyclic carbene (NHC) unit. These are very strongly σ donating and NHC complexes are generally stable to oxidation.⁶⁰

Mechanistic studies including the formation of complexes and deuterium labelling studies may be carried out in order to try and understand the mechanism of hydrogenation with this type of ligand, and therefore enable the design of new ligands.

Chapter 2. Synthesis of Macrocyclic Ligands

Ligands

2.1. Introduction

Macrocyclic ligands are large cyclic molecules which are generally made up of carbon frames with heteroatoms interspersed which are capable of binding to metal atoms.⁶¹ There are many naturally occurring macrocyclic ligands including the porphyrin ring found in the iron complex haem, the corrin core to vitamin B₁₂ and the chlorin ring found in chlorophyll (**Figure 42**).⁶²

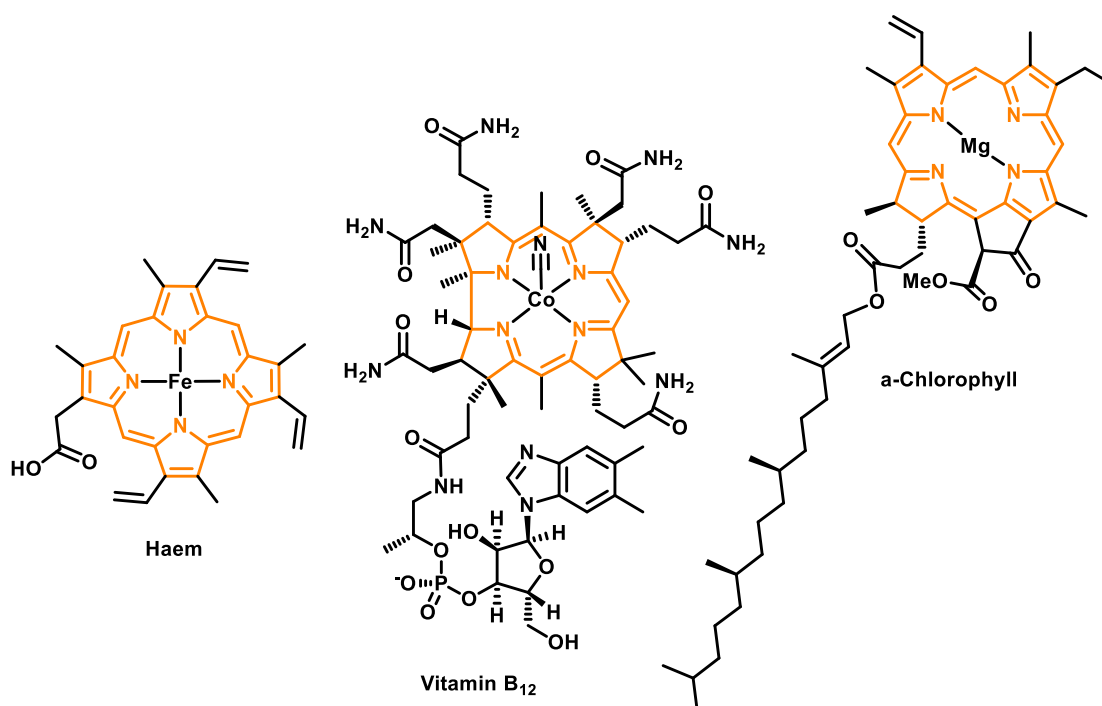


Figure 42 – Examples of macrocyclic ligands found in nature.

Macrocyclic ligands are desirable because they form more stable complexes due to the macrocyclic effect. This effect is similar to the chelate effect, which is the greater stability of the resulting complex compared to a complex with analogous monodentate ligands. The chelate effect is due to the increase in entropy when a multidentate ligand displaces monodentate ligands.⁶³ The macrocyclic effect is a combination of the increase in entropy, plus an additional energetic contribution coming from the pre-organised arrangement of the coordinating groups.⁶³ Also, once coordinated, macrocyclic ligands are

less likely to dissociate because if one donor atom dissociates, it is still held in close proximity to the metal ion by the rest of the ligand framework.⁶¹

The success of a macrocyclisation reaction depends on many different factors including thermodynamic and kinetic factors. There are two main ways to make macrocycles; one way is the condensation of two or more fragments under high dilution conditions, and the other way is template synthesis where the fragments are first coordinated to a metal and then react around the metal to form the macrocycle.⁶⁴

High dilution favours intramolecular reactions leading to cyclisation over intermolecular reactions leading to oligomerisation or polymerisation. One reactant is usually added slowly to the other reactant in a high volume of solvent so only a very small amount is present in the reaction at any one time. The cyclisation step requires the open-chain precursor to have an appropriate conformation which places the reactive groups in close proximity for cyclisation. Template synthesis can induce an appropriate conformation by the coordination of the open-chain precursor(s) to a metal before cyclisation.⁶⁴

An example of the high dilution method is the synthesis of the macrocyclic ligand **23** (**Figure 43**).¹ Dialdehyde **45** reacts with 1,2-diaminocyclohexane at high dilution in the presence of sodium sulfate to remove the water, giving the imine macrocycle in 75% yield. This is followed by reduction with sodium borohydride in ethanol to give the final amine macrocycle **23** in 60% overall yield.

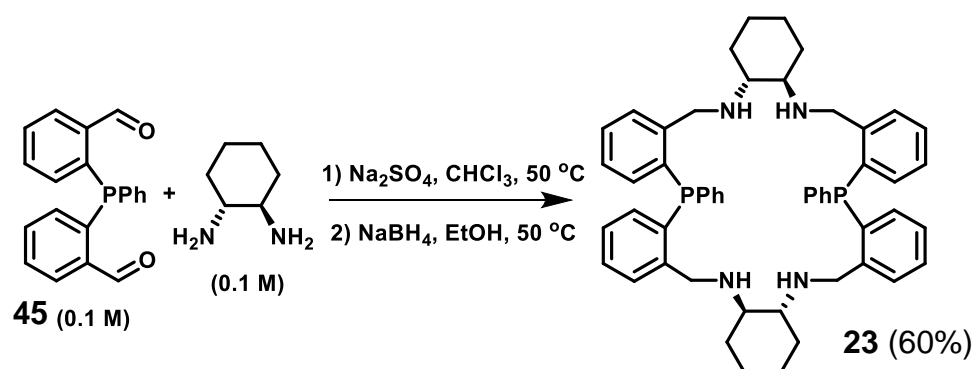


Figure 43 – High dilution synthesis of macrocyclic ligand **23**.¹

Another example of a macrocycle made by the high dilution method is macrocyclic ligand **29** (**Figure 44**) used in complex **22** (see also **Figure 29**).⁵²

Dialdehyde **28** is reacted with 1,2-diaminocyclohexane at 0.01 M in ethanol to give the imine macrocycle (67% yield) which is then reduced using lithium aluminium hydride to give the amine macrocycle **29** in 69% yield.

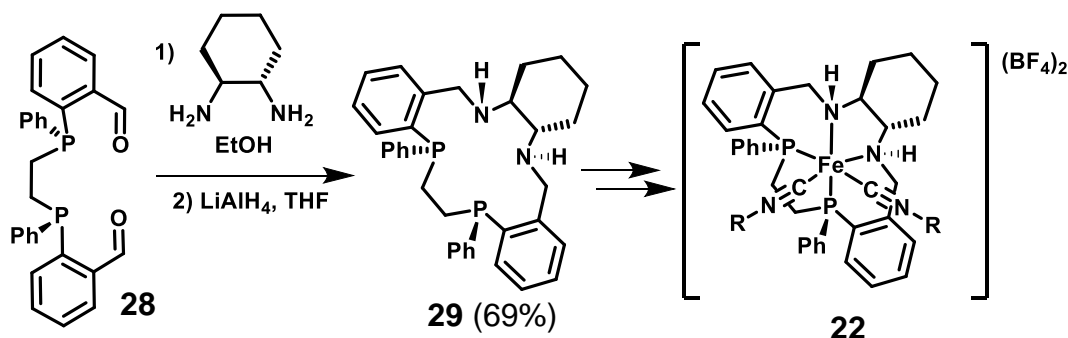


Figure 44 – High dilution synthesis of macrocyclic ligand **29**.⁵²

An example of the template method is the synthesis of P_2N_2 macrocyclic ligand **34** (**Figure 45**).⁶⁵ The NPPN ligand **30** is coordinated to nickel to give the dicationic complex **31**. This is then deprotonated by triethylamine to give the neutral complex **32** where the nitrogen atoms have nucleophilic activity. Reaction with 1,3-propanediol di-p-tosylate in toluene at reflux in the presence of potassium carbonate gives the macrocyclic complex **33**. The nickel is then removed using an aqueous solution of cyanide to give the free ligand **34**.

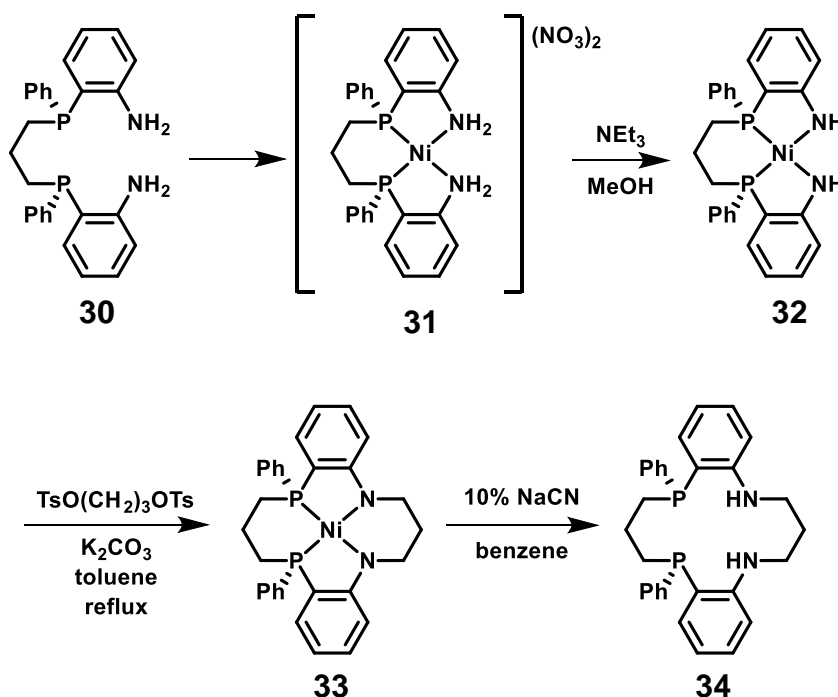


Figure 45 – Template synthesis of P_2N_2 macrocyclic ligand.⁶⁵

The method used in this project is the high dilution method. The synthesis of the diamine precursors proved to be quite challenging. Two synthetic routes

were studied; the first route did not work, but the second route worked well and a variety of macrocycles were synthesised.

2.2. Route 1

To prepare ligands having features similar to the most efficient ligand **23**, we targeted ligands of the type **37** (**Figure 46**). The R group and the linker that ring closes **36** are variable, making **37** modular and therefore increasing the likelihood of finding a more effective ligand for AH or ATH with iron.

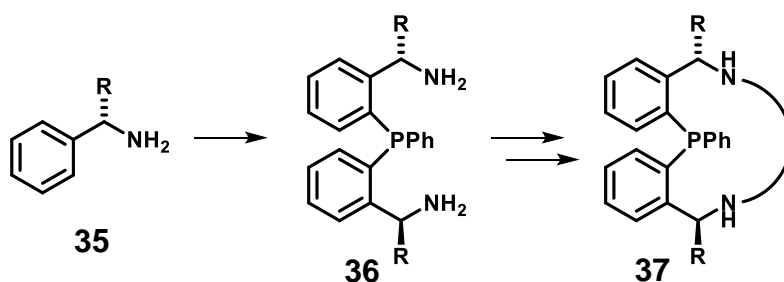


Figure 46 – The first synthetic route towards macrocycles.

The first synthetic route (**Figure 46**) started from (*S*)-phenylethylamine **35a** (R = Me), following the same method used to make (*S*)-1-[2-(diphenylphosphino)phenyl]ethylamine **81** from literature (**Figure 47**).¹² Firstly, one equivalent of *n*-BuLi was added to deprotonate the amine, and then trimethylsilylchloride was added as a protecting group. Next, more *n*-BuLi was added to deprotonate the aromatic ring in the ortho position, followed by the addition of Cl₂PPh (**Figure 47**).

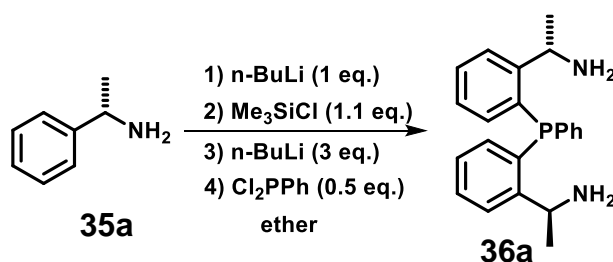


Figure 47 – The synthesis of diamine **36a**.

After purification by column chromatography, a pale-yellow oil was obtained, which was a mixture of two very similar products. There were two singlets in the phosphine region of the ³¹P NMR spectrum at -29.8 and -30.5 ppm, and the ¹H NMR spectrum contained two overlapped multiplets at 5.0 and 4.9 ppm,

which is where the peak for the hydrogen adjacent to the phenyl ring would be expected ($\text{ArCH}(\text{Me})\text{NH}_2$). These two products ran very closely on TLC and were therefore difficult to separate by column chromatography. A mass spectrum of this mixture was obtained which indicated that the expected product **36a** had not been formed.

On inspection of the details of the method used, it was decided to attempt the reaction using a smaller amount of *n*-BuLi for the ortholithiation step (step 3, **Figure 47**). The reaction was repeated twice, first using 1.2 equivalents, and the second using 2.2 equivalents. A mixture of different products was formed for each attempt, but mass spectrometry revealed that none of the expected product **36a** had been formed.

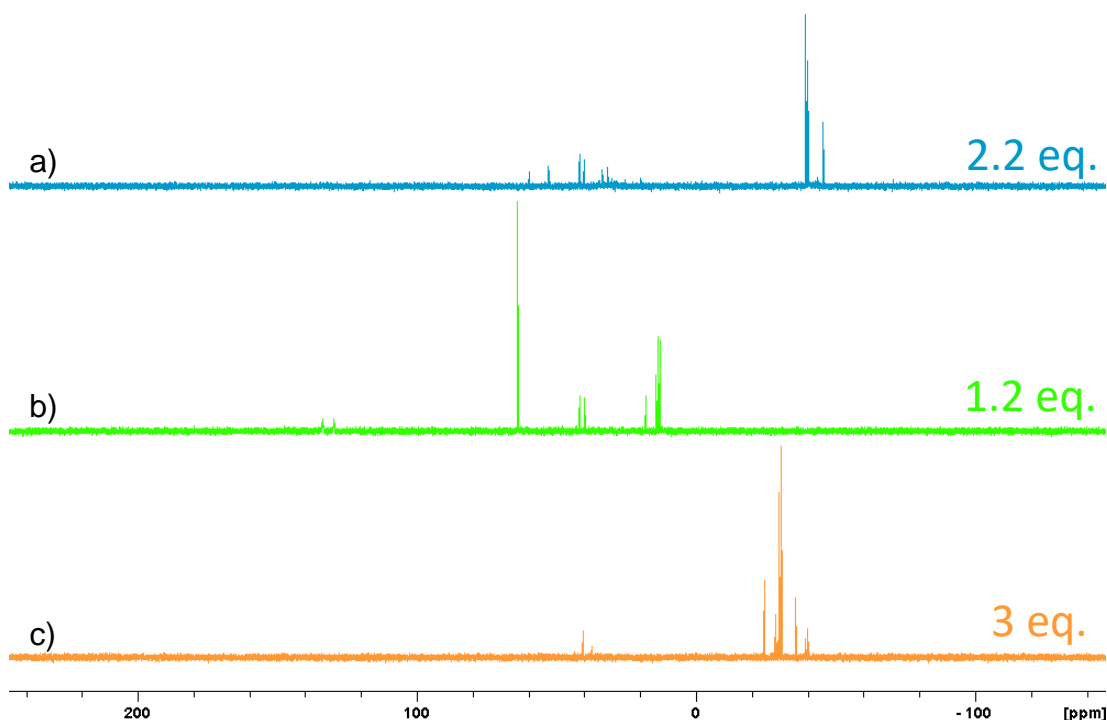


Figure 48 – A comparison of the $^{31}\text{P}\{^1\text{H}\}$ NMR spectra of the crude products, using (a) 2.2, (b) 1.2 or (c) 3 equivalents of *n*-BuLi for the ortholithiation step.

A comparison of the $^{31}\text{P}\{^1\text{H}\}$ NMR spectra of the crude products (**Figure 48**) shows the considerably different results obtained for each reaction. The use of 2.2 or 3 equivalents of *n*-BuLi produces a mixture of different products in the phosphine region of the spectrum, whereas the use of 1.2 equivalents shows no product in the phosphine region. All three spectra show the absence of dichlorophenylphosphine ($\delta^{31}\text{P}$ approx. 160 ppm).

In order to simplify the reaction mixture, it was decided to try to synthesise and isolate the TMS protected amine **38** (**Figure 49**), to avoid any by-products of this step interfering with any subsequent steps. One equivalent of *n*-BuLi was added dropwise to a solution of **35a** in dry ether at -35 °C. This mixture was stirred for 15 minutes and 1.1 equivalents of trimethylsilylchloride were added slowly. The mixture was stirred for one hour at -35 °C and then was slowly warmed to room temperature, filtered and the solvent was removed. However, this gave no product **38** and 67% of the starting material **35a** was recovered.

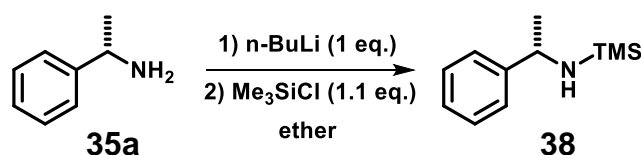


Figure 49 – The synthesis of TMS protected (*S*)-phenylethylamine.

A subsequent literature search revealed that mono-TMS protected primary amines are deprotonated by *n*-BuLi.⁶⁶⁻⁶⁸ This was unexpected since TMS was used as a protecting group for the synthesis of related primary amines. However, this may provide an explanation as to why such amines are only obtained in low yield.¹²

Therefore, the synthesis of bis-TMS protected phenylethylamine **39** was attempted by addition of one equivalent of *n*-BuLi to deprotonate the amine followed by one equivalent of trimethylsilylchloride, then repeating this sequence once more (**Figure 50**, top). However, workup by addition of water and extraction with ether gave recovered starting material **35a**.

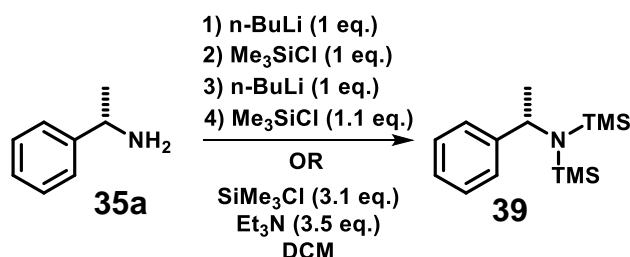


Figure 50 - The synthesis of bis-TMS protected (*S*)-phenylethylamine.

Another method for the synthesis of bis-TMS protected primary amines was found,⁶⁹ which used triethylamine as the base (**Figure 50**, bottom). Both triethylamine and trimethylsilyl chloride were used in excess (3.5 and 3.1 equivalents respectively) and the mixture was stirred in DCM at room

temperature overnight. The next day, the volatiles were removed under vacuum and the residue was extracted with hexane. This gave a mixture of starting material and a new product. Purification by vacuum distillation gave a yellow oil, but this was mono-TMS protected phenylethylamine **38** (42% yield) instead of the bis-TMS protected amine **39**. The ^1H NMR spectrum of **38** agreed with the literature,^{70, 71} showing a singlet at -0.01 ppm with an integration of 9 for the three methyl groups on silicon, a doublet at 1.37 ppm with an integration of 3 for the methyl group on the chiral centre, and a multiplet at 4.04 ppm with an integration of 1 for the hydrogen on the chiral centre.

The reaction was repeated at a higher temperature (reflux) to try and encourage formation of the bis-TMS protected amine **39**; however, this also did not work.

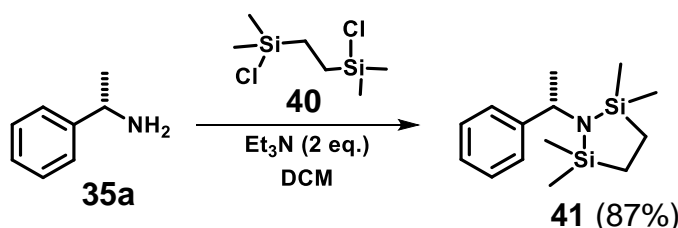


Figure 51 – The synthesis of ‘Stabase’ protected (S)-phenylethylamine.⁷²

A literature search revealed a silicon based protecting group **40**, called ‘Stabase’, which is a cyclic version of bis-TMS protected amine (**Figure 51**).⁷² The formation of a ring would be more entropically favourable than adding two separate TMS groups, and the product **41** may be more stable than **39**.

A solution of **40** in anhydrous DCM was added dropwise to a solution of **35a** in DCM with 2 equivalents of triethylamine. Upon addition, the solution became cloudy and white. The mixture was stirred for 2 hours at room temperature and was then filtered through sintered glass, which removed a white solid. This gave the product **41** as a pale-yellow oil in 87% yield (**Figure 51**). Two singlets were present in the ^1H NMR spectrum at -0.14 and 0.05 ppm with integrations of 6 for the methyl groups on silicon, there was a singlet at 0.68 ppm with an integration of 4 for the CH_2 groups, a doublet at 1.51 ppm with an integration of 3 for the methyl group on the chiral centre and a quartet at 4.34 ppm with an integration of 1 for the hydrogen on the chiral centre.

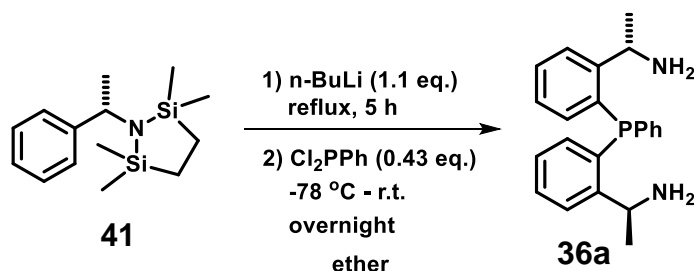


Figure 52 – The synthesis of (1*S*,1'*S*)-1,1'-((phenylphosphanediyl))bis(2,1-phenylene))bis(ethan-1-amine).

In an attempt to prepare **36a**, this Stabase protected (*S*)-phenylethylamine **41** was reacted with just over one equivalent of *n*-BuLi overnight at room temperature, followed by the addition of dichlorophenylphosphine. A mixture of many products was formed, however, none of the products were **36a**.

Next, the reaction was repeated but was heated under reflux for 5 hours in order to deprotonate the phenyl ring (**Figure 52**), following a procedure for the deprotonation of *N,N*-dimethylbenzylamine.⁷³ To this was added dichlorophenylphosphine at -78 °C and the mixture was left to react overnight. Unfortunately, no product **36a** was obtained from this reaction and some phenylethylamine **35a** was recovered.

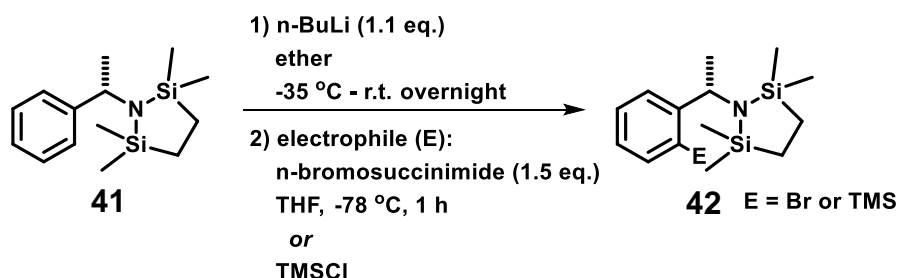


Figure 53 – The addition of different electrophiles to Stabase protected phenylethylamine.

Next, in an attempt to help to determine if the ortholithiation step takes place, two different electrophiles were added after the deprotonation step, instead of Cl_2PPh (**Figure 53**). Firstly, *n*-bromosuccinimide was added to put a bromine atom in the ortho position,⁷⁴ but no product **42** was obtained from this reaction. TMSCl ⁶⁷ was tried next which also failed, as only starting material **41** was recovered from this reaction.

Different conditions for the deprotonation step were tried next (**Figure 54**), using hexane as the solvent and t-butyl methyl ether as an additive (1.5 eq.).⁷⁵ This reaction also gave recovered starting material **41**.

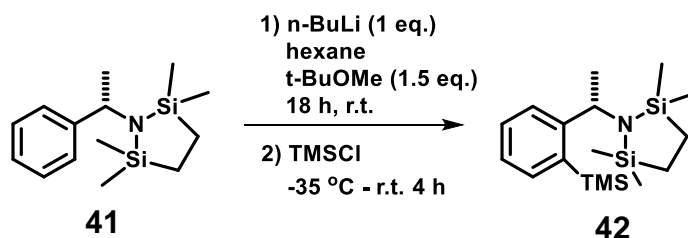


Figure 54 – The use of different conditions for the ortholithiation step.

A literature search on directing groups for ortholithiation revealed that -NMe₂ works well.⁷³ Therefore, (*S*)-*N,N*-dimethyl-1-phenylethan-1-amine **43** was synthesised from (*S*)-phenylethylamine **35a** using formaldehyde and formic acid,⁷⁶ to give product **43** in 53% yield (**Figure 55**).

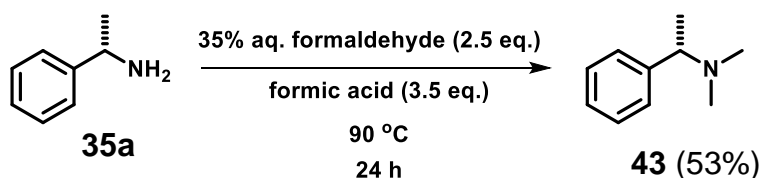


Figure 55 – The synthesis of (*S*)-*N,N*-dimethyl-1-phenylethan-1-amine.⁷⁶

This then underwent ortholithiation and reaction with Cl₂PPh to give **44** in 52% yield (**Figure 56**).⁷³ The ¹H NMR spectrum showed two doublets at 1.04 and 1.16 ppm with integrations of 3 which correspond to the methyl groups at the chiral centres. A singlet at 2.14 ppm with an integration of 12 corresponds to the four methyl groups on the amines, and two quintets at 3.98 and 4.11 ppm correspond to the hydrogens on the chiral centres. The ³¹P{¹H} NMR spectrum showed a singlet at -29.4 ppm.

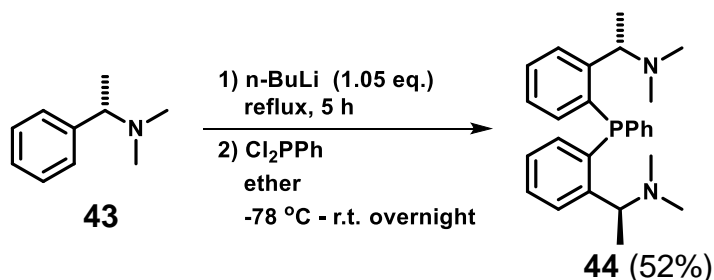


Figure 56 – The synthesis of (1*S*,1'*S*)-1,1'-((phenylphosphanediy)bis(2,1-phenylene))bis(*N,N*-dimethylethan-1-amine).⁷³

Two papers were found in which $R\text{-NMe}_2$ was converted into $R\text{-NH}_2$ through conversion into a good leaving group, followed by substitution with ammonia (**Figure 57** and **Figure 58**).^{77, 78} However, the papers did not present any explanation as to how there was retention of stereochemistry, since theoretically it could go either via S_N1 or S_N2 . Retention also occurs without the presence of the phosphine or sulfide group and earlier papers suggest participation of the iron.^{79, 80} No other papers could be found which showed that the conversion of $R\text{-NMe}_2$ into $R\text{-NH}_2$ could proceed with clean retention or inversion of stereochemistry.

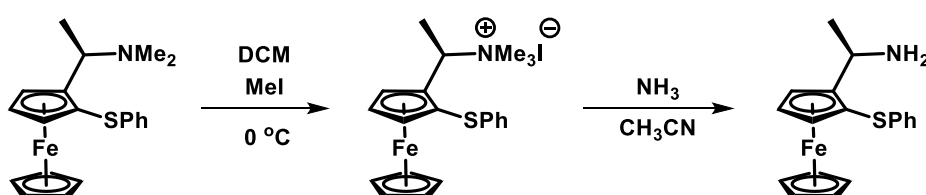


Figure 57 – Conversion of $R\text{-NMe}_2$ into $R\text{-NH}_2$ via an ammonium salt.⁷⁷

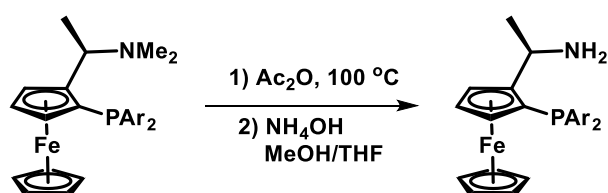


Figure 58 – Conversion of $R\text{-NMe}_2$ into $R\text{-NH}_2$ via an acetate.⁷⁸

In conclusion, method 1 was unsuccessful because a suitable protecting group for the primary amine was not found.

2.3. Route 2

Therefore, a different route towards the chiral diamine **36** was pursued (**Figure 59**), which adds the phosphorus before the amine, and avoids the requirement of a protecting group for the primary amine. This route starts from dialdehyde **45** which can be converted to diimine **46** using a chiral sulfinamide. Chiral sulfinamides, particularly *t*-butanesulfinamide, are popular reagents for the synthesis of chiral amines.⁸¹ Factors which make these reagents popular include the availability of both enantiomers at reasonable prices, and the straightforward and robust synthetic steps towards chiral amines with a broad substrate scope. The chiral diimine **46** can then undergo diastereoselective

Grignard addition to give the chiral diamine **47**, which can be converted to the free diamine **36** by removal of the sulfoxide groups. An advantage of this route is that a variety of different Grignard reagents can be added to generate a series of chiral diamines **36** with different chiral groups. The disadvantage of this route is the greater number of steps.

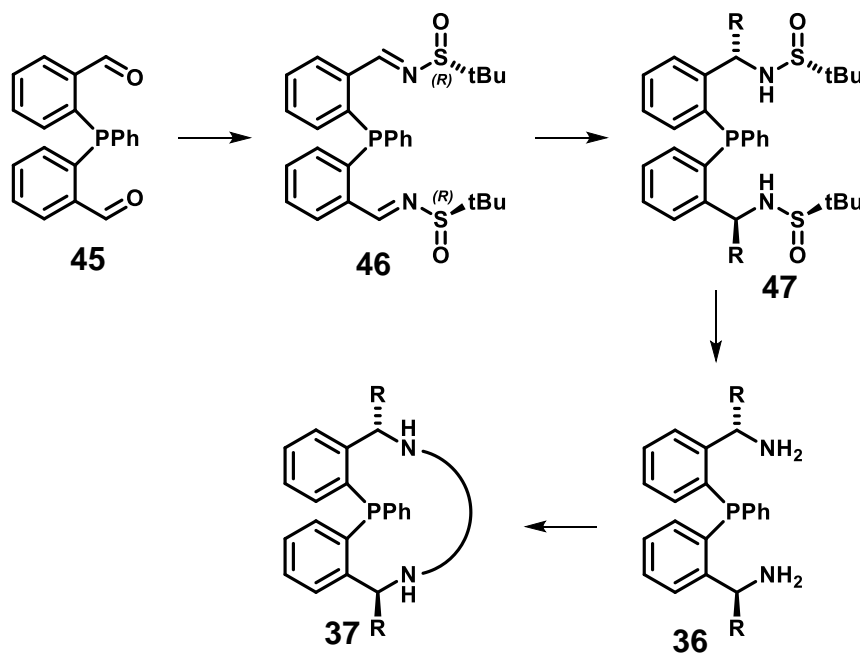


Figure 59 – The second synthetic route towards macrocycles.

2.2.1. Synthesis of dialdehyde **45**

Dialdehyde **45** is a known compound and was synthesised according to **Figure 60**.⁸²

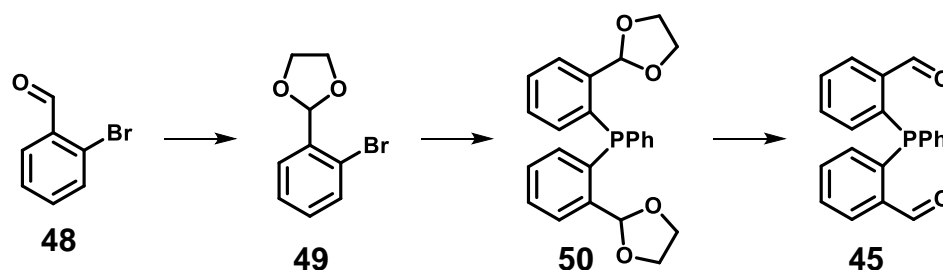


Figure 60 – An outline of the synthesis of 2,2'-(phenylphosphanediyldibenzaldehyde).⁸²

2-Bromobenzaldehyde **48** was reacted in refluxing toluene with ethylene glycol, catalysed by *p*-toluenesulfonic acid, to give **49** in 92% yield after purification by column chromatography (**Figure 61**).⁸³ Dean-Stark apparatus

was used to remove the water from the reaction as it was formed. The workup involved the addition of ethanolic potassium hydroxide to neutralise the acid catalyst, before washing with water. By allowing more time (about 30 mins) for the acid catalyst to be neutralised, the yield was increased to 99% and there was no need for purification.

A commercial sample of product **49** was obtained, but this gave much lower yields (around 30%) for the next step (**Figure 62**). This commercial sample was not kept under an inert atmosphere, so it could have contained water and/or 2-bromobenzaldehyde **48**, both of which would react with the n-BuLi, decreasing the yield of **50**.

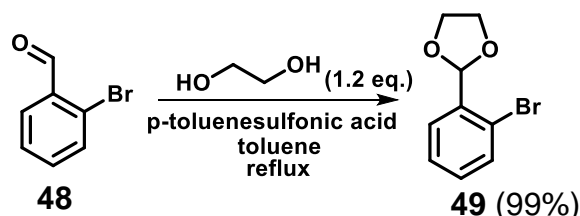


Figure 61 – The synthesis of 2-(2-bromophenyl)-1,3-dioxolane.⁸³

This protected product **49** then underwent lithium-halogen exchange with n-BuLi at -78 °C, followed by reaction with dichlorophenylphosphine to give the protected dialdehyde **50**. This was recrystallized from hot methanol to give the pure product in 60% yield. The yield was increased to 73% by increasing the time for lithium-halogen exchange from 1 hour to 2 hours (**Figure 62**).⁸² The ¹H NMR spectrum showed a multiplet at 4.0 ppm with an integration of 8 corresponding to the four CH₂ groups, and a doublet (coupling to P) at 6.37 ppm with integration of 2 corresponding to the hydrogens on the carbons adjacent to the aromatic rings. The ³¹P{¹H} NMR spectrum showed a singlet at -26.2 ppm and the IR spectrum showed a C-O stretch at 1087 cm⁻¹.

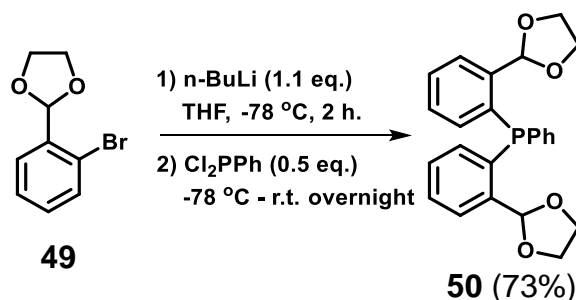


Figure 62 – The synthesis of bis(2-(1,3-dioxolan-2-yl)phenyl)(phenyl)phosphane.⁸²

Deprotection of **50** in acetone catalysed by *p*-toluenesulfonic acid initially gave the dialdehyde **45** in around 40% yield (**Figure 63**), which was much lower than the literature yield of 97%.⁸²

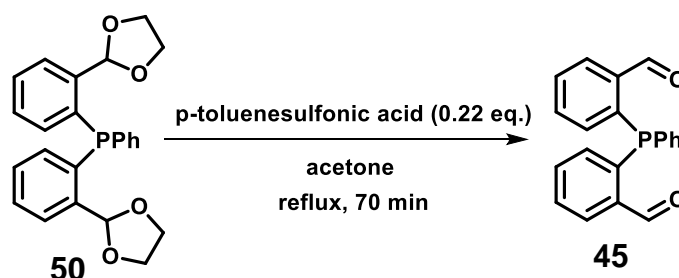


Figure 63 – Deprotection to give the dialdehyde.⁸²

However, the literature does not mention whether the acetone used was dry or not, so 2 equivalents of water were added to try and improve the yield. This increased the yield to around 60%, but another product was observed which was the oxidation-reduction of the dialdehyde **45** by water, giving the product **51** (**Figure 64**).⁸⁴ The product **51** was characterised by ¹H NMR, ³¹P{¹H} NMR and mass spectrometry and the data agrees with the literature.⁸⁴ It exists as a mixture of two diastereoisomers and the ³¹P{¹H} NMR showed two singlets at 33.3 and 27.5 ppm.

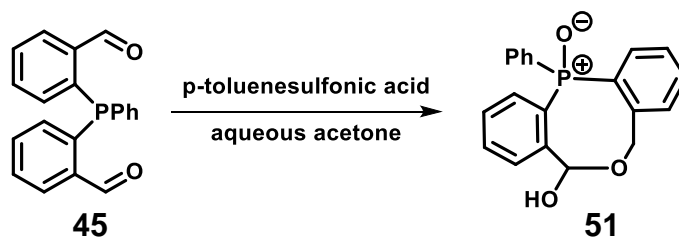


Figure 64 – Oxidation-reduction of dialdehyde **45** by water.⁸⁴

The reaction is similar to a previous report involving the reaction of (2-phenylethynylphenyl)phosphines with water,⁸⁵ which suggests that the mechanism involves intramolecular nucleophilic attack of phosphorus onto the alkyne followed by addition of water. Oxidation-reduction does not occur with the mono-aldehyde,⁸⁴ which suggests that the both aldehydes must be involved in the mechanism. This leads to the suggested mechanism shown in **Figure 65**.

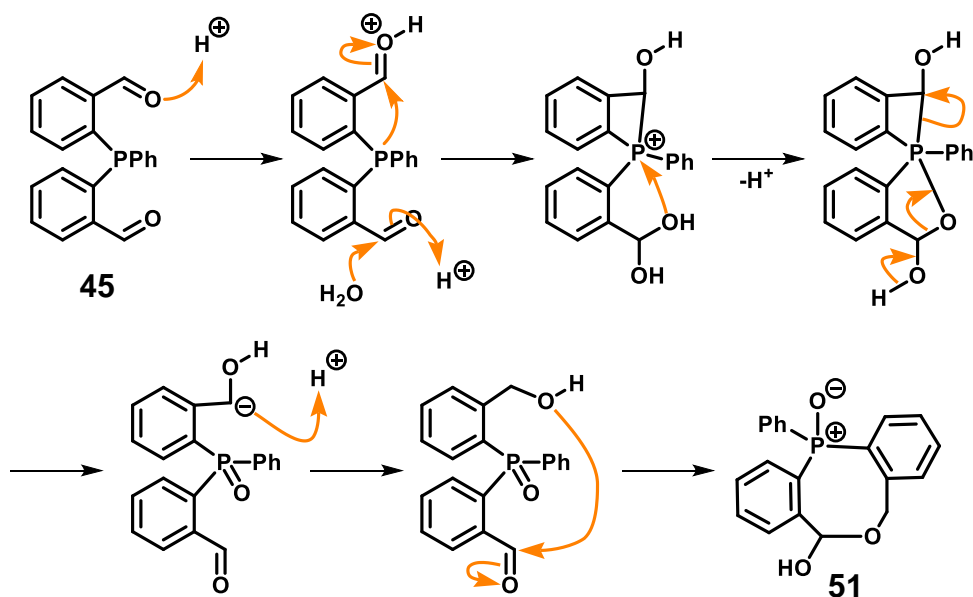


Figure 65 – Suggested mechanism of oxidation-reduction of dialdehyde **45** to give **51**.

Due to the low yield of dialdehyde **45**, it was decided to try and optimise the conditions for this step (**Figure 63**). The workup for this reaction involves addition of water and then evaporation of acetone to produce a yellow precipitate which is filtered, washed with water and dried.⁸² This precipitation step was often very difficult to achieve since it tended to form a thick yellow oil rather than a solid, and multiple attempts were required. Therefore, in order to simplify the workup, and also to see any other products being formed, the workup was changed to neutralise the acid catalyst using a solution of potassium carbonate, then evaporate the acetone, extract with DCM and wash with water. The results are summarised in **Table 1** below.

Table 1 – Optimisation of reaction conditions for the formation of dialdehyde **45** (**Figure 63**).

	percentage of product from the ^{31}P NMR of the crude products					time (min)	water (eq.)	notes
	45	50	53	51	52			
1	38	2	37	23	-	70	0	original workup was attempted first, before neutralisation and extraction with DCM
2	77	-	21	-	2	110	0	
3	87	-	6	-	7	170	0	
4	84	-	4	4	8	70	2	

Conditions: Protected dialdehyde **50** (0.087 M), *p*-toluenesulfonic acid (0.22 eq.), water, acetone, reflux. Workup – add $\text{K}_2\text{CO}_3(\text{aq.})$ (0.04 M, 0.22 eq.), evaporate acetone, extract with DCM, wash with water, dry with MgSO_4 .

In the first entry (**Table 1**), after 70 mins reaction time the original workup was attempted first, as recommended by the paper.⁸² Then, since no precipitate could be obtained, the mixture was neutralised and extracted with DCM. The ^{31}P NMR spectrum of the crude product showed only 38% of the dialdehyde **45**. A small amount of starting material **50** remained (2%), 37% was half-protected product **53** (**Figure 67**) and 23% was the oxidation-reduction with water product **51**. This result may explain why the precipitation step was difficult to achieve. The next two entries (entry 2 and 3) show no formation of oxidation-reduction product **51**, which indicates that the neutralisation of the acid catalyst stops the oxidation-reduction with water occurring. Increased reaction time produces more product, but also increases the oxidation-reduction with acetone, giving product **52** (**Figure 66**).⁸⁴ Adding 2 equivalents of water (entry 4) requires a much shorter reaction time. The crude product could be taken to the next step without further purification. However, if a purer product was needed it could be obtained by crystallisation with water/acetone.

The dialdehyde **45** was characterised by ^1H NMR, $^{31}\text{P}\{^1\text{H}\}$ NMR, $^{13}\text{C}\{^1\text{H}\}$ NMR, mass spectrometry and CHN and the data agrees with the literature,^{84, 86} showing a singlet in the $^{31}\text{P}\{^1\text{H}\}$ NMR spectrum at -16.2 ppm, and in the ^1H NMR there is a doublet (coupling to P) at 10.5 ppm with an integration of 2 corresponding to the hydrogens on the aldehydes.

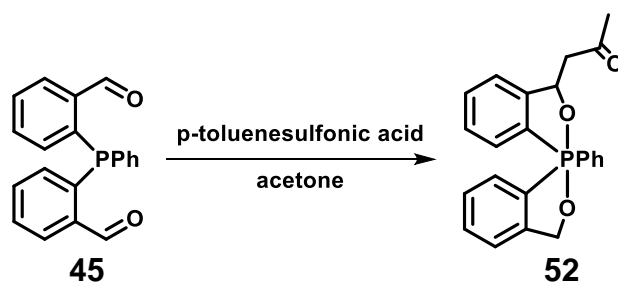


Figure 66 – Oxidation-reduction of dialdehyde **45** by acetone.⁸⁴

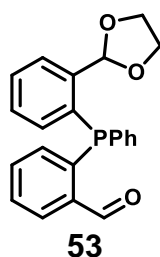


Figure 67 – Half-protected product.

During the optimisation process, in order to try and prevent the formation of the oxidation-reduction products **51** and **52**, the phosphorus atom of **50** was protected with BH_3 in THF at -78°C to give **54** (**Figure 68**).⁸⁷ The $^{31}\text{P}\{^1\text{H}\}$ NMR spectrum showed a singlet at 20.9 ppm. Unfortunately, it was difficult to purify this product. This protection with BH_3 was not optimised any further since the optimisation of the formation of dialdehyde **45** in **Table 1** resulted in a good yield of dialdehyde **45** (84 - 87% yield compared to 97% literature yield).⁸²

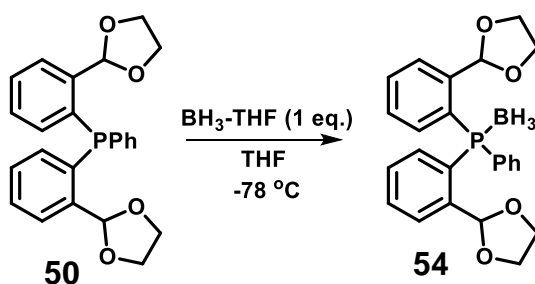


Figure 68 – Protection of **50** with BH_3 .

2.2.2. Synthesis of chiral diimine **46**

Next, the diimine **46** was made by reaction of the dialdehyde **45** with chiral sulfinamide **55** in THF at 50°C . Titanium isopropoxide acts as both a Lewis acid and a water scavenger (**Figure 69**).⁸⁸ This worked relatively well and, after purification by column chromatography, the pure product was obtained in up to 70% yield. The only difficulty with this step was the purification because

there was an impurity which ran very closely to the product on TLC; some mixed fractions were always obtained which required further purification. The ^1H NMR spectrum of **46** showed two singlets at 0.99 and 1.09 ppm each with an integration of 9 for the methyl groups on the t-butyl groups, and two doublets (coupling to P) at 8.95 and 9.07 ppm each with an integration of 1 for the imine hydrogens. The $^{31}\text{P}\{^1\text{H}\}$ NMR spectrum showed a singlet at -15.1 ppm and the IR spectrum showed a C=N stretch at 1574 cm^{-1} .

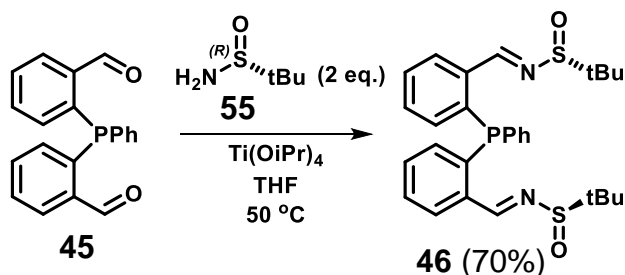


Figure 69 – The synthesis of the chiral diimine.

2.2.3. Diastereoselective Grignard addition to diimine **46**

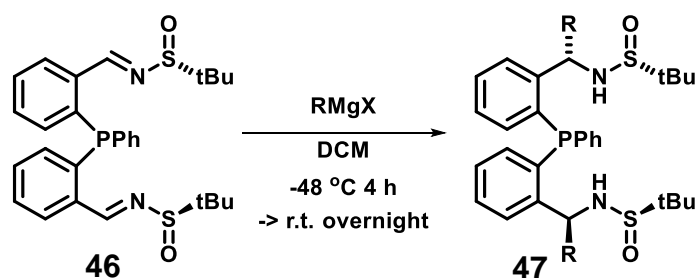


Figure 70 – Diastereoselective Grignard addition to the chiral diimine **46**.

The diimine **46** was then reacted with various Grignard reagents at $-48\text{ }^{\circ}\text{C}$ in DCM to give the corresponding chiral diamines **47** (**Figure 70**).⁸⁹ The reaction is diastereoselective and goes via the 6-membered ring transition state **56** shown in **Figure 71**.⁸¹ The bulky tertiary butyl group and the R^1 group on the imine strongly prefer equatorial positions, while the lone pair and the hydrogen can occupy the axial positions. The metal coordinates to the sulfoxide oxygen as the R^2 group adds into the imine carbon.

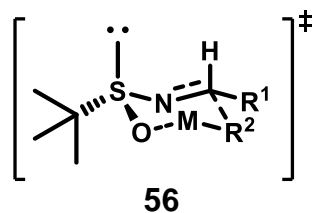


Figure 71 – Diastereoselective Grignard addition via a 6-membered ring transition state.⁸¹

An open transition state **57** (**Figure 72**)⁸¹ occurs in the presence of coordinating solvents such as THF, which leads to the formation of the opposite diastereoisomer. The solvent coordinates to the metal which prevents the 6-membered ring transition state **56** from forming.

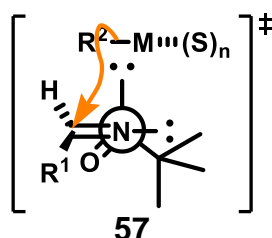


Figure 72 – Open transition state in the presence of coordinating solvents.⁸¹
(M = metal, S = solvent)

There are three possible diastereoisomers: SS, RR and SR (**Figure 73**). If the reaction goes via transition state **56**, the favoured diastereoisomer should be SS. However, if it goes via transition state **57**, RR will be preferred. In practice, a mixture of all three diastereoisomers is formed. A summary of the various Grignard additions is shown in **Table 2** below.

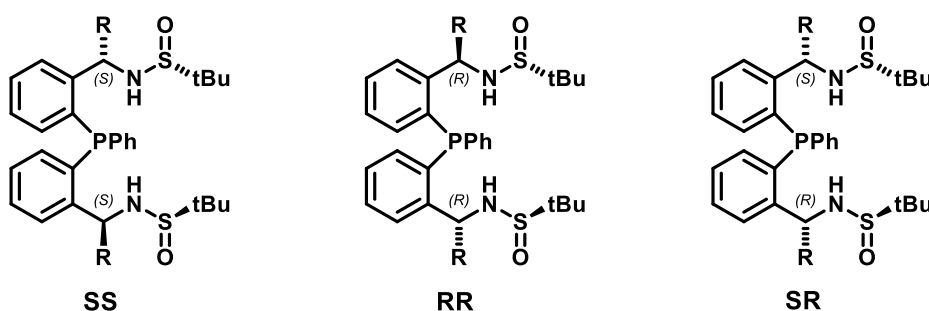


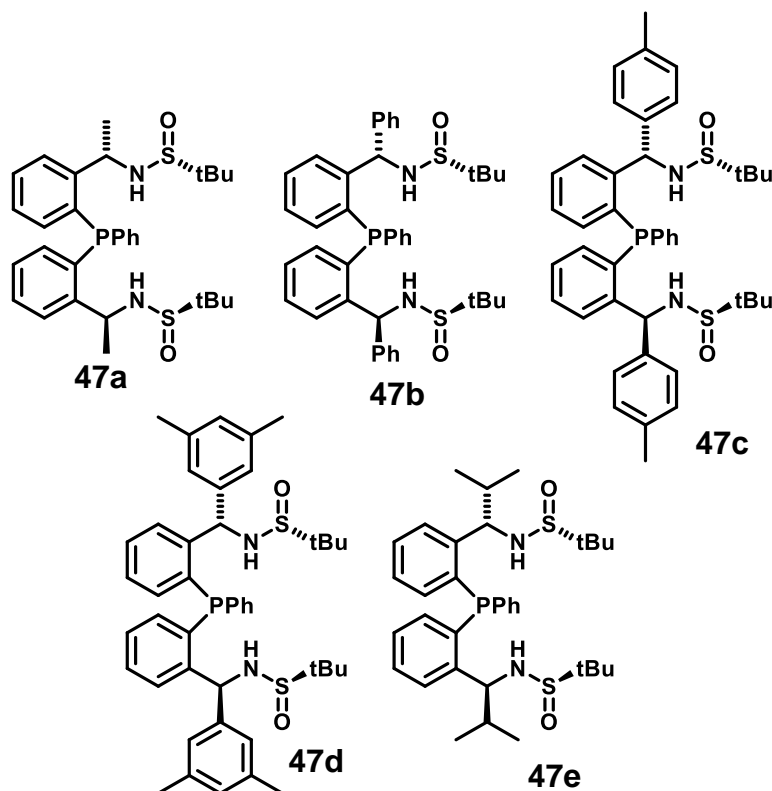
Figure 73 – Possible diastereoisomers from Grignard addition.

Table 2 – A summary of the Grignard additions.

	Grignard reagent	concentration/solvent	DCM:Grignard reagent ratio (by volume)	diastereoselectivity*	dr of major product(s) after purification
1	MeMgBr	3 M / ether	3:1	19 : 62 : 18	83 : 17
2	PhMgBr	3 M / ether	3:1	4 : 85 : 11	98 : 2
3	PhMgBr	3 M / ether	6:1	3 : 86 : 11	98 : 2
4	p-TolMgBr	0.5 M / ether	1:2	1 : 66 : 33	95 : 5
5	p-TolMgBr	0.5 M / ether	3:1	4 : 83 : 13	98 : 2
6	3,5-XylMgBr	0.5 M / THF	3:1	5 : 62 : 33	100
7	iPrMgCl	2 M / ether	6:1	38 : 39 : 23	96 : 4 84 : 16

*the ratio of peaks in the $^{31}\text{P}\{^1\text{H}\}$ NMR of the crude product.

The first Grignard reagent used was methylmagnesium bromide (entry 1) to give **47a** (Figure 74). This had poor diastereoselectivity and one of the minor diastereoisomers was unable to be separated from the major product. The $^{31}\text{P}\{^1\text{H}\}$ NMR spectrum of this mixture had two singlets at -28.9 and -28.6 ppm. Also, this final mixture contained 40% oxidation products. All attempts to purify this mixture further, either by crystallisation or column chromatography, failed.

**Figure 74** – Products from Grignard addition to diimine **46**.

Next, phenylmagnesium bromide was used (entry 2), which gave better diastereoselectivity and these diastereoisomers were separable by column

chromatography to give the main diastereoisomer **47b** in good yield. The ^1H NMR spectrum showed two doublets at 3.59 and 3.85 ppm each with an integration of 1 corresponding to the hydrogens on the chiral centre. The $^{31}\text{P}\{^1\text{H}\}$ NMR spectrum showed a singlet at -27.8 ppm and the IR spectrum showed an N-H stretch at 3195 cm^{-1} .

p-Tolylmagnesium bromide was used next, which gave a lower diastereoselectivity at first (entry 4). However, the selectivity was increased by adjusting the amount of DCM to give a DCM:Grignard reagent ratio of 3:1 (entry 5) as previously used, taking into account the lower concentration of the Grignard reagent. This gave the product **47c** in good yield. The ^1H NMR spectrum showed two singlets, each with an integration of 3, at 2.15 and 2.20 ppm for the methyl groups on the tolyl groups, and two doublets at 3.55 and 3.76 ppm for the hydrogens on the chiral centre. The $^{31}\text{P}\{^1\text{H}\}$ NMR spectrum showed a singlet at -27.8 ppm and the IR spectrum showed an N-H stretch at 3214 cm^{-1} .

3,5-Dimethylphenylmagnesium bromide (entry 6) gave slightly lower diastereoselectivity, possibly due to the more strongly coordinating solvent (THF compared to ether). The diastereoisomers were easily separated by column chromatography to give a single diastereoisomer **47d** in moderate yield. The methyl groups on the aromatic rings give two singlets in the ^1H NMR spectrum at 2.03 and 2.08 ppm, each with integrations of 6. The hydrogens on the chiral centres gave two doublets (coupling to P) at 3.59 and 3.97 ppm. The $^{31}\text{P}\{^1\text{H}\}$ NMR spectrum showed a singlet at -28.4 ppm and the IR spectrum showed an N-H stretch at 3223 cm^{-1} .

Finally, isopropylmagnesium chloride gave very poor diastereoselectivity (entry 7), so that it was unclear which diastereoisomer was the desired one (**47e**). One of the diastereoisomers was separated by column chromatography which had a singlet at -27.5 ppm in the $^{31}\text{P}\{^1\text{H}\}$ NMR spectrum. The other two diastereoisomers were unable to be separated and also contained 39% oxide products. The $^{31}\text{P}\{^1\text{H}\}$ NMR spectrum had singlets at -27.6 and -26.7 ppm plus oxide peaks at 37.5 and 38.1 ppm.

2.2.4. Removal of the sulfoxide groups

The sulfoxide groups from the diamines **47** can then be removed by acid catalysed hydrolysis to give the free diamines **36** (**Figure 75**).⁹⁰ The products **47a** and **47e** (R = Me, iPr) were not continued since they could not be purified, and also the configuration of **47e** was unknown.

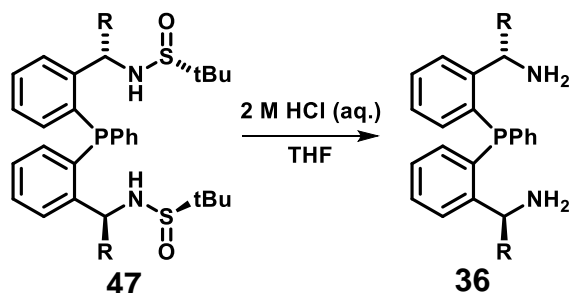


Figure 75 – Removal of the sulfoxide groups by acid hydrolysis.

The sulfinamides **47** were dissolved in THF, 2 M HCl was added and the reaction was stirred at room temperature for 3 days. The mixture was then basified with sodium hydroxide and extracted with ethyl acetate. The first eluent tried for the column chromatography (EtOAc/hexane/Et₃N) gave a mixture of many extra products in the phosphine region which were not present in the crude product. Changing the eluent to methanol/DCM gave the pure diamines **36** in around 70% yield (**Figure 76**).

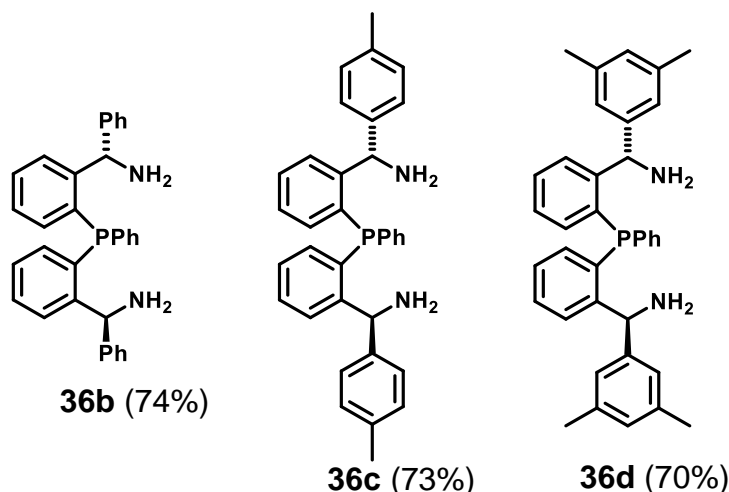


Figure 76 – Chiral diamines.

The hydrogens on the chiral centres gave peaks in the ¹H NMR spectra at 5.88 and 6.06 ppm for **36b**, 5.79 and 6.01 ppm for **36c**, and 5.96 and 6.02 ppm for **36d**. The ³¹P{¹H} NMR spectra showed singlets at -26.7 ppm for **36b**, -26.7 ppm for **36c** and -27.8 ppm for **36d**.

2.2.5. Cyclisation

Next, the cyclisation of the diamine **36b** with various dialdehydes was carried out at 50 °C in chloroform at high dilution in the presence of sodium sulfate (**Figure 77**). High dilution reduces the possibility of polymerisation and sodium sulfate removes the water to prevent the reaction from running backwards.

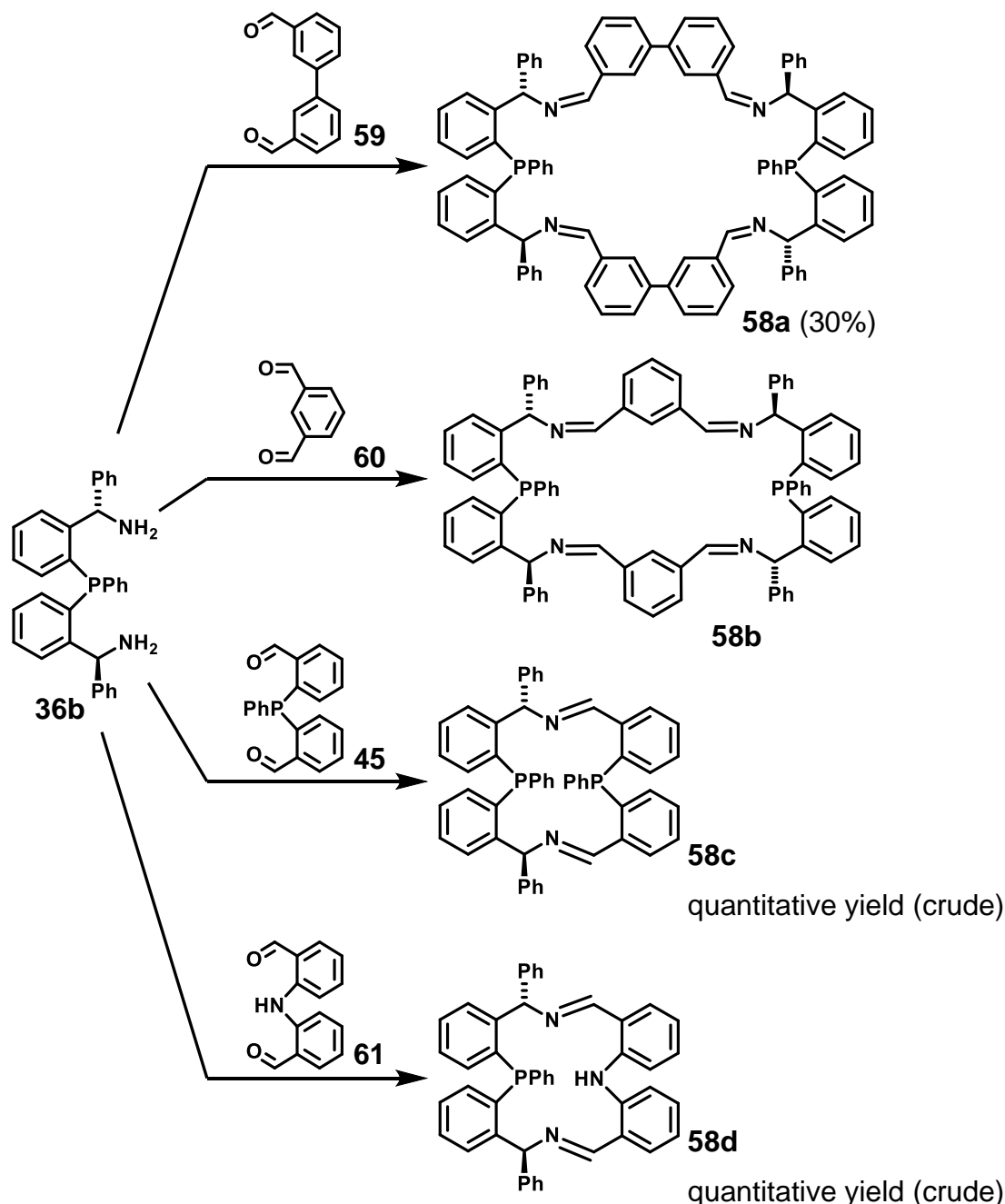


Figure 77 – Cyclisation of diamine **36b** with various dialdehydes.
 Conditions: **36b** (0.002 M), dialdehyde (1 eq.) Na₂SO₄ (13 eq.), chloroform, 50 °C, 48 h.

The first cyclisation was carried out by Dr George Cheng from the Xiao group using [1,1'-biphenyl]-3,3'-dicarbaldehyde **59** (**Figure 77**). This was purified by

column chromatography to give the pure product **58a** in 30% yield. At first, it was unclear whether the product was the 1+1 macrocycle or the 2+2 macrocycle (**Figure 78**).

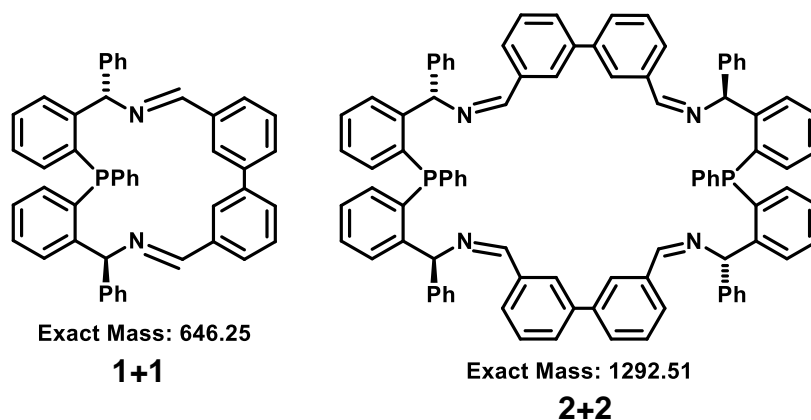


Figure 78 – 1+1 vs 2+2 macrocycles.

Confusion could occur between these two possible products, since the analytical data would be very similar. Mass spectrometry showed a peak at m/z 647.26, which could either correspond to the $[M+H]^+$ ion for the 1+1 macrocycle, or the $[M+2H]^{2+}$ ion for the 2+2 macrocycle. A peak at m/z 1293.51 was also present which could either correspond to the $[M+H]^+$ ion for the 2+2 macrocycle, or a dimer of the 1+1 macrocycle. The deciding factor was the presence of another peak at m/z 647.76, with equal intensity to m/z 647.26. These peaks indicate doubly charged species since they are 0.5 mass units apart. Therefore, the product is the 2+2 macrocycle **58a**.

The next dialdehyde used was isophthalaldehyde **60** (**Figure 77**), which gave a complicated mixture of products. The reaction was repeated at a higher concentration, which still gave the same mixture of products but in different ratios. The $^{31}\text{P}\{^1\text{H}\}$ NMR spectra for the crude mixtures are shown in **Figure 79** and the peak for the starting diamine **36b** is marked with an asterisk. A broad peak at -28.2 ppm could correspond to a polymer or oligomer product. A pair of doublets at -26.0 and -25.1 with similar integration and coupling constants (9.2 Hz) could correspond to a 2+2 macrocycle where the phosphorus atoms are inequivalent, possibly due to isomers of the imine bonds or the phenyl rings on phosphorus. The peak at -23.9 ppm looks as though it could be a doublet, but since there is no coupling partner, it must be a mixture of peaks. The mass spectra of the crude product mixtures indicated

that the desired product **58b** had been formed, but attempts to purify or reduce these mixtures failed.

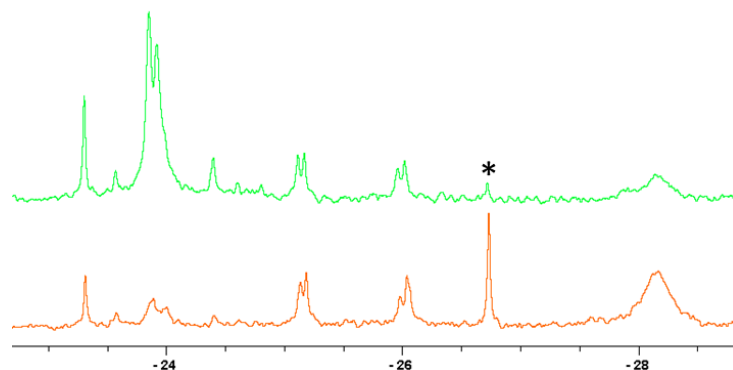


Figure 79 $^{31}\text{P}\{^1\text{H}\}$ NMR spectra for the crude products from reaction of **36b** with **60**.

The starting concentration of **36b** = 0.1 M (top), 0.00184 M (bottom).
The peak for the starting diamine **36b** is at -26.7 ppm (marked with *).

Dialdehyde **45** was used next which, in contrast to the previous two dialdehydes, gave the 1+1 macrocycle **58c** in quantitative yield (**Figure 77**). The ^1H NMR spectrum showed two doublets (coupling to P) for the imine hydrogens at 9.54 and 10.27 ppm. The $^{31}\text{P}\{^1\text{H}\}$ NMR spectrum for this product is interesting as it shows two doublets with coupling constants of 8.9 Hz, which indicates that the two phosphorus atoms couple to each other, even though they are 8 bonds away from each other. Through-space P-P couplings are obtained when the phosphorus lone pairs point toward each other and overlap, enabling the transmission of nuclear spin information.⁹¹ A phosphorus-phosphorus COSY was performed to confirm this (**Figure 80**).

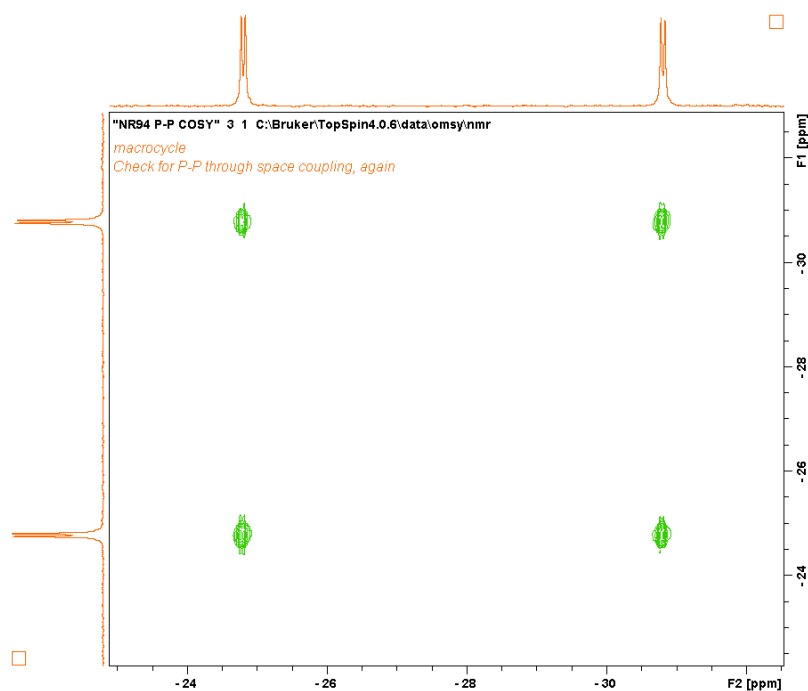


Figure 80 – A P-P COSY spectrum of **58c**.

The next macrocycle was made by cyclisation with 2,2'-iminobisbenzaldehyde **61** (**Figure 77**) which gave one major product **58d** in quantitative yield. The ^1H NMR spectrum showed two singlets for the imine hydrogens at 8.31 and 9.10 ppm and the $^{31}\text{P}\{^1\text{H}\}$ NMR spectrum showed a singlet at -15.4 ppm.

The cyclisation with dialdehyde **45** was repeated with the corresponding diamines **36c** and **36d** to give macrocycles **58e** and **58f** in quantitative yields (**Figure 81**).

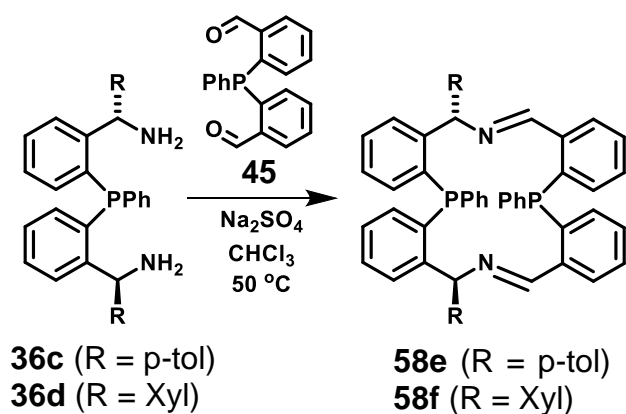


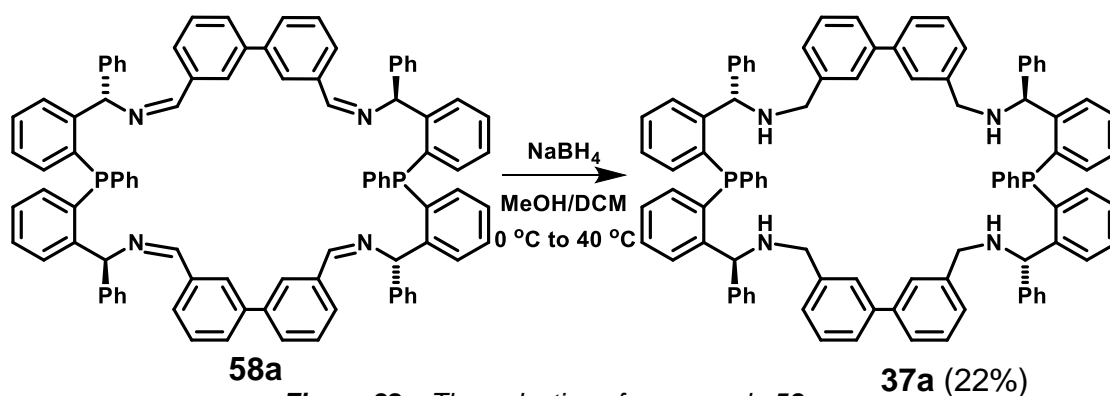
Figure 81 – Cyclisation with dialdehyde **45** with diamines **36c** and **36d**.

2.2.6. Reduction of imine macrocycles

The imine macrocycles were then reduced to the amine macrocycles using sodium borohydride.

The reduction of imine macrocycle **58a** using sodium borohydride in methanol failed, which may have been due to the insolubility of **58a** in methanol. The synthesis of the macrocycle **58a** was repeated by MChem student Liam Williams, under my supervision. It was found that reduction of the crude product **58a** worked by using a mixture of methanol and DCM. After purification by column chromatography, the amine macrocycle **37a** was obtained as a 4:1 mixture of products in 22% yield (**Figure 82**). The $^{31}\text{P}\{^1\text{H}\}$ NMR spectrum showed two singlets at -26.6 and -27.3 ppm in a ratio 4:1. The NMR spectra for the two products were very similar, so it was speculated that it was stereoisomerism at phosphorus (with the phenyl rings on the phosphorus atoms either both pointing the same way, or opposite ways). Attempts to crystallise this product failed. A pure product could possibly be obtained by purifying the imine macrocycle before reduction.

The ^1H NMR spectrum of **37a** showed four doublets for the CH_2 groups at 3.05, 3.40, 3.48 and 3.57 ppm in contrast to the imine hydrogen peak for **58a** at 8.28 ppm.



The imine macrocycle **58c** was also insoluble in methanol, so a mixture of methanol/DCM was used for the reduction using sodium borohydride to give the amine macrocycle **37b**. At first, the method involved dissolving the macrocycle in methanol/DCM and then adding sodium borohydride to this. However, this method gave a significant amount of phosphine oxide product. The method was improved by putting the sodium borohydride in the flask first,

flushing with nitrogen, then adding a solution of imine macrocycle in DCM, followed by the slow addition of methanol. This gave the product **37b** in good yield (**Figure 83**).

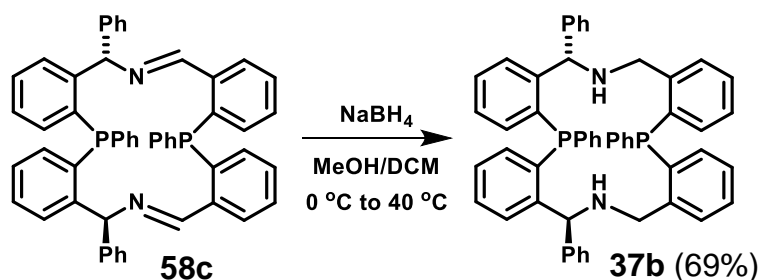


Figure 83 – Reduction of imine macrocycle **58c**.

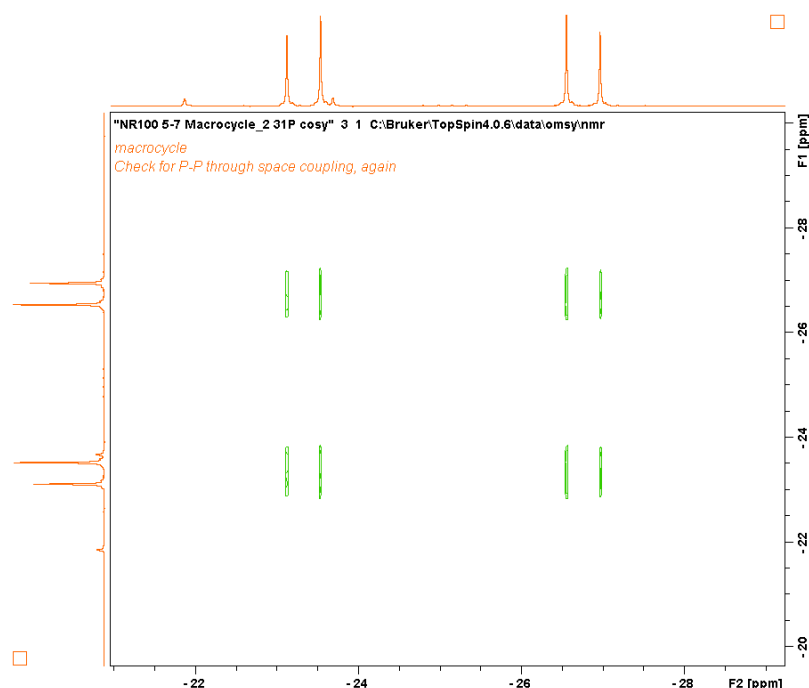


Figure 84 – A P-P COSY spectrum of **37b**.

The ^1H NMR spectrum showed two doublets and two doublets of doublets for the CH_2 groups. The $^{31}\text{P}\{^1\text{H}\}$ NMR spectrum of **37b** (**Figure 84**) had a much larger P-P coupling than **58c** of 66.5 Hz, which indicates that the lone pairs on the phosphorus atoms overlap more and therefore couple more strongly.

A crystal structure of the protonated macrocycle **62** was obtained which is shown in **Figure 85** (see **Figure 101** for formation of **62**). This confirms the size of the macrocycle (1+1 not 2+2), the chirality (S,S) as predicted by transition state **56** and the P-P distance (4.17 Å) which is in the range previously observed for through-space P-P coupling.⁹¹

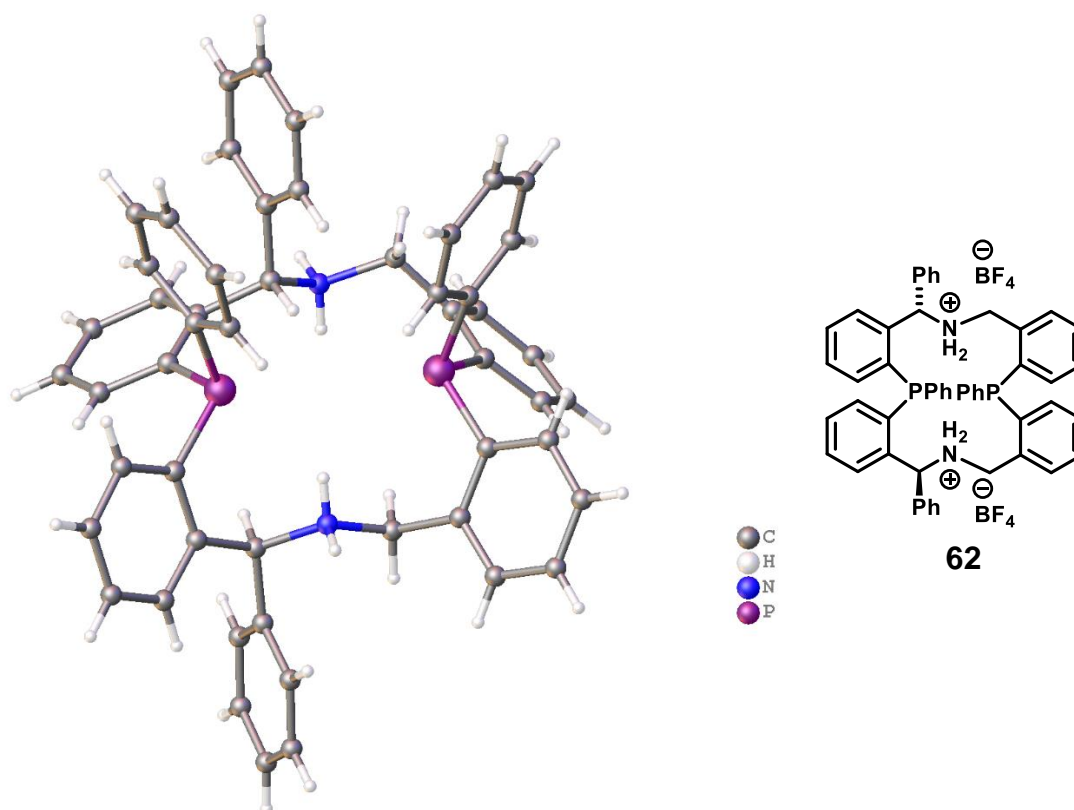


Figure 85 – Crystal structure of the protonated macrocycle **62**. BF₄ counter ions and solvent (chloroform) are omitted for clarity.

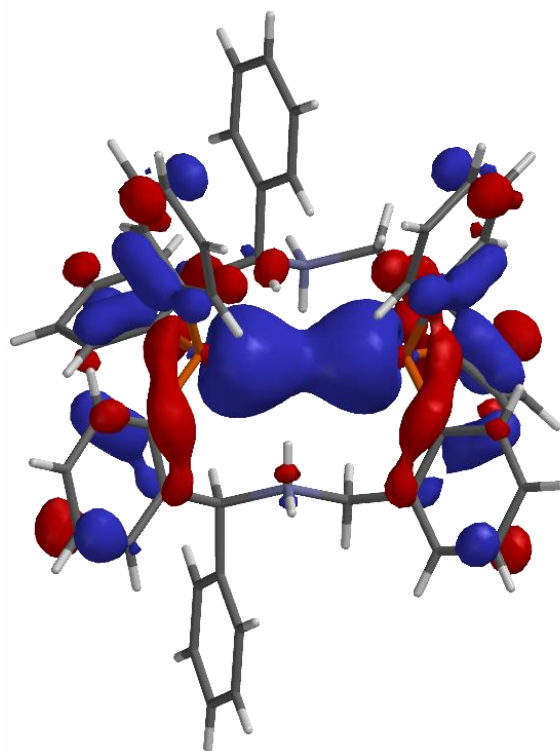


Figure 86 – The HOMO{-2} molecular orbital of **62**, showing overlap between the two phosphorus atoms. Calculated using Density Functional ω B97x-D 6-31* in Spartan (Spartan 16 Wavefunction Inc. Irvine CA).

The molecular orbitals of crystal structure **62** were calculated using Spartan. The HOMO{-2} molecular orbital shows overlap between the two phosphorus atoms (**Figure 86**), which adds further support for the idea that the phosphorus lone pairs must overlap.

The imine macrocycles **58e** and **58f** were also reduced using sodium borohydride in methanol/DCM to give the corresponding amine macrocycles **37c** and **37d**. The ^1H NMR spectra show peaks for the CH_2 groups at 3.40, 3.48, 4.12 and 4.46 ppm for **37c** and 3.44, 3.53, 4.10 and 4.44 for **37d**. The $^{31}\text{P}\{^1\text{H}\}$ NMR spectra show doublets at -26.7 and -23.3 ppm for **37c** and -26.6 and -23.3 ppm for **37d**.

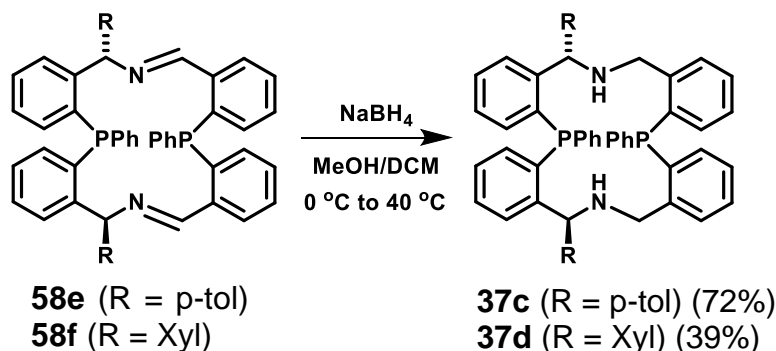


Figure 87 – Reduction of the imine macrocycles **58e** and **58f**.

The crude imine macrocycle **58d** was also reduced using sodium borohydride in methanol/DCM to give, after purification by column chromatography, **37e** in 51% yield (**Figure 88**). The ^1H NMR spectrum showed a doublet with integration of 2, and two doublets with integration of 1 for the CH_2 groups. The $^{31}\text{P}\{^1\text{H}\}$ NMR spectrum showed a singlet at -18.1 ppm.

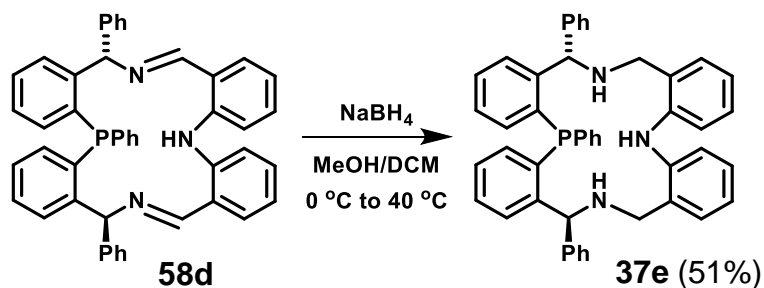


Figure 88 – Reduction of imine macrocycle **58d**.

2.4. Other macrocycles

Method 2, via a sulfinamide, can be adapted to synthesise a variety of different macrocycles (**Figure 89**) by starting with a different dialdehyde. These macrocycles show varying size, denticity and donor groups. An analogue of the 22-membered macrocycle **23** from literature is also synthesised (macrocycle **65**).¹

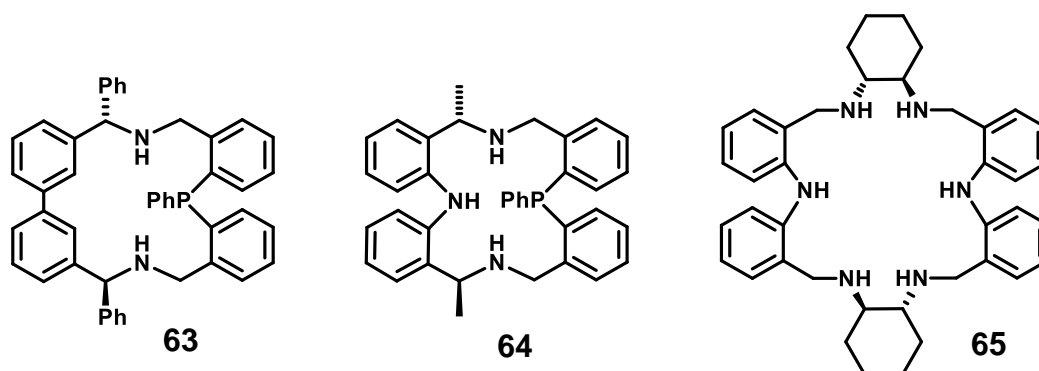


Figure 89 – Other macrocycles.

2.4.1. Synthesis of macrocycle 63

The macrocycle **63** was synthesised by MChem student Zac Ellis, under my supervision. The synthesis (**Figure 90**) follows the same route as in **Figure 59** (p 39) but starts with a different dialdehyde.

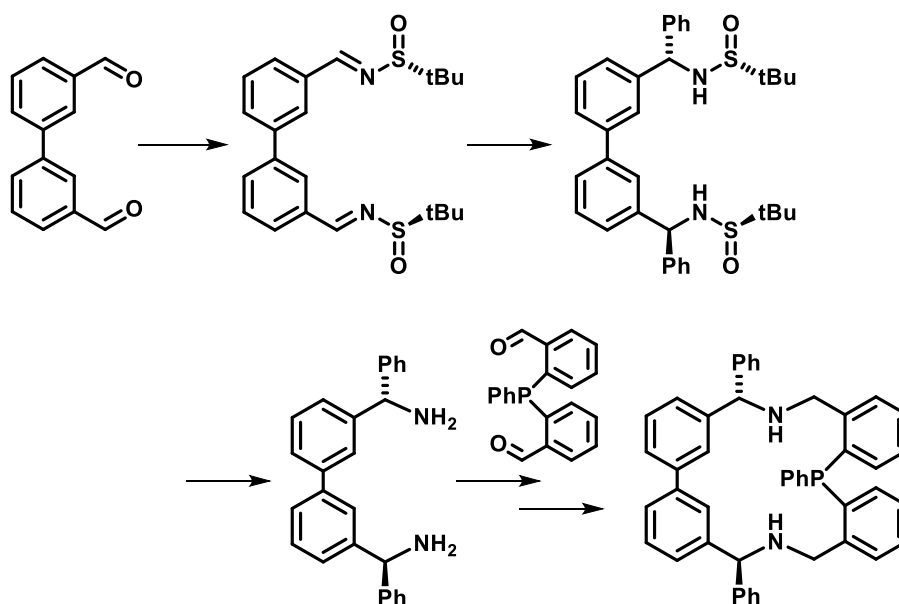


Figure 90 – An outline of the synthesis of macrocycle **63**.

The required dialdehyde **59** was made via a Suzuki coupling between 3-bromobenzaldehyde **66** and 3-formylphenylboronic acid **67**, giving the product **59** in excellent yield (**Figure 91**).⁹² The ¹H NMR spectrum showed a singlet at 10.12 ppm with an integration of 2 for the hydrogens on the aldehydes.

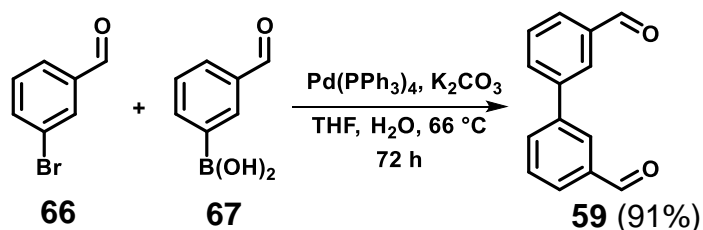


Figure 91 - Suzuki coupling to make dialdehyde **59**.⁹²

Next, chiral sulfinamide **55** was added to produce chiral diimine **68** in good yield (**Figure 92**), following the same procedure as in **Figure 69** above. The ¹H NMR spectrum showed a singlet for the imine hydrogens at 8.67 ppm, and a singlet at 1.28 ppm with an integration of 18 for the hydrogens on the tertiary butyl groups. This was followed by diastereoselective Grignard addition to produce **69**. The problem with this step was the separation of diastereoisomers. After purifying by column chromatography, TLC analysis showed only one product, but the ¹H NMR spectrum showed an 8:1 mixture of diastereoisomers. When the same TLC plate was run a second time, this separated out into two spots. Many different eluents were tried in order to separate the products in one TLC run, but none succeeded. Therefore, a longer column was run which improved the diastereomeric ratio to 15:1. The yield is low because only a few fractions were pure and the mixed fractions were discarded. The ¹H NMR spectrum of **69** showed a doublet at 5.70 ppm for the hydrogens on the chiral centres.

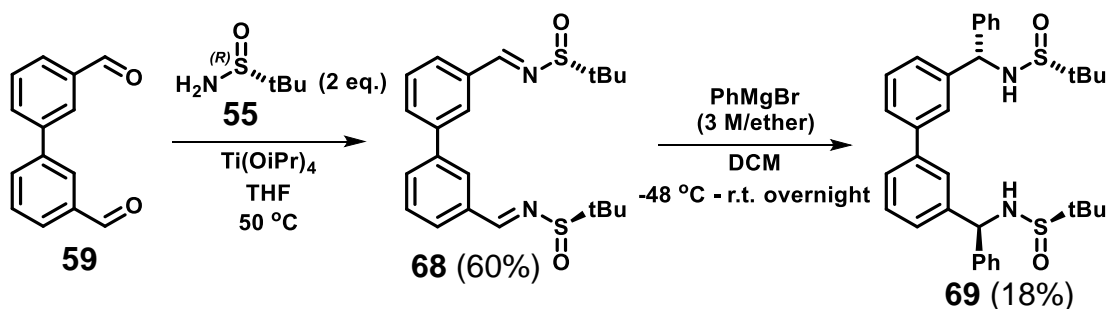


Figure 92 – The synthesis of the chiral diimine **68**, followed by Grignard addition.

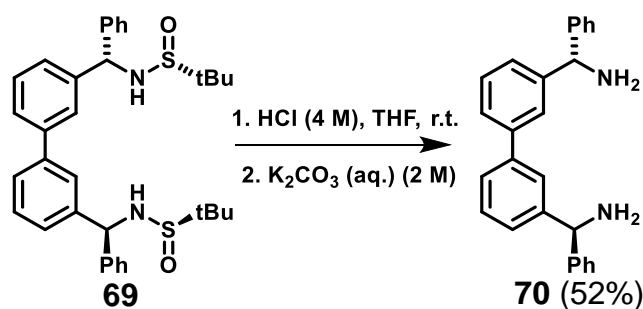


Figure 93 – Removal of the sulfoxide groups by acid hydrolysis.

After this, the sulfoxide groups were removed by acid catalysed hydrolysis as above, using 4 M hydrochloric acid, to give the diamine **70** in 52% yield (**Figure 93**). The workup was slightly different from before because the HCl salt precipitated out of the reaction, which could then be filtered off and potassium carbonate was added to give the free diamine **70** with no further purification needed. The ^1H NMR spectrum showed a singlet at 5.27 ppm with an integration of 2 for the hydrogens on the chiral centres.

Cyclisation with dialdehyde **45** was carried out at high dilution in chloroform with sodium sulfate at 50 °C, giving one major product **71** in quantitative yield. This crude product was reduced with sodium borohydride in MeOH/DCM to give the final macrocycle **63** in good yield (**Figure 94**). The ^1H NMR spectrum of **71** showed peaks for the imine hydrogens at 8.85 and 9.14 ppm and the ^1H NMR spectrum of **63** showed peaks for the CH_2 groups at 3.75, 3.84, 4.15 and 4.27 ppm. The $^{31}\text{P}\{^1\text{H}\}$ NMR spectrum of **71** showed a singlet at -18.1 ppm and the $^{31}\text{P}\{^1\text{H}\}$ NMR spectrum of **63** showed a singlet at -23.1 ppm.

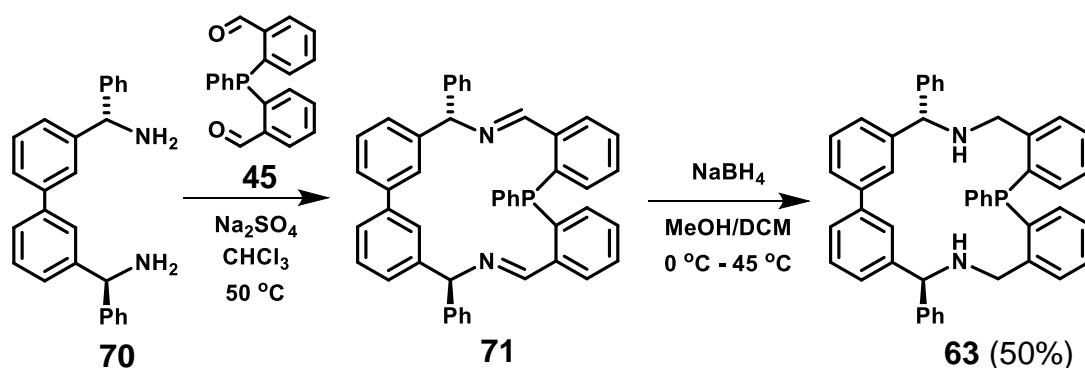


Figure 94 – Cyclisation followed by reduction.

2.4.2. Synthesis of macrocycle **64**

The synthesis of macrocycle **64** (**Figure 89**) also follows the same route as in **Figure 59** (p 39) but starts with dialdehyde **61** (**Figure 95**). A sample of dialdehyde **61** was available in the lab, which is accessible via Ullmann coupling of **72** and **73** to give the diester **74**, followed by reduction to the dialcohol **75** by lithium aluminium hydride and then oxidation to the dialdehyde **61** by MnO_2 .⁹³

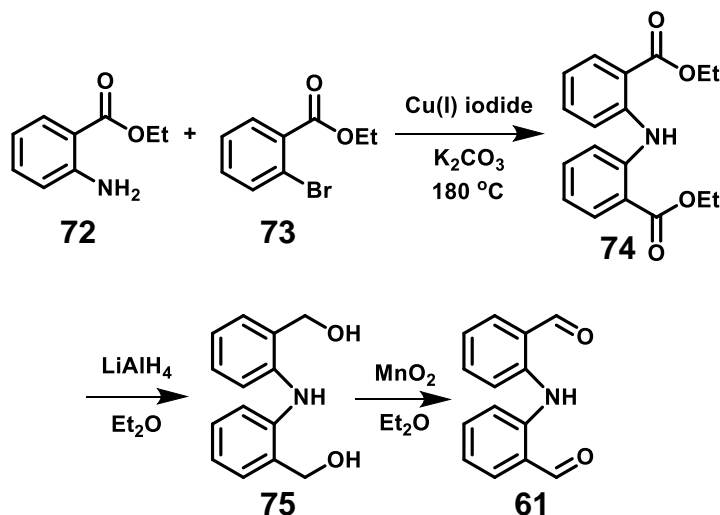


Figure 95 – The synthesis of dialdehyde **61**.⁹³

The addition of sulfinamide **55** to dialdehyde **61**, catalysed by titanium isopropoxide, gave the product **76** in good yield (**Figure 96**). The ^1H NMR spectrum showed a singlet at 8.67 ppm with an integration of 2 for the imine hydrogens. This then underwent diastereoselective Grignard addition with methylmagnesium bromide and the diastereoisomers were separated by column chromatography to give **77** in 69% yield (**Figure 96**). The ^1H NMR spectrum showed a doublet at 1.60 ppm with an integration of 6 for the two CH_3 groups on the chiral centres, plus a doublet of quartets at 4.82 ppm for the two hydrogens on the chiral centres.

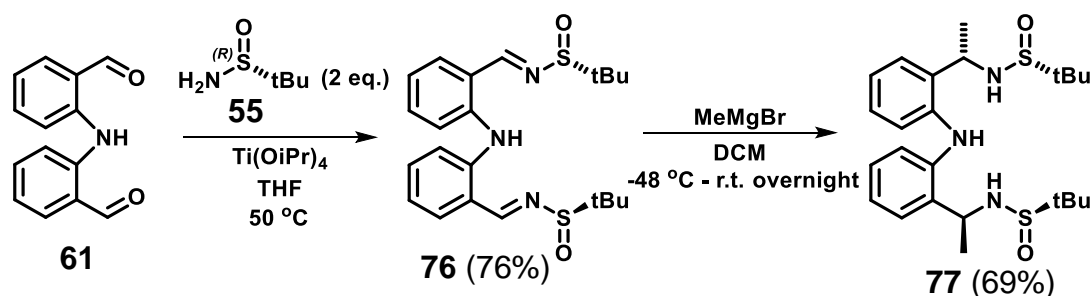


Figure 96 – Formation of chiral diimine followed by diastereoselective Grignard addition.

Removal of the sulfoxide groups by acid catalysed hydrolysis was first performed using aqueous hydrochloric acid, followed by addition of sodium hydroxide and extraction with ethyl acetate. However, this crude product was very difficult to purify. Performing the reaction with hydrochloric acid in dioxane resulted in precipitation of the HCl salt which was filtered off, treated with aqueous potassium carbonate and extracted with ethyl acetate to give the pure product **78** in 62% yield (**Figure 97**). The ^1H NMR spectrum showed a doublet at 1.47 ppm with an integration of 6 for the two CH_3 groups, coupling to a quartet at 4.33 ppm with an integration of 2 for the two hydrogens on the chiral centres. A broad singlet was present at 8.88 ppm for the NH group in between the aromatic rings.

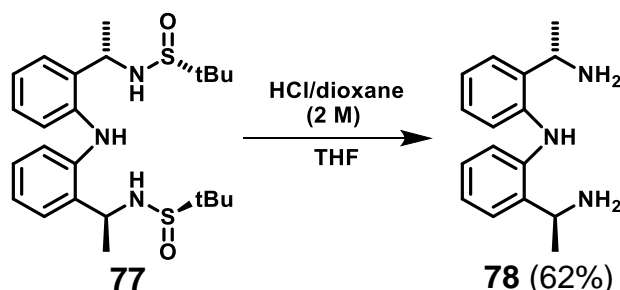


Figure 97 – Removal of the sulfoxide groups by acid catalysed hydrolysis.

Cyclisation with dialdehyde **45** at high dilution in chloroform gave the imine macrocycle **79** with a singlet in the $^{31}\text{P}\{^1\text{H}\}$ NMR spectrum at -24.3 ppm. Reduction with sodium borohydride in methanol/DCM then gave the final macrocycle **64** in 42% yield (**Figure 98**). The ^1H NMR spectrum showed two doublets for the CH_3 groups at 1.09 and 1.49 ppm, four peaks for the CH_2 groups and two quartets at 3.99 and 4.07 ppm for the hydrogens on the chiral centres. The $^{31}\text{P}\{^1\text{H}\}$ NMR spectrum showed a singlet at -24.3 ppm.

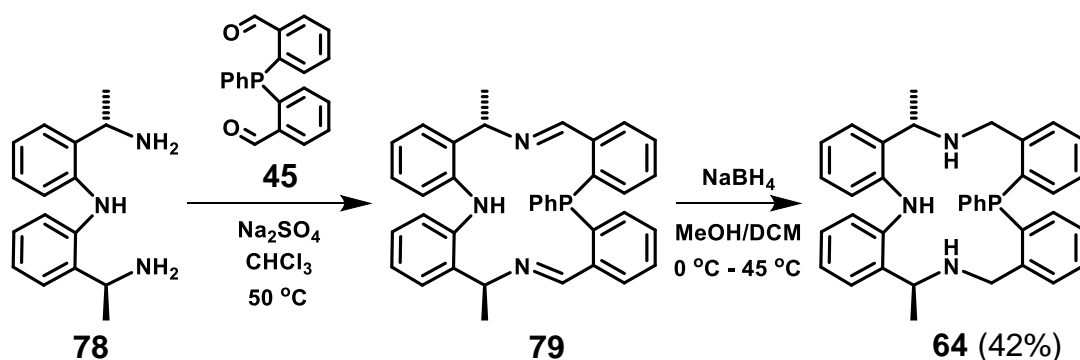


Figure 98 – Cyclisation followed by reduction to give the final macrocycle **64**.

2.4.3. Synthesis of macrocycle **65**

The availability of dialdehyde **61** also gave access to the final macrocycle **65**, which is an analogue of the 22-membered macrocycle **23** from literature. Cyclisation of dialdehyde **61** with 1,2-diaminocyclohexane gave crude product **80**. Attempts to purify this product by crystallisation failed, but mass spectrometry confirmed the existence of the desired product. Reduction of this crude product gave the 22-membered macrocycle **65** (**Figure 99**). The ^1H NMR spectrum showed two doublets at 3.51 and 3.74 ppm for the CH_2 groups adjacent to the aromatic rings.

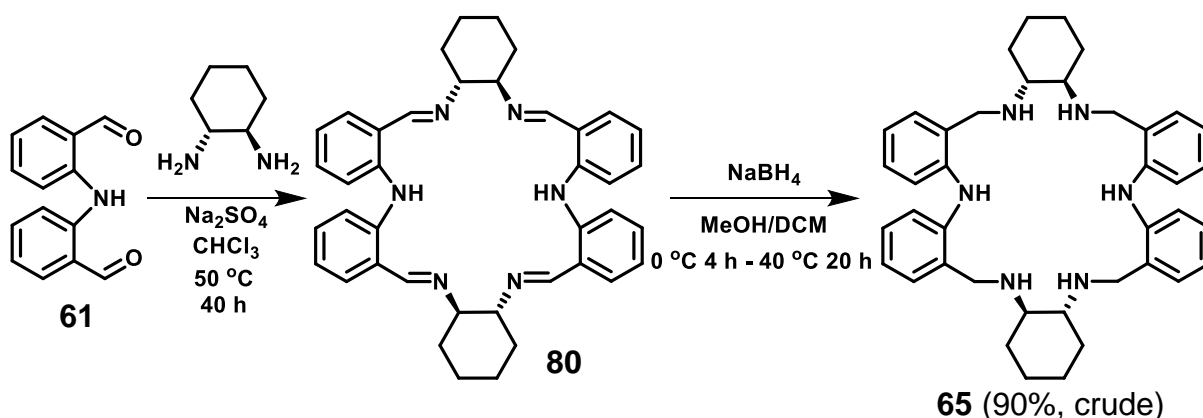


Figure 99 – Cyclisation followed by reduction.

2.5. Attempted formation of metal complexes

The synthesis of complexes was carried out in order to try and obtain a better understanding of the complexes which may form in the catalytic cycle. Complex formation with macrocyclic ligand **37b** was attempted using iron bromide in THF at room temperature overnight (**Figure 100**).⁹⁴ The dark red

solid formed gave a very broad NMR spectrum, and so was likely paramagnetic. However, the mass spectrum showed only the mass of the ligand.

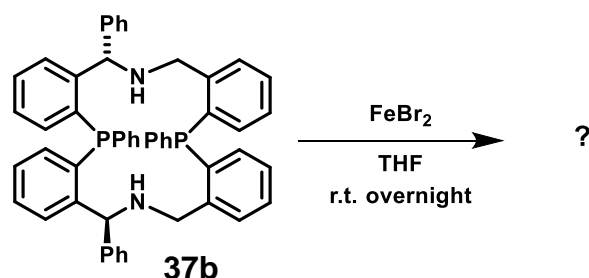


Figure 100 – An attempt at forming a complex.

A different method was used next with iron(II) tetrafluoroborate hexahydrate as the iron source in acetonitrile/DCM at 50 °C.⁵² However, this protonated the macrocycle instead of forming an iron complex (**Figure 101**). The $^{31}\text{P}\{^1\text{H}\}$ NMR showed two doublets at -28.7 and -26.4 ppm with a coupling constant of 105 Hz (See **Figure 85** for the crystal structure of **62**).

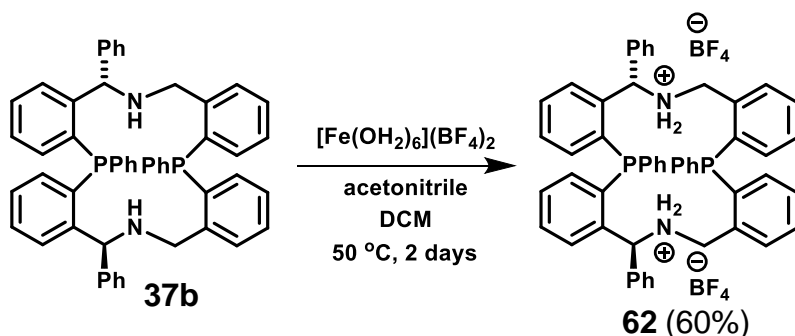


Figure 101 – Another attempt at complex formation.

2.6. Summary

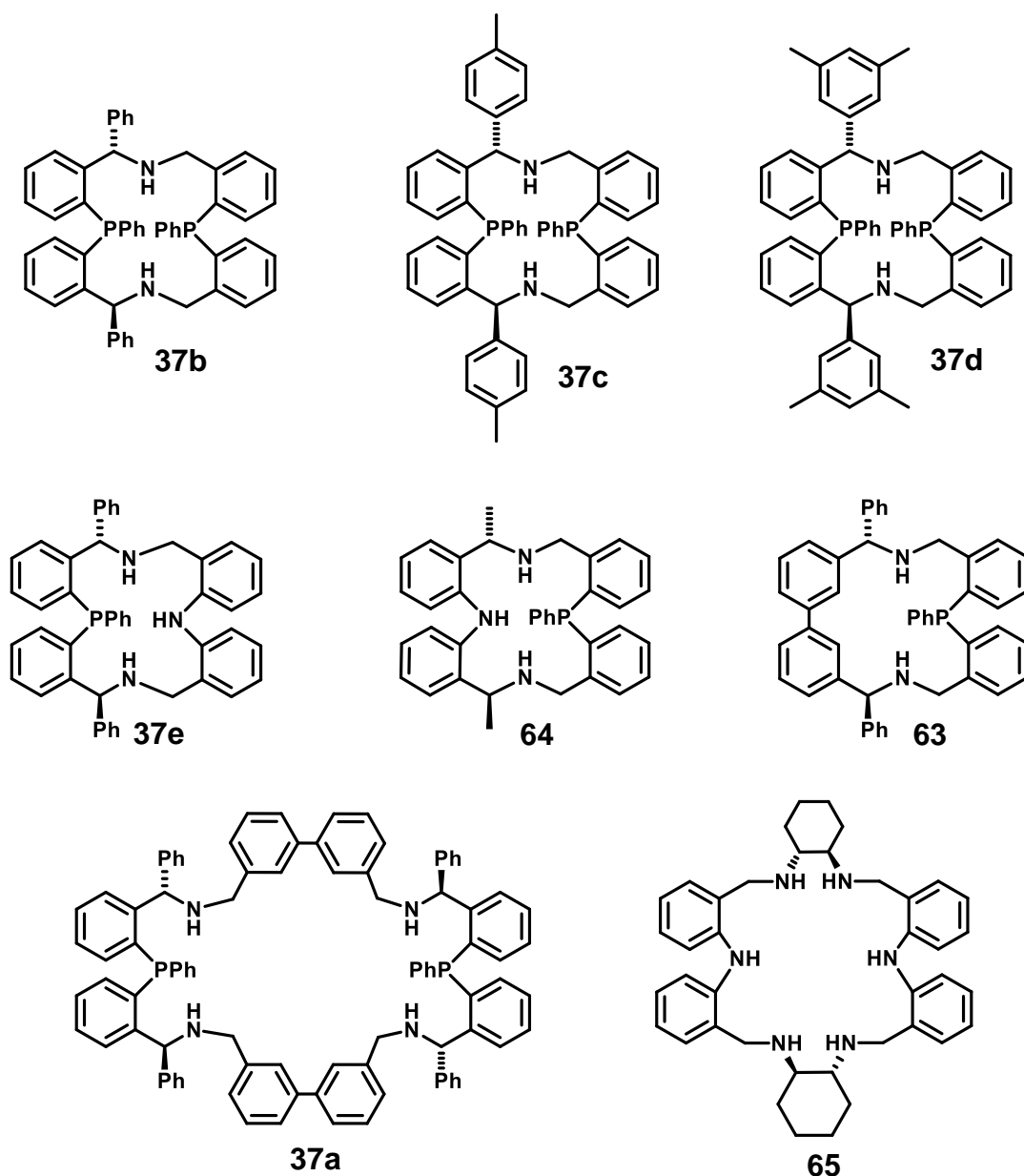


Figure 102 – A summary of the macrocyclic ligands synthesised.

In summary, the first synthetic route starting from the primary amine **35** was unsuccessful due to the difficulty in finding a suitable protecting group for the ortholithiation step. However, the second route via Grignard addition to a sulfinamide (section 2.3, p 38) worked well and eight different macrocyclic ligands have been synthesised (**Figure 102**), plus their imine analogues. A selection of ring sizes has been made, from 16 to 34 membered rings. The denticity has been varied from three to six, and the combination of donor groups (P_2N_2 , P_2N_3 , PN_2 , P_2N_4 , N_6) has also been varied. Also, a range of chiral groups has been used (Me, Ph, p-tol and 3,2-dimethylphenyl, Cy).

Chapter 3. Synthesis of Acyclic Ligands

The acyclic ligands studied in this project are multidentate, containing phosphorus and nitrogen donor atoms, because these have been shown to have some success with iron catalysed AH and ATH previously (see section 1.6, page 11).

Complexes with multidentate ligands have a greater stability compared to analogous complexes with monodentate ligands. This is because of the chelate effect, which is mainly due to the increase in entropy when a multidentate ligand displaces monodentate ligands.⁶³ Another factor to consider is that once one of the donor atoms in a multidentate ligand has coordinated, the other donor atoms are then held in close proximity to the metal and will therefore be more likely to coordinate. This factor also makes a multidentate ligand less likely to dissociate once coordinated. The size of the chelate ring formed is an important aspect to consider when choosing the linkage between donor atoms – 5 membered rings are the most favoured, but 6 membered rings are also common. A ring size of 8 or more is not expected to show a chelate effect.⁹⁵

A general route towards tetradentate PNNP ligands, such as those made by Morris's group (**Figure 103**), is shown in **Figure 104**.⁹⁶ Two equivalents of a phosphino-aldehyde react with a diamine to give the free PNNP ligand, followed by complexation with iron. Alternatively, a template synthesis can lead directly to the iron complexes.

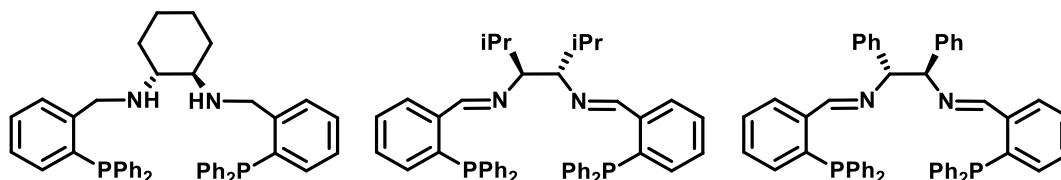


Figure 103 – Acyclic PNNP ligands synthesised previously.^{36, 42, 58}

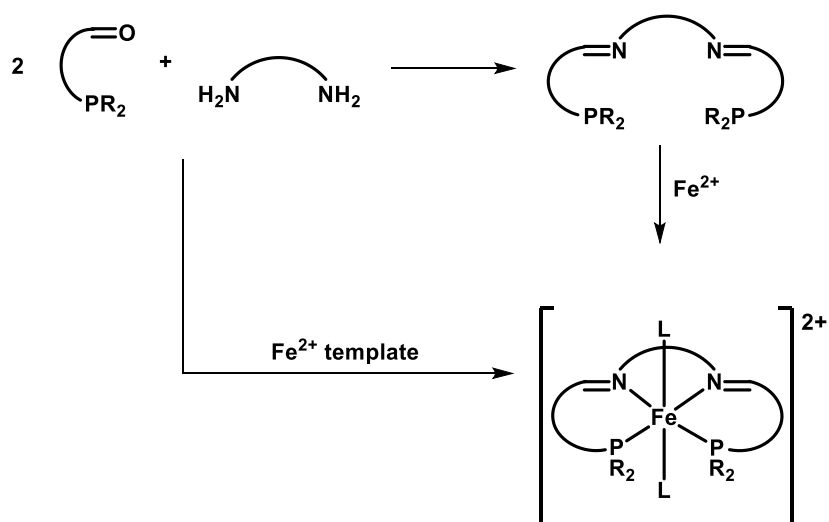


Figure 104 – General synthetic route towards acyclic PNNP ligands and iron complexes.⁹⁶

The PNNP ligands which have been made previously (**Figure 103**, see also section 1.6, page 11) have their chiral groups in between the two nitrogen atoms. However, the target PNNP ligands in this project (**82** and **86**, **Figure 105**) have the chiral group on the other side of the amine. This means a different approach is needed. The ligand synthons, and possible PN ligands, **81** and **85** need to be synthesised first and then these can be joined together via a dihalide or dialdehyde.

Not only do these ligands expand the toolbox of multidentate chiral ligands, they can also be used to compare with the macrocyclic ligands in Chapter 2, providing insight into a possible macrocyclic effect on catalytic activity and selectivity in iron catalysed AH and ATH reactions.

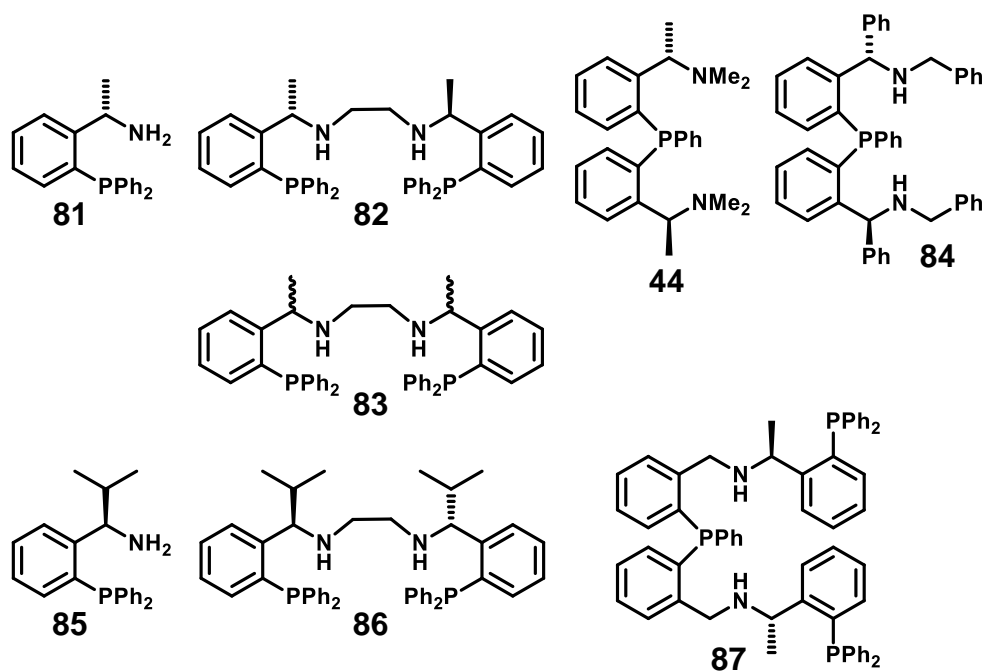


Figure 105 – Acyclic ligands synthesised.

The synthesis of NPN ligand **44** was already discussed in Chapter 2.2 on page 37 (**Figure 56**). The NPN ligand **84** is a modification of the chiral diamine **36b** which was discussed in the previous chapter (page 49). The diamine **36b** is reacted with benzaldehyde, followed by reduction. The pentadentate ligand **87** is made by reaction of PN ligand **81** with the dialdehyde **45** discussed in the previous chapter (page 39).

3.1. Synthesis of bidentate PN ligands

3.1.1. Synthesis of PN ligand 81

Ligand **81** is a known compound and was synthesised following a procedure from literature (**Figure 106**).¹²

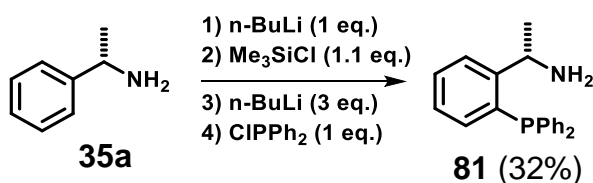


Figure 106 – Synthesis of (S)-1-[2-(diphenylphosphino)phenyl]ethylamine.¹²

One equivalent of n-BuLi was added to (S)-phenylethylamine **35a** to deprotonate the amine, and then trimethylsilyl chloride was used to add a TMS protecting group. Next, more n-BuLi (3 eq.) was added to deprotonate the

benzene ring. The nitrogen coordinates to the lithium to direct the deprotonation ortho to the substituent. Next, chlorodiphenylphosphine was added to put a PPh_2 substituent at that position. The reaction was finished by workup with aqueous 1 M HCl which removes the TMS protecting group and quenches any unreacted ClPPh_2 or $n\text{-BuLi}$. Extraction with ether and purification by column chromatography gave the product **81**, a white solid, in 32% yield (**Figure 106**).

The product was much more polar than expected, given the eluent system used for column chromatography in the paper (hexane/acetate, 8/1).¹² TLC analysis showed that the product was on the baseline using this eluent system. Ethyl acetate/hexane (60/40) plus 2% triethylamine worked much better. The triethylamine neutralises the acid sites on the silica gel which stops the product from sticking to the column. For TLC analysis using this type of eluent system, it is important to soak the TLC plate in the eluent with 2% triethylamine first, then let it dry, add the product and run the TLC. If the TLC plate was not soaked beforehand, the 2% triethylamine had little effect on the R_f values.

3.1.2. Synthesis of PN ligand **85**

The first method for the synthesis of the second PN ligand **85** started from aldehyde **88**, which was reacted with chiral sulfinamide **55** in THF at 50 °C using titanium isopropoxide as Lewis acid and water scavenger (**Figure 107**).⁸⁸ After purification by column chromatography, the chiral imine **89** was obtained in 68% yield, showing a doublet at 9.12 ppm in its ^1H NMR spectrum for the imine hydrogen and a singlet in the $^{31}\text{P}\{^1\text{H}\}$ NMR spectrum at -12.3 ppm.

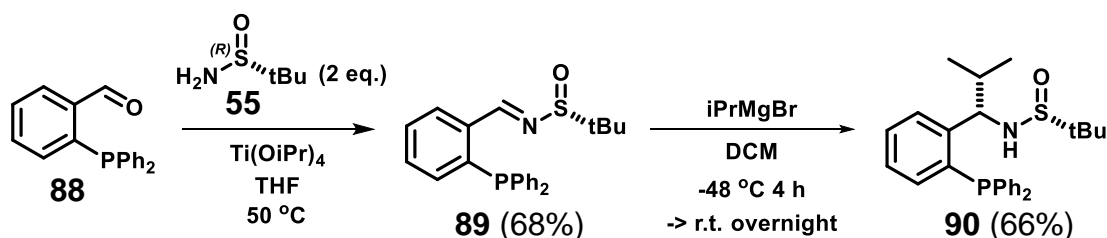


Figure 107 – Synthesis of chiral imine **89**, followed by diastereoselective Grignard addition.

This then underwent diastereoselective Grignard addition with isopropylmagnesium bromide (**Figure 107**).⁸⁹ After purification by column chromatography, the product was obtained in 66% yield. The ^1H NMR spectrum showed a peak at 1 ppm for the CH_3 groups, a doublet of doublets at 4.43 ppm for the CH on the isopropyl group, and a doublet of doublet of doublets at 4.64 ppm for the hydrogen on the chiral centre. The $^{31}\text{P}\{^1\text{H}\}$ NMR spectrum showed a singlet at -16.3 ppm. Unfortunately, the sulfoxide group from **90** could not be removed without the phosphorus getting oxidised.

Therefore, a second route towards PN ligand **85** was pursued in which the phosphorus atom was added at a later stage. This started from the addition of sulfinamide **55** to isobutyraldehyde **91**, following a procedure from literature (**Figure 108**).⁹⁷ This gave the product **92** in 72% yield, showing a doublet in its ^1H NMR spectrum at 7.99 ppm for the imine hydrogen. Diastereoselective addition of phenylmagnesium bromide, followed by separation of the diastereoisomers by column chromatography, gave the product **93** in 72% yield. The ^1H NMR spectrum showed a triplet at 4.16 ppm for the hydrogen on the chiral centre.

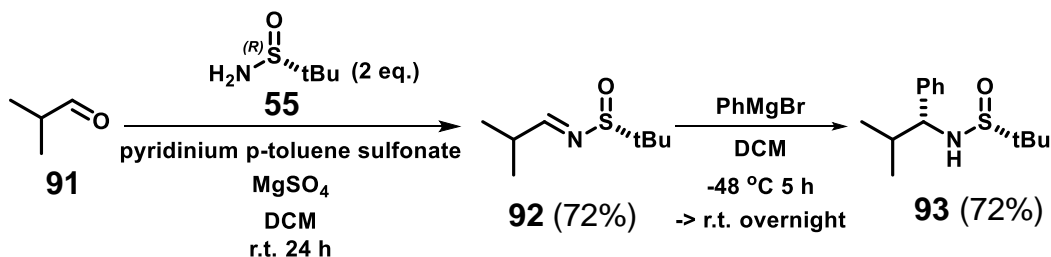


Figure 108 – Addition of chiral sulfinamide followed by diastereoselective Grignard addition.⁹⁷

Removal of the sulfoxide group by acid-catalysed hydrolysis gave the chiral amine **94** in excellent yield. Then ortholithiation with $n\text{-BuLi}$, followed by addition of chlorodiphenylphosphine gave **85** in 18% yield (**Figure 109**). The ^1H NMR spectrum showed two doublets for the CH_3 groups at 0.67 and 1.00 ppm, an octet at 1.96 ppm for the CH on the isopropyl group, and a triplet at 4.46 ppm for the hydrogen on the chiral centre. The $^{31}\text{P}\{^1\text{H}\}$ NMR spectrum showed a singlet at -16.7 ppm.

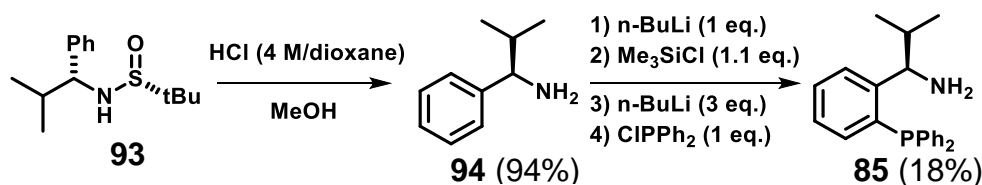


Figure 109 – Removal of the sulfoxide group followed by addition of chlorodiphenylphosphine.

3.2. Synthesis of tetradentate PNNP ligands

3.2.1. Synthesis of PNNP ligand **82**

The tetradentate PNNP ligand **82** could be prepared via several methods. The method initially attempted is shown in **Figure 110**, where two molecules of product **81** were joined together via a dihalide to produce **82**.

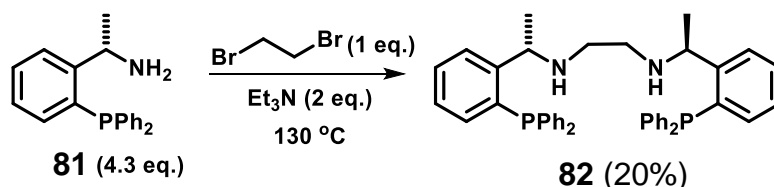


Figure 110 – The synthesis of PNNP ligand **82**.

First of all, a method used to join two molecules of norephedrine was followed,⁹⁸ in which a mixture of the amine **81** (1 eq.) and 1,2-dibromoethane (0.5 eq.) were heated together at 100 °C for 8 h. The mixture became very thick during this time and was unable to stir. Aqueous sodium hydroxide (0.5 M) was added and the product was extracted with chloroform. ³¹P{¹H} NMR analysis of the crude product showed there was only 22% product.

Next, since the mixture was too thick to stir, the reaction was carried out using DMF as solvent. Unfortunately, this gave no product. Next, the reaction was repeated using Na₂CO₃ in the reaction mixture with DMF as solvent, which gave about 15% product.

Another method was found in which an excess of the amine was used (4.3 equivalents).⁹⁹ Triethylamine was added to this followed by 1,2-dibromoethane at 110 °C under a nitrogen atmosphere. The mixture was stirred for 22 h at 110-130 °C. Workup by addition of a saturated KOH solution and extraction with DCM gave a mixture of starting material and product (40% product by NMR). Purification by column chromatography using 10%

MeOH/DCM gave the product **82**, a white solid, in 20% isolated yield (**Figure 110**). The ^1H NMR showed a doublet at 1.25 ppm with an integration of 6 for the two CH_3 groups, a broad singlet at 2.50 ppm with an integration of 4 for the CH_2 groups and a multiplet at 4.61 ppm with an integration of 2 for the hydrogens on the chiral centres. The $^{31}\text{P}\{^1\text{H}\}$ NMR showed a singlet at -17.2 ppm.

Due to the low yield, two other methods were tried. Firstly, **81** was dissolved in isopropanol, then an aqueous solution of glyoxal was added and the mixture was heated to 70 °C for 1 h (**Figure 111**).¹⁰⁰ This gave mainly recovered starting material **81**, plus oxide products.

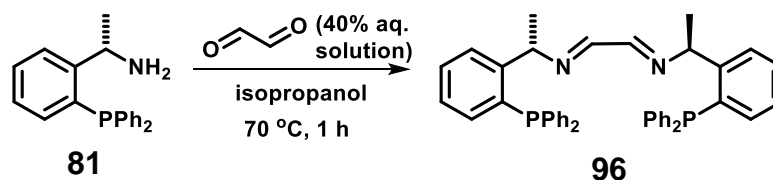


Figure 111 – Reaction of **81** with glyoxal.

The next method (**Figure 112**) used glyoxal trimer dihydrate **95** following a method used to make N,N'-bis-((S)-1-phenylethyl)ethane-1,2-diimine.¹⁰¹ On the first attempt, this appeared to work well, giving one major product in quantitative yield, with a peak at -16.5 ppm in the $^{31}\text{P}\{^1\text{H}\}$ NMR spectrum. The ^1H NMR spectrum showed a singlet at 7.56 ppm for the imine hydrogens, a multiplet at 5.32 ppm for the hydrogens on the chiral centres, and a doublet at 1.37 ppm for the hydrogens on methyl groups.

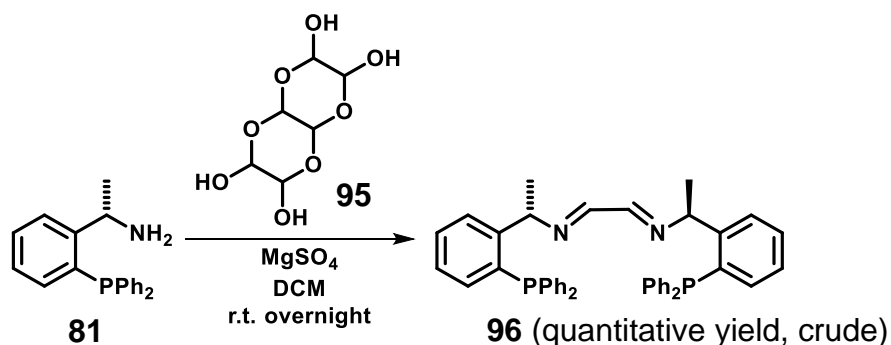


Figure 112 – Reaction of **81** with glyoxal trimer dihydrate **95**.

The reduction of this crude product was carried out using sodium borohydride in methanol/DCM (**Figure 113**). This resulted in a mixture of many products, including some left-over starting material. This crude product was re-dissolved

in DCM and was added to more sodium borohydride, followed by the addition of methanol. The reaction was continued for another day, but this still resulted in a mixture of many products. It was later discovered that the methanol bottle actually contained acetone, so this would explain why the reaction was unfinished because the sodium borohydride would have reacted with the acetone.

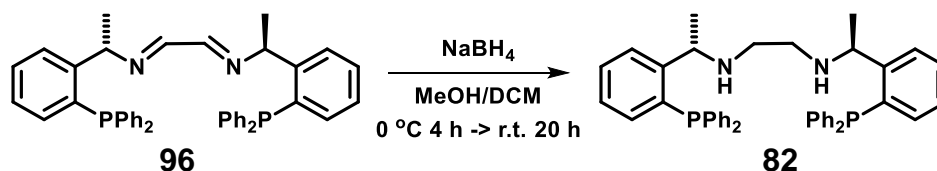


Figure 113 – Attempted reduction of the diimine **96**.

Unfortunately, the reaction in **Figure 112** could not be repeated, as any further attempts resulted in either a mixture of many products, or just remaining starting material **81**. Therefore, the dibromoethane method in **Figure 110** was chosen for further reactions. Even though the yield was low for this method, the reaction is clean and the starting material can be recovered and reused.

3.2.2. Synthesis of racemic PNNP ligand **83**

The racemic analogue of **82** was synthesised in order to be able to measure the ee of **82**. This followed exactly the same method, but starting from racemic phenylethylamine **97** (**Figure 114**). A mixture of diastereoisomers of **83** were formed which were difficult to separate, so only a very small amount of pure product could be obtained (3%).

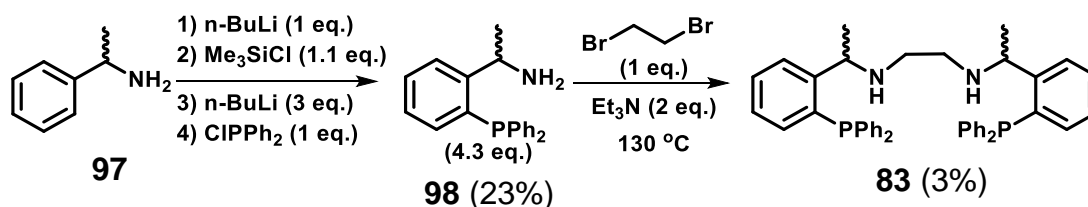


Figure 114 – Synthesis of the racemic analogue **83**.

Unfortunately, the enantiomers of **83** could not be separated by chiral HPLC; so, the ee of **82** was not determined.

3.2.3. Synthesis of PNNP ligand **86**

Next, two molecules of **85** were joined together in the same way, to produce tetradentate PNNP ligand **86** in 50% yield (**Figure 115**).

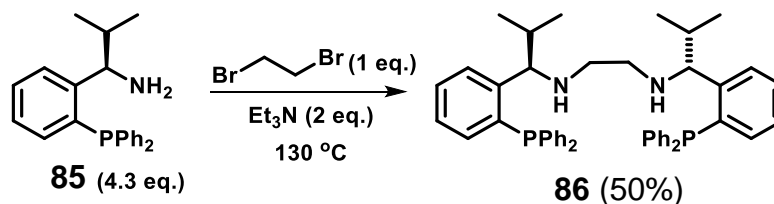


Figure 115 – The synthesis of PNNP ligand **86**.

The peaks in the NMR spectra for ligand **86** were very broad, but the resolution was improved with increased concentration, as can be seen from the comparison of the spectra in **Figure 116**. The peaks for the CH₂ groups (CH₂CH₂, 2.26 and 2.49 ppm) and the CH in the isopropyl group (CH(CH₃)₂, 2.08 ppm) are indistinguishable at low concentration as they are very broad and overlap. The peaks for the methyl groups (CH₃, 0.59 and 1.05 ppm) appear as broad singlets at low concentration but are doublets at higher concentration.

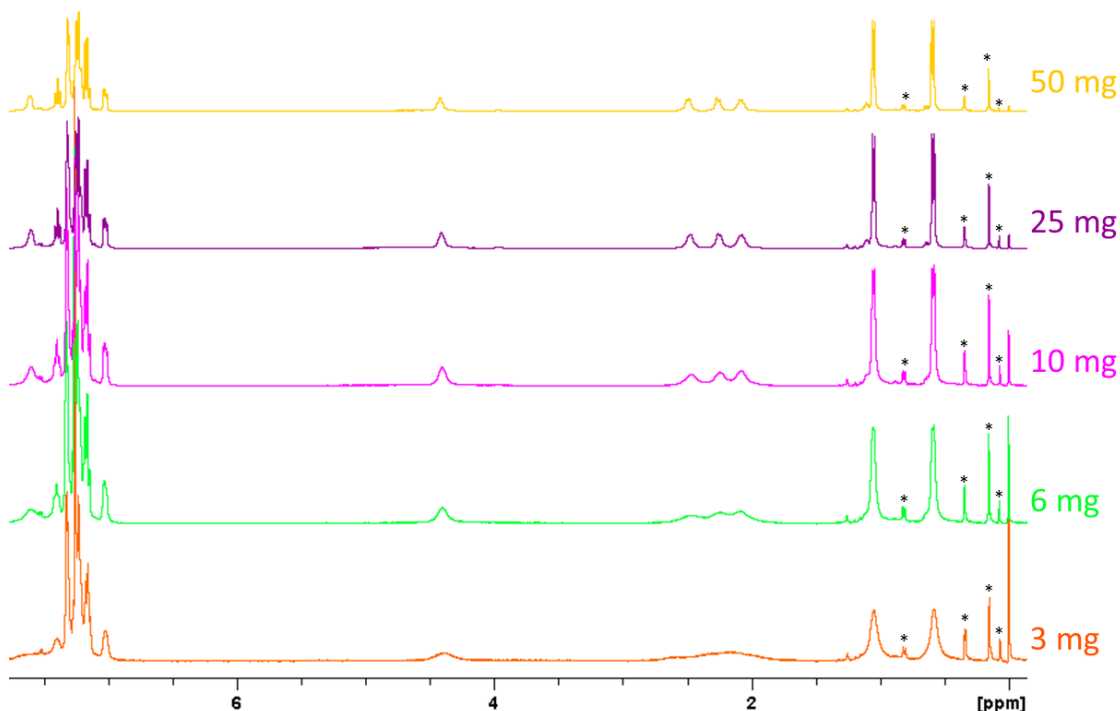


Figure 116 – ¹H NMR spectra of PNNP ligand **86** at different concentrations in CDCl₃. The amounts of ligand shown at the right-hand side are the amount per 0.6 ml of chloroform. Impurities are marked with a *.

This effect is also observed in the ^1H NMR spectrum of PNNP ligand **82**, but is not so noticeable. This is unusual because the resolution of an NMR spectrum normally decreases with increased concentration, due to intermolecular chemical exchange. Chemical exchange means that a nucleus moves between a set of magnetic environments,¹⁰² consequently varying the chemical shift slightly, producing a broad peak. Increased concentration would produce more intermolecular interactions, increasing the amount of chemical exchange, reducing the resolution.

3.3. Synthesis of tridentate NPN ligands

The synthesis of the tridentate NPN ligand **44** was already discussed in Chapter 2.2 on page 37 (**Figure 56**). To expand the scope of the NPN ligands, compound **84** was targeted.

The NPN ligand **84** was synthesised from the chiral diamine **36b** (see **Figure 75**) by reaction with benzaldehyde to give diimine **99**, followed by reduction with sodium borohydride to give NPN ligand **84** in 42% yield (**Figure 117**). The ^1H NMR spectrum showed two doublets with integrations of 1 and a singlet with an integration of 2 for the two CH_2 groups, and two doublets (coupling to P) for the two hydrogens on the chiral centres. The $^{31}\text{P}\{^1\text{H}\}$ NMR showed a singlet at -26.0 ppm.

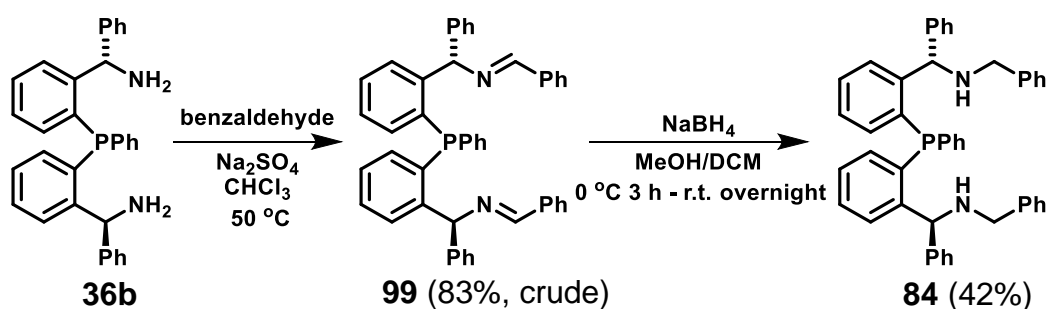


Figure 117 – Synthesis of NPN ligand **84**.

3.4. Synthesis of pentadentate ligand **87**

In addition to the tetradentate and tridentate ligands described, a pentadentate ligand **87** was synthesised by reaction of dialdehyde **45** with PN ligand **81**, followed by reduction with sodium borohydride in methanol/DCM to give **87** in

excellent yield (**Figure 118**). The ^1H NMR spectrum showed two doublets at 0.87 and 0.89 ppm for the CH_3 groups, and a multiplet at 4.53 ppm for the two hydrogens on the chiral centres. The $^{31}\text{P}\{^1\text{H}\}$ NMR showed three peaks with equal integrations at -25.8, -17.9 and -17.6 ppm.

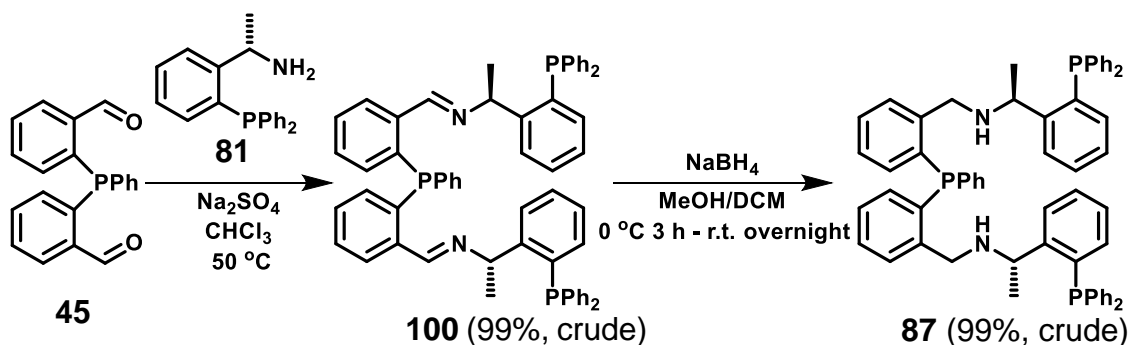


Figure 118 – Synthesis of pentadentate ligand **87**.

3.5. Complex formation

Complex formation with the PNNP ligands **82** ($\text{R} = \text{Me}$) and **86** ($\text{R} = \text{iPr}$) was carried out using $[\text{Rh}(\text{COD})\text{Cl}]_2$ in deuterated DCM in an NMR tube under nitrogen (**Figure 119**). The synthesis of rhodium complexes was carried out with the aim of gaining a better understanding of what kind of complexes may form in the catalytic cycle.

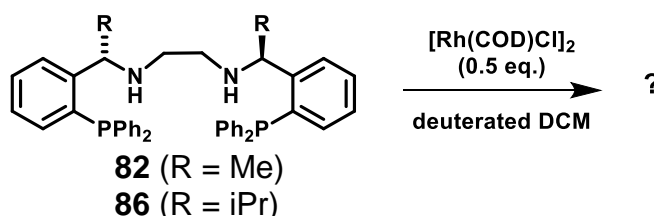


Figure 119 – Complex formation using $[\text{Rh}(\text{COD})\text{Cl}]_2$.

Rhodium was used because it is NMR active. The presence of Rh-P coupling in the NMR spectra confirms coordination of the ligand, and the position of the other donor groups in the complex strongly influences the size of the coupling. The ligand *trans* to phosphorus affects the coupling constants much more than the ligands *cis* to phosphorus.^{103, 104} The *trans* influence is the extent to which a ligand weakens the bond *trans* to itself, decreasing the metal-ligand coupling constant.⁶³ The *trans* influence depends on the electronic properties (e.g. σ -donor or π -acceptor) of the ligand, metal oxidation state, coordination number and geometry.¹⁰⁵

There are 4 possible ligands which could be *trans* to phosphorus in this reaction: chloride, amine, phosphine or alkene. **Table 3** summarises the different values of $J_{\text{Rh-P}}$ for different *trans* ligands and geometries.

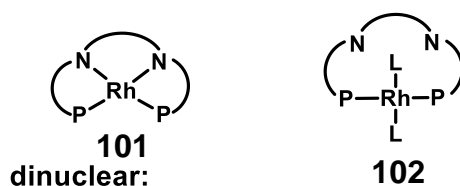
Table 3 – Values found in literature of $J_{\text{Rh-P}}$ for different geometries and *trans* ligands.

Ligand <i>trans</i> to P	range of values for $J_{\text{Rh-P}}$ (Hz)			
	Square planar ¹⁰⁶⁻¹⁰⁸	Trigonal bipyramidal ¹⁰⁹⁻¹¹³	square based pyramid ^{111, 114}	Octahedral (Rh(III)) ^{103, 113}
chloride	186-200	108-120	134-156	111-113
amine	172-173			96-107
phosphine	130-142	94-108	84-108	69-84
alkene	119-147			

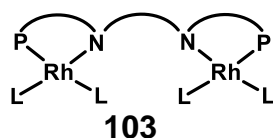
The vast majority of rhodium(I) complexes are 4-coordinate square planar, but 5-coordinate trigonal bipyramidal or square based pyramid geometries are also a possibility.^{111, 115} In trigonal bipyramidal complexes, a further consideration is that the rhodium to equatorial phosphine coupling is typically 20-30% larger than the coupling to the axial phosphorus.^{109, 111}

There is a small number of reports in the literature of similar PNNP ligands reacting with $[\text{Rh}(\text{COD})\text{Cl}]_2$, forming square planar complexes **101** (**Figure 120**).^{107, 108, 116, 117} In contrast to the $^{31}\text{P}\{^1\text{H}\}$ NMR spectra reported here, Gao et al.^{116, 117} report singlets in the $^{31}\text{P}\{^1\text{H}\}$ NMR spectra, which is an unexpected observation given resolvable Rh-P couplings are expected. Thus, both Cooper et al.¹⁰⁷ and Marxen et al.¹⁰⁸ report a doublet in the $^{31}\text{P}\{^1\text{H}\}$ NMR of complex **101** with a coupling constant of 172 - 173 Hz. Other acyclic PNNP ligands have been shown to give *trans*-spanning rhodium complexes **102**,^{107, 118} which have rhodium-phosphorus coupling constants of 130 - 135 Hz.¹¹⁸ Dinuclear rhodium PNNP complexes **103** have also been reported.¹¹⁹ Trigonal bipyramidal rhodium(I) complexes with tripodal tetradentate ligands have been reported.¹²⁰ No papers with trigonal bipyramidal rhodium(I) complexes with linear tetradentate ligands have been found, although there is an example with zinc.¹²¹

square planar:



dinuclear:



trigonal bipyramidal:

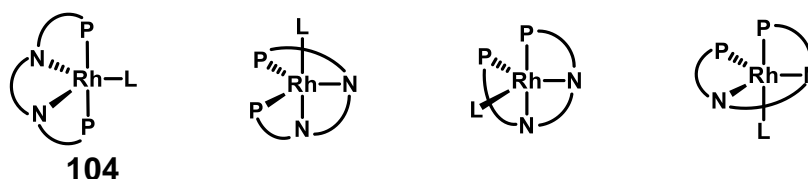


Figure 120 – Possible structures of the rhodium PNP complexes.
L = unspecified ligand.

The reaction proved to be more complicated than anticipated because a mixture of products is formed for each ligand, as can be seen from the $^{31}\text{P}\{^1\text{H}\}$ NMR spectra shown in **Figure 121** and **Figure 127**. Intermediate complexes are seen after 1 h for both ligands, however, free ligand is no longer seen after 4 days using ligand **82** (**Figure 121**, top) but is still seen after 8 days with ligand **86** (**Figure 127**, top). This might indicate either that the later steps in the substitution reaction sequence are considerably slower with the bulkier ligand **86**, or that the reaction is an equilibrium and the position of equilibrium is influenced by the steric bulk of the ligand.

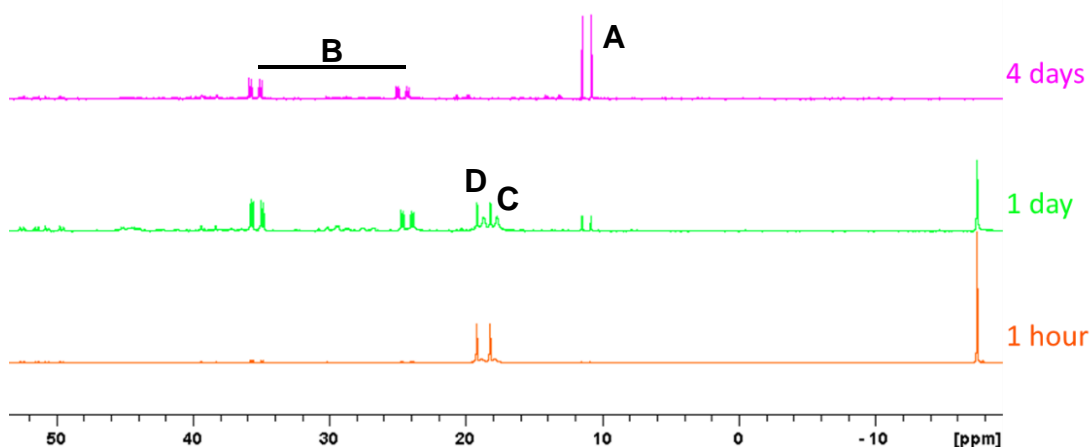


Figure 121 – The $^{31}\text{P}\{^1\text{H}\}$ NMR spectra of complex formation with PNP ligand **82**.

The $^{31}\text{P}\{^1\text{H}\}$ NMR spectrum at 4 days reaction time with ligand **82** in **Figure 121** is dominated by the resonances of two complexes; a doublet at 11.1 ppm with a coupling constant of 106 Hz corresponding to Rh-P coupling, complex **A**, and a pair of doublets of doublets of doublets at 24.6 and 35.4 ppm, complex **B**.

Complex **A** with doublet at 11.1 ppm and a coupling constant of 106 Hz must come from a complex where the phosphorus atoms are equivalent and are coordinated to Rh. Mass balance indicates it is unlikely that this is a dinuclear complex **103** because there is no free ligand left. The Rh-P coupling constant (106 Hz) is much smaller than previously reported square planar complexes **101** with P *trans* to N (172-173 Hz),^{107, 108} indicating that a complex analogous to **101** is unlikely. A square planar complex with P *trans* to P such as *trans*-spanning complex **102** would be expected to have $J_{\text{Rh-P}}$ around 130-135 Hz,¹¹⁸ while a trigonal bipyramidal complex with axial phosphines such as **104** (**Figure 122**) would be consistent with the observed small value of the Rh-P coupling constant.^{109, 111} Another possibility for this complex is a complex with P *trans* to alkene such as **105** or **106** (**Figure 122**), which would again be consistent with a small value for $J_{\text{Rh-P}}$ due to the high *trans*-influence of the alkene.

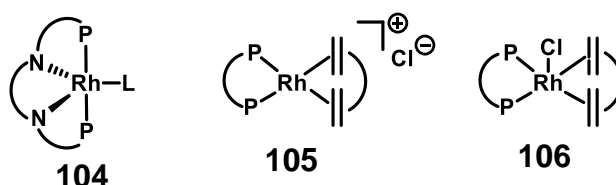


Figure 122 – Possible structures for complex **A** with P *trans* to P or alkene.¹⁰⁶

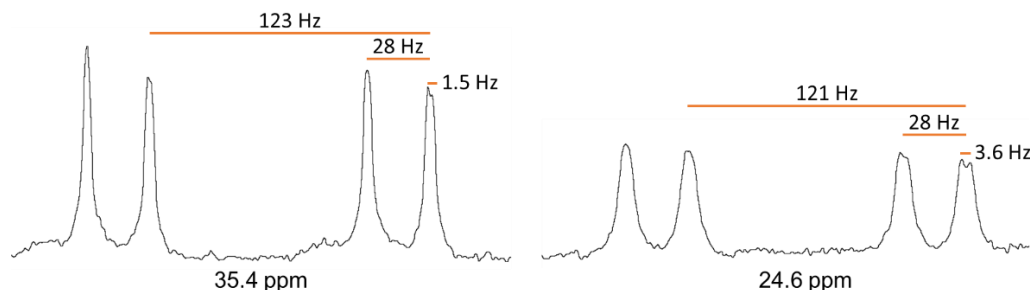


Figure 123 – Expansions of the $^{31}\text{P}\{^1\text{H}\}$ NMR spectrum for complex **B** in **Figure 121** showing two doublets of doublets of doublets.

Complex **B** shows doublets of doublets of doublets at 24.6 and 35.4 ppm (see **Figure 123** for expansions). These integrate close to 1:1 in all spectra; the

differing intensities are due to the degree of overlap of the lines of the small doublet splitting assigned to $^3J_{\text{Rh-P}}$ (3.6 Hz for the peak at 24.6, and 1.5 Hz for the peak at 35.4). The coupling constant of 28 Hz is the same in both doublets of doublets and can be assigned to P-P coupling, and the largest coupling constants (121 and 123 Hz, respectively) correspond to one-bond Rh-P coupling. The presence of $^3J_{\text{Rh-P}}$ coupling in **B** confirms that **B** is a dimer complex with two inequivalent phosphine donors, i.e. the ligand chelates the rhodium - a bridging ligand, although possible, is unlikely. Possible structures for **B** are complexes **107** or **108** (**Figure 124**) in which the phosphorus centres are made inequivalent by the conformation of the ligand backbones. However, the Rh-P coupling constants (121-123 Hz) are too small for P *trans* to chloride (186-200 Hz).¹⁰⁶ Trigonal bipyramidal structures, such as complexes **109** or **110**, in which the axial Ps are mutually *trans* could account for the small Rh-P coupling.

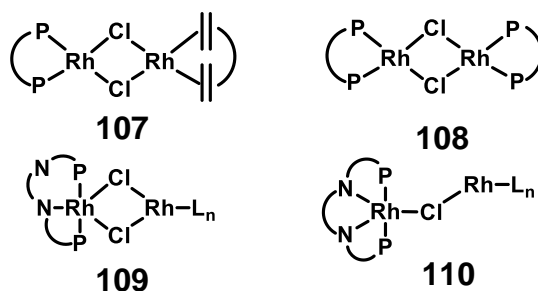


Figure 124 – Possible structures for complex **B**.¹⁰⁶ (L=ligand)

At shorter reaction times (bottom two spectra in **Figure 121**), two additional sets of resonances are seen: a broad doublet at 18.2 ppm with a coupling constant of 160 Hz, complex **C**, and a sharp doublet at 18.7 ppm with a coupling constant of 157 Hz, complex **D**.

Complex **C**, since it is broad, might be an intermediate complex where only one of the phosphorus atoms has coordinated, although the expected corresponding broad singlet near to the free ligand peak is not seen in **Figure 121**. Instead, we favour an analogous reaction to that reported for the reaction of *bis*-(2-diphenylphosphino)phenyl ether (DPEPhos) with $[\text{Rh}(\text{COD})\text{Cl}]_2$ to form a mixture of complexes **107**, showing a sharp doublet, and **108**, overlapping with a broad doublet (**Figure 125**). However, we note that much

larger $J_{\text{Rh-P}}$ (205 and 201 Hz) are reported for the DPEPhos complexes than are observed here (157 and 160 Hz).¹⁰⁶

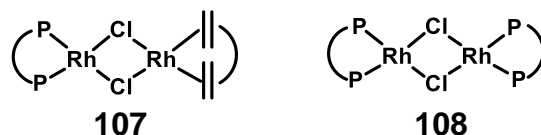


Figure 125 – Possible structures for **C** and **E** (**107**) and **D** and **G** (**108**).

The NMR spectra in **Figure 127** for the reaction of PNNP ligand **86** ($R = i\text{Pr}$) are more complicated. After 1.5 h reaction time, there are 3 doublets at 19.2, 18.0 and 17.6 ppm, complexes **E**, **F**, and **G**. The doublet for complex **E** is sharp with Rh-P coupling of 160 Hz, whereas for complexes **F** and **G** the doublets are broad, with Rh-P coupling constants of 158 Hz. A broad singlet is also present at -19.3 ppm, next to the free ligand peak, which integrates roughly 1:1 compared to the broad doublet for complex **F** and, in the bottom spectrum, it integrates 1:1 compared to the resonance of free ligand. This indicates that in complex **F** only one of the phosphorus donors is coordinated to the metal, such as complex **111** (**Figure 126**). The breadth of the resonances indicates a dynamic process is occurring. The differential broadening of the free ligand and decoordinated end of **86** in complex **F** indicates that the ends of the coordinated ligand exchange more rapidly than the exchange of coordinated and free **86**, indicating either an intramolecular process, or that **86** does not leave the solvation shell of the complex during the exchange. A second slower exchange process can then exchange free and coordinated **86**. Complexes **E** and **G** are assigned as the dimer complexes **107** and **108**, as discussed above (**Figure 125**).

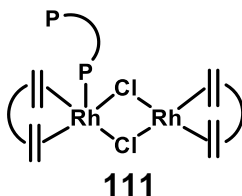


Figure 126 – Possible structure of complex **F**.

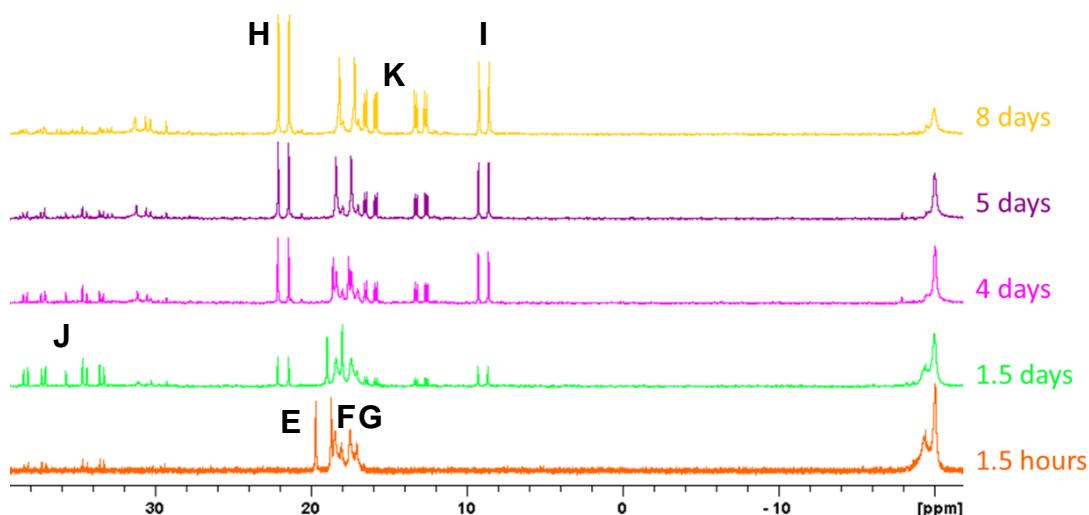


Figure 127 – The $^{31}\text{P}\{^1\text{H}\}$ NMR spectra of complex formation with PNNP ligand **86**.

At longer reaction times in **Figure 127**, the resonances of 4 additional complexes are seen: two doublets at 21.8 and 9.0 ppm, complexes **H** and **I**, and two sets of doublets of doublets at 36 ppm, complex **J**, and 14.6 ppm, complex **K**.

The Rh-P coupling constants for **H** and **I** are 111 and 106 Hz, respectively, which would be consistent with P *trans* to P in a trigonal bipyramidal complex **104**, or a square planar complex with P *trans* to alkene such as **105** or **106** (**Figure 128**), as discussed above.

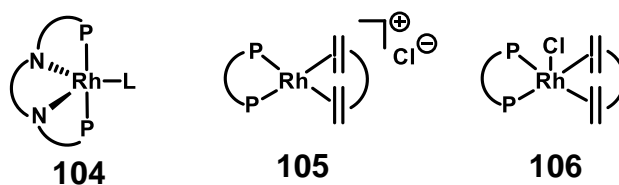


Figure 128 – Possible structures for **H** and **I**.

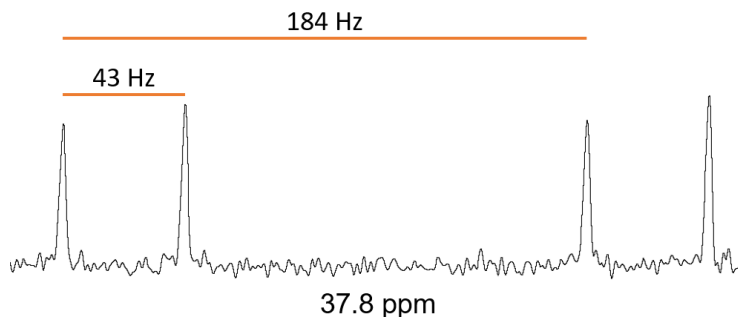


Figure 129 – An expansion of the $^{31}\text{P}\{^1\text{H}\}$ NMR of the doublet of doublets at 37.8 ppm for complex **J** in **Figure 127**.

For complexes **J** and **K**, the doublets of doublets show no coupling to a remote rhodium, as for the complex with **82** above, and the lines are very sharp which indicates that there are no unresolved Rh-P couplings (**Figure 129**). This means that these complexes are most likely not dimers. This may be due to the increased steric bulk of the ligand which makes the formation of a dimer complex less likely.

Complex **J** has P-P coupling constants of 43 Hz and Rh-P coupling constants of 184 and 176 Hz. The large Rh-P coupling constants would suggest a structure where one P is *trans* to Cl and the other *trans* to N. An example of a complex which fulfils these requirements would be a square based pyramid structure **112** (**Figure 130**), although this looks like an unusual coordination geometry for the PNNP ligand.

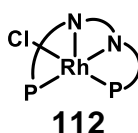


Figure 130 – A possible structure for complex **J**, with one P *trans* to N and the other *trans* to Cl.

Complex **K** has P-P coupling constants of 23.6 Hz and Rh-P coupling constants of 105 and 106 Hz. The small Rh-P coupling constants would suggest either a trigonal bipyramidal complex with P *trans* to P or a square planar complex with P *trans* to alkene. However, it is difficult to imagine such complexes having inequivalent phosphorus atoms. Another possibility would be the oxidation of Rh(I) to Rh(III) to form an octahedral complex, which are known to have smaller Rh-P coupling constants (see **Table 3**).¹¹¹

The observations above suggest that the sterically more demanding ligand **86** is less likely to coordinate to a metal centre than ligand **82**.

Unfortunately, no crystals were obtained from these NMR solutions.

3.6. Summary

In summary, eight acyclic ligands were synthesised (**Figure 105**), with varying denticity (bidentate, tridentate, tetradentate and pentadentate) and chiral groups (Me, iPr, Ph). The PNNP ligands were reacted with [Rh(COD)Cl]₂ and

the NMR spectra show rhodium-phosphorus coupling which confirms complex formation. However, the ease of complex formation appears to vary with the ligand's steric property, with the bulkier one less likely to coordinate to a metal centre.

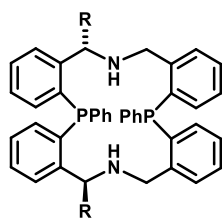
Chapter 4. Catalysis

As mentioned in the introduction, until recently asymmetric hydrogenation (AH) and asymmetric transfer hydrogenation (ATH) reactions have mainly used expensive and toxic rhodium, ruthenium and iridium metal catalysts. In recent years a considerable amount of research has gone into AH and ATH reactions which use base metals instead of precious metals.²⁵⁻³³ Iron is the most abundant metal in the earth's crust and is also an essential element in nature.³⁴ This means it is a lot cheaper and less toxic than the precious metals, making iron a good candidate for the replacement of precious metals.

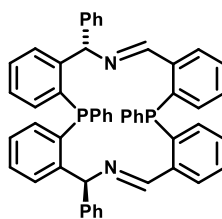
Examples of iron catalysed hydrogenations are given in section 1.6 (page 11), including the use of the 22-membered macrocycle **23** which is the most enantioselective ligand for iron catalysed AH of ketones so far. However, it has a low TOF, high H₂ pressure is needed (50 bar), and it is unable to hydrogenate other substrates such as imines.²

Therefore, the macrocyclic and acyclic ligands described in Chapter 2 and Chapter 3 were tested for the iron catalysed AH and ATH of acetophenone, with the hope of obtaining an iron catalyst with increased activity and substrate scope. The initial reaction conditions were based on those for the AH and ATH using the 22-membered macrocyclic ligand **23** from literature.^{1, 2} The conditions for the best ligand were optimised and a variety of ketones and one imine were reduced to demonstrate the substrate scope.

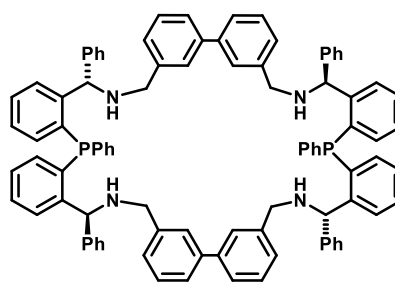
The following ligands were tested for iron catalysed hydrogenation:



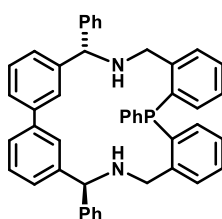
37b (R=Ph)
37c (R=p-Tol)
37d (R=Xyl)



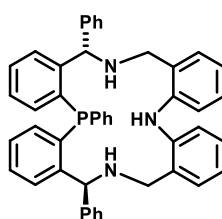
58c



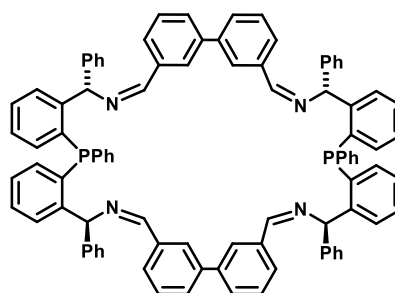
37a



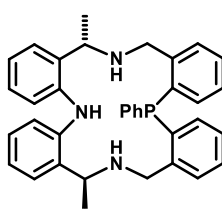
63



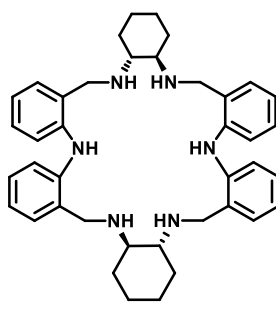
37e



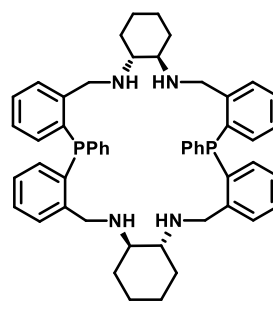
58a



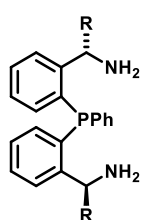
64



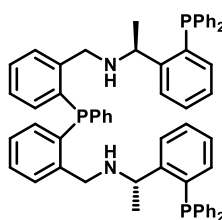
65



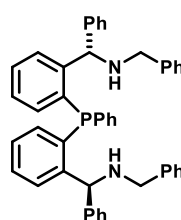
23



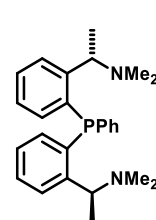
36b (R=Ph)
36c (R=p-Tol)
36d (R=Xyl)



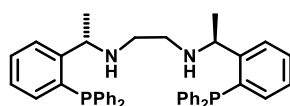
87



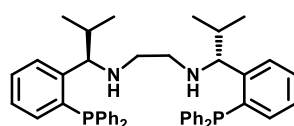
84



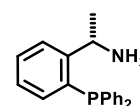
44



82



86



81

4.1. Asymmetric Hydrogenation (AH)

AH of acetophenone was studied first and this was undertaken at AstraZeneca in Macclesfield from July-September 2018. All of the ligands synthesised were sent over in order to test them using the screening equipment available at AstraZeneca. The AH experiments were based on the procedure used for the 22-membered macrocycle **23** from literature (**Figure 131**), with the catalyst formed in situ.² In the literature procedure, the iron source ($\text{Fe}_3(\text{CO})_{12}$) and the ligand are placed into a dry autoclave under nitrogen, followed by the addition of dry methanol. Then the autoclave is filled with hydrogen and the mixture is stirred at 45 °C under 5 bar of hydrogen for 1 h. After this, KOH in methanol is added followed by acetophenone. Then 50 bar of hydrogen is added and the mixture is stirred at 45 °C.²

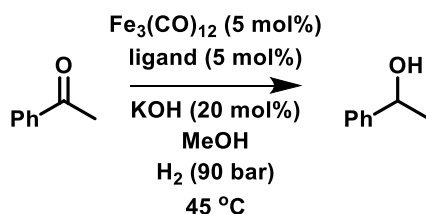


Figure 131 – The AH of acetophenone.

At AstraZeneca, the ligands were weighed out in air and then taken into a glovebox under nitrogen. Then $\text{Fe}_3(\text{CO})_{12}$ was weighed out into these vials using an automatic weighing machine inside the glovebox. Unfortunately, this was not always very accurate, so the ratios of iron/ligand were sometimes unusual. Potassium hydroxide was also weighed out in the glovebox into a large vial to make a solution in methanol to which acetophenone was added. Then an appropriate amount of this solution was added to each reaction vial. The reaction vials were placed into a 48-well metal plate which was then placed into a hydrogenation reactor. This was tightened up before removing it from the glovebox and installing it in the hydrogenation machine. 90 bar of hydrogen was added and the reactions were heated to 45 °C and were left overnight.

Samples were taken from each reaction and were analysed using SFC. No product was obtained from any of the reactions apart from the 22-membered macrocycle **23** from literature (76% conversion).

Next, a slightly different method was used in which the ligand and $\text{Fe}_3(\text{CO})_{12}$ were stirred in methanol under 5 bar of hydrogen for 1 hour at 45 °C before cooling and adding a solution of KOH and acetophenone in methanol. Then 90 bar of hydrogen was added and the mixtures were stirred overnight at 45 °C. Unfortunately, this method also gave no product.

4.2. ATH under Schlenk conditions

The ATH experiments were based on the literature procedure used for the 22-membered macrocycle **23** (Figure 132).¹ The reactions were performed under nitrogen using a Schlenk line. In the literature procedure, the iron source, ligand and NaBH_4 are placed in a tube under nitrogen. Isopropanol is then added, and the mixture is stirred at 65 °C for 30 min before the addition of base in isopropanol. The mixture is stirred for a further 10 min before the addition of ketone.¹

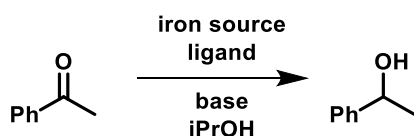


Figure 132 – The ATH of acetophenone.

Table 4 – The screening of ligands for the ATH of acetophenone.

	ligand	time (h)	conversion ^b (%)	ee ^c (%)
i ^a	37a	19	0	-
ii	37b	16	0	-
iii	37e	19	0	-
iv	37c	16	3	-
v	37d	16	0.5	-
vi	36b	16	2	-
vii	84	16	0	-
viii ^a	84	17	0	-
ix	63	15	0	-
x	65	18	0.5	-
xi	82	16	99	50
xii	87	17	1	-

conditions: acetophenone (0.3 mmol), ligand (0.5 mol%), $\text{Fe}_3(\text{CO})_{12}$ (0.5 mol%), KOH (12 mol%), iPrOH (3 ml), 55 °C.

^a NH_4Cl additive (6 mol%).

^b Determined by ^1H NMR.

^c Determined by chiral HPLC.

Firstly, the exact conditions used for the 22-membered macrocycle were used, apart from the additive since the role of this is unknown and was only shown to increase the conversion by 5%.¹ Very low conversions ($\leq 3\%$) were observed for almost all ligands (**Table 4**). However, the PNNP ligand **82** gave 99% conversion and about 50% ee (entry xi).

Table 5 – Screening of metals, bases and ligands for ATH of acetophenone.

	ligand	metal source	base	time (h)	conversion ^d (%)	ee ^e (%)
i	37b	Fe ₃ (CO) ₁₂	KOH	21	0.3	-
ii	37b	Fe ₃ (CO) ₁₂	KOtBu	23	4	-
iii	37b	Fe ₃ (CO) ₁₂	K ₂ CO ₃	22	0.6	-
iv	37b	FeBr ₂	KOH	20	9	-
v	37b	FeSO ₄ ·7H ₂ O	KOH	23	7	-
vi	37b	Fe ₂ (CO) ₉	KOH	22	8	-
vii	37b	Fe(OAc) ₂	KOH	23	16	4
viii	37b	Fe(OAc) ₂	KOtBu	22	12	3
ix ^b	37b	Fe(OAc) ₂	KOH	24	57	1
x ^c	37b	[Ru(p-cymene)Cl ₂] ₂	KOH	24	92	3
xi	58c	Fe ₃ (CO) ₁₂	KOH	21	0	-
xii	36b	Fe ₃ (CO) ₁₂	KOH	22	4	-
xiii	37e	Fe ₃ (CO) ₁₂	KOH	23	0	-
xiv	37e	Fe(OAc) ₂	KOH	23	17	-
xv	37e	FeSO ₄ ·7H ₂ O	KOH	23	13	-
xvi	23	Fe ₃ (CO) ₁₂	KOH	1	42	95
xvii ^a	23	Fe ₃ (CO) ₁₂	KOH	1	89	96

conditions: acetophenone (0.3 mmol), ligand (1.7 mol%), metal source (1.7 mol%), base (12 mol%), 90 °C.

^a ligand (0.5 mol%), Fe₃(CO)₁₂ (0.5 mol%), NH₄Cl additive (6 mol%), 55 °C.

^b 50 mol% base

^c metal source (0.85 mol%)

^d Determined by ¹H NMR.

^e Determined by chiral HPLC.

Next, various iron sources and bases were tested, and the catalyst loading and the temperature were increased. The results are summarised in **Table 5** above. The first ligand tested was the macrocyclic ligand **37b** (entries i-x). Fe₃(CO)₁₂ gave very low conversions (entry i-iii) but was slightly improved with a stronger base (entry ii). Other iron sources (entry iv-viii) improved the yield slightly, however these have different iron/ligand ratios so they may not be directly comparable. The best iron source was Fe(OAc)₂ and the conversion was improved by increasing the amount of base to 50 mol% giving 57% conversion (entry ix). However, there was no enantioselectivity. A ruthenium source gave 92% conversion (entry x) but still no enantioselectivity.

The imine version of this macrocycle (**58c**) was also tried with $\text{Fe}_3(\text{CO})_{12}$ (entry xi) but gave no conversion. The free diamine **36b** gave 4% conversion under the same conditions (entry xii).

Macrocycle **37e** was tested with three different iron sources (entries xiii-xv). $\text{Fe}_3(\text{CO})_{12}$ gave no conversion whereas iron acetate and iron sulfate gave low conversions.

The ATH using the 22-membered macrocycle from literature was repeated as a comparison, which gave 42% conversion and 95% ee (entry xvi). This was increased to 89% conversion and 96% ee (entry xvii) by using the exact conditions used in the paper, which is comparable to the literature results (97% conversion, 98% ee).

4.3. ATH in a glovebox

The ATH of acetophenone was also examined at AstraZeneca (**Figure 133**) and was carried out in small glass vials inside a glovebox under nitrogen.

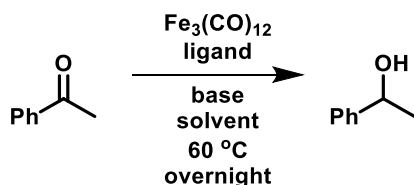


Figure 133 – The ATH of acetophenone in a glovebox at AZ.

The first ligand to be tested was the macrocyclic ligand **37b** (**Table 6**). This had given very low conversions previously (see section 4.2) when Schlenk techniques were used. However, in a glovebox it gave very high conversions, but still low ee ($\leq 15\%$). The low ee may be the result of reaction reversibility which can cause racemization of the product on longer reaction times.⁴⁷ Future work should include shorter reaction times to test this.

The conversion was improved with stronger base (compare entries i and ii). A mixture of toluene and isopropanol was tested next (entry iii) since the ligand is not very soluble in isopropanol, but this gave a lower conversion. The use of formic acid/triethylamine as a hydrogen source gave no product (entry iv).

Increasing the mol% of ligand and iron to 2% (entry v) increased the conversion to >99%.

Table 6 – ATH of acetophenone using ligand **37b**.

ligand	mol% ligand	mol% $\text{Fe}_3(\text{CO})_{12}$	base	solvent	conversion ^b (%)	ee ^b (%)
i	0.5	0.5	KOH	iPrOH	73	14
ii	0.5	0.5	KOtBu	iPrOH	92	12
iii	0.5	0.5	KOtBu	toluene/iPrOH (1/4)	66	8
iv	0.5	0.5	-	HCOOH/Et ₃ N iPrOH	0	-
v	2	2	KOtBu	iPrOH	>99	8
vi ^a	2	1.4	KOH	iPrOH	96	15
vii	2	1.4	KOH	iPrOH	98	12

conditions: acetophenone (0.1 M), $\text{Fe}_3(\text{CO})_{12}$, ligand, base (12 mol%), solvent, 60 °C, overnight.

^a2.5 μl of water was added (0.14 mol%).

^b Determined by chiral SFC.

In order to understand why the reaction did not work in a Schlenk flask, a small amount of water (2.5 μl) was added (entry vi). This had a minimal effect on the results (compare entries vi and vii), which would suggest that the reaction may be air sensitive rather than water sensitive.

The next ligand to be tested was macrocyclic ligand **64** (Table 7). Very low conversion was obtained when KOH was used as the base (entry i), but a stronger base (KOtBu) gave a higher conversion and moderate ee (entry ii). The addition of toluene to try and increase the solubility of the ligand resulted in a slightly lower conversion and ee (entry iii). Formic acid/Et₃N as the hydrogen source gave no product (entry iv).

Table 7 – ATH of acetophenone using macrocyclic ligand **64**.

ligand	mol% ligand	mol% $\text{Fe}_3(\text{CO})_{12}$	base	solvent	conversion ^a (%)	ee ^a (%)
i	0.5	0.5	KOH	iPrOH	4	2
ii	0.5	0.5	KOtBu	iPrOH	22	44
iii	0.5	0.5	KOtBu	toluene/iPrOH (1/4)	15	20
iv	0.5	0.5	-	HCOOH/Et ₃ N iPrOH	0	-

conditions: acetophenone (0.1 M), $\text{Fe}_3(\text{CO})_{12}$, ligand, base (12 mol%), solvent, 60 °C, overnight.

^a Determined by chiral SFC.

The bidentate PN ligand **81** was also tested (Table 8). This gave low conversions but moderate ee using KOH as base (entries i and ii). An

increased amount of ligand and iron source, plus KOtBu as base, gave 64% conversion and 66% ee (entry iii).

Table 8 – ATH of acetophenone using PN ligand **81**.

ligand	mol% ligand	mol% $\text{Fe}_3(\text{CO})_{12}$	base	conversion ^a (%)	ee ^a (%)
i	0.5	0.5	KOH	6	32
ii	1	0.5	KOH	6	26
iii	2	2	KOtBu	64	66
iv	6	5	KOtBu	12	64
v	12	3.6	KOtBu	13	47
vi	18	2.1	KOtBu	21	48
vii	2	1.4	NaOtBu	22	38
viii	2	1.3	KOH	18	67
ix	2	1.4	KOtBu	29	59

conditions: acetophenone (0.1 M), $\text{Fe}_3(\text{CO})_{12}$, ligand, base (12 mol%), solvent, 60 °C, overnight.

^a Determined by chiral SFC.

An excess of ligand compared to iron (entries iv-vi) gave lower conversions and ee than a 1:1 mixture (entry iii). A comparison of bases (entries vii-ix) showed that KOtBu was the best in terms of conversion, but KOH gave the best ee.

PNNP ligand **82** consistently gave full conversions (**Table 9**), apart from when a great excess of iron was used (entry iii) which gave no conversion. However, the ee was not reliable.

Table 9 – ATH of acetophenone using PNNP ligand **82**.

ligand	mol% ligand	mol% $\text{Fe}_3(\text{CO})_{12}$	base	conversion ^a (%)	ee ^a (%)
i	2	2	KOtBu	100	20
ii	2	1.4	KOtBu	98	0.4
iii	2	11.5	KOH	0	-
iv	2	1.5	KOH	99	2
v	2	1.5	KOtBu	98	8

conditions: acetophenone (0.1 M), $\text{Fe}_3(\text{CO})_{12}$, ligand, base (12 mol%), iPrOH, 60 °C, overnight.

^a Determined by chiral SFC.

Various other ligands were also tested (**Table 10**). PNP ligand **44** gave very low conversion (entry i) and the use of a stronger base and increased catalyst loading did not improve this (entry ii). The macrocyclic ligand **37a**, along with its imine analogue **58a**, gave low conversion and ee (entries iii and xi). The macrocyclic ligands **63** and **37e** gave both low conversions and ee (entries viii

and iv), whereas macrocyclic ligands **37c** and **37d** gave good conversions but low ee (entries v and vi).

Table 10 – ATH of acetophenone in a glovebox at AZ.

	ligand	mol% ligand	mol% Fe ₃ (CO) ₁₂	base	conversion ^a (%)	ee ^a (%)
i	44	0.5	0.5	KOH	2	-
ii	44	2	2	KOtBu	0	-
iii	37a	2	2	KOtBu	8	4
iv	37e	2	2	KOtBu	2	12
v	37c	2	2	KOtBu	85	8
vi	37d	2	2	KOtBu	69	12
vii	65	2	2	KOtBu	0	-
viii	63	2	2	KOtBu	4	12
ix	87	2	2	KOtBu	0	-
x	84	2	2	KOtBu	4	6
xi	58a	2	2	KOtBu	10	4
xii	23	2	2	KOtBu	98	80

conditions: acetophenone (0.1 M), Fe₃(CO)₁₂, ligand, base (12 mol%), iPrOH, 60 °C, overnight.

^a Determined by chiral SFC.

The macrocyclic ligand **65**, which is an amino analogue of the 22-membered macrocycle **23** from literature, gave no conversion (entry vii) compared to 98% conversion for **23** (entry xii). The pentadentate ligand **87** gave no conversion (entry ix). The benzyl protected PNP diamine ligand **84** gave low conversion and ee (entry x).

A comparison of the macrocyclic ligands suggests that the phosphorus donor atoms are important for activity. The 22-membered macrocycle **23** from literature which has 2 phosphorus atoms gave 98% conversion (entry xii) whereas the amino analogue **65** gave no conversion (entry vii). Also, the macrocyclic ligands **37b**, **37c** and **37d** which have 2 phosphorus donors gave good conversions whereas **37e**, where one of the phosphorus atoms is replaced with an NH, and **63**, where one of the phosphorus atoms is removed, gave very low conversions.

4.4. Optimisation of PNNP ligand **82**

After returning from AstraZeneca, the PNNP ligand **82** was optimised under Schlenk conditions. This ligand was chosen to be optimised because it gave

good conversions and the ATH can be carried out under Schlenk conditions, unlike the macrocyclic ligand **37b** which only works in a glovebox.

Firstly, some control experiments were conducted (**Table 11**) which show that each component of the reaction is essential to its success.

Table 11 – Control experiments.

	ligand	base	iron source	conversion ^a (%)
i	-	KOH	Fe ₃ (CO) ₁₂	0
ii	82	-	Fe ₃ (CO) ₁₂	0
iii	82	KOH	-	0

acetophenone (0.3 mmol), Fe₃(CO)₁₂ (0.5 mol%), ligand **82** (0.5 mol%), KOH (12 mol%), iPrOH (3 ml), 55 °C, 1 hour.

^a Determined by ¹H NMR.

Secondly, the reaction time was varied (**Table 12**). No change in conversion was observed until the reaction time was decreased to 30 minutes, showing the catalyst formed to be highly active. The ee appears to increase slightly on shorter reaction times, but not to any significant extent. This would suggest that the reaction is not easily reversible because this would result in racemisation of the product with prolonged reaction times.⁴² The optimum reaction time chosen was 1 hour.

Table 12 – Optimisation of reaction time.

	time	conversion ^a (%)	ee ^b (%)
i	16 h	98	50
ii	2 h	98	46
iii	1 h	98	51
iv	30 min	96	57
v	10 min	20	56

acetophenone (0.3 mmol), Fe₃(CO)₁₂ (0.5 mol%), ligand **82** (0.5 mol%), KOH (12 mol%), iPrOH (3 ml), 55 °C.

^a Determined by ¹H NMR.

^b Determined by chiral HPLC.

Next, different reaction temperatures were tried (**Table 13**). The conversion decreases slightly with lower temperature, as would be expected, but the ee remains around the same value. The chosen temperature was 55 °C.

Table 13 – Optimisation of reaction temperature.

	temperature (°C)	conversion ^a (%)	ee ^b (%)
i	25	82	55
ii	35	92	46
iii	55	98	51
iv	80	99	47

acetophenone (0.3 mmol), Fe₃(CO)₁₂ (0.5 mol%), ligand **82** (0.5 mol%), KOH (12 mol%), iPrOH (3 ml), 1 hour.

^a Determined by ¹H NMR.

^b Determined by chiral HPLC.

Different bases were tried next (**Table 14**). A series of hydroxides was examined (entries i-iv). Lithium and potassium hydroxide gave the same results, whereas sodium hydroxide gave a much lower conversion and enantioselectivity, and caesium hydroxide still gave good conversion but lower ee. Strength of base was examined next; a weaker base (potassium carbonate, entry v) gave no conversion, and a stronger base (potassium t-butoxide, entry vi) gave lower conversion and enantioselectivity. The base of choice was potassium hydroxide since this is readily soluble in isopropanol.

Table 14 – Choice of base.

	base	conversion ^a (%)	ee ^b (%)
i	LiOH	98	52
ii	NaOH	14	36
iii	KOH	98	51
iv	CsOH	95	31
v	K ₂ CO ₃	0	-
vi	KOtBu	11	40

acetophenone (0.3 mmol), Fe₃(CO)₁₂ (0.5 mol%), ligand **82** (0.5 mol%), base (12 mol%), iPrOH (3 ml), 55 °C, 1 hour.

^a Determined by ¹H NMR.

^b Determined by chiral HPLC.

The amount of base was also varied (**Table 15**). Either an increase or decrease in the amount of base lowered both the conversion and enantioselectivity. Therefore, the mol% KOH was kept at 12 mol%.

Table 15 – Variation of mol% KOH.

	mol% KOH	conversion ^a (%)	ee ^b (%)
i	6	22	32
ii	12	98	51
iii	30	6	12

acetophenone (0.3 mmol), Fe₃(CO)₁₂ (0.5 mol%), ligand **82** (0.5 mol%), iPrOH (3 ml), 55 °C, 1 hour.

^a Determined by ¹H NMR.

^b Determined by chiral HPLC.

The ligand/iron ratio was investigated next (**Table 16**). The ligand/iron ratio used so far has been 1/1, following the literature method for the 22-membered macrocycle **23**.¹ The reaction time was reduced to 10 minutes in order to see any difference in conversion. The conversion is increased with increasing amounts of ligand up until the ratio 3/1. However, increasing the amount of ligand further decreases the conversion. This would suggest that the active catalyst may be an iron complex containing one iron atom with one ligand coordinated. Further ligand may coordinate to the active sites of the catalyst, blocking the coordination of substrate and therefore lowering the conversion.

Table 16 – The variation of ligand/iron ratio.

	L/Fe ₃ (CO) ₁₂	conversion ^a (%)	ee ^b (%)
i	1/1	20	56
ii	2/1	29	52
iii	3/1	84	50
iv	4/1	42	48

acetophenone (0.3 mmol), Fe₃(CO)₁₂ (0.5 mol%), ligand **82**, KOH (12 mol%), iPrOH (3 ml), 55 °C, 10 min.

^a Determined by ¹H NMR.

^b Determined by chiral HPLC.

Finally, PPh₃ was added (**Table 17**) which did not have any effect on the conversion, but the ee was lowered slightly. This may suggest that the reaction is homogeneous because PPh₃ can be used as a poison which strongly binds to a metal, blocking substrate access. However, further experiments must be conducted in order to distinguish homogenous from heterogeneous catalysis as there is no single definitive experiment for making this distinction.¹²²

Table 17 – Investigating the effect of an additive.

	additive	conversion ^a (%)	ee ^b (%)
i	PPh ₃	97	39
ii	-	98	55

acetophenone (0.3 mmol), Fe₃(CO)₁₂ (0.5 mol%), ligand **82** (1.5 mol%), PPh₃ (1.5 mol%), KOH (12 mol%), iPrOH (3 ml), 55 °C, 1 hour.

^a Determined by ¹H NMR.

^b Determined by chiral HPLC.

The isopropyl analogue of this ligand, PNNP ligand **86**, was also tested in the hope that the bulkier isopropyl groups would improve the ee (**Table 18**). However, the conversion was only 1% when the optimised conditions for PNNP ligand **82** were used (entry i). Increasing the temperature to 80 °C only increased the conversion to 4% (entry ii). Leaving the reaction overnight (entry iii) gave 32% conversion but only 3% ee. These results indicate that the formation of an active iron catalyst is highly sensitive to the steric property of the ligands.

Table 18 – The ATH of acetophenone using PNNP ligand **86**.

	temperature (°C)	time (h)	conversion ^a (%)	ee ^b (%)
i	55	1	1	-
ii	80	1	4	-
iii	80	24	32	3

acetophenone (0.3 mmol), Fe₃(CO)₁₂ (0.5 mol%), ligand **86** (1.5 mol%), KOH (12 mol%), iPrOH (3 ml).

^a Determined by ¹H NMR.

^b Determined by chiral HPLC.

4.5. Substrate scope of PNNP ligand **82**

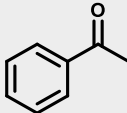
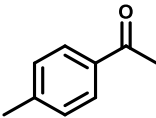
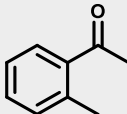
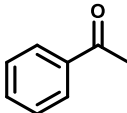
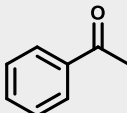
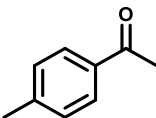
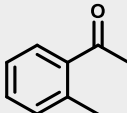
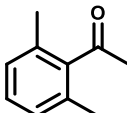
Following the optimisation of the conditions for the ATH of acetophenone using PNNP ligand **82** (section 4.4), various substrates were reduced using the optimised conditions to demonstrate the substrate scope (**Table 19**).

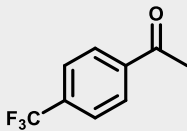
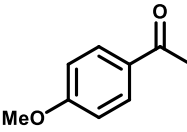
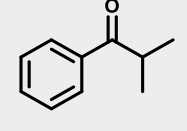
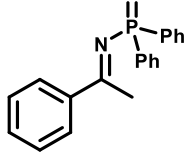
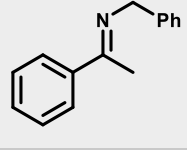
The first substrates were tried before the optimisation of the ligand/iron ratio (entries i-iii). Increasing steric bulk of the substrate increases the ee but lowers the conversion. A comparison of entry (i) and entry (iv) shows that increasing the ligand/iron ratio to 3/1 has little effect on the ee.

From entry (v) lower ees were obtained using exactly the same conditions (compare entries v and i). One reason for this could be that a new batch of ligand was used. There was no difference in the NMR spectra, but there could

potentially be an undetectable impurity which could affect the ee. It is unlikely that this batch of ligand had been racemised because this would result in a mixture of diastereoisomers which would be distinguishable by NMR. Another reason for the decrease in ee could be that a new solution of KOH/iPrOH was made. The KOH solutions were made by crushing a KOH pellet and then weighing it out into a glass vial. During this time the KOH sometimes appeared to get wet. The amount of water would differ depending on the humidity of the lab and the time taken to weigh it out. Therefore, the amount of KOH used may have been different which would affect the ee (see **Table 15**).

Table 19 – The ATH of different acetophenone type substrates.

	substrate	L/Fe ₃ (CO) ₁₂	conversion ^a (%)	ee ^b (%)	notes
i		1/1	98	51	
ii		1/1	89	57	
iii		1/1	88	74	
iv		3/1	98	55	
v		1/1	98	40	new batch of ligand from this row, giving lower ee (compare to row i)
vi		3/1	96	29	slight overlap with an unknown peak in HPLC
vii		3/1	>99	68	
viii		3/1	6	71	

	substrate	L/ $\text{Fe}_3(\text{CO})_{12}$	conversion ^a (%)	ee ^b (%)	notes
ix		3/1	>99	23	enantiomers slightly overlap in HPLC
x		3/1	82	35	
xi		3/1	98	58	
xii		3/1	98	49	a mixture of products was formed, including amine and alcohol
xiii		3/1	0	-	

substrate (0.3 mmol), $\text{Fe}_3(\text{CO})_{12}$ (0.5 mol%), ligand **82**, KOH (12 mol%), *i*PrOH (3 ml), 55 °C, 1 hour.

^a Determined by ^1H NMR.

^b Determined by chiral HPLC.

A methyl group in the para position (entry vi) appears to give lower ee compared to acetophenone (entry v), but there was a slight overlap of peaks in the HPLC so this may be misleading. A methyl group in the ortho position (entry vii) gave full conversion, compared to only 64% conversion using macrocyclic ligand **23** from literature (in 2 hours at 75 °C),¹ and a higher ee (68%) than acetophenone (40%, entry v). A methyl group in both of the ortho positions (entry viii) decreased the conversion considerably (6%) but the ee was increased to 71%.

An electron withdrawing group in the para position (entry ix) gave full conversion but lower ee. Unfortunately, the peaks for enantiomers were slightly overlapping in the HPLC so the ee is only approximate. The macrocyclic ligand **23** from literature required much longer reaction times for electron withdrawing groups in the para position (*p*-cyanoacetophenone needed 3 h to achieve full conversion).¹

An electron donating group in the para position (entry x) gave a slightly lower conversion (82%) which is comparable to the macrocyclic ligand **23** from literature (86% conversion, 30 min, 75 °C).¹ A similar ee is obtained (35%) in comparison to acetophenone (40%, entry v).

The next substrate contained two extra methyl groups on the other side of the ketone (entry xi) which gave 98% conversion and higher ee (58%) than acetophenone. The conversion is much better than macrocyclic ligand **23**, which gave only 90% conversion after 12 h at 75 °C.¹

A couple of imine substrates were also tried (entries xii and xiii). The phosphinyl imine (xii) gave a mixture of products including the expected amine product, but also some 1-phenylethanol resulting from hydrolysis of the imine before reduction. The ratio between the amine and alcohol products in the ¹H NMR spectrum of the crude product was 1:1.1. The amine product was separated from the mixture in 20% isolated yield and the ee was 49%. The benzyl imine (xiii) gave no product.

4.6. Summary

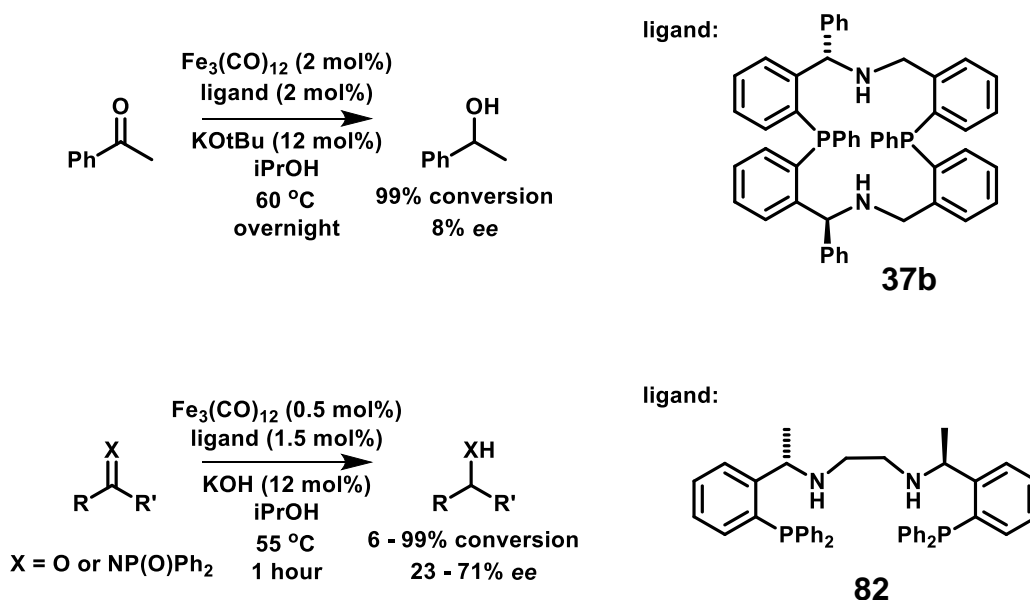


Figure 134 – The best ligands for the iron catalysed ATH.

In summary, all of the ligands were tested for the AH and ATH of acetophenone. All of them were unsuccessful for AH, but some worked for ATH (**Figure 134**). The best ligands were macrocyclic ligand **37b**, giving full

conversion but low ee, and PNNP acyclic ligand **82** giving full conversion and moderate ee. The conditions for ATH with PNNP ligand **82** were optimised, including reaction time, temperature, base, mol% base and ligand/iron ratio. Then a range of ketones and one imine were reduced, demonstrating the substrate scope.

Chapter 5. Conclusions and suggestions for future work

for future work

A variety of new chiral macrocyclic ligands containing phosphorus and nitrogen donor atoms (**Figure 135**) have been synthesised by the condensation of a variety of chiral diamines with a selection of dialdehydes under high dilution conditions.

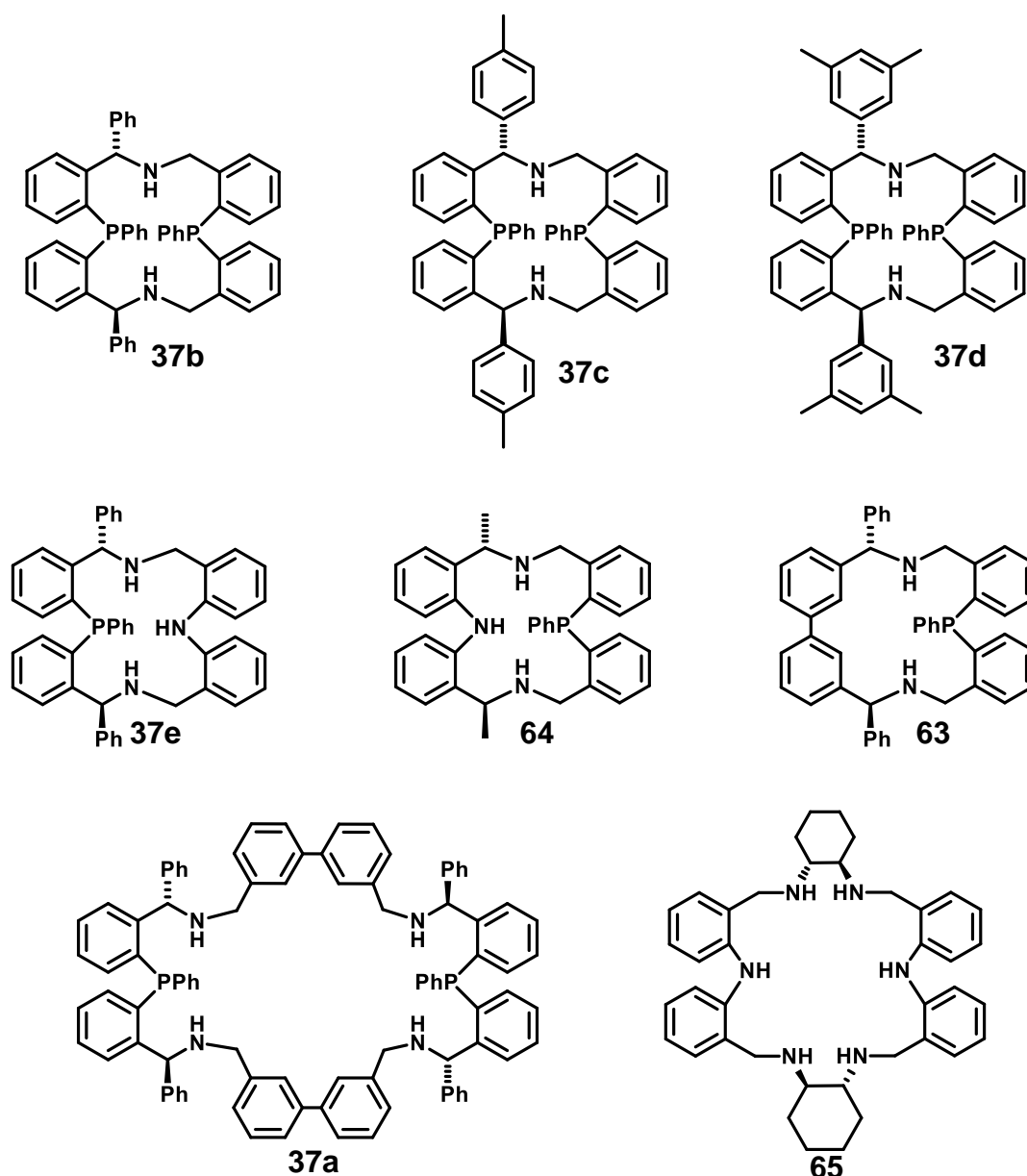


Figure 135 – Macrocyclic ligands synthesised.

The first synthetic route towards the chiral diamines was unsuccessful due to the difficulty in finding a suitable protecting group for the ortholithiation step; however, the second route via Grignard addition to a chiral sulfinamide worked

well. The collection of macrocycles exhibits a selection of ring sizes from 16 to 34 membered rings, denticity ranging from three to six, variations in the combination of donor groups (P_2N_2 , P_2N_3 , PN_2 , P_2N_4 , N_6), and a range of chiral groups (Me, Ph, p-tol and 3,2-dimethylphenyl, Cy).

Eight acyclic ligands containing phosphorus and nitrogen donor atoms have also been made (**Figure 136**) with varying size, denticity and chiral groups (Me, iPr, Ph). The PNNP ligands **82** and **86** were reacted with $[Rh(COD)Cl]_2$ and the NMR spectra show rhodium-phosphorus coupling which confirms complex formation.

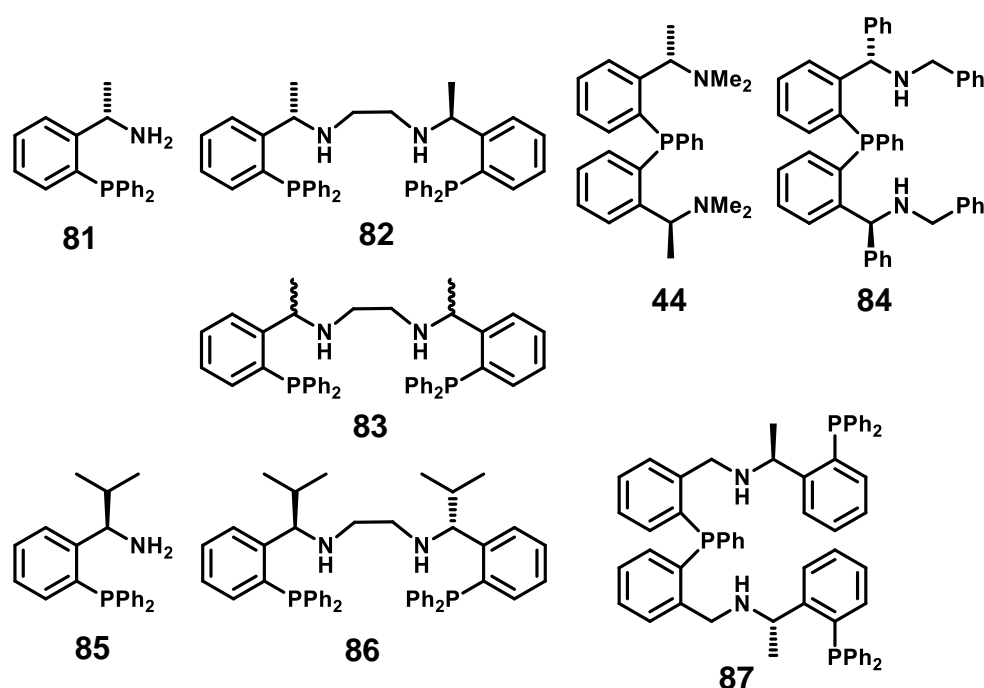


Figure 136 – Acyclic ligands synthesised.

All of these ligands were tested for the iron catalysed AH and ATH of acetophenone. Unfortunately, none of the ligands worked for the AH of acetophenone under the conditions examined, but some ligands did work for the ATH. The best macrocyclic ligand was **37b** (when used in a glovebox) which gave full conversion but low ee. The PNNP acyclic ligand **82** has good activity, better than the macrocyclic ligand **23** in some cases,¹ and gave the products with moderate ee (**Figure 137**).

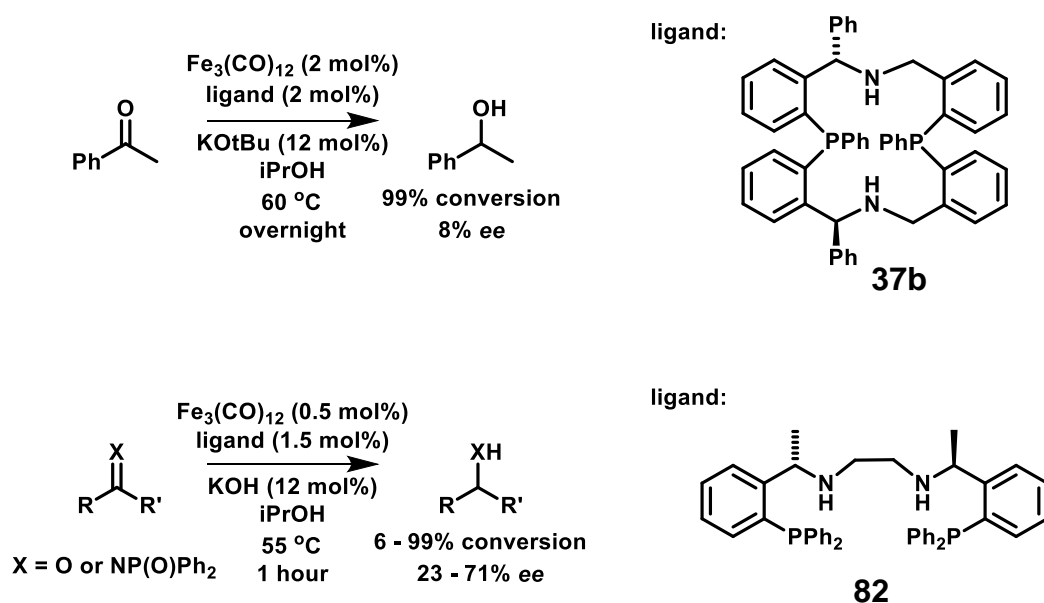


Figure 137 – The best ligands for iron catalysed ATH.

The conditions for the ATH of acetophenone were optimised for PNNP ligand **82**, including reaction time, temperature, base, mol% of base, and ligand/iron ratios. Once the optimum conditions were found, a variety of acetophenone type substrates were reduced to demonstrate the substrate scope, including one imine substrate.

A comparison of the macrocyclic ligands tested for the iron catalysed ATH suggests that the phosphorus donor atoms are important for activity. The 22-membered macrocycle **23** from literature which has 2 phosphorus atoms gave 98% conversion (entry xii) whereas the amino analogue **65** gave no conversion (entry vii). Also, the macrocyclic ligands **37b**, **37c** and **37d** which have 2 phosphorus donors gave good conversions whereas **37e**, where one of the phosphorus atoms is replaced with an NH, and **63**, where one of the phosphorus atoms is removed, gave very low conversions.

Suggestions for future work include the testing of different conditions for the ATH using the macrocyclic ligands **37b**, **37c** and **37d** in a glovebox. Firstly, shorter reaction times should be investigated to see if there is any racemisation due to reaction reversibility. Then other conditions such as base, temperature, metal sources and ligand/iron ratio could be investigated.

Also, different conditions for the in-situ formation of the catalyst should be investigated, such as time and temperature. This may be especially important

for PNNP ligand **86**, because the complex formation with rhodium (**Figure 127**) was much slower than for PNNP ligand **82**. Some procedures in literature leave the ligand and metal stirring overnight before the addition of base and substrate.^{15, 37, 38}

The synthesis of well-defined iron complexes using the PNNP ligands **82** and **86**, similar to Morris's group,^{41, 42, 45, 58} could help to understand the mechanism. Mechanistic studies, for example, deuterium labelling studies or following the reaction by NMR, could be carried out.

The use of different base metals, such as nickel, manganese, and cobalt could also be investigated for all ligands.

Suggestions for other ligands to be made (**Figure 138**) would include PNNP ligand **113** which could be compared with PNNP ligands previously made where the phenyl groups are in between the nitrogens.³⁶ Also, macrocyclic ligand **114** could be made, which is the macrocyclic version of the PNNP ligand **82** and could be compared to the 22-membered macrocycle **23**.

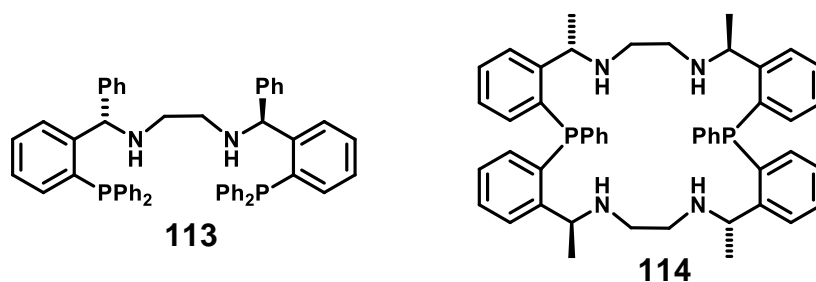


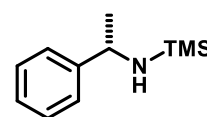
Figure 138 – Suggestions for other ligands.

Chapter 6. Experimental

Chemicals were purchased from commercial suppliers and were used without further purification. Solvents were dried using an MBraun SPS 5 800. NMR spectra were recorded using a Bruker 400 MHz spectrometer at 298 K. Me₄Si was used as the internal standard, *J* values are recorded in Hz and chemical shifts are given in ppm. Multiplicities are abbreviated as s (singlet), d (doublet), t (triplet), q (quartet), sept (septet), m (multiplet), br (broad). Mass Spectrometry was performed using either Agilent QTOF 7200/6530B or Micromass LCT mass spectrometer. CHN analysis was performed using a Thermo Flash Smart instrument and CHNS analysis was performed using an Elementar Vario Micro Cube instrument. Analytical TLC was performed with 0.25 mm silica gel plates which were visualised under UV light or with iodine. A Cellulose-C column was used for chiral HPLC.

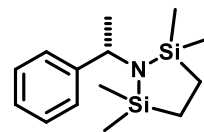
6.1. Synthesis of (S)-1,1,1-trimethyl-N-(1-phenylethyl)silanamine **38**

Triethylamine (4.95 ml, 35.5 mmol, 3.5 eq.) was added to a solution of (S)-phenylethylamine **35a** (1.29 ml, 10 mmol) in DCM (20 ml). The mixture was cooled to 0 °C and trimethylsilyl chloride (3.96 ml, 31.2 mmol, 3.1 eq.) was added dropwise. On addition, the solution turns from clear and colourless to cloudy and white. This was allowed to warm to room temperature and was stirred overnight (16.5 h). The next day, the volatiles were removed under vacuum and the residue was extracted with hexane (5 x 10 ml). The solvent was evaporated to give a yellow oil. This was purified by vacuum distillation to give yellow oil **38** (0.81 g, 42%). ¹H NMR (400 MHz; CDCl₃; Me₄Si) -0.01 (9H, s, Si(CH₃)₃), 1.37 (3H, d, *J* = 6.6, CHCH₃), 1.55 (1H, br s, NH), 4.04 (1H, m, CHCH₃), 7.16-7.40 (5H, m, Ar-H); CAS number 121443-77-4.



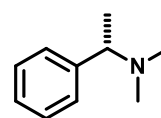
6.2. Synthesis of (S)-2,2,5,5-tetramethyl-1-(1-phenylethyl)-1,2,5-azadisilolidine **41**⁷²

A solution of 1,2-bis(chlorodimethylsilyl)ethane (2.16 g, 10 mmol) in anhydrous DCM (3.75 ml) was added dropwise over 25 minutes to a solution of (S)-phenylethylamine **35a** (1.29 ml, 10 mmol) in DCM (6.25 ml) containing triethylamine (2.79 ml, 20 mmol, 2 eq.). On addition, there was a very slight increase in temperature and the clear colourless solutions turned cloudy and white. The mixture was stirred at room temperature under nitrogen for 2 hours and was then filtered through sintered glass. A white solid was filtered off, but some still remained in the filtrate. The solvent was evaporated and the residue was dissolved in petroleum ether (~20 ml). The mixture was filtered again and the solvent removed to give a pale-yellow oil **41** (2.3 g, 87%). ¹H NMR (400 MHz; CDCl₃; Me₄Si) -0.14 (6H, s, Si(CH₃)₂), 0.05 (6H, s, Si(CH₃)₂), 0.68 (4H, s, SiCH₂CH₂Si), 1.51 (3H, d, *J* = 6.9, CH(CH₃)), 4.34 (1H, q, *J* = 6.9, CH(CH₃)), 7.15-7.36 (5H, m, Ar-H); *m/z* (CI) 264.2 (M+H)⁺ (calculated: 264.2), 248.1 (M-CH₃)⁺, 122.1 (M-SiMe₂CH₂CH₂SiMe₂)⁺, 105.1 (M-NSiMe₂CH₂CH₂SiMe₂)⁺.



6.3. Synthesis of (S)-N,N-dimethyl-1-phenylethan-1-amine **43**⁷⁶

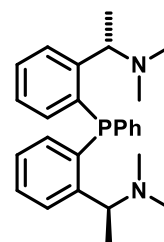
Formic acid (2.7 ml, 70.4 mmol, 3.5 eq.) and formaldehyde (35% aq., 3.7 ml, 50.3 mmol, 2.5 eq.) were added to (S)-phenylethylamine **35a** (2.6 ml, 20.1 mmol). The mixture was heated to 90 °C and stirred for 24h. The solution was then cooled to room temperature and 6 M HCl (7 ml, 2.1 eq.) was added. The resulting mixture was extracted with ether (3 x 6 ml). The aqueous layer was made basic using 50% aq. NaOH solution (5 ml) and was extracted with ether (3 x 6 ml). The organics were dried with MgSO₄ and the solvent removed to give a yellow oil (2.04 g). This was purified by column chromatography (EtOAc/hexane 20/80 to 50/50) to give a slightly yellow oil **43** (1.58 g, 53%). ¹H NMR (400 MHz; CDCl₃; Me₄Si) 1.37 (3H, d, *J* = 6.7, (CH₃)CH), 2.20 (6H, s, (CH₃)₂N), 3.24 (1H, q, *J* = 6.7, CH(CH₃)), 7.2-7.35 (5H, m, Ar-H); *m/z* (CI) 172.1 (M+Na)⁺



(calculated: 172.1), 171.1 ($M+Na-H$)⁺, 105.1 ($M-N(CH_3)_2$)⁺; CAS number 17279-31-1.

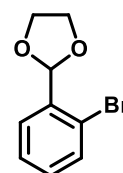
6.4. Synthesis of (1*S*,1'*S*)-1,1'-((phenylphosphanediyl)bis-(2,1-phenylene))bis(*N,N*-dimethylethan-1-amine) **44**⁷³

To a solution *n*-BuLi (2.5 M, 2.8 ml) in hexane (6.7 ml) in oven-dried glassware under a nitrogen atmosphere were added ether (5 ml) and (*S*)-*N,N*-dimethyl-1-phenylethylamine **43** (1.1 ml, 6.7 mmol). The mixture was refluxed for 5h and then was cooled to -78 °C and a solution of dichlorophenylphosphine (0.51 ml, 2.85 mmol, 0.425 eq.) in ether (3.4 ml) was added dropwise. After stirring overnight, the solvent was evaporated and ethanol (0.5 ml) then water (5 ml) were added. The product was extracted with DCM (3 x 5 ml), then dried with MgSO₄ and the solvent removed to give a thick yellow oil (1.37 g). This was purified by column chromatography (90% hexane/EtOAc + 2% Et₃N) to give a clear oil **44** (0.60 g, 52%). ¹H NMR (400 MHz; CDCl₃; Me₄Si) 1.04 (3H, d, *J* = 6.5, (CH₃)CH), 1.16 (3H, d, *J* = 6.5, (CH₃)CH), 2.14 (12H, s, 2x(CH₃)₂N), 3.98 (1H, quintet, *J* = 6.5, CH(CH₃)), 4.11 (1H, quintet, *J* = 6.5, CH(CH₃)), 6.82 (2H, m, Ar-*H*), 7.10 (2H, tdd, *J* = 7.5, 3.4, 1.2, Ar-*H*), 7.21 (2H, m, Ar-*H*), 7.28-7.38 (5H, m, Ar-*H*), 7.58 (2H, m, Ar-*H*); ³¹P{¹H} NMR (162 MHz; CDCl₃) -29.4 (s); *m/z* (CI) 405.2 ($M+H$)⁺ (calculated: 405.25), 360.2 ($M-NMe_2$)⁺.



6.5. Synthesis of 2-(2-bromophenyl)-1,3-dioxolane **49**⁸³

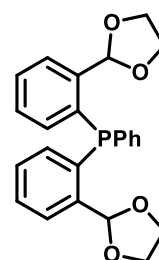
2-Bromobenzaldehyde (10 ml, 85.7 mmol) was dissolved in toluene (36 ml), and ethylene glycol (5.73 ml, 102.8 mmol) and *p*-toluenesulfonic acid (91 mg, 0.48 mmol) were added. The solution was refluxed in Dean-Stark apparatus (not under nitrogen) until water no longer condensed. The mixture was then made slightly basic using ethanolic potassium hydroxide (1 M, ~0.7 ml), then diluted with toluene (40 ml), washed with water (50 ml), dried with potassium carbonate and concentrated to give a clear colourless oil **49** (19.4 g, 99%). ¹H NMR (400 MHz; CDCl₃; Me₄Si) 4.1 (4H, m, OCH₂CH₂O), 6.1 (1H, s, Ar-CH), 7.2 (1H, dt, *J* = 1.8, 7.6,



Ar-*H*), 7.3 (1H, dt, $J = 1.0, 7.5$, Ar-*H*), 7.56 (1H, dd, $J = 1.1, 8.0$, Ar-*H*), 7.60 (1H, dd, $J = 1.8, 7.7$, Ar-*H*); m/z (CI) 229 (M+H)⁺ (calculated: 228.99), 231 (M+H)⁺, 185 (M-OCH₂CH₂)⁺, 187 (M-OCH₂CH₂)⁺, 149.1 (M-Br)⁺, 73 (M-PhBr)⁺; CAS number 34824-58-3.

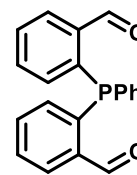
6.6. Synthesis of bis(2-(1,3-dioxolan-2-yl)phenyl)-(phenyl)phosphane **50**⁸²

2-(2-bromophenyl)-1,3-dioxolane **49** (19 g, 82.9 mmol) was dissolved in dry THF (225 ml) under a nitrogen atmosphere in an oven-dried round bottomed flask and cooled to -78 °C. A solution of *n*-BuLi in hexane (2.5 M, 36.2 ml, 90.4 mmol 1.09 eq.) was added dropwise over 40 minutes. The mixture was stirred for 2 hours at -78 °C and then dichlorophenylphosphine (5.63 ml, 41.5 mmol, 0.5 eq.) was added dropwise and the reaction mixture was stirred overnight at room temperature. The next day, water was added cautiously (~28 ml) and the layers were separated and the aqueous phase was extracted with toluene (2 x 60 ml). The organics were washed with water (160 ml) and dried with MgSO₄, filtered and concentrated to give a yellow oil. Recrystallisation using methanol gave white crystals **50** (12.3 g, 73%). ¹H NMR (400 MHz; CDCl₃; Me₄Si) 4.0 (8H, m, CH₂CH₂), 6.37 (2H, d, $J_{HP} = 5.0$, Ar-CH), 6.93 (2H, ddd, $J_{HH} = 1.1, 7.7, J_{HP} = 4.5$, Ar-*H*), 7.17-7.34 (7H, m, Ar-*H*), 7.39 (2H, td, $J = 1.2, 7.7$, Ar-*H*), 7.68 (2H, ddd, $J_{HH} = 1.0, 7.7, J_{HP} = 4.1$, Ar-*H*); ³¹P{¹H} NMR (162 MHz; CDCl₃) -26.2 (s); ¹³C{¹H} NMR (100 MHz; CDCl₃) 65.4 (s, CH₂CH₂), 101.7 (d, $J_{CP} = 24.1$, CH-O), 126.6 (d, $J_{CP} = 5.9$, Ar), 128.4 (m, Ar), 129.2 (d, $J_{CP} = 19.7$, Ar), 133.9 (d, $J_{CP} = 19.9$, Ar), 134.3 (s, Ar), 135.9 (d, $J_{CP} = 18.2$, Ar), 136.6 (d, $J_{CP} = 9.9$, Ar), 141.5 (d, $J_{CP} = 21.8$, Ar); m/z (CI) 407.1 (M+H)⁺ (calculated: 407.14), 363.1 (M-OCH₂CH₂)⁺, 349.1 (M-OCH₂CH₂O)⁺, 259.1 (M-(Ar-COCH₂CH₂O))⁺; CHN C₂₄H₂₃O₄P calculated: C 70.93, H 5.70, found: C 70.78, H 5.71; IR ν_{max}/cm^{-1} 2890 (C-H), 1478 (C=C), 1087 (C-O).



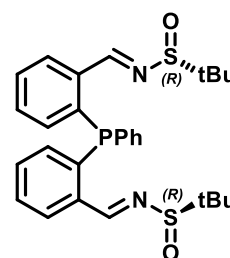
6.7. Synthesis of 2,2'-(phenylphosphanediyl)-dibenzaldehyde **45**⁸²

Bis(2-(1,3-dioxolan-2-yl)phenyl)-(phenyl)phosphane **50** (4.3 g, 10.58 mmol) was dissolved in acetone (120 ml) under a nitrogen atmosphere and p-toluenesulfonic acid (0.44 g, 2.34 mmol, 0.22 eq.) and water (0.38 ml, 21.16 mmol, 2 eq.) were added. The mixture was refluxed for 70 minutes. After allowing the reaction to cool to room temperature, water (30.2 ml) was added, and the acetone was removed on a rotary evaporator until yellow crystals formed. These were filtered off, washed with water and dried (1.84 g, 55%). ¹H NMR (400 MHz; CDCl₃; Me₄Si) 6.94 (2H, ddd, *J* = 1.0, 4.5, 7.5, Ar-*H*), 7.22-7.32 (2H, m, Ar-*H*), 7.32-7.42 (3H, m, Ar-*H*), 7.45 (2H, td, *J* = 1.4, 7.5, Ar-*H*), 7.53 (2H, td, *J* = 1.1, 7.6, Ar-*H*), 8.00 (2H, ddd, *J* = 1.3, 3.9, 7.6, Ar-*H*), 10.5 (2H, d, *J*_{HP} = 5.5, *H*-C=O); ³¹P{¹H} NMR (162 MHz; CDCl₃) -16.2 (s); ¹³C{¹H} NMR (100 MHz, CDCl₃) 129.0 (d, *J* = 7.6, Ar), 129.2 (s, Ar), 129.5 (s, Ar), 131.5 (d, *J* = 4.3, Ar), 133.9 (d, *J* = 37.0, Ar), 134.59 (d, *J* = 21.6, Ar), 135.3 (d, *J* = 10.0, Ar), 138.5 (d, *J* = 15.6, Ar), 140.4 (d, *J* = 24.9, Ar), 191.7 (d, *J* = 18.3, CHO); *m/z* (CI) 319.1 (M+H)⁺ (calculated: 319.09), 291.1 ((M+H)-CO)⁺; CHN C₂₀H₁₅O₂P calculated: C 75.47, H 4.75, found: C 75.17, H 4.83.



6.8. Synthesis of N,N'-((1E,1'E)-((phenylphosphanediyl)-bis(2,1-phenylene))bis(methanylylidene))bis(2-methylpropane-2-sulfinamide) **46**

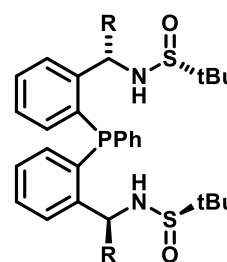
2,2'-(Phenylphosphanediyl)dibenzaldehyde **45** (1.7 g, 5.36 mmol) and (*R*)-2-methylpropane-2-sulfinamide **55** (1.3 g, 10.73 mmol, 2 eq.) were dissolved in dry THF (22 ml) under a nitrogen atmosphere in an oven-dried 2-necked round bottomed flask fitted with a condenser. Titanium(IV) tetraisopropoxide (6.35 ml, 21.45 mmol, 4 eq.) was added and the reaction mixture stirred overnight at 50 °C. The next day, the mixture was cooled to room temperature, diluted with ethyl acetate (25 ml) and poured into brine (70 ml) with rapid stirring. The resulting mixture, containing a white solid, was



filtered through Celite. The filtrate was transferred to a separatory funnel and the organic layer was washed with an equal volume of brine. The organic layer was dried with MgSO_4 , filtered and concentrated to give the crude product, a yellow solid. This was purified by column chromatography (70% hexane/EtOAc) to give the product, a white-yellow solid **46** (2.03 g, 72%). ^1H NMR (400 MHz; CDCl_3 ; Me_4Si) 0.99 (9H, s, $\text{C}(\text{CH}_3)_3$), 1.09 (9H, s, $\text{C}(\text{CH}_3)_3$), 6.87 (2H, m, Ar-H), 7.18-7.52 (9H, m, Ar-H), 7.96 (2H, m, Ar-H) 8.95 (1H, d, $J_{\text{HP}} = 4.10$, $\text{HC}=\text{N}$), 9.07 (1H, d, $J_{\text{HP}} = 5.13$, $\text{HC}=\text{N}$); $^{31}\text{P}\{^1\text{H}\}$ NMR (162 MHz; CDCl_3) -15.1 (s); $^{13}\text{C}\{^1\text{H}\}$ NMR (100 MHz, CDCl_3), 22.2 (s, $(\text{CH}_3)_3$), 22.3 (s, $(\text{CH}_3)_3$), 57.3 (s, $\text{CH}(\text{CH}_3)_3$), 57.4 (s, $\text{CH}(\text{CH}_3)_3$), 128.8 (d, $J_{\text{CP}} = 7.5$, Ar), 128.9 (d, $J_{\text{CP}} = 4.6$, Ar), 129.2 (s, Ar), 130.3 (d, $J_{\text{CP}} = 4.4$, Ar), 131.5 (d, $J_{\text{CP}} = 3.9$, Ar), 131.6 (d, $J_{\text{CP}} = 14.6$, Ar), 133.7 (s, Ar), 134.5 (s, Ar), 134.7 (s, Ar), 134.9 (s, Ar), 136.0 (d, $J_{\text{CP}} = 10.8$, Ar), 136.9 (d, $J_{\text{CP}} = 18.3$, Ar), 137.3 (d, $J_{\text{CP}} = 17.7$, Ar), 138.9 (d, $J_{\text{CP}} = 24.7$, Ar), 139.4 (d, $J_{\text{CP}} = 20.1$, Ar), 161.5 (s, $\text{C}=\text{N}$), 161.7 (s, $\text{C}=\text{N}$), 161.9 (s, $\text{C}=\text{N}$); m/z (ES) 547.2 ($\text{M}+\text{Na}$) $^+$ (calculated: 547.16), 525.2 ($\text{M}+\text{H}$) $^+$; CHN $\text{C}_{28}\text{H}_{33}\text{N}_2\text{O}_2\text{PS}_2$ calculated: C 64.10, H 6.34, N 5.34, found: C 63.76, H 6.33, N 5.24; IR $\nu_{\text{max}}/\text{cm}^{-1}$ 3053 (C-H imine), 2922 (C-H), 1594 (C=C), 1574 (C=N), 1086 (S=O).

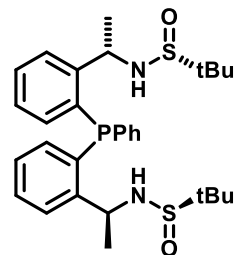
6.9. General method for Grignard addition to diimine **46**

A solution of the Grignard reagent in ether or THF (4 eq.) was added to a solution of the diimine **46** (1 eq.) in DCM (DCM:Grignard reagent ratio = 3:1) at $-48\text{ }^\circ\text{C}$ under a nitrogen atmosphere in oven-dried glassware. The mixture was stirred at this temperature for 4 hours, then warmed to room temperature and stirred overnight. The next day, aqueous NH_4Cl was added dropwise and the mixture was diluted with ethyl acetate. The aqueous layer was extracted with ethyl acetate (x2), and the combined organic layers were dried with Na_2SO_4 , filtered and concentrated. The crude product was purified by column chromatography (ethyl acetate/hexane) to give the pure products in good yields.



6.9.1. *N,N'*-((1*S*,1'*S*)-((phenylphosphanediy)bis(2,1-phenylene))bis(ethane-1,1-diyl))bis(2-methylpropane-2-sulfinamide) 47a

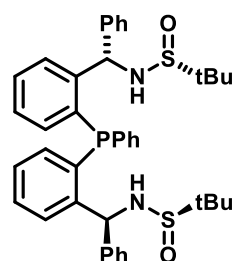
Mixture of diastereoisomers, d.r. 17:83 (0.36 g, about 70%). $^{31}\text{P}\{^1\text{H}\}$ NMR (162 MHz; CDCl_3) -28.9 (s), -28.6 (s); m/z (ES) 579.2 ($\text{M}+\text{Na}^+$) (calculated: 579.22).



6.9.2. *N,N'*-((1*S*,1'*S*)-((phenylphosphanediy)bis(2,1-phenylene))-bis(phenylmethylene))bis(2-methylpropane-2-sulfinamide) 47b

Major diastereoisomer (theoretically (S,S)):

(0.6 g, 46%) ^1H NMR (400 MHz; CDCl_3 ; Me_4Si) 1.15 (9H, s, tBu), 1.22 (9H, s, tBu), 1.68 (2H, br s, NH), 3.59 (1H, d, $J = 2.6$, $\text{CH}(\text{Ph})\text{NH}$), 3.85 (1H, d, $J = 3.6$, $\text{CH}(\text{Ph})\text{NH}$), 6.39 (1H, dd, $J_{\text{HH}} = 2.9$, $J_{\text{HP}} = 8.1$, Ar-*H*), 6.53 (1H, dd, $J_{\text{HH}} = 3.6$, $J_{\text{HP}} = 8.3$, Ar-*H*), 6.67 (1H, ddd, $J_{\text{HH}} = 0.8$, 6.8, $J_{\text{HP}} = 4.1$, Ar-*H*), 6.88 (1H, ddd, $J_{\text{HH}} = 0.9$, 6.9, $J_{\text{HP}} = 4.1$, Ar-*H*), 6.92-7.24 (15H, m, Ar-*H*), 7.31 (1H, td, $J = 0.8$, 7.6, Ar-*H*), 7.39 (1H, td, $J = 0.7$, 7.5, Ar-*H*), 7.64 (1H, dd, $J_{\text{HH}} = 7.5$, $J_{\text{HP}} = 4.2$, Ar-*H*), 7.68 (1H, dd, $J_{\text{HH}} = 7.3$, $J_{\text{HP}} = 4.4$, Ar-*H*); $^{31}\text{P}\{^1\text{H}\}$ NMR (162 MHz; CDCl_3) -27.8 (s); $^{13}\text{C}\{^1\text{H}\}$ NMR (100 MHz, CDCl_3) 22.6 (s, CH_3), 22.8 (s, CH_3), 55.9 (s, $\text{C}(\text{CH}_3)_3$), 56.1 (s, $\text{C}(\text{CH}_3)_3$), 59.3 (d, $J = 10.5$, $\text{CH}(\text{Ph})\text{NH}$), 59.8 (d, $J = 9.8$, $\text{CH}(\text{Ph})\text{NH}$), 127.2 (d, $J = 5.6$, Ar), 127.4 (s, Ar), 127.7 (s, Ar), 128.1 (d, $J = 5.6$, Ar), 128.2 (m, Ar), 128.6 (s, Ar), 128.7 (d, $J = 4.9$, Ar), 129.0 (s, Ar), 129.2 (s, Ar), 134.1 (s, Ar), 134.3 (m, Ar), 134.4 (s, Ar), 134.6 (s, Ar), 135.0 (m, Ar), 135.7 (d, $J = 15.2$, Ar), 141.2 (s, Ar), 141.6 (s, Ar), 145.8 (d, $J = 23.8$, Ar), 146.1 (d, $J = 23.8$, Ar); m/z (ES) 703.2551 ($\text{M}+\text{Na}^+$) (calculated: 703.2558); $\text{CHNS C}_{40}\text{H}_{45}\text{N}_2\text{O}_2\text{PS}_2$ calculated: C 70.56, H 6.66, N 4.11, S 9.42, found: C 70.23, H 6.72, N 3.96, S 9.11; IR $\nu_{\text{max}}/\text{cm}^{-1}$ 3195 (N-H), 2959 (C-H), 1600 (C=C), 1062 (S=O).



Other diastereoisomer (unknown configuration):

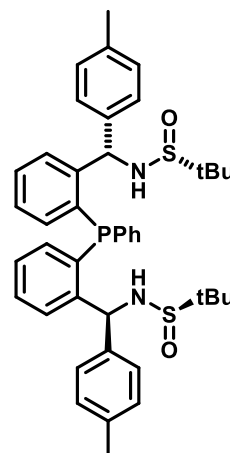
(0.14 g, 11%) ^1H NMR (400 MHz; CDCl_3 ; Me_4Si) 1.07 (9H, s, tBu), 1.16 (9H, s, tBu), 1.66 (2H, br s, NH), 3.99 (1H, s, $\text{CH}(\text{Ph})\text{NH}$), 4.75 (1H, s, $\text{CH}(\text{Ph})\text{NH}$), 6.69 (2H, d, $J_{\text{HP}} = 9.5$, Ar-*H*), 6.78-6.98 (4H, m, Ar-*H*), 7.03-7.25 (9H, m, Ar-*H*), 7.29-7.37 (3H, m, Ar-*H*), 7.39 (1H, t, $J_{\text{HH}} = 7.6$, Ar-*H*), 7.44 (2H, d, $J_{\text{HH}} =$

7.5, Ar-*H*), 7.55 (1H, dd, $J_{HH} = 7.3$, $J_{HP} = 4.6$, Ar-*H*), 7.93 (1H, dd, $J_{HH} = 7.3$, $J_{HP} = 4.8$, Ar-*H*); $^{31}\text{P}\{^1\text{H}\}$ NMR (162 MHz; CDCl_3) -30.0 (s); $^{13}\text{C}\{^1\text{H}\}$ NMR (100 MHz, CDCl_3) 22.7 (s, CH_3), 22.8 (s, CH_3), 55.9 (s, $\text{C}(\text{CH}_3)_3$), 56.0 (s, $\text{C}(\text{CH}_3)_3$), 58.8 (d, $J = 27.9$, $\text{CH}(\text{Ph})\text{NH}$), 60.6 (d, $J = 29.2$, $\text{CH}(\text{Ph})\text{NH}$), 115.6 (s, Ar), 119.5 (s, Ar), 127.3 (s, Ar), 127.6 (d, $J = 22.8$, Ar), 128.2 (d, $J = 6.6$, Ar), 128.3 (m, Ar), 128.6 (s, Ar), 128.8 (d, $J = 5.0$, Ar), 129.2 (d, $J = 5.0$, Ar), 129.3 (s, Ar), 129.6 (d, $J = 6.6$, Ar), 133.8 (m, Ar), 134.0 (s, Ar), 134.9 (m, Ar), 135.0 (d, $J = 13.1$, Ar), 135.3 (d, $J = 13.6$, Ar), 141.0 (s, Ar), 141.2 (s, Ar), 146.8 (d, $J = 23.9$, Ar), 147.5 (d, $J = 23.1$, Ar); m/z (ES) 703.2547 ($\text{M}+\text{Na}$)⁺ (calculated: 703.2558); $\text{CHNS C}_{40}\text{H}_{45}\text{N}_2\text{O}_2\text{PS}_2$ calculated: C 70.56, H 6.66, N 4.11, S 9.42, found: C 70.02, H 6.65, N 3.79, S 8.89; IR $\nu_{\text{max}}/\text{cm}^{-1}$ 3181 (N-H), 2978 (C-H), 1591 (C=C), 1059 (S=O).

6.9.3. *N,N'*-((1*S*,1'*S*)-((phenylphosphanediy)bis(2,1-phenylene))bis(*p*-tolylmethylene))bis(2-methylpropane-2-sulfinamide) 47c

Major diastereoisomer (theoretically (*S,S*)):

(0.74 g, 47%) ^1H NMR (400 MHz; CDCl_3 ; Me_4Si) 1.15 (9H, s, tBu), 1.22 (9H, s, tBu), 1.66 (2H, br s, NH), 2.15 (3H, s, Ar- CH_3), 2.20 (3H, s, Ar- CH_3), 3.55 (1H, d, $J = 2.5$, $\text{CH}(\text{Ar})\text{NH}$), 3.76 (1H, d, $J = 3.4$, $\text{CH}(\text{Ar})\text{NH}$), 6.30 (1H, dd, $J = 2.5$, 7.6, Ar-*H*), 6.48 (1H, dd, $J = 3.2$, 8.1, Ar-*H*), 6.63 (1H, dd, $J = 4.1$, 7.3, Ar-*H*), 6.75 (2H, d, $J = 7.9$, Ar-*H*), 6.81-6.91 (4H, m, Ar-*H*), 6.91-7.04 (4H, m, Ar-*H*), 7.08-7.23 (4H, m, Ar-*H*), 7.30 (1H, t, $J = 7.6$, Ar-*H*), 7.38 (1H, t, $J = 7.4$, Ar-*H*), 7.66 (2H, m, Ar-*H*); $^{31}\text{P}\{^1\text{H}\}$ NMR (162 MHz; CDCl_3) -27.8 (s); m/z (CI) 731 ($\text{M}+\text{Na}$)⁺ (calculated: 731.29); $\text{CHNS C}_{42}\text{H}_{49}\text{N}_2\text{O}_2\text{PS}_2$ calculated: C 71.16, H 6.97, N 3.95, S 9.04, found: C 69.6, H 6.85, N 3.64, S 8.91; IR $\nu_{\text{max}}/\text{cm}^{-1}$ 3214 (br N-H), 2919 (C-H), 1511 (C=C), 1062 (S=O).



Minor diastereoisomer (unknown configuration):

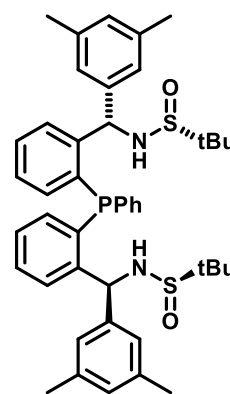
(0.17 g, 11%) ^1H NMR (400 MHz; CDCl_3 ; Me_4Si) 1.07 (9H, s, tBu), 1.16 (9H, s, tBu), 1.64 (2H, br s, NH), 2.19 (3H, s, Ar- CH_3), 2.27 (3H, s, Ar- CH_3), 3.95 (1H, s, $\text{CH}(\text{Ar})\text{NH}$), 4.67 (1H, s, $\text{CH}(\text{Ar})\text{NH}$), 6.61 (2H, d, $J = 9.1$, Ar-*H*), 6.72 (1H, d, $J = 8.4$, Ar-*H*), 6.91 (5H, m, Ar-*H*), 7.03 (2H, d, $J = 7.8$, Ar-*H*), 7.13 (4H,

m, Ar-*H*), 7.20 (2H, d, $J = 7.8$, Ar-*H*), 7.31 (2H, d, $J = 7.8$, Ar-*H*), 7.38 (1H, t, $J = 7.3$, Ar-*H*), 7.57 (1H, dd, $J = 4.7$, 7.16, Ar-*H*), 7.91 (1H, dd, $J = 4.5$, 7.16, Ar-*H*); $^{31}\text{P}\{^1\text{H}\}$ NMR (162 MHz; CDCl_3) -29.7 (s); m/z (CI) 731 ($\text{M}+\text{Na}^+$) (calculated: 731.29); $\text{CHNS C}_{42}\text{H}_{49}\text{N}_2\text{O}_2\text{PS}_2$ calculated: C 71.16, H 6.97, N 3.95, S 9.04, found: C 70.72, H 6.98, N 3.53, S 8.37; IR $\nu_{\text{max}}/\text{cm}^{-1}$ 3193 (br N-H), 2920 (C-H), 1512 (C=C), 1058 (S=O).

6.9.4. *N,N'*-((1*S*,1'*S*)-((phenylphosphanediyl)bis(2,1-phenylene))bis((3,5-dimethylphenyl)methylene))bis(2-methylpropane-2-sulfonamide) 47d

Major diastereoisomer (theoretically (*S,S*)):

(0.4 g, 54%) ^1H NMR (400 MHz; CDCl_3 ; Me_4Si) 1.13 (9H, s, tBu), 1.26 (9H, s, tBu), 1.83 (2H, br s, NH), 2.03 (6H, s, Ar- CH_3), 2.08 (6H, s, Ar- CH_3), 3.59 (1H, d, $J_{\text{HP}} = 2.2$, $\text{CH}(\text{Ar})\text{NH}$), 3.97 (1H, d, $J_{\text{HP}} = 3.5$, $\text{CH}(\text{Ar})\text{NH}$), 6.52 (2H, m, Ar-*H*), 6.62 (4H, s, Ar-*H*), 6.70 (1H, s, Ar-*H*), 6.76 (1H, dd, $J_{\text{HH}} = 7.5$, $J_{\text{HP}} = 3.9$, Ar-*H*) 6.87 (1H, dd, $J_{\text{HH}} = 7.5$, $J_{\text{HP}} = 4.0$, Ar-*H*), 7.00 (1H, t, $J = 7.4$, Ar-*H*), 7.07 (2H, t, $J = 7.5$, Ar-*H*), 7.16 (2H, m, Ar-*H*), 7.22 (1H, d, $J = 7.3$, Ar-*H*), 7.35 (2H, t, $J = 7.5$, Ar-*H*), 7.55 (1H, dd, $J = 4.3$, 7.6, Ar-*H*), 7.74 (1H, dd, $J = 4.4$, 7.6, Ar-*H*); $^{31}\text{P}\{^1\text{H}\}$ NMR (162MHz; CDCl_3) -28.4 (s); m/z (ES) 759.3156 ($\text{M}+\text{Na}^+$) (calculated: 759.3184); $\text{CHNS C}_{44}\text{H}_{53}\text{N}_2\text{O}_2\text{PS}_2$ calculated: C 71.71, H 7.25, N 3.80, S 8.70, found: C 70.91, H 7.31, N 3.57, S 8.29; IR $\nu_{\text{max}}/\text{cm}^{-1}$ 3223 (N-H), 3195 (C-H), 1601 (C=C), 1064 (S=O).



Another diastereoisomer (unknown configuration):

(0.19 g, 27%) ^1H NMR (400 MHz; CDCl_3 ; Me_4Si) 1.03 (9H, s, tBu), 1.18 (9H, s, tBu), 1.63 (2H, br s, NH), 2.10 (6H, s, Ar- CH_3), 2.23 (6H, s, Ar- CH_3), 3.62 (1H, br s, $\text{CH}(\text{Ar})\text{NH}$), 4.96 (1H, br s, $\text{CH}(\text{Ar})\text{NH}$), 6.57 (1H, d, $J_{\text{HP}} = 9.8$, Ar-*H*), 6.61 (1H, d, $J_{\text{HP}} = 10.0$, Ar-*H*), 6.68 (1H, s, Ar-*H*), 6.83 (1H, s, Ar-*H*), 6.84-6.89 (1H, m, Ar-*H*), 6.90 (2H, s, Ar-*H*), 7.03 (2H, t, J_{HH} and $J_{\text{HP}} = 7.4$, Ar-*H*), 7.07 (2H, s, Ar-*H*), 7.13 (2H, td, $J_{\text{HH}} = 3.0$, 7.2, Ar-*H*), 7.19 (2H, t, $J_{\text{HH}} = 6.8$, Ar-*H*), 7.31 (1H, t, $J_{\text{HH}} = 7.4$, Ar-*H*), 7.38 (1H, t, $J_{\text{HH}} = 7.6$, Ar-*H*), 7.54 (1H, dd, $J_{\text{HH}} = 7.3$, $J_{\text{HP}} = 4.6$, Ar-*H*), 7.94 (1H, dd, $J_{\text{HH}} = 7.3$, $J_{\text{HP}} = 4.6$, Ar-*H*); $^{31}\text{P}\{^1\text{H}\}$ NMR (162 MHz; CDCl_3) -29.8 (s); m/z (ES) 759.3170 ($\text{M}+\text{Na}^+$) (calculated:

759.3184); CHNS C₄₄H₅₃N₂O₂PS₂ calculated: C 71.71, H 7.25, N 3.80, S 8.70, found: C 70.72, H 7.25, N 3.61, S 8.48; IR ν_{max} /cm⁻¹ 3196 (N-H), 2915 (C-H), 1601 (C=C), 1060 (S=O).

Minor diastereoisomer (unknown configuration):

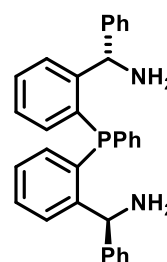
(0.013 g, 2%, not pure) ¹H NMR (400 MHz; CDCl₃; Me₄Si) 1.07 (9H, s, tBu), 1.15 (9H, s, tBu), 1.75 (2H, br s, NH), 1.98 (6H, s, Ar-CH₃), 2.07 (6H, s, Ar-CH₃), 3.56 (1H, d, J_{HP} = 2.5, CH(Ar)NH), 3.62 (1H, d, J_{HP} = 3.0, CH(Ar)NH), 6.18-7.73 (19H, m, Ar-H); ³¹P{¹H} NMR (162MHz; CDCl₃) -27.1 (s).

6.10. Synthesis of (1S,1'S)-((phenylphosphanediyl)bis(2,1-phenylene))bis(phenylmethanamine) 36b

N,N'-((1S,1'S)-((phenylphosphanediyl)bis(2,1-phenylene))bis-

(phenylmethanamine))bis(2-methylpropane-2-sulfinamide) **47b**

(1.92 g, 2.81 mmol) was dissolved in THF (6.2 ml) under a nitrogen atmosphere and 4 M HCl (2.8 ml, 11.26 mmol, 4 eq.) was added. The mixture was stirred at room temperature for 3

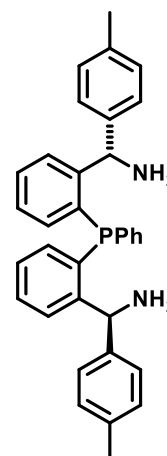


days, then 1 M NaOH (~11.5 ml) was added to basify the mixture. The product was extracted with ethyl acetate (3 x 30 ml) and washed with 1 M NaOH (30 ml), then water (30 ml). The organic layer was dried with MgSO₄, filtered and concentrated to give the crude product (1.33 g). This was purified by column chromatography to give the pure product, a white solid (0.99 g, 74%). ¹H NMR (400 MHz; CDCl₃; Me₄Si) 1.25 (4H, s, NH), 5.88 (1H, d, J_{HP} = 7.9, CH(Ph)NH₂), 6.06 (1H, d, J_{HP} = 7.7, CH(Ph)NH₂), 6.82 (1H, ddd, J = 0.7, 4.2, 7.5, Ar-H), 6.93 (1H, ddd, J = 1.0, 4.1, 7.6, Ar-H), 7.01-7.42 (20H, m, Ar-H), 7.48 (1H, dd, J = 4.6, 7.4, Ar-H); ³¹P{¹H} NMR (162 MHz; CDCl₃) -26.7 (s); ¹³C{¹H} NMR (100 MHz, CDCl₃) 56.2 (d, J = 15.2, CH(NH₂)), 56.5 (d, J = 15.7, CH(NH₂)), 126.6 (d, J = 14.6, Ar), 127.1 (d, J = 11.4, Ar), 127.2 (d, J = 18.4, Ar), 127.7 (d, J = 2.6, Ar), 127.8 (d, J = 2.4, Ar), 128.1 (d, J = 10.6, Ar), 128.6 (d, J = 7.0, Ar), 128.9 (s, Ar), 129.6 (d, J = 15.8, Ar), 134.1 (d, J = 5.7, Ar), 134.2 (d, J = 12.2, Ar), 134.3 (d, J = 20.1, Ar), 134.9 (d, J = 12.7, Ar), 136.1 (d, J = 9.6, Ar), 144.6 (d, J = 12.2, Ar), 150.0 (d, J = 2.2, Ar), 150.3 (d, J = 1.5, Ar); m/z (ES) 473.2

(M+H)⁺ (calculated: 473.2), 472.2 (M⁺), 471.2 (M-H), 456.2 (M-NH₂); CHN C₃₂H₂₉N₂P calculated: C 81.33, H 6.19, N 5.93, found: C 80.68, H 6.17, N 5.83.

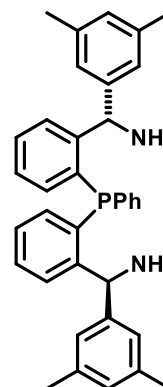
6.11. Synthesis of (1S,1'S)-((phenylphosphanediy)bis(2,1-phenylene))bis(p-tolylmethanamine) **36c**

N,N'-((1S,1'S)-((phenylphosphanediy)bis(2,1-phenylene))bis(p-tolylmethanamine))bis(2-methylpropane-2-sulfonamide) **47c** (0.74 g, 1.04 mmol) was dissolved in a mixture of THF (2.3 ml) and DCM (4.3 ml) under a nitrogen atmosphere. 4 M HCl (1.04 ml, 4.18 mmol, 4 eq.) was added and the reaction was stirred at room temperature for 3 days. 1 M NaOH (6.2 ml) was added to basify the mixture which was then extracted with ethyl acetate (3 x 16 ml). The organics were washed with 1 M NaOH (16 ml) and then water (16 ml). The organic solution was dried with MgSO₄, filtered and the solvent was removed under reduced pressure to give the crude product (0.47 g). This was purified by column chromatography (10% MeOH/DCM) to give the pure product, a white solid **36c** (0.38 g, 73%). ¹H NMR (400 MHz, CDCl₃, Me₄Si) 2.18 (3H, s, CH₃), 2.25 (3H, s, CH₃), 5.79 (1H, d, J_{HP} = 7.9, CH(Ar)NH₂), 6.01 (1H, d, J_{HP} = 7.4, CH(Ar)NH₂), 6.79 (1H, dd, J_{HH} = 7.7, J_{HP} = 4.3, Ar-H), 6.94 (5H, m, Ar-H), 7.04 (1H, t, J_{HH} = 7.5, Ar-H), 7.08-7.37 (12H, m, Ar-H), 7.39 (1H, dd, J_{HH} = 7.4, J_{HP} = 4.4, Ar-H), 7.51 (1H, dd, J_{HH} = 7.6, J_{HP} = 4.4, Ar-H); ³¹P{¹H} NMR (162 MHz, CDCl₃) -26.7 (s); ¹³C{¹H} NMR (100 MHz, CDCl₃) 20.9 (s, CH₃), 21.0 (s, CH₃), 56.0 (d, J = 25.4, CH(Ar)NH₂), 56.2 (d, J = 25.9, CH(Ar)NH₂), 126.9 (d, J = 1.2, Ar), 127.0 (s, Ar), 127.1 (d, J = 1.1, Ar), 127.3 (s, Ar), 127.6 (d, J = 5.1, Ar), 127.7 (d, J = 5.1, Ar), 128.6 (d, J = 6.9, Ar), 128.8 (d, J = 11.9, Ar), 129.6 (d, J = 26.6, Ar), 134.0 (s, Ar), 134.2 (d, J = 4.0, Ar), 134.4 (s, Ar), 134.5 (s, Ar), 134.9 (d, J = 13.1, Ar), 136.0 (s, Ar), 136.2 (d, J = 9.5, Ar), 136.3 (s, Ar), 141.6 (d, J = 17.8, Ar), 150.1 (d, J = 5.8, Ar), 150.3 (d, J = 6.3, Ar); m/z (CI) 501.2 (M+H)⁺ (calculated: 501.2), 485.2 (M-NH₂)⁺, 484.2 (M-CH₃)⁺, 468.2 (M-(2xNH₂))⁺; CHN C₃₄H₃₃N₂P calculated: C 81.57, H 6.64, N 5.60, found: C 81.34, H 6.79, N 5.37; IR ν_{max}/cm⁻¹ 3360 (br N-H), 3282 (br N-H), 2856-3050 (C-H), 1584 (C=C), 1177 (C-N); [α]_D = -42.3° (c 1.42, DCM).



6.12. Synthesis of (1S,1'S)-((phenylphosphanediyl)bis(2,1-phenylene))bis((3,5-dimethylphenyl)methanamine) **36d**

N,N'-((1S,1'S)-((phenylphosphanediyl)bis(2,1-phenylene))bis((3,5-dimethylphenyl)methylene))bis(2-methylpropane-2-sulfonamide) **47d** (0.82 g, 1.11 mmol) was dissolved in THF (2.4 ml) under a nitrogen atmosphere. 4 M HCl (1.1 ml, 4.45 mmol, 4 eq.) was added and the mixture was stirred at room temperature for 3 days. 1 M NaOH (6.5 ml) was added to basify the mixture, which was then extracted with ethyl acetate (3 x 20 ml). The organics were washed with 1 M NaOH (20 ml) and water (20 ml) and then dried with MgSO₄. This was filtered off and the solvent was removed under reduced pressure to produce the crude product (0.55 g). This was purified by column chromatography (10% MeOH/DCM) to give the pure product, an off-white solid **36d** (0.41 g, 70%). ¹H NMR (400 MHz, CDCl₃, Me₄Si) 2.11 (6H, s, CH₃), 2.12 (6H, s, CH₃), 5.96 (1H, d, *J*_{HP} = 8.6, CH(Ar)NH₂), 6.02 (1H, d, *J*_{HP} = 8.1, CH(Ar)NH₂), 6.70 (2H, s, Ar-H), 6.72 (2H, s, Ar-H), 6.79 (2H, s, Ar-H), 6.85 (1H, dd, *J*_{HH} = 7.5, *J*_{HP} = 4.2, Ar-H), 6.92 (1H, dd, *J*_{HH} = 7.6, *J*_{HP} = 4.2, Ar-H), 7.06 (1H, t, *J*_{HH} = 7.4, Ar-H), 7.15 (1H, t, *J*_{HH} = 7.4, Ar-H), 7.21 (2H, m, Ar-H), 7.27-7.37 (5H, m, Ar-H), 7.48 (2H, td, *J*_{HH} = 8.8, *J*_{HP} = 4.7, Ar-H); ³¹P{¹H} NMR (162 MHz, CDCl₃) -27.8 (s); ¹³C{¹H} NMR (100 MHz, CDCl₃) 21.2 (CH₃), 21.3 (CH₃), 56.0 (d, *J* = 11.5, CH(NH₂)), 56.2 (d, *J* = 11.8, CH(NH₂)), 124.9 (d, *J* = 2.1, Ar), 126.9 (s, Ar), 127.2 (s, Ar), 127.7 (d, *J* = 5.1, Ar), 127.9 (d, *J* = 4.6, Ar), 128.2 (s, Ar), 128.3 (s, Ar), 128.5 (d, *J* = 7.1, Ar), 128.7 (s, Ar), 129.7 (s, Ar), 134.0 (d, *J* = 11.3, Ar), 134.3 (s, Ar), 134.4 (d, *J* = 25.3, Ar), 135.0 (d, *J* = 12.7, Ar), 136.1 (d, *J* = 8.9, Ar), 137.5 (d, *J* = 13.6, Ar), 144.3 (d, *J* = 18.5, Ar), 150.5 (s, Ar); *m/z* (ES) 529.2765 (M+H)⁺ (calculated: 529.2773); CHN C₃₆H₃₇N₂P calculated: C 81.79, H 7.05, N 5.30, found: C 80.82, H 7.13, N 4.98.



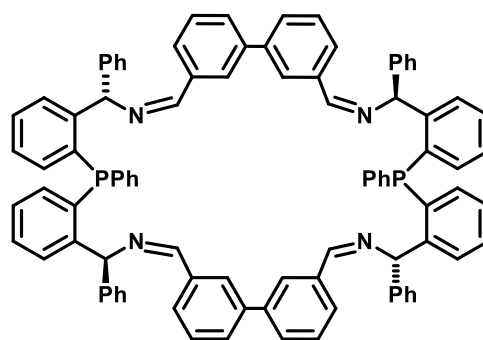
6.13. General method for cyclisation

The diamine (1 eq.) and sodium sulfate (13 eq.) were placed in a 2-necked flask fitted with a condenser. Degassed chloroform (dried with molecular

sieves overnight) was added so that the concentration of the diamine was 0.002 M. This mixture was heated to 50 °C and a solution of the dialdehyde (1 eq., 0.023 M in chloroform) was added dropwise via a dropping funnel over 8-10 hours. After the addition, the reaction was stirred for 48 hours, then cooled to room temperature, filtered and concentrated to give the crude product.

6.13.1. (3Z,5S,9S,10Z,14Z,16S,20S,21Z)-5,7,9,16,18,20-hexaphenyl-4,10,15,21-tetraaza-7,18-diphospha-1,2,12,13(1,3),6,8,17,19(1,2)-octabenzenacyclodocosaphane-3,10,14,21-tetraene 58a

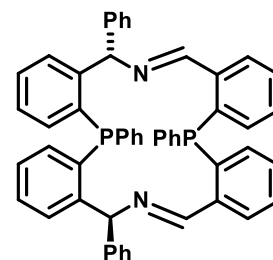
(0.09 g, 30%) ¹H NMR (400 MHz, CDCl₃, Me₄Si) 6.23 (2H, d, *J*_{HP} = 7.6, CH(Ph)N), 6.67 (2H, d, *J*_{HP} = 8.0, CH(Ph)N), 6.82 (2H, dd, *J*_{HH} = 7.0, *J*_{HP} = 3.6, Ar-*H*), 6.86 (2H, dd, *J*_{HH} = 7.2, *J*_{HP} = 4.0, Ar-*H*), 6.93 (2H, t, *J*_{HH} = 7.2, Ar-*H*), 7.00 (2H, d, *J*_{HH} = 7.6, Ar-*H*), 7.05-7.11 (4H, m, Ar-*H*), 7.16



(4H, t, *J*_{HH} = 7.6, Ar-*H*), 7.24 (2H, m, Ar-*H*), 7.36 (20H, m, Ar-*H*), 7.55 (10H, m, Ar-*H*), 7.71 (4H, m, Ar-*H*), 8.06 (2H, d, *J*_{HH} = 8.0, Ar-*H*), 8.18 (2H, dd, *J*_{HH} = 7.2, *J*_{HP} = 4.0, Ar-*H*), 8.28 (2H, s, N=CH); ³¹P{¹H} NMR (162 MHz, CDCl₃) -23.1 (s); *m/z* (ES) 1293.5142 (M+H)⁺ (calculated: 1293.5154).

6.13.2. (10S,11E,22E,24S)-5,10,17,24-tetraphenyl-5,10,17,24-tetrahydrotetrabenzo[*c,f,k,n*][1,9]diazabenzodiphenylphosphacyclohexa-decine 58c

(1.22 g, 96%) ¹H NMR (400 MHz; CDCl₃; Me₄Si) 6.06 (1H, d, *J*_{HP} = 7.1, CH(Ph)N), 6.54 (1H, d, *J*_{HP} = 5.1, CH(Ph)N), 6.87-7.70 (34H, m, Ar-*H*), 8.16 (1H, m, Ar-*H*), 8.42 (1H, m, Ar-*H*), 9.54 (1H, d, *J*_{HP} = 4.1, HC=N), 10.27 (1H, d, *J*_{HP} = 7.8, HC=N); ³¹P{¹H} NMR (162 MHz;



CDCl₃) -30.81 (1P, d, *J* = 8.9), -24.81 (1P, d, *J* = 8.9); *m/z* (ES) 755.274 (M+H)⁺ (calculated: 755.2745); CHN C₅₂H₄₀N₂P₂ calculated: C 82.74, H 5.34, N 3.71, found: C 79.92, H 5.51, N 3.51.

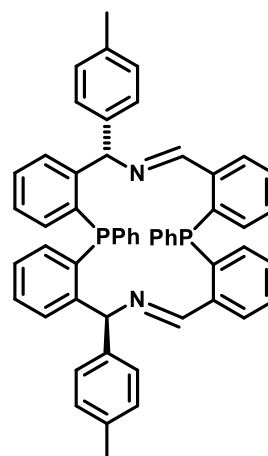
6.13.3. (10*S*,11*E*,22*E*,24*S*)-5,17-diphenyl-10,24-di-*p*-tolyl-5,10,17,24-tetrahydrotetrabenzo[*c,f,k,n*][1,9]diazaphosphacyclohexa-decine 58e

(0.37 g, quantitative) ^1H NMR (400 MHz, CDCl_3 , Me_4Si)

2.20 (3H, s, CH_3), 2.25 (3H, s, CH_3), 6.01 (1H, d, $J_{\text{HP}} = 7.0$, $\text{CH}(\text{Ar})\text{N}$), 6.49 (1H, d, $J_{\text{HP}} = 5.1$, $\text{CH}(\text{Ar})\text{N}$), 6.80 (2H, m, Ar-*H*), 6.87 (3H, m, Ar-*H*), 6.98 (4H, m, Ar-*H*), 7.13 (5H, m, Ar-*H*), 7.33 (13H, m, Ar-*H*), 7.44 (3H, m, Ar-*H*), 7.52 (1H, dd, $J_{\text{HH}} = 7.7$, $J_{\text{HP}} = 4.2$, Ar-*H*), 7.60 (2H, br s, Ar-*H*), 8.15 (1H, m, Ar-*H*), 8.41 (1H, m, Ar-*H*), 9.51 (1H, d, $J_{\text{HP}} = 4.0$, $\text{HC}=\text{N}$), 10.24 (1H, d, $J_{\text{HP}} = 7.9$, $\text{HC}=\text{N}$);

$^{31}\text{P}\{^1\text{H}\}$ NMR (162 MHz, CDCl_3) -30.77 (1P, d, $J = 9.4$), -

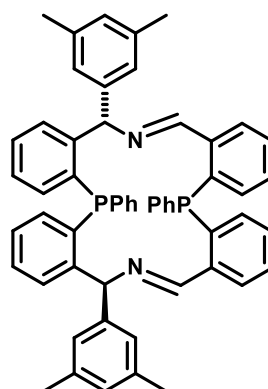
25.66 (1P, d, $J = 9.4$); $^{13}\text{C}\{^1\text{H}\}$ NMR (100 MHz, CDCl_3) 19.9 (s, CH_3), 20.0 (s, CH_3), 73.5 (d, $J = 19.5$, $\text{CH}(\text{Ar})\text{N}$), 73.8 (d, $J = 17.4$, $\text{CH}(\text{Ar})\text{N}$), 126.0 (s, Ar), 126.2 (m, Ar), 126.4 (s, Ar), 127.4 (s, Ar), 127.6 (m, Ar), 127.8 (m, Ar), 128.2 (d, $J = 11.5$, Ar), 128.7 (s, Ar), 129.0 (m, Ar), 129.2 (d, $J = 5.2$, Ar), 129.4 (s, Ar), 129.9 (s, Ar), 130.5 (s, Ar), 132.6 (d, $J = 19.1$, Ar), 132.9 (s, Ar), 133.2 (d, $J = 10.7$, Ar), 133.4 (s, Ar), 133.6 (d, $J = 14.5$, Ar), 134.3 (s, Ar), 134.4 (s, Ar), 134.5 (m, Ar), 134.9 (s, Ar), 135.0 (s, Ar), 135.1 (s, Ar), 135.2 (d, $J = 2.9$, Ar), 135.4 (s, Ar), 136.0 (d, $J = 3.8$, Ar), 137.4 (d, $J = 19.7$, Ar), 139.1 (d, $J = 20.5$, Ar), 139.5 (s, Ar), 139.8 (d, $J = 22.1$, Ar), 140.3 (s, Ar), 146.1 (d, $J = 7.9$, Ar), 146.3 (d, $J = 7.6$, Ar), 158.7 (dd, $J = 3.5$, $J = 25.3$, $\text{C}=\text{N}$), 160.0 (dd, $J = 4.5$, $J = 35.2$, $\text{C}=\text{N}$); m/z (ES) 783.3072 ($\text{M}+\text{H}^+$) (calculated: 703.3058); CHN $\text{C}_{54}\text{H}_{44}\text{N}_2\text{P}_2$ calculated: C 82.84, H 5.67, N 3.58, found: C 77.63, H 5.60, N 3.13.



6.13.4. (10*S*,11*E*,22*E*,24*S*)-10,24-bis(3,5-dimethylphenyl)-5,17-diphenyl-5,10,17,24-tetrahydrotetrabenzo[*c,f,k,n*][1,9]diazaphosphacyclohexadecine

(0.37 g, quantitative) ^1H NMR (400 MHz, CDCl_3 , Me_4Si)

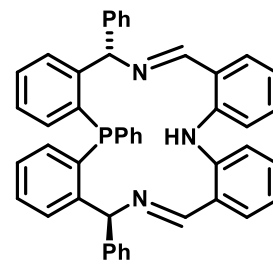
2.11 (6H, s, 2 x CH_3), 2.15 (6H, s, 2 x CH_3), 5.96 (1H, d, $J_{\text{HP}} = 6.9$, $\text{CH}(\text{Ar})\text{N}$), 6.53 (2H, s, Ar-*H*), 6.57 (1H, d, $J_{\text{HP}} = 6.0$, $\text{CH}(\text{Ar})\text{N}$), 6.64 (2H, s, Ar-*H*), 6.68 (1H, s, Ar-*H*),



6.75 (1H, s, Ar-*H*), 6.92 (1H, m, Ar-*H*), 7.08-7.19 (4H, m, Ar-*H*), 7.29-7.42 (12H, m, Ar-*H*), 7.46 (4H, m, Ar-*H*), 7.61 (3H, m, Ar-*H*), 8.16 (1H, m, Ar-*H*), 8.46 (1H, m, Ar-*H*), 9.48 (1H, d, $J_{\text{HP}} = 4.0$, HC=N), 10.29 (1H, d, $J_{\text{HP}} = 8.2$, HC=N); $^{31}\text{P}\{^1\text{H}\}$ NMR (162 MHz, CDCl_3) -31.24 (1P, d, $J = 8.2$), -24.45 (1P, d, $J = 8.2$); $^{13}\text{C}\{^1\text{H}\}$ NMR (100 MHz, CDCl_3) 21.3 (s, CH_3), 21.3 (s, CH_3), 75.2 (d, $J = 13.2$, CH(Ar)N), 75.4 (d, $J = 14.1$, CH(Ar)N), 124.9 (s, Ar), 125.3 (s, Ar), 127.1 (s, Ar), 127.2 (m, Ar), 127.4 (s, Ar), 128.1 (s, Ar), 128.5-128.9 (m, Ar), 129.2 (d, $J = 14.7$, Ar), 129.8 (s, Ar), 130.0 (m, Ar), 130.2 (d, $J = 5.0$, Ar), 130.5 (s, Ar), 130.9 (s, Ar), 131.5 (s, Ar), 133.5 (s, Ar), 133.7 (m, Ar), 134.2 (m, Ar), 134.5 (m, Ar), 134.7 (s, Ar), 135.1 (d, $J = 11.1$, Ar), 135.7 (s, Ar), 135.9 (s, Ar), 136.1 (s, Ar), 136.3 (d, $J = 6.8$, Ar), 136.4 (s, Ar), 137.1 (s, Ar), 137.5 (s, Ar), 143.2 (s, Ar), 144.2 (s, Ar), 147.0 (d, $J = 22.3$, Ar), 147.5 (d, $J = 22.3$, Ar), 159.7 (dd, $J = 2.7$, $J = 26.7$, C=N), 160.9 (dd, $J = 3.8$, $J = 36.0$, C=N); m/z (ES) 811.3369 ($\text{M}+\text{H}^+$) (calculated: 811.3371); CHN $\text{C}_{56}\text{H}_{48}\text{N}_2\text{P}_2$ calculated: C 82.94, H 5.97, N 3.45, found: C 79.87, H 6.11, N 2.98.

6.13.5. (10*E*,12*S*,22*S*,23*E*)-12,17,22-triphenyl-5,12,17,22-tetrahydrotetrabenzo[*c,f,k,n*][1,5,9]triazaphosphacyclohexa-decine 58d

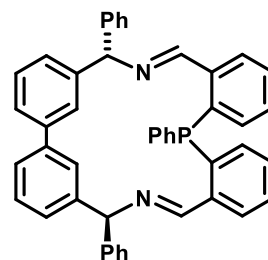
(0.34 g, quantitative) ^1H NMR (400 MHz, CDCl_3 , Me_4Si) 6.55 (1H, s, CH(Ph)N), 6.71 (1H, d, $J = 9.4$, CH(Ph)N), 6.79 (1H, t, $J = 7.2$, Ar-*H*), 6.84 (1H, m, Ar-*H*), 6.88-6.95 (3H, m, Ar-*H*), 6.98 (2H, d, $J = 7.2$, Ar-*H*), 7.06-7.53 (22H, m, Ar-*H*), 7.59 (1H, d, $J = 8.0$, Ar-*H*), 8.01 (1H, d, $J = 7.7$, Ar-*H*), 8.31 (1H, s, HC=N), 9.10 (1H, s, HC=N), 12.23 (1H, s, NH); $^{31}\text{P}\{^1\text{H}\}$ NMR (162 MHz, CDCl_3) -15.4 (s); $^{13}\text{C}\{^1\text{H}\}$ NMR (100 MHz, CDCl_3) 73.0 (s, CH(Ph)N), 73.2 (s, CH(Ph)N), 111.8 (s, Ar), 116.8 (s, Ar), 118.6 (s, Ar), 123.6 (s, Ar), 126.3 (s, Ar), 127.0 (m, Ar), 127.4 (s, Ar), 127.9 (m, Ar), 128.2 (s, Ar), 128.7 (s, Ar), 128.9 (d, $J = 7.7$, Ar), 129.6 (s, Ar), 130.3 (s, Ar), 130.5 (s, Ar), 130.7 (s, Ar), 130.8 (d, $J = 4.6$, Ar), 131.3 (s, Ar), 131.4 (d, $J = 5.1$, Ar), 132.4 (s, Ar), 134.2 (s, Ar), 136.1 (d, $J = 22.1$, Ar), 137.5 (d, $J = 21.1$, Ar), 140.7 (s, Ar), 141.1 (s, Ar), 144.5 (s, Ar), 146.2 (s, Ar), 160.6 (d, $J = 2.8$, C=N), 164.6 (s, C=N); m/z (ES) 662.2728 ($\text{M}+\text{H}^+$) (calculated: 662.2725).



6.13.6. (3*S*,4*E*,9*E*,11*S*)-3,7,11-triphenyl-4,10-diaza-7-phospha-1,2(1,3),6,8(1,2)-tetrabenzenacycloundecaphane-4,9-diene 71

¹H NMR (400 MHz, CDCl₃, Me₄Si) 5.63 (1H, s, C-H(Ph)N), 5.98 (1H, s, CH(Ph)N), 6.80 (1H, dd, *J* = 7.3, *J* = 3.8, Ar-*H*), 6.93 (1H, dd, *J* = 7.6, *J* = 3.4, Ar-*H*), 6.96-7.62 (26H, m, Ar-*H*), 7.85 (2H, m, Ar-*H*), 8.29 (1H, s, Ar-*H*), 8.85 (1H, s, HC=N), 9.14 (1H, d, *J* = 2.2, HC=N);

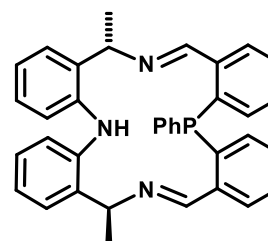
³¹P{¹H} NMR (162 MHz, CDCl₃) -18.1 (s); *m/z* 647.3 (M+H)⁺ (calculated: 647.26).



6.13.7. (10*S*,11*E*,22*E*,24*S*)-10,24-dimethyl-17-phenyl-5,10,17,24-tetrahydrotetrabenzo[*c,f,k,n*][1,5,9]triazaphosphacyclohexa-decine 79

(0.094 g, quantitative) Note: the ¹H NMR spectrum for this compound was too impure to assign the peaks.

³¹P{¹H} NMR (162 MHz, CDCl₃) -24.3 (s).

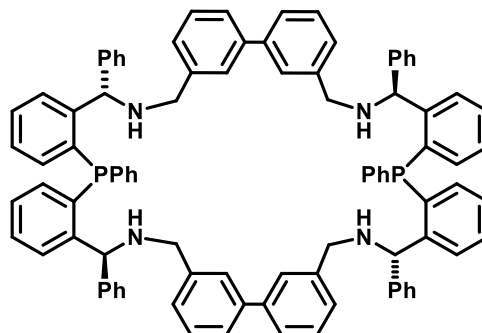


6.14. General procedure for the reduction of the imine macrocycles

Sodium borohydride (52 eq.) was put into an oven-dried 2-necked round bottomed flask fitted with a condenser under nitrogen. To this was added a solution of the imine macrocycle in DCM (0.066 M) at 0 °C. An equal volume of methanol was added slowly and this mixture was stirred for 4 hours at 0 °C, and then heated to 40 °C for 24 hours. The reaction mixture was allowed to cool to room temperature and water was added slowly. The mixture was extracted with ethyl acetate (x 5), washed with water and brine, dried with Na₂SO₄ and concentrated to give the crude product. This was purified by column chromatography to give the pure product.

6.14.1. (5*S*,9*S*,16*S*,20*S*)-5,7,9,16,18,20-hexaphenyl-4,10,15,21-tetraaza-7,18-diphospha-1,2,12,13(1,3),6,8,17,19(1,2)-octabenzenacyclodocosaphane 37a

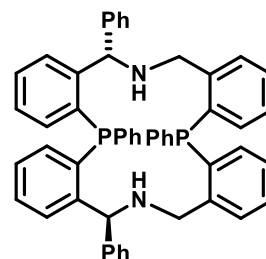
(0.11 g, 22%) ^1H NMR (400 MHz; CDCl_3 , Me_4Si) 3.05 (2H, d, $J_{\text{HH}} = 12.6$, CH_2), 3.40 (2H, d, $J_{\text{HH}} = 12.6$, CH_2), 3.48 (2H, d, $J_{\text{HH}} = 13.0$, CH_2), 3.57 (2H, d, $J_{\text{HH}} = 13.0$, CH_2), 5.69 (2H, d, $J_{\text{HP}} = 8.4$, $\text{CH}(\text{Ph})\text{NH}$), 5.89 (2H, d, $J_{\text{HP}} = 8.0$, $\text{CH}(\text{Ph})\text{NH}$), 6.76 (2H, dd, $J_{\text{HH}} = 7.5$, $J_{\text{HP}} = 4.2$, Ar-*H*), 6.84



(2H, dd, $J_{\text{HH}} = 7.7$, $J_{\text{HP}} = 3.8$, Ar-*H*), 6.92 (2H, s, Ar-*H*), 6.97-7.48 (52H, m, Ar-*H*), 7.53 (2H, dd, $J_{\text{HH}} = 7.8$, $J_{\text{HP}} = 4.2$, Ar-*H*), 7.92 (2H, dd, $J_{\text{HH}} = 7.6$, $J_{\text{HP}} = 4.4$, Ar-*H*); $^{31}\text{P}\{^1\text{H}\}$ NMR (162 MHz; CDCl_3) -26.62 (s); $^{13}\text{C}\{^1\text{H}\}$ NMR (100 MHz, CDCl_3) 52.4 (s, CH_2), 52.8 (s, CH_2), 63.5 (d, $J = 24.6$, $\text{CH}(\text{Ph})\text{NH}$), 64.4 (d, $J = 24.6$, $\text{CH}(\text{Ph})\text{NH}$), 125.7 (m, Ar), 126.7 (m, Ar), 126.9 (s, Ar), 127.1 (m, Ar), 127.4 (s, Ar), 127.7 (s, Ar), 127.9 (s, Ar), 128.0 (s, Ar), 128.2 (d, $J = 10.8$, Ar), 128.6 (m, Ar), 128.8 (s, Ar), 129.4 (s, Ar), 129.8 (s, Ar), 134.1 (d, $J = 17.4$, Ar), 134.6 (d, $J = 20.3$, Ar), 135.4 (d, $J = 12.8$, Ar), 136.1 (d, $J = 10.5$, Ar), 141.0 (m, Ar), 143.1 (d, $J = 15.1$, Ar), 148.0 (d, $J = 23.7$, Ar), 148.3 (d, $J = 23.1$, Ar); m/z (ES) 1301.5769 ($\text{M}+\text{H}$) $^+$ (calculated:1301.5780); CHN $\text{C}_{92}\text{H}_{78}\text{N}_4\text{P}_2$ calculated: C 84.90, H 6.04, N 4.30, found: C 83.28, H 6.23, N 4.13.

6.14.2. (10*S*,24*S*)-5,10,17,24-tetraphenyl-5,10,11,12,17,22,23,24-octahydrotetrabenzo[*c,f,k,n*][1,9]diazapenta[5,13]diphosphacyclohexa-decine 37b

(0.67 g, 69%) ^1H NMR (400 MHz; CDCl_3 ; Me_4Si) 3.42 (1H, d, $J_{\text{HH}} = 11.0$, $\text{CH}(\text{H})\text{NH}$), 3.49 (1H, d, $J_{\text{HH}} = 11.4$, $\text{CH}(\text{H})\text{NH}$), 4.14 (1H, dd, $J_{\text{HH}} = 11.4$, $J_{\text{HP}} = 3.8$, $\text{CH}(\text{H})\text{NH}$), 4.50 (1H, dd, $J_{\text{HH}} = 11.0$, $J_{\text{HP}} = 5.7$, $\text{CH}(\text{H})\text{NH}$), 5.49 (1H, d, $J_{\text{HP}} = 5.7$, $\text{CH}(\text{Ph})\text{NH}$), 5.66 (1H,

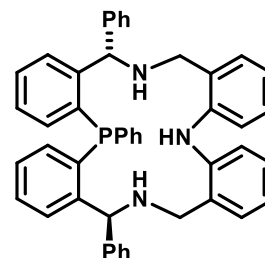


d, $J_{\text{HP}} = 4.8$, $\text{CH}(\text{Ph})\text{NH}$), 6.75 (1H, dd, $J_{\text{HH}} = 6.8$, $J_{\text{HP}} = 3.8$, Ar-*H*), 6.79 (1H, dd, $J_{\text{HH}} = 7.5$, $J_{\text{HP}} = 3.8$, Ar-*H*), 6.88 (1H, dd, $J_{\text{HH}} = 6.8$, $J_{\text{HP}} = 3.8$, Ar-*H*), 7.00 (1H, dd, $J_{\text{HH}} = 6.5$, $J_{\text{HP}} = 3.8$, Ar-*H*), 7.03-7.64 (32H, m, Ar-*H*); $^{31}\text{P}\{^1\text{H}\}$ NMR (162 MHz; CDCl_3 ; Me_4Si) -26.8 (1P, d, $J = 66.5$), -23.4 (1P, d, $J = 66.5$); $^{13}\text{C}\{^1\text{H}\}$

NMR (100 MHz, CDCl₃) 51.9 (d, $J = 17.9$, CH₂), 52.2 (s, $J = 15.7$, CH₂), 65.1 (d, $J = 12.2$, CH(Ph)NH), 65.3 (d, $J = 14.5$, CH(Ph)NH), 126.9 (d, $J = 1.4$, Ar), 127.6 (s, Ar), 127.7 (s, Ar), 127.8 (s, Ar), 128.2 (d, $J = 3.9$, Ar), 128.4 (d, $J = 10.3$, Ar), 128.6 (m, Ar), 128.9 (d, $J = 6.7$, Ar), 129.3 (s, Ar), 129.4 (s, Ar), 129.5 (d, $J = 4.4$, Ar), 129.6 (s, Ar), 129.8 (d, $J = 4.6$, Ar), 131.0 (dd, $J = 4.9$, $J = 9.5$, Ar), 133.5 (m, Ar), 133.9 (s, Ar), 134.2 (d, $J = 14.2$, Ar), 134.8 (d, $J = 14.8$, Ar), 135.0 (s, Ar), 135.2 (s, Ar), 135.7 (d, $J = 11.9$, Ar), 136.2 (d, $J = 13.1$, Ar), 136.5 (d, $J = 5.9$, Ar), 136.6 (d, $J = 3.0$, Ar), 136.8 (d, $J = 10.7$, Ar), 141.5 (d, $J = 8.9$, Ar), 143.9 (d, $J = 25.5$, Ar), 144.4 (d, $J = 26.7$, Ar), 147.5 (d, $J = 23.2$, Ar), 147.9 (d, $J = 23.7$, Ar); m/z (ES) 759.3066 (M+H)⁺ (calculated: 759.3058); CHN C₅₂H₄₄N₂P₂ calculated: C 82.30, H 5.84, N 3.69, found: C 81.34, H 5.93, N 3.62.

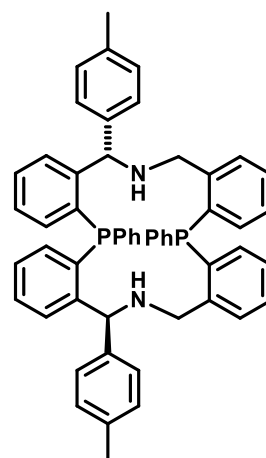
6.14.3. (12*S*,22*S*)-12,17,22-triphenyl-5,10,11,12,17,22,23,24-octahydrotetrabenzo[*c,f,k,n*][1,5,9]triazaphosphacyclohexadecine 37e

(0.15 g, 51%) ¹H NMR (400MHz, CDCl₃, Me₄Si) 3.60 (2H, d, $J = 12.2$, CH₂), 3.78 (1H, d, $J = 11.9$, CH(H)NH), 4.01 (1H, d, $J = 12.2$, CH(H)NH), 5.18 (1H, d, $J = 4.3$, CH(Ph)NH), 5.25 (1H, s, CH(Ph)NH), 6.49 (1H, d, $J = 7.3$, Ar-*H*), 6.66 (3H, m, Ar-*H*), 6.79 (2H, m, Ar-*H*), 6.91 (3H, m, Ar-*H*), 6.99-7.19 (5H, m, Ar-*H*), 7.20-7.43 (17H, m, Ar-*H*), 7.54 (1H, d, $J = 7.9$, Ar-*H*), 8.07 (1H, s, Ar(NH)Ar); ³¹P{¹H} NMR (162 MHz, CDCl₃) -18.1 (s); ¹³C{¹H} NMR (100 MHz, CDCl₃) 49.4 (s, CH₂), 51.2 (s, CH₂), 60.5 (d, $J = 19.0$, CH(Ph)NH), 65.4 (d, $J = 12.7$, CH(Ph)NH), 114.7 (s, Ar), 119.2 (s, Ar), 121.3 (d, $J = 26.8$, Ar), 126.4 (s, Ar), 126.9 (s, Ar), 127.2 (s, Ar), 127.3 (s, Ar), 127.7 (s, Ar), 127.9 (s, Ar), 128.2 (d, $J = 1.5$, Ar), 128.3 (s, Ar), 128.5 (d, $J = 5.0$, Ar), 128.7 (d, $J = 8.1$, Ar), 128.9 (d, Ar), 129.2 (d, $J = 5.0$, Ar), 129.4 (m, Ar), 129.5 (s, Ar), 131.3 (s, Ar), 131.6 (s, Ar), 132.4 (s, Ar), 133.7 (s, Ar), 135.3 (m, Ar), 137.1 (d, $J = 12.5$, Ar), 139.8 (s, Ar), 141.0 (s, Ar), 143.1 (s, Ar), 143.6 (s, Ar), 146.6 (d, $J = 22.9$, Ar), 147.0 (d, $J = 21.5$, Ar); m/z (ES) 666.3030 (M+H)⁺ (calculated: 666.3038); CHN C₄₆H₄₀N₃P calculated: C 82.98, H 6.06, N 6.31, found: C 82.24, H 6.13, N 6.04.



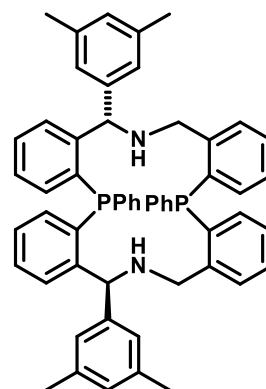
6.14.4. (10*S*,24*S*)-5,17-diphenyl-10,24-di-*p*-tolyl-5,10,11,12,17,22,23,24-octahydrotetrabenzo[*c,f,k,n*][1,9]diazabenzodiposphacyclohexadecine 37c

(0.21 g, 72%) ^1H NMR (400 MHz, CDCl_3 , Me_4Si) 2.28 (3H, s, CH_3), 2.29 (3H, s, CH_3), 3.40 (1H, d, $J_{\text{HH}} = 11.4$, $\text{CH}(\text{H})\text{NH}$), 3.48 (1H, d, $J_{\text{HH}} = 11.3$, $\text{CH}(\text{H})\text{NH}$), 4.12 (1H, m, $\text{CH}(\text{H})\text{NH}$), 4.46 (1H, dd, $J_{\text{HH}} = 11.1$, $J_{\text{HP}} = 5.4$, $\text{CH}(\text{H})\text{NH}$), 5.45 (1H, d, $J_{\text{HP}} = 5.6$, $\text{CH}(\text{Ar})\text{NH}$), 5.64 (1H, d, $J_{\text{HP}} = 4.8$, $\text{CH}(\text{Ar})\text{NH}$), 6.73 (1H, dd, $J_{\text{HH}} = 7.3$, $J_{\text{HP}} = 3.4$, Ar-*H*), 6.79 (1H, dd, $J_{\text{HH}} = 7.6$, $J_{\text{HP}} = 3.0$, Ar-*H*), 6.86 (1H, dd, $J_{\text{HH}} = 7.5$, $J_{\text{HP}} = 3.8$, Ar-*H*), 6.98 (1H, dd, $J_{\text{HH}} = 7.3$, $J_{\text{HP}} = 3.1$, Ar-*H*), 7.01-7.25 (18H, m, Ar-*H*), 7.27-7.36 (5H, m, Ar-*H*), 7.40-7.61 (7H, m, Ar-*H*); $^{31}\text{P}\{^1\text{H}\}$ NMR (162 MHz, CDCl_3) -26.66 (1P, d, $J = 67.0$), -23.29 (1P, d, $J = 67.0$); $^{13}\text{C}\{^1\text{H}\}$ NMR (100 MHz, CDCl_3) 21.1 (m, CH_3), 52.1 (dd, $J = 13.8$, $J = 23.0$, CH_2), 64.9 (dd, $J = 16.5$, $J = 22.4$, $\text{CH}(\text{Ar})\text{NH}$), 127.5 (Ar), 127.6 (s, Ar), 128.1 (d, $J = 6.1$, Ar), 128.5 (m, Ar), 128.7-129.5 (m, Ar), 129.6 (s, Ar), 129.7 (d, $J = 4.7$, Ar), 131.0 (dd, $J = 5.0$, $J = 9.8$, Ar), 133.5 (m, Ar), 133.9 (s, Ar), 134.1 (d, $J = 7.2$, Ar), 134.7 (d, $J = 15.2$, Ar), 135.0 (m, Ar), 135.0 (m, Ar), 135.7 (s, Ar), 135.8 (s, Ar), 136.0 (s, Ar), 136.2 (s, Ar), 136.4 (s, Ar), 136.4 (s, Ar), 136.5 (s, Ar), 136.7 (s, Ar), 136.9 (d, $J = 10.8$, Ar), 138.4 (d, $J = 8.8$, Ar), 144.2 (dd, $J = 27.1$, $J = 44.7$, Ar), 147.9 (dd, $J = 23.6$, $J = 36.5$, Ar); m/z (ES) 787.3367 ($\text{M}+\text{H}^+$) (calculated: 787.3371); CHN $\text{C}_{54}\text{H}_{48}\text{N}_2\text{P}_2$ calculated: C 82.42, H 6.15, N 3.56, found: C 81.50, H 6.15, N 3.39.



6.14.5. (10*S*,24*S*)-10,24-bis(3,5-dimethylphenyl)-5,17-diphenyl-5,10,11,12,17,22,23,24-octahydrotetrabenzo[*c,f,k,n*][1,9]diazabenzodiposphacyclohexadecine 37d

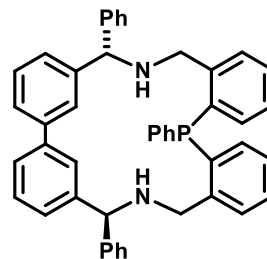
(0.13 g, 39%) ^1H NMR (400 MHz, CDCl_3 , Me_4Si) 2.20 (12H, s, CH_3), 3.44 (1H, d, $J_{\text{HH}} = 11.4$, $\text{CH}(\text{H})\text{NH}$), 3.53 (1H, d, $J_{\text{HH}} = 11.4$, $\text{CH}(\text{H})\text{NH}$), 4.10 (1H, dd, $J_{\text{HH}} = 11.0$, $J_{\text{HP}} = 4.3$, $\text{CH}(\text{H})\text{NH}$), 4.44 (1H, dd, $J_{\text{HH}} = 11.0$, $J_{\text{HP}} = 5.5$, $\text{CH}(\text{H})\text{NH}$), 5.42 (1H, d, $J_{\text{HP}} = 6.0$, $\text{CH}(\text{Ar})\text{NH}$), 5.70 (1H, d, $J_{\text{HP}} = 6.2$, $\text{CH}(\text{Ar})\text{NH}$), 6.71-6.82 (8H, m, Ar-*H*), 6.88



(1H, dd, $J_{HH} = 7.6$, $J_{HP} = 3.9$, Ar-*H*), 7.00-7.35 (16H, m, Ar-*H*), 7.41-7.61 (7H, m, Ar-*H*); $^{31}\text{P}\{^1\text{H}\}$ NMR (162 MHz, CDCl_3) -26.62 (1P, d, $J = 65.0$), -23.26 (1P, d, $J = 65.0$); $^{13}\text{C}\{^1\text{H}\}$ NMR (100 MHz, CDCl_3) 21.4 (m CH_3), 52.2 (dd, $J = 10.4$, $J = 23.2$, CH_2), 65.2 (dd, $J = 14.6$, $J = 22.7$, $\text{CH}(\text{Ar})\text{NH}$), 125.9 (d, $J = 6.8$, Ar), 127.4 (s, Ar), 127.6 (m, Ar), 128.5 (m, Ar), 128.9 (m, Ar), 129.3 (m, Ar), 129.5 (d, $J = 4.2$, Ar), 129.7 (m, Ar), 130.9 (m, Ar), 133.5 (s, Ar), 133.7 (d, $J = 14.3$, Ar), 133.9 (d, $J = 7.2$, Ar), 134.1 (s, Ar), 134.9 (d, $J = 15.2$, Ar), 135.3 (s, Ar), 135.5 (s, Ar), 135.8 (d, $J = 12.6$, Ar), 136.2 (d, $J = 12.8$, Ar), 136.5 (d, $J = 14.9$, Ar), 136.8 (dd, $J = 12.4$, $J = 21.6$, Ar), 137.4 (s, Ar), 137.6 (d, $J = 7.1$, Ar), 141.4 (d, $J = 15.6$, Ar), 144.2 (dd, $J = 26.6$, $J = 41.2$, Ar), 147.9 (dd, $J = 7.8$, $J = 24.5$, Ar); m/z (ES) 815.3678 ($\text{M}+\text{H}$) $^+$ (calculated: 815.3684); CHN $\text{C}_{56}\text{H}_{52}\text{N}_2\text{P}_2$ calculated: C 82.53, H 6.43, N 3.44, found: C 81.56, H 6.47, N 3.25.

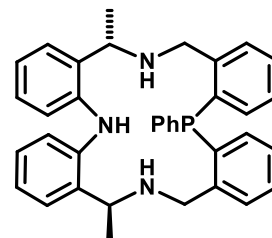
6.14.6. (3*S*,11*S*)-3,7,11-triphenyl-4,10-diaza-7-phospha-1,2(1,3),6,8(1,2)-tetrabenzenacycloundecaphane 63

(0.14 g, 50%) ^1H NMR (400 MHz, CDCl_3 , Me_4Si) 3.75 (1H, d, $J_{HH} = 12.6$, $\text{CH}(\text{H})\text{NH}$), 3.84 (1H, d, $J_{HH} = 13.6$, $\text{CH}(\text{H})\text{NH}$), 4.15 (1H, d, $J_{HH} = 13.6$, $\text{CH}(\text{H})\text{NH}$), 4.27 (1H, dd, $J_{HH} = 12.4$, $J_{HP} = 3.3$, $\text{CH}(\text{H})\text{NH}$), 4.93 (1H, s, $\text{CH}(\text{Ph})\text{NH}$), 5.05 (1H, s, $\text{CH}(\text{Ph})\text{NH}$), 6.86 (1H, dd, $J_{HH} = 7.5$, $J_{HP} = 4.6$, Ar-*H*), 6.89-7.00 (3H, m, Ar-*H*), 7.09-7.17 (4H, m, Ar-*H*), 7.19-7.24 (6H, m, Ar-*H*), 7.26-7.37 (9H, m, Ar-*H*), 7.40-7.49 (3H, m, Ar-*H*), 7.50-7.59 (3H, m, Ar-*H*), 8.14 (1H, s, Ar-*H*), 8.48 (1H, s, Ar-*H*); $^{31}\text{P}\{^1\text{H}\}$ NMR (162 MHz, CDCl_3) -23.1 (s); $^{13}\text{C}\{^1\text{H}\}$ NMR (100 MHz, CDCl_3) 50.7 (d, $J = 19.6$, CH_2), 51.6 (d, $J = 18.5$, CH_2), 65.7 (s, $\text{CH}(\text{Ph})\text{NH}$), 67.0 (s, $\text{CH}(\text{Ph})\text{NH}$), 125.0 (d, $J = 2.7$, Ar), 125.9 (d, $J = 5.5$, Ar), 126.4 (s, Ar), 127.0 (d, $J = 10.9$, Ar), 127.2 (d, $J = 8.7$, Ar), 127.5 (s, Ar), 127.7 (s, Ar), 128.4 (d, $J = 12.8$, Ar), 128.5 (m, Ar), 128.8 (d, $J = 4.3$, Ar), 129.0 (s, Ar), 129.7 (d, $J = 4.8$, Ar), 133.8 (d, $J = 20.9$, Ar), 134.5 (d, $J = 14.3$, Ar), 136.0 (d, $J = 15.8$, Ar), 136.6 (d, $J = 15.4$, Ar), 137.2 (d, $J = 9.5$, Ar), 140.9 (d, $J = 19.5$, Ar), 143.5 (s, Ar), 143.9 (d, $J = 8.6$, Ar), 144.1 (d, $J = 9.5$, Ar), 144.3 (d, $J = 6.8$, Ar), 144.7 (s, Ar), 145.0 (s, Ar); m/z (ES) 651.2923 ($\text{M}+\text{H}$) $^+$ (calculated: 651.2929).



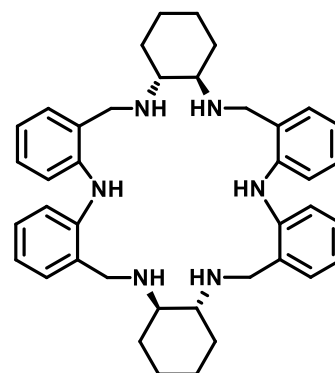
6.14.7. (10S,24S)-10,24-dimethyl-17-phenyl-5,10,11,12,17,22,23,24-octahydrotetrabenzo[*c,f,k,n*][1,5,9]triazia[13]phosphacyclohexa-decine 64

(0.042 g, 42%) ^1H NMR (400 MHz, CDCl_3 , Me_4Si) 1.09 (3H, d, $J = 6.3$, CH_3), 1.49 (3H, d, $J = 6.7$, CH_3), 3.55 (1H, d, $J = 12.1$, $\text{CH}(\text{H})\text{NH}$), 3.63 (1H, dd, $J = 11.6$, $J = 1.7$, $\text{CH}(\text{H})\text{NH}$), 3.90 (1H, dd, $J = 11.5$, $J = 2.7$, $\text{CH}(\text{H})\text{NH}$), 3.99 (1H, q, $J = 6.7$, $\text{CH}(\text{CH}_3)$), 4.07 (1H, q, $J = 6.3$, $\text{CH}(\text{CH}_3)$), 4.17 (1H, dd, $J = 12.1$, $J = 4.6$, $\text{CH}(\text{H})\text{NH}$), 6.72 (1H, dd, $J = 7.5$, $J = 4.2$, Ar-*H*), 6.82-6.97 (5H, m, Ar-*H*), 7.06-7.43 (15H, m, Ar-*H*), 8.80 (1H, s, ArNHAr); $^{31}\text{P}\{^1\text{H}\}$ NMR (162 MHz, CDCl_3) -24.33 (s); $^{13}\text{C}\{^1\text{H}\}$ NMR (100 MHz, CDCl_3) 20.1 (s, CH_3), 20.2 (s, CH_3), 50.6 (d, $J = 22.9$, CH_2), 52.2 (d, $J = 17.5$, CH_2), 53.6 (s, $\text{CH}(\text{Me})\text{NH}$), 59.5 (s, $\text{CH}(\text{Me})\text{NH}$), 116.8 (s, Ar), 119.8 (s, Ar), 120.2 (s, Ar), 127.2 (d, $J = 5.2$, Ar), 127.6 (s, Ar), 127.7 (s, Ar), 128.4 (d, $J = 7.4$, Ar), 128.8 (s, Ar), 129.0 (s, Ar), 129.3 (s, Ar), 129.5 (s, Ar), 129.6 (d, $J = 4.8$, Ar), 130.7 (d, $J = 4.3$, Ar), 131.9 (s, Ar), 132.0 (s, Ar), 133.3 (s, Ar), 133.8 (s, Ar), 134.5 (d, $J = 21.2$, Ar), 136.5 (m, Ar), 142.2 (s, Ar), 143.2 (s, Ar); m/z (ES) 542.2707 ($\text{M}+\text{H}$) $^+$ (calculated: 542.2725); CHN $\text{C}_{36}\text{H}_{36}\text{N}_3\text{P}$ calculated: C 79.83, H 6.70, N 7.76, found: C 78.38, H 6.68, N 7.05.



6.14.8. (11aR,15aR,28aR,32aR)-5,10,11,11a,12,13,14,15,15a,16,17,22,27,28,28a,29,30,31,32,32a,33,34-docosahydrohexabenzo[*b,f,i,m,q,t*][1,4,8,12,15,19]hexaazacyclodocosine 65

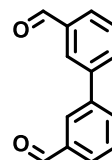
(0.058 g, 90%) ^1H NMR (400 MHz, CDCl_3 , Me_4Si) 1.08 (5H, m, Cy), 1.17 (4H, m, Cy), 1.66 (5H, d, $J = 6.8$, Cy), 2.07 (2H, br s, Cy), 2.26 (4H, br s, Cy), 3.51 (4H, d, $J = 11.7$, 2 x CH_2Ar), 3.74 (4H, d, $J = 11.7$, 2 x CH_2Ar), 6.75 (4H, t, $J = 7.4$, Ar-*H*), 7.08 (4H, d, $J = 7.3$, Ar-*H*), 7.12 (4H, t, $J = 7.3$, Ar-*H*), 7.33 (4H, d, $J = 8.0$, Ar-*H*), 8.35 (2H, s, ArNHAr); $^{13}\text{C}\{^1\text{H}\}$ NMR (100 MHz, CDCl_3) 25.2 (CH_2CH_2), 33.1 (CH_2CHNH), 50.6 (Ar CH_2NH), 62.5 (CHNH), 116.6 (Ar), 119.5 (Ar), 127.9 (Ar), 128.5 (Ar), 130.4 (Ar), 143.3 (Ar); m/z (ES) 615.4171 ($\text{M}+\text{H}$) $^+$ (calculated: 615.4175); CHN



C₄₀H₅₀N₆ calculated: C 78.14, H 8.20, N 13.67, found: C 77.08, H 8.41, N 12.70.

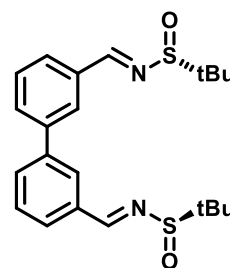
6.15. Synthesis of [1,1'-biphenyl]-3,3'-dicarbaldehyde **59**

To a degassed mixture of water (120 ml) and THF (300 ml) under nitrogen was added 3-bromobenzaldehyde **66** (4.44 g, 24.1 mmol), 3-formylphenylboronic acid **67** (5.4 g, 35.9 mmol), potassium carbonate (6 g) and Pd(PPh₃)₄ (0.6 g, 2 mol%). The mixture was heated to 80 °C for 62 hours. The THF was removed on a rotary evaporator and the aqueous solution was extracted with DCM (3 x 120 ml). The organic layers were dried with MgSO₄, filtered and concentrated to give the crude product, a pale-yellow solid. This was purified by column chromatography (100% DCM) to give a white solid **59** (4.57 g, 91%). ¹H NMR (400 MHz, CDCl₃, Me₄Si) 7.67 (2H, t, *J* = 7.7 Hz, Ar-*H*), 7.92 (4H, dd, *J* = 7.5, 4.5 Hz, Ar-*H*), 8.15 (2H, s, Ar-*H*), 10.12 (2H, s, CHO); ¹³C{¹H} NMR (100 MHz, CDCl₃) 128.00 (Ar), 129.46 (Ar), 129.79 (Ar), 132.98 (Ar), 137.11 (Ar), 140.71 (Ar), 192.00 (CHO).



6.16. Synthesis of (R,R)-N,N'-((1E,1'E)-[1,1'-biphenyl]-3,3'-diylbis(methaneylylidene))bis(2-methylpropane-2-sulfinamide) **68**

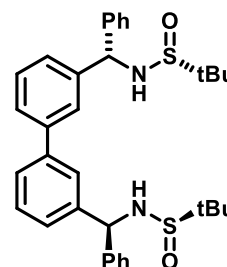
Dialdehyde **59** (2.1 g, 10 mmol) was dissolved in THF (30 ml) in an oven-dried flask under nitrogen. Ti(OiPr)₄ (12 ml, 40 mmol) was added and the resulting solution was stirred for 10 minutes. A solution of (*R*)-*t*-butanesulfinamide (2.42 g, 20 mmol) in THF (10 ml) was added and the mixture was stirred at 50 °C for 18 h. The reaction was quenched with brine and filtered through Celite. The filtrate was washed with brine, and the organics were dried over anhydrous Na₂SO₄, filtered and concentrated. The crude product was purified by column chromatography (30% EtOAc, 70% petroleum ether) to give **68** (2.46 g, 60%) as a white solid. ¹H NMR (400 MHz, CDCl₃, Me₄Si) 1.28



(18H, s, 6 x CH_3), 7.60 (2H, t, $J = 8.0$, Ar- H), 7.78 (2H, d, $J = 8.0$, Ar- H), 7.87 (2H, d, $J = 7.6$, Ar- H), 8.11 (2H, s, Ar- H), 8.67 (2H, s, 2 x $\text{HC}=\text{N}$); $^{13}\text{C}\{^1\text{H}\}$ NMR (100 MHz, CDCl_3) 22.7 (CH_3), 57.9 ($\text{CH}(\text{CH}_3)_3$), 127.7 (Ar), 129.0 (Ar), 129.6 (Ar), 131.1 (Ar), 141.0 (Ar), 162.5 ($\text{C}=\text{N}$); m/z 439.1 ($\text{M}+\text{Na}$) $^+$ (calculated: 439.1).

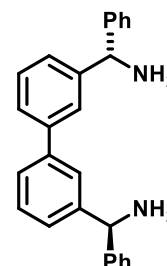
6.17. Synthesis of (R,R)-N,N'-((1S,1'S)-[1,1'-biphenyl]-3,3'-diylbis(phenylmethyle))bis(2-methylpropane-2-sulfinamide) **69**

A solution of **68** (1.95 g, 4.68 mmol) in DCM (13.7 ml) in an oven-dried round bottomed flask under nitrogen was cooled to $-48\text{ }^\circ\text{C}$ and PhMgBr (15 ml, 3.0 M/ Et_2O , 15.44 mmol) was added over 20 minutes. The mixture was stirred at this temperature for 50 minutes and was allowed to warm to room temperature overnight. The reaction was quenched with saturated ammonium chloride and extracted with EtOAc (x 2). The combined organics were dried over anhydrous Na_2SO_4 , filtered, and concentrated. The residue was purified by column chromatography (100% EtOAc) to give **69** (0.6 g, 18%). ^1H NMR (400 MHz, CDCl_3 , Me_4Si) 1.28 (18H, s, 6 x CH_3), 3.73 (2H, d, $J = 2.2$, NH), 5.70 (2H, d, $J = 2.2$, $\text{CH}(\text{Ph})\text{NH}$), 7.23-7.28 (2H, m, Ar- H), 7.33 (4H, t, $J = 7.7$, Ar- H), 7.37-7.48 (10H, m, Ar- H), 7.60 (2H, s, Ar- H); $^{13}\text{C}\{^1\text{H}\}$ NMR (100 MHz, CDCl_3) 22.7 (CH_3), 53.4 ($\text{C}(\text{CH}_3)_3$), 55.9 ($\text{CH}(\text{Ph})$), 62.2 ($\text{CH}(\text{Ph})$), 126.5 (Ar), 126.7 (Ar), 126.9 (Ar), 127.3 (Ar), 128.9 (Ar), 129.1 (Ar), 141.2 (Ar), 141.8 (Ar), 142.6 (Ar); m/z 573.3 ($\text{M}+\text{H}$) $^+$ (calculated: 573.26).



6.18. Synthesis of (1S,1'S)-[1,1'-biphenyl]-3,3'-diylbis(phenylmethan-amine) **70**

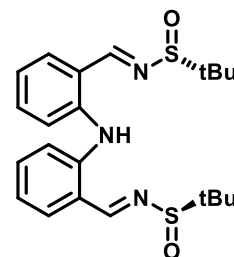
To a solution of **69** (0.6 g, 1 mmol) in THF (6.6 ml) was added a solution of HCl in 1,4-dioxane (4 M, 2.1 ml, 8.4 mmol) at room temperature. The resulting mixture was then stirred at room temperature for 72 h. The precipitate was filtered and washed



with diethyl ether to give the white HCl salt. To this salt was added dropwise a 2 M K₂CO₃ solution until the mixture reached pH 11. The mixture was extracted with ethyl acetate and the combined organics were washed with brine, dried over Na₂SO₄, filtered, and the solvent removed to give **70** (0.2 g, 52%). ¹H NMR (400 MHz, CDCl₃, Me₄Si) 5.27 (2H, s, 2 x CH(Ph)NH₂), 7.23 (2H, m, Ar-H), 7.29-7.45 (14H, m, Ar-H), 7.60 (2H, s, Ar-H); ¹³C{¹H} NMR (100 MHz, CDCl₃) 59.84 (CH(Ph)NH), 125.80 (Ar), 125.92 (Ar), 126.93 (Ar), 127.01 (Ar), 128.52 (Ar), 128.88 (Ar), 141.40 (Ar), 145.48 (Ar), 146.10 (Ar); m/z 364.2 (M⁺) (calculated: 364.2).

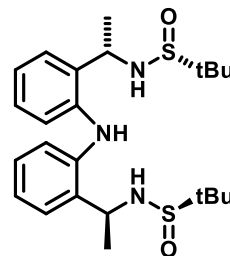
6.19. Synthesis of (R,R)-N,N'-((1E,1'E)-(azanediylbis(2,1-phenylene))-bis(methaneylylidene))bis(2-methylpropane-2-sulfinamide) **76**

Dialdehyde **61** (0.29 g, 1.3 mmol) and sulfinamide **55** (0.35 g, 2.86 mmol) were dissolved in THF (5.2 ml) in an oven-dried round bottomed flask under nitrogen. Ti(OiPr)₄ (1.5 ml, 5.2 mmol) was added and the mixture was heated to 50 °C overnight. Next day, the mixture was cooled to room temperature and diluted with ethyl acetate (5.2 ml). The mixture was poured into brine (15 ml) with rapid stirring, and then filtered through Celite. The filtrate was washed with brine, dried with MgSO₄, filtered and concentrated to give the crude product as a thick yellow oil. This was purified by column chromatography (70% hexane/ethyl acetate) to give the pure product **76** as a thick yellow oil which slowly solidifies (0.43 g, 76%). ¹H NMR (400 MHz, CDCl₃, Me₄Si) 1.16 (18H, s, 6 x CH₃), 7.05 (2H, td, *J* = 1.0, *J* = 7.4, Ar-H), 7.39 (2H, td, *J* = 1.4, *J* = 7.8, Ar-H), 7.54 (2H, d, *J* = 8.2, Ar-H), 7.66 (2H, dd, *J* = 1.5, *J* = 7.6, Ar-H), 8.67 (2H, 2 x HC=N), 10.79 (1H, s, NH); ¹³C{¹H} NMR (100 MHz, CDCl₃) 22.41 (CH₃), 57.69 (C(CH₃)₃), 118.52 (Ar), 121.20 (Ar), 121.94 (Ar), 132.93 (Ar), 134.85 (Ar), 143.22 (Ar), 162.25 (C=N); m/z (ES) 432.1785 (M+H)⁺ (calculated: 432.1779).



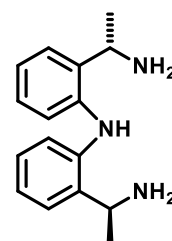
6.20. Synthesis of (R,R)-N,N'-((1S,1'S)-(azanediylbis(2,1-phenylene))-bis(ethane-1,1-diyl))bis(2-methylpropane-2-sulfinamide) **77**

The chiral diimine **76** (0.12 g, 0.28 mmol) was dissolved in dry DCM (2.2 ml) in an oven-dried round bottomed flask under nitrogen. The solution was cooled to -48 °C and methylmagnesium bromide (0.37 ml, 3 M/ether, 1.1 mmol) was added dropwise over 10 minutes, during which time the solution turned from clear yellow to red. This was stirred for 4 hours at -48 °C, then left at room temperature overnight. The next day, aqueous ammonium chloride (1.5 ml) was added slowly, during which time the mixture became warm. Ethyl acetate (approx. 2 ml) was added and the layers were separated. The aqueous layer was extracted with ethyl acetate (2 x 3 ml) and the organics were dried with Na₂SO₄, filtered and concentrated to give the crude product. This was purified by column chromatography (70% ethyl acetate/petroleum ether + 2% Et₃N) to give the pure product **77** as a thick orange oil (0.09 g, 69%). ¹H NMR (400 MHz, CDCl₃, Me₄Si) 1.20 (18H, s, CH(CH₃)₃), 1.60 (6H, d, *J* = 6.8, CH(CH₃)NH), 3.75 (2H, d, *J* = 3.3, NH), 4.82 (2H, dq, *J* = 3.6, *J* = 6.7, CH(CH₃)NH), 6.56 (1H, s, ArNHAr), 6.93 (2H, dd, *J* = 0.8, *J* = 8.0, Ar-H), 6.98 (2H, dt, *J* = 1.0, *J* = 7.5, Ar-H), 7.17 (2H, dt, *J* = 1.5, *J* = 7.9, Ar-H), 7.34 (2H, dd, *J* = 1.4, *J* = 7.7, Ar-H); *m/z* (ES) 486.2232 (M+Na)⁺ (calculated: 486.2225).



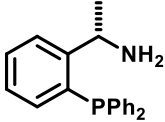
6.21. Synthesis of bis(2-((S)-1-aminoethyl)phenyl)amine **78**

The disulfonamide **77** (0.16 g, 0.34 mmol) was dissolved in THF (2.3 ml) and a solution of HCl in dioxane (1.35 ml, 2 M, 8 eq.) was added slowly. The mixture was stirred for 3 days at room temperature and then the white precipitate was filtered off and washed with ether. This was then dissolved in water (5 ml) and a 2 M solution of potassium carbonate was added until the mixture became pH 10. The product was extracted with ethyl acetate (5 x 5 ml) and the organics were washed with water and brine, dried with Na₂SO₄, filtered and the solvent



removed to give a light orange-brown oil **78** (0.055 g, 62%). ^1H NMR (400 MHz, CDCl_3 , Me_4Si) 1.47 (6H, d, $J = 6.5$, CH_3), 4.33 (2H, q, $J = 6.2$, $\text{CH}(\text{CH}_3)\text{NH}$), 6.88 (2H, t, $J = 7.3$, Ar- H), 7.13 (2H, t, $J = 7.6$, Ar- H), 7.22 (2H, d, $J = 8.1$, Ar- H), 7.29 (2H, d, $J = 7.6$, Ar- H), 8.88 (1H, br s, ArNHAr); m/z (ES) 256.1809 ($\text{M}+\text{H}$) $^+$ (calculated: 256.1814).

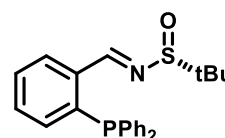
6.22. Synthesis of (S)-1-[2-(diphenylphosphino)phenyl]-ethylamine **81**

(S)-Phenylethylamine **35a** (1.26 ml, 10 mmol) was dissolved in dry ether (10 ml) in an oven-dried round bottomed flask under nitrogen. The solution was cooled to $-35\text{ }^\circ\text{C}$ (using a ) MeOH/ H_2O /dry ice bath), and *n*-butyllithium (2.5 M in hexanes, 4 ml, 10 mmol) was added dropwise with stirring. On addition of *n*-BuLi, the solution turned from clear and colourless to cloudy and white. After the solution was stirred at $-35\text{ }^\circ\text{C}$ for 20 minutes, Me_3SiCl (1.39 ml, 11 mmol) was added slowly. After stirring at $-35\text{ }^\circ\text{C}$ for 1 hour, more *n*-BuLi (2.5 M in hexanes, 12 ml, 30 mmol) was added dropwise, during which time the reaction mixture turned slightly yellow. This was then left to stir for 3 hours at $-35\text{ }^\circ\text{C}$, then warmed to room temperature and left to stir overnight. The next day, the yellow solution was cooled to $-35\text{ }^\circ\text{C}$ and a solution of ClPPh_2 (1.8 ml, 10 mmol) in dry ether (10 ml) was added dropwise over 45 minutes. The solution was stirred for 3 hours at $-35\text{ }^\circ\text{C}$ and then warmed to room temperature and stirred for 4 hours. 1 M HCl was added slowly until the reaction mixture became clear. During the addition of HCl, the mixture became slightly warm. The layers were separated and the aqueous layer was extracted with ether (4 x 10 ml). The organic layers were combined, dried with Na_2SO_4 and concentrated using a rotary evaporator to give the crude product as an orange oil (3.6 g). This was purified by column chromatography (hexane/EtOAc, 8/1 to 1/1, with 1-2% triethylamine) to give the product **81**, a white solid (0.9768 g, 32%). ^1H NMR (400 MHz; CDCl_3 ; Me_4Si) 1.24 (3H, d, $J = 6.2$, $\text{CH}(\text{CH}_3)\text{NH}_2$), 1.48 (2H, br s, NH_2), 4.90 (1H, m, $J = 6.6$, $\text{CH}(\text{CH}_3)\text{NH}_2$), 6.84 (1H, ddd, $J = 1.2, 4.4, 7.6$, Ar- H), 7.13 (1H, td, $J = 1.2, 7.4$, Ar- H), 7.20 – 7.42 (11H, m, Ar- H), 7.60 (1H, ddd, $J = 1.0, 4.2, 7.7$, Ar- H); $^{31}\text{P}\{^1\text{H}\}$ NMR (162 MHz; CDCl_3) -16.44 (s); m/z (CI) 306.14 ($\text{M}+\text{H}$) $^+$

(calculated: 306.14), 289.1 (M-NH₃)⁺, 228.1 (M-Ph)⁺, 187.1 (M-PhCH(CH₃)NH₂)⁺.

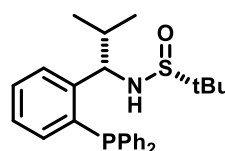
6.23. Synthesis of (R)-N-(2-(diphenylphosphaneyl)-benzylidene)-2-methylpropane-2-sulfinamide **89**

2-(diphenylphosphaneyl)benzaldehyde **88** (2 g, 6.89 mmol) and sulfinamide **55** (0.84 g, 6.89 mmol) were dissolved in THF (28 ml) to form a yellow solution. Titanium isopropoxide (4.1 ml, 13.78 mmol, 2 eq.) was added which turned the solution orange. The mixture was heated to 50 °C and was left to stir overnight. The next day, the mixture was cooled to room temperature and diluted with ethyl acetate (20 ml). Then the mixture was poured into brine (40 ml) with rapid stirring. The mixture was filtered through Celite, removing a white solid. The filtrate was washed with brine, dried with MgSO₄, filtered and the solvent removed to give the crude product as a thick orange oil (2.6 g). This was purified by column chromatography (85% hexane/ethyl acetate) to give the pure product **89** as a thick yellow oil (1.85 g, 68%). ¹H NMR (400 MHz, CDCl₃, Me₄Si) 1.08 (9H, s, CH₃), 6.96 (1H, dd, *J*_{HH} = 7.5, *J*_{HP} = 4.3, Ar-*H*), 7.20-7.27 (4H, m, Ar-*H*), 7.28-7.39 (7H, m, Ar-*H*), 7.45 (1H, t, *J* = 7.6, Ar-*H*), 7.98 (1H, dd, *J*_{HH} = 7.0, *J*_{HP} = 3.2, Ar-*H*), 9.12 (1H, d, *J*_{HP} = 4.7, HC=N); ³¹P{¹H} NMR (162 MHz, CDCl₃) -12.3.



6.24. Synthesis of (R)-N-((S)-1-(2-(diphenylphosphaneyl)-phenyl)-2-methylpropyl)-2-methylpropane-2-sulfinamide **90**

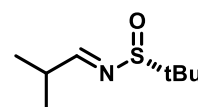
The chiral imine **89** (0.3 g, 0.76 mmol) was dissolved in dry DCM (6 ml) in an oven-dried round bottomed under nitrogen. The solution was cooled to -48 °C and isopropylmagnesium bromide (0.52 ml, 1.52 mmol, 2 M/ether, 2 eq.) was added slowly. After stirring for 4 hours at -48 °C, the mixture was allowed to warm to room temperature and was left to stir overnight. The next day, the mixture was cooled to 0 °C and a saturated solution of ammonium chloride



(3.9 ml) was added slowly. Ethyl acetate (10 ml) was added and the layers were separated. The aqueous layer was extracted with ethyl acetate (2 x 8 ml) and the organics were dried with Na₂SO₄, filtered and the solvent was removed to give the crude product (0.29 g). This was purified by column chromatography (50% ethyl acetate/hexane) to give the pure product **90** (0.22 g, 66%). ¹H NMR (400 MHz, CDCl₃, Me₄Si) 0.98-1.11 (15H, m, 5 x CH₃), 3.44 (1H, br m, NH), 4.43 (1H, dd, *J* = 7.9, *J* = 14.0, CH(CH₃)₂), 4.64 (1H, ddd, *J*_{HH} = 5.4, *J*_{HH} = 14.0, *J*_{HP} = 1.9, CH(iPr)NH), 6.92 (1H, ddd, *J*_{HH} = 7.5, *J*_{HP} = 4.3, *J*_{HP} = 0.9, Ar-*H*), 7.18-7.28 (4H, m, Ar-*H*), 7.29-7.38 (8H, m, Ar-*H*), 7.47 (1H, dd, *J*_{HH} = 7.5, *J*_{HP} = 4.6, Ar-*H*); ³¹P{¹H} NMR (162 MHz, CDCl₃) -16.3 (s); *m/z* (ES) 438.2020 (M+H)⁺ (calculated: 438.2020).

6.25. Synthesis of (R)-2-methyl-N-(2-methylpropylidene)-propane-2-sulfinamide **92**⁹⁷

(*R*)-*t*-butanesulfinamide **55** (10.51 g, 86.73 mmol), pyridinium *p*-toluenesulfonate (1.1 g, 4.34 mmol), and magnesium sulfate

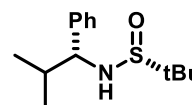


(52 g, 434 mmol) were placed into a round bottomed flask.

DCM (145 ml) was added followed by isobutyraldehyde **91** (15.8 ml, 173.5 mmol). This mixture was stirred for 24 hours at room temperature, then filtered through Celite. The solvent was evaporated to give the crude product (16.6 g). This was purified by column chromatography (75% hexane/ethyl acetate) to give the pure product **92** as a clear, colourless oil (11.0 g, 72%). ¹H NMR (400 MHz, CDCl₃, Me₄Si) 1.16 (3H, d, CH(CH₃)), 1.18 (3H, d, *J* = 1.8, CH(CH₃)), 1.19 (9H, s, *J* = 2.1, C(CH₃)₃), 2.72 (1H, m, CH(CH₃)₂), 7.99 (1H, d, *J* = 4.3, HC=N); ¹³C{¹H} NMR (100 MHz, CDCl₃) 18.9 (CH(CH₃)₂), 22.3 (C(CH₃)₃), 34.8 (CH(CH₃)₂), 56.4 (C(CH₃)₃), 173.5 (C=N); *m/z* (ES) 176.1106 (M+H)⁺ (calculated: 176.1109).

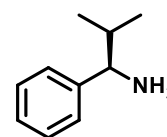
6.26. Synthesis of (R)-2-methyl-N-((R)-2-methyl-1-phenylpropyl)propane-2-sulfinamide **93**⁹⁷

The chiral sulfinimine **92** (1.4 g, 7.99 mmol) was dissolved in dry DCM (48 ml) in an oven-dried round bottomed flask under nitrogen. The solution was cooled to -48 °C and phenylmagnesium bromide (5.3 ml, 15.97 mmol, 3M/ether) was added slowly. This was stirred for 5 hours at -48 °C, then was allowed to warm to room temperature and was stirred overnight. A solution of saturated ammonium chloride (16.6 ml) was added slowly and the mixture was extracted with ethyl acetate (3 x 25 ml). The organics were dried with Na₂SO₄, filtered and the solvent was removed to give the crude product as a yellow oil (2.1 g). This was purified by column chromatography (50% ethyl acetate/hexane) to give the pure product **93** as a white solid (1.46 g, 72%). ¹H NMR (400 MHz, CDCl₃, Me₄Si) 0.81 (3H, d, *J* = 6.8, CH(CH₃)), 0.93 (3H, d, *J* = 6.8, CH(CH₃)), 1.24 (9H, s, C(CH₃)₃), 2.22 (1H, octet, *J* = 6.8, CH(CH₃)₂), 3.45 (1H, d, *J* = 5.2, NH), 4.16 (1H, t, *J* = 5.8, CH(Ph)NH), 7.23-7.29 (3H, m, Ar-*H*), 7.29-7.35 (2H, m, Ar-*H*); ¹³C{¹H} NMR (100 MHz, CDCl₃) 18.0 (CH(CH₃)), 19.3 (CH(CH₃)), 22.7 (C(CH₃)₃), 32.9 (CH(CH₃)₂), 56.0 (C(CH₃)₃), 65.0 (CH(Ph)NH), 127.5 (Ar), 127.7 (Ar), 128.3 (Ar), 140.9 (Ar); *m/z* (ES) 276.1394 (M+Na)⁺ (calculated: 276.1398).



6.27. Synthesis of (R)-2-methyl-1-phenylpropan-1-amine **94**⁹⁷

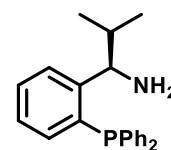
The amine **93** (9.6 g, 38.1 mmol) was dissolved in MeOH (19.5 ml). A solution of HCl in dioxane (19 ml, 76.1 mmol, 4 M, 2 eq.) was added and the solution was stirred for 30 minutes at room temperature. Most of the solvent was removed on a rotary evaporator and then diethyl ether was added and the precipitate was filtered (6.6 g, 94%). This was dissolved in MeOH (20 ml) and 2 M potassium carbonate (40 ml) was added. The product was extracted with DCM (3 x 40 ml), washed with brine (100 ml), dried with Na₂SO₄, filtered and concentrated to give the pure product **94** as a pale yellow oil (5.32 g, 94%). ¹H NMR (400 MHz, CDCl₃, Me₄Si) 0.77 (3H, d, *J* = 6.7, CH₃), 0.98 (3H, d, *J* = 6.7, CH₃), 1.46 (2H, br s, NH), 1.85 (1H,



octet, $J = 6.7$, $\text{CH}(\text{CH}_3)_2$), 3.60 (1H, d, $J = 7.2$, $\text{CH}(\text{iPr})\text{NH}_2$), 7.19-7.34 (5H, m, Ar- H); $^{13}\text{C}\{^1\text{H}\}$ NMR (100 MHz, CDCl_3) 18.9 (CH_3), 19.8 (CH_3), 35.5 ($\text{CH}(\text{CH}_3)_2$), 62.5 ($\text{CH}(\text{iPr})\text{NH}_2$), 126.8 (Ar), 127.0 (Ar), 128.2 (Ar), 145.5 (Ar); m/z (ES) 150.1276 ($\text{M}+\text{H}^+$) (calculated: 150.1283).

6.28. Synthesis of (R)-1-(2-(diphenylphosphaneyl)phenyl)-2-methylpropan-1-amine **85**

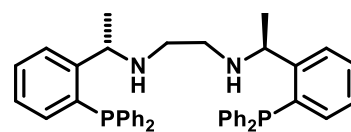
(*R*)-2-methyl-1-phenylpropan-1-amine **94** (0.67 g, 4.5 mmol) was dissolved in dry ether (4.5 ml) in an oven-dried round bottomed flask under nitrogen. The solution was cooled to -35 °C (using a MeOH/ H_2O /dry ice bath), and *n*-butyllithium (2.5 M in hexanes, 1.79 ml, 4.5 mmol, 1 eq.) was added dropwise with stirring. On addition of *n*-BuLi, the solution turned slightly yellow. After the solution was stirred at -35 °C for 15 minutes, Me_3SiCl (0.63 ml, 4.9 mmol, 1.1 eq.) was added slowly. After stirring at -35 °C for 1 hour, more *n*-BuLi (2.5 M in hexanes, 5.38 ml, 13.5 mmol, 3 eq.) was added dropwise. This was then left to stir for 3 hours at -35 °C, then warmed to room temperature and left to stir overnight. The next day, the cloudy yellow solution was cooled to -35 °C and a solution of ClPPh₂ (0.80 ml, 4.5 mmol, 1 eq.) in dry ether (4.5 ml) was added dropwise over 45 minutes. The solution was stirred for 3 hours at -35 °C and then warmed to room temperature and stirred for 4 hours. 1 M HCl was added slowly until the reaction mixture became clear. During the addition of HCl, the mixture became slightly warm. The layers were separated and the aqueous layer was extracted with ether (3 x 5 ml). The organic layers were combined, dried with Na_2SO_4 and concentrated using a rotary evaporator to give the crude product as a yellow oil (1.63 g). This was purified by column chromatography (40% ethyl acetate/hexane + 2% Et₃N) to give the product **85**, a yellow-orange oil (0.28 g, 18%). ^1H NMR (400 MHz, CDCl_3 , Me_4Si) 0.67 (3H, d, $J = 6.8$, CH_3), 1.00 (3H, d, $J = 6.6$, CH_3), 1.44 (2H, br s, NH_2), 1.96 (1H, octet, $J = 6.8$, $\text{CH}(\text{CH}_3)_2$), 4.46 (1H, t, $J = 8.1$, $\text{CH}(\text{iPr})\text{NH}_2$), 6.90 (1H, ddd, $J = 1.0$, $J = 4.1$, $J = 7.7$, Ar- H), 7.13 (1H, dt, $J = 1.1$, $J = 7.5$, Ar- H), 7.22-7.41 (11H, m, Ar- H), 7.51 (1H, dd, $J = 4.2$, $J = 8.3$, Ar- H); $^{31}\text{P}\{^1\text{H}\}$ NMR (162 MHz, CDCl_3) -16.7 (s); $^{13}\text{C}\{^1\text{H}\}$ NMR (100 MHz, CDCl_3) 16.7 (s, CH_3), 18.2 (s, CH_3), 32.9 (d, $J = 1.3$, $\text{CH}(\text{CH}_3)_2$), 56.7 (d,



$J = 24.2$, $\text{CH}(\text{iPr})\text{NH}_2$), 124.3 (d, $J = 5.3$, Ar), 124.7 (s, Ar), 126.3-126.6 (m, Ar), 127.2 (s, Ar), 131.4-131.7 (m, Ar), 132.0 (d, $J = 19.8$, Ar), 133.2 (d, $J = 12.0$, Ar), 134.7 (d, $J = 10.9$, Ar), 135.3 (d, $J = 10.9$, Ar), 148.5 (d, $J = 22.8$, Ar); m/z (ES) 334.1725 ($\text{M}+\text{H}$)⁺ (calculated: 334.1725).

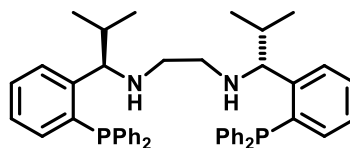
6.29. Synthesis of N1,N2-bis((S)-1-(2-(diphenylphosphanyl)phenyl)ethyl)ethane-1,2-diamine **82**

Dibromoethane (36 μl , 0.413 mmol, 1 eq.) was added slowly to a mixture of (S)-1-[2-(diphenylphosphino)phenyl]ethylamine **81** (0.54 g, 1.77 mmol, 4.3 eq.) and triethylamine (0.12 ml, 0.825 mmol, 2 eq.) at 110 °C under a nitrogen atmosphere. (The triethylamine was dried with molecular sieves overnight prior to use). After about 5 minutes stirring, the mixture became thick. The temperature was increased to 130 °C and the mixture was stirred for 22 h at this temperature. The mixture was then allowed to cool and 0.6 ml of a saturated KOH solution was added carefully. DCM (3 ml) was added, the layers were separated and the aqueous layer was extracted with DCM (3 x 3 ml). The organics were washed with H₂O (5 ml) and saturated brine (5 ml), dried with Na₂SO₄ and the solvent was removed under vacuum. Purification by column chromatography (10% MeOH/DCM) gave the product **82**, a white solid (0.0524 g, 20%). ¹H NMR (400 MHz; CDCl₃; Me₄Si) 1.25 (6H, d, $J = 6.6$, CH₃), 2.5 (4H, br s, CH₂CH₂), 2.65 (2H, br s, NH), 4.61 (2H, m, $J = 6.6$, CH(CH₃)NH), 6.87 (2H, ddd, $J = 1.0, 4.2, 7.6$, Ar-*H*), 7.11 – 7.41 (24H, m, Ar-*H*), 7.62 (2H, dd, $J = 4.1, 7.4$, Ar-*H*); ³¹P{¹H} NMR (162 MHz; CDCl₃) -17.2 (s); ¹³C{¹H} NMR (100 MHz, CDCl₃) 22.5 (s, CH₃), 44.7 (s, CH₂), 54.0 (d, $J = 27.1$, CH(CH₃)NH), 126.4 (d, $J = 4.8$, Ar), 127.8 (s, Ar), 128.6 (d, $J = 3.2$, Ar), 128.7 (d, $J = 2.9$, Ar), 128.9 (d, $J = 10.5$, Ar), 129.9 (s, Ar), 133.5 (s, Ar), 133.9 (d, $J = 9.4$, Ar), 134.2 (d, $J = 9.4$, Ar), 135.6 (d, $J = 13.4$, Ar), 135.9 (d, $J = 9.2$, Ar), 136.4 (d, $J = 10.2$, Ar); m/z (ES) 637.3 ($\text{M}+\text{H}$)⁺ (calculated: 637.29), 289.1 ($\text{M}-\text{NHCH}_2\text{CH}_2\text{NHCH}(\text{CH}_3)\text{PhPPh}_2$)⁺; CHN C₄₂H₄₂N₂P₂ calculated: C 79.22, H 6.65, N 4.40, found: C 75.70, H 6.41, N 4.13.



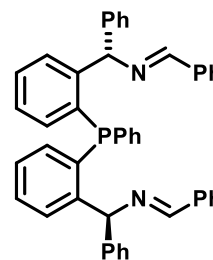
6.30. Synthesis of N1,N2-bis((R)-1-(2-(diphenylphosphaneyl)phenyl)-2-methylpropyl)ethane-1,2-diamine **86**

(*R*)-1-(2-(diphenylphosphaneyl)phenyl)-2-methylpropan-1-amine **85** (1.57 g, 4.7 mmol) was transferred to an oven-dried Schlenk flask under nitrogen. Triethylamine (0.31 ml, 2.19 mmol) was added and the mixture was heated to 110 °C. Dibromoethane (94 µl, 1.09 mmol) was added and the temperature was increased to 130 °C and was stirred at this temperature overnight. The next day, the mixture was cooled to 60 °C and a saturated KOH solution (1.64 ml) was added carefully. After cooling to room temperature, the product was extracted with DCM (3 x 7 ml) and washed with water (20 ml) and brine (20 ml). The organic layer was dried with Na₂SO₄, filtered and concentrated to give the crude product (1.5 g). This was purified by column chromatography (10% MeOH/DCM) to give the pure product **86** as a white solid (0.38 g, 50%). ¹H NMR (400 MHz, CDCl₃, Me₄Si) 0.59 (6H, d, *J* = 6.8, 2 x CH₃), 1.05 (6H, d, *J* = 6.7, 2 x CH₃), 2.08 (2H, br m, CH(CH₃)₂), 2.26 (2H, br d, *J* = 8.0, CH₂), 2.49 (2H, br d, *J* = 8.0, CH₂), 4.42 (2H, br m, CH(*i*Pr)NH), 4.68 (2H, br s, NH), 7.02 (2H, dd, *J* = 3.9, *J* = 7.4, Ar-*H*), 7.12-7.34 (18H, m, Ar-*H*), 7.39 (2H, t, *J* = 7.6, Ar-*H*), 7.6 (2H, br s, Ar-*H*); ³¹P{¹H} NMR (162 MHz, CDCl₃, Me₄Si) -19.1 (s); ¹³C{¹H} NMR (100 MHz, CDCl₃) 17.1 (s, CH₃), 18.0 (s, CH₃), 32.0 (s, CH(CH₃)₂), 42.9 (br s, CH₂), 62.7 (m, CH(*i*Pr)NH), 125.2 (br s, Ar), 126.3 (d, *J* = 6.9, Ar), 126.5 (d, *J* = 21.4, Ar), 127.5 (s, Ar), 131.4 (d, *J* = 19.5, Ar), 131.8 (d, *J* = 20.2, Ar), 132.5 (s, Ar), 133.9 (m, Ar), 134.4 (d, *J* = 14.1, Ar), 134.8 (d, *J* = 10.8, Ar); *m/z* (ES) 693.3523 (M+H)⁺ (calculated: 693.3527); CHN C₄₆H₅₀N₂P₂ calculated: C 79.74, H 7.27, N 4.04, found: C 76.30, H 7.20, N 3.96.



6.31. Synthesis of (1E,1'E)-N,N'-((1S,1'S)-((phenylphosphanediyl)bis(2,1-phenylene))bis(phenylmethylene))-bis(1-phenylmethanimine) **99**

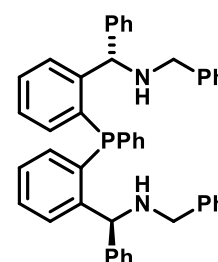
The diamine **36b** (50 mg, 0.11 mmol) and Na₂SO₄ (0.18 g, 1.27 mmol, 12 eq.) were placed in an oven-dried reaction tube under nitrogen. Chloroform (1.2 ml) was added followed by benzaldehyde (22.5 mg, 0.21 mmol, 2 eq.).



The mixture was heated to 50 °C overnight, then cooled to room temperature, filtered and the solvent was removed to give the crude imine product **99** (0.057 g, 83%). ¹H NMR (400 MHz, CDCl₃, Me₄Si) 6.33 (1H, d, *J*_{HP} = 7.5, CH(Ph)N), 6.49 (1H, d, *J*_{HP} = 7.5, CH(Ph)N), 6.79 (2H, m, Ar-*H*), 6.95 (1H, t, *J* = 7.5, Ar-*H*), 7.07 (2H, t, *J* = 7.8, Ar-*H*), 7.12-7.21 (3H, m, Ar-*H*), 7.23-7.37 (15H, m, Ar-*H*), 7.39 (2H, d, *J* = 7.6, Ar-*H*), 7.44 (4H, d, *J* = 7.6, Ar-*H*), 7.54-7.58 (2H, m, Ar-*H* and HC=N), 7.66 (1H, dd, *J*_{HH} = 7.7, *J*_{HP} = 4.4, Ar-*H*), 7.73 (1H, s, HC=N), 7.77 (1H, dd, *J*_{HH} = 6.9, *J*_{HP} = 4.4, Ar-*H*); ³¹P{¹H} NMR (162 MHz, CDCl₃) -23.9 (s); *m/z* (ES) 649.2775 (M+H)⁺ (calculated: 649.2773).

6.32. Synthesis of (1S,1'S)-1,1'-((phenylphosphane-diyl)bis(2,1-phenylene))bis(N-benzyl-1-phenylmethanamine) **84**

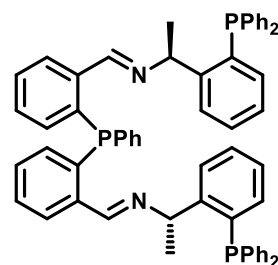
Sodium borohydride (0.15 g, 4.01 mmol, 52 eq.) was placed in an oven-dried Radley's tube under nitrogen. A solution of the diimine **99** (50 mg, 0.077 mmol) in DCM (1.1 ml) was added at 0 °C. Methanol (1.1 ml) was added slowly and the mixture was stirred at 0 °C for 3 hours and then was warmed to 40 °C and left to stir overnight. The next day, the mixture was cooled to room temperature and water (1.2 ml) was added slowly. The product was extracted with ethyl acetate (3 x 3 ml), washed with water and brine, dried with Na₂SO₄, filtered and concentrated to give the crude product (0.039 g). This was purified by column chromatography (85% hexane/ethyl acetate) to give the pure product **84**, a white solid (0.021 g, 42%). ¹H NMR (400 MHz, CDCl₃, Me₄Si) 2.97 (1H, d, *J*_{HH} = 12.8, CH(H)), 3.26 (1H, d, *J*_{HH} = 12.8, CH(H)), 3.51



(2H, s, CH_2), 5.57 (1H, d, $J_{\text{HP}} = 7.8$, $\text{CH}(\text{Ph})\text{NH}$), 5.87 (1H, d, $J_{\text{HP}} = 7.4$, $\text{CH}(\text{Ph})\text{NH}$), 6.76 (1H, dd, $J_{\text{HH}} = 7.6$, $J_{\text{HP}} = 3.8$, Ar- H), 6.91 (1H, dd, $J_{\text{HH}} = 6.8$, $J_{\text{HP}} = 4.1$, Ar- H), 6.97 (2H, d, $J_{\text{HH}} = 6.8$, Ar- H), 7.03 (1H, t, $J_{\text{HH}} = 7.6$, Ar- H), 7.06-7.39 (24H, m, Ar- H), 7.45 (4H, m, Ar- H), 7.57 (1H, dd, $J_{\text{HH}} = 7.6$, $J_{\text{HP}} = 4.3$, Ar- H), 7.73 (1H, dd, $J_{\text{HH}} = 7.6$, $J_{\text{HP}} = 4.3$, Ar- H); $^{31}\text{P}\{^1\text{H}\}$ NMR (162 MHz, CDCl_3) -26.0 (s); $^{13}\text{C}\{^1\text{H}\}$ NMR (100 MHz, CDCl_3) 52.3 (CH_2), 52.4 (CH_2), 63.8 (d, $J = 8.1$, $\text{CH}(\text{Ph})\text{NH}$), 64.0 (d, $J = 7.2$, $\text{CH}(\text{Ph})\text{NH}$), 126.7 (s, Ar), 126.8 (d, $J = 1.5$, Ar), 126.9 (s, Ar), 127.3 (d, $J = 15.6$, Ar), 127.7 (d, $J = 1.7$, Ar), 127.9-128.3 (m, Ar), 128.7 (d, $J = 7.3$, Ar), 128.9 (s, Ar), 129.3 (s, Ar), 129.7 (s, Ar), 134.1 (d, $J = 10.9$, Ar), 134.5 (d, $J = 20.6$, Ar), 134.9 (d, $J = 13.3$, Ar), 135.4 (d, $J = 12.7$, Ar), 136.3 (d, $J = 10.3$, Ar), 140.5 (s, Ar), 143.1 (s, Ar), 143.3 (s, Ar), 147.9 (d, $J = 22.9$, Ar), 148.2 (d, $J = 23.2$, Ar); m/z (ES) 653.3088 ($\text{M}+\text{H}$)⁺ (calculated: 653.3086).

6.33. Synthesis of 1,1'-((phenylphosphanediy)bis(2,1-phenylene))bis(N-((S)-1-(2-(diphenylphosphaneyl)-phenyl)ethyl)methanimine) **100**

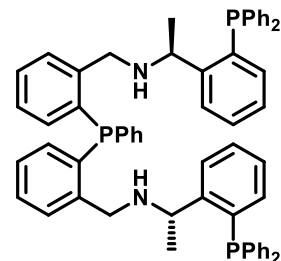
2,2'-(phenylphosphanediy)-dibenzaldehyde **45** (0.2 g, 0.63 mmol), (S)-1-[2-(diphenylphosphino)phenyl]ethylamine **81** (0.38 g, 1.26 mmol, 2 eq.) and sodium sulfate (1.16 g, 8.17 mmol, 13 eq.) were placed in an oven-dried round bottomed flask fitted with a condenser under



nitrogen. Chloroform (2 ml) was added and the mixture was heated to 50 °C for 2 days. Then the mixture was filtered and the solvent was evaporated to give the crude diimine **100** (0.56 g, 99%). ^1H NMR (400 MHz, CDCl_3 , Me_4Si) 1.08 (3H, d, $J = 6.4$, CH_3), 1.13 (3H, d, $J = 6.4$, CH_3), 5.25 (2H, sept, $J = 6.4$, $\text{CH}(\text{CH}_3)\text{N}$), 6.74-6.84 (4H, m, Ar- H), 7.03 (2H, t, $J = 6.6$, Ar- H), 7.12-7.36 (40H, m, Ar- H), 7.42 (1H, dd, $J = 4.5$, $J = 7.7$, Ar- H), 7.68 (2H, m, Ar- H), 8.53 (1H, d, $J = 4.5$, $\text{HC}=\text{N}$), 8.56 (1H, d, $J = 4.4$, $\text{HC}=\text{N}$); $^{31}\text{P}\{^1\text{H}\}$ NMR (162 MHz, CDCl_3) -17.3 (1P, s), -16.8 (1P, s), -16.7 (1P, s); m/z (ES) 893.3314 ($\text{M}+\text{H}$)⁺ (calculated: 893.3343).

6.34. Synthesis of (1S,1'S)-N,N'-(((phenylphosphanediyl)-bis(2,1-phenylene))bis(methylene))bis(1-(2-(diphenylphosphaneyl)phenyl)ethan-1-amine) **87**

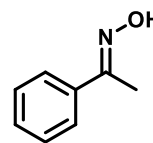
Sodium borohydride (1.16 g, 30.66 mmol) was placed in an oven-dried 2-necked flask under nitrogen. A solution of the diimine **100** (0.53 g, 0.59 mmol) in DCM (8.4 ml) was added at 0 °C, followed by the slow addition of methanol (8.4 ml). The mixture was stirred for 4 hours



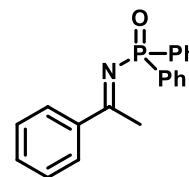
at 0 °C, then warmed to 40 °C and stirred overnight. The next day, more DCM (7 ml) was added and the mixture was stirred for a further 6 hours. Then the mixture was cooled to room temperature and water (8.8 ml) was added slowly. After stirring for 1h45m the product was extracted with ethyl acetate (3 x 20 ml), washed with water and brine, dried with Na₂SO₄, filtered and concentrated to give the crude product, a white solid (0.52 g, 99%). ¹H NMR (400 MHz, CDCl₃, Me₄Si) 0.87 (3H, d, *J*_{HH} = 6.5, CH₃), 0.89 (3H, d, *J*_{HH} = 6.5, CH₃), 3.56 (1H, d, *J*_{HH} = 12.7, CH(H)), 3.67 (2H, s, CH₂), 3.72 (1H, dd, *J*_{HH} = 12.4, *J*_{HP} = 1.6, CH(H)), 4.53 (2H, m, CH(CH₃)NH), 6.75-6.87 (4H, m, Ar-H), 7.09 (4H, m, Ar-H), 7.17-7.33 (34H, m, Ar-H), 7.45 (3H, m, Ar-H), 7.59 (1H, m, Ar-H); ³¹P{¹H} NMR (162 MHz, CDCl₃) -25.8 (1P, s), -17.9 (1P, s), -17.6 (1P, s); ¹³C{¹H} NMR (100 MHz, CDCl₃) 23.6 (s, CH₃), 23.7 (s, CH₃), 50.4 (d, *J* = 2.3, CH₂), 50.6 (d, *J* = 2.2, CH₂), 54.6 (dd, *J* = 11.6, 25.2, CH(Me)NH), 126.1 (t, *J* = 4.4, Ar), 126.7 (s, Ar), 127.2 (s, Ar), 128.4-128.7 (m, Ar), 128.9 (d, *J* = 2.5, Ar), 129.4 (s, Ar), 129.9 (d, *J* = 4.5, Ar), 133.5 (d, *J* = 8.9, Ar), 133.7 (s, Ar), 133.9 (m, Ar), 134.2 (d, *J* = 3.1, 20.1, Ar), 134.4 (s, Ar), 134.9 (dd, *J* = 5.3, 13.9, Ar), 135.6 (d, *J* = 13.7, Ar), 136.0 (d, *J* = 13.4, Ar), 136.9 (m, Ar), 137.0 (m, Ar), 137.4 (d, *J* = 8.1, Ar), 137.5 (d, *J* = 8.4, Ar), 144.9 (dd, *J* = 5.3, 24.8, Ar), 150.2 (dd, *J* = 7.3, 22.2, Ar); *m/z* (ES) 897.3652 (M+H)⁺ (calculated: 897.3656); CHN C₆₀H₅₅N₂P₃ calculated: C 80.34, H 6.18, N 3.12, found: C 78.93, H 6.76, N 2.69.

6.35. Synthesis of 1-phenylethan-1-one oxime¹²³

Acetophenone (0.58 ml, 5 mmol), hydroxylamine hydrochloride (0.52 g, 7.5 mmol, 1.5 eq.), sodium acetate (1.03 g, 12.5 mmol, 2.5 eq.), ethanol (4 ml) and water (12 ml) were placed in a round bottomed flask fitted with a condenser. The mixture was heated to reflux overnight. The next day, the mixture was cooled to room temperature, poured into a beaker and cooled to 0 °C. The precipitate was filtered off, washed with water and dried under vacuum to give the product as a fluffy white solid (0.37 g, 54%). ¹H NMR (400 MHz, CDCl₃, Me₄Si) 2.3 (3H, s, CH₃), 7.39 (3H, m, Ar-H), 7.63 (2H, m, Ar-H), 8.47 (1H, s, OH); m/z (ES) 136.0758 (M+H)⁺ (calculated: 136.0762).

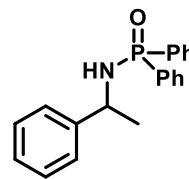
**6.36. Synthesis of P,P-diphenyl-N-(1-phenylethylidene)phosphinic amide**¹²⁴

1-phenylethan-1-one oxime (0.36 g, 2.66 mmol) and triethylamine (0.74 ml, 5.33 mmol, 2 eq.) were placed in an oven-dried flask under nitrogen. A 1/1 mixture of n-pentane and DCM (5.3 ml) was added and the mixture was cooled to -78 °C. Chlorodiphenylphosphine (0.48 ml, 2.66 mmol, 1 eq.) was added slowly over 15 minutes, during which time the clear colourless solution turned cloudy and slightly yellow. The mixture was stirred for 40 minutes at -78 °C, then was allowed to warm to room temperature overnight. The next day, the mixture was filtered through Celite and the filtrate was washed with water and brine, dried with MgSO₄, filtered and concentrated to give the crude product as a yellow oil (0.9 g). This was purified by column chromatography (85% ethyl acetate/hexane) to give the pure product as a white solid (0.56 g, 66%). ¹H NMR (400 MHz, CDCl₃, Me₄Si) 2.97 (3H, d, J_{HP} = 2.1, CH₃), 7.40-7.51 (8H, m, Ar-H), 7.53-7.58 (1H, m, Ar-H), 7.98 (4H, ddd, J_{HH} = 7.5, J_{HH} = 1.4, J_{HP} = 11.9, Ar-H), 8.09 (2H, m, Ar-H); ³¹P{¹H} NMR (162 MHz, CDCl₃) 18.9 (s); m/z (ES) 342.1023 (M+Na)⁺ (calculated: 342.1024).



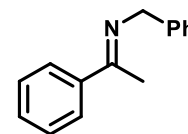
6.37. Synthesis of P,P-diphenyl-N-(1-phenylethyl)-phosphinic amide⁵⁴

P,P-diphenyl-N-(1-phenylethylidene)phosphinic amide (30 mg, 0.094 mmol) was dissolved in THF (0.3 ml) and sodium borohydride (14 mg, 0.37 mmol, 4 eq.) was added. The mixture was stirred overnight at room temperature. A saturated solution of ammonium chloride (3 ml) was added carefully and the product was extracted with DCM (3 x 3 ml), dried with MgSO₄, filtered and concentrated to give the crude product (0.0316 g, quantitative yield). ¹H NMR (400 MHz, CDCl₃, Me₄Si) 1.58 (3H, d, *J* = 6.8, CH₃), 3.17 (1H, dd, *J* = 5.5, *J* = 9.7, NH), 4.40 (1H, m, CH(CH₃)NH), 7.21-7.40 (10H, m, Ar-*H*), 7.40-7.54 (6H, m, Ar-*H*), 7.79-7.86 (2H, m, Ar-*H*), 7.88-7.97 (3H, m, Ar-*H*); ³¹P{¹H} NMR (162 MHz, CDCl₃) 22.5 (s); *m/z* (CI) 322.1360 (M+H)⁺ (calculated: 322.1361).



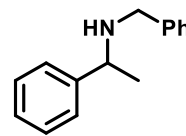
6.38. Synthesis of N-benzyl-1-phenylethan-1-imine¹²⁵

Acetophenone (1.75 ml, 15 mmol), benzylamine (1.64 ml, 15 mmol) and *p*-toluenesulfonic acid monohydrate (0.031 g, 0.17 mmol, 0.011 eq.) were dissolved in toluene (50 ml) in a round bottomed flask fitted with a Dean-Stark trap. The mixture was heated to reflux overnight during which time, the clear colourless mixture turned yellow. Then the mixture was cooled to room temperature during which time it became cloudy. This was filtered through Celite, and the solvent was evaporated to give the crude product as a yellow-orange oil (2.6 g). This was dissolved in petroleum ether and cooled in the freezer overnight to give a pale-yellow solid which was filtered off and dried (1.68 g, 54%). ¹H NMR (400 MHz, CDCl₃, Me₄Si) 2.34 (3H, s, CH₃), 4.75 (2H, s, CH₂), 7.25 (1H, m, Ar-*H*), 7.32-7.45 (1H, m, Ar-*H*), 7.87 (2H, m, Ar-*H*); ¹³C{¹H} NMR (100 MHz, CDCl₃) 15.9 (CH₃), 55.7 (CH₂), 126.6 (Ar), 126.8 (Ar), 127.7 (Ar), 128.3 (Ar), 128.4 (Ar), 129.6 (Ar), 140.6 (Ar), 141.1 (Ar), 166.0 (C=N); *m/z* (CI) 210.1273 (M+H)⁺ (calculated: 210.1283); CAS number 14428-98-9.



6.39. Synthesis of N-benzyl-1-phenylethan-1-amine

N-benzyl-1-phenylethan-1-imine (0.1 g, 0.53 mmol) was dissolved in ethanol (0.5 ml) and sodium borohydride (30 mg, 0.79 mmol, 1.5 eq.) was added. The mixture was stirred for 4 hours at room temperature, then was diluted with water (1.8 ml), transferred to a separating funnel adding ethyl acetate (5.3 ml) and water (5.3 ml). The product was extracted with ethyl acetate (2 x 3.5 ml), washed with brine (5.3 ml), dried with Na₂SO₄, filtered and concentrated to give the product (0.107 g, 96%). ¹H NMR (400 MHz, CDCl₃, Me₄Si) 1.37 (3H, d, *J* = 6.7, CH₃), 3.59 (1H, d, *J* = 13.0, CH(H)), 3.66 (1H, d, *J* = 13.0, CH(H)), 3.81 (1H, q, *J* = 6.7, CH(CH₃)NH), 7.21-7.38 (10H, m, Ar-H); ¹³C{¹H} NMR (100 MHz, CDCl₃) 24.5 (CH₃), 51.7 (CH₂), 57.5 (CH(CH₃)NH), 126.7 (Ar), 126.9 (Ar), 127.0 (Ar), 128.2 (Ar), 128.4 (Ar), 128.5 (Ar), 140.6 (Ar), 145.6 (Ar); *m/z* (CI) 212.1442 (M+H)⁺ (calculated: 212.1439); CAS number 3193-62-2.

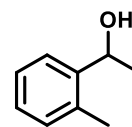


6.40. General procedure for the synthesis of racemic alcohols

The ketone (1 eq.) was dissolved in ethanol (1 M) and sodium borohydride (1.5 eq.) was added. The reaction was stirred at room temperature for 1 - 2 hours, then diluted with water. The mixture was transferred to a separating funnel and ethyl acetate and water were added. The product was extracted with ethyl acetate (x 2), washed with brine and dried with Na₂SO₄, filtered and concentrated to give the products.

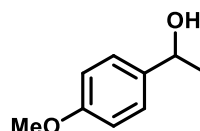
6.40.1. 1-(*o*-tolyl)ethan-1-ol

(0.38 g, 94%) ¹H NMR (400 MHz, CDCl₃, Me₄Si) 1.47 (3H, d, *J* = 6.3, CH₃CH(OH)), 1.71 (1H, s, OH), 2.35 (3H, s, Ar-CH₃), 5.13 (1H, q, *J* = 6.4, CH(OH)CH₃), 7.15 (2H, m, Ar-H), 7.23 (1H, m, Ar-H), 7.51 (1H, d, *J* = 7.6, Ar-H); ¹³C{¹H} NMR (100 MHz, CDCl₃) 18.9 (Ar-CH₃), 23.9 (CH₃), 66.8 (CH(OH)), 124.5 (Ar), 126.4 (Ar), 127.2 (Ar), 130.4 (Ar), 134.2 (Ar), 143.9 (Ar); *m/z* (CI) 119.0852 (M-OH)⁺ (calculated: 119.0861); CAS number 7287-82-3.

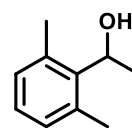


6.40.2. 1-(4-methoxyphenyl)ethan-1-ol

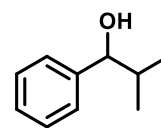
(0.45 g, 99%) ^1H NMR (400 MHz, CDCl_3 , Me_4Si) 1.48 (3H, d, $J = 6.5$, $\text{CH}_3\text{CH}(\text{OH})$), 1.74 (1H, s, OH), 3.81 (3H, s, Ar- CH_3), 4.86 (1H, q, $J = 6.5$, $\text{CH}(\text{OH})$), 6.88 (2H, d, $J = 8.6$, Ar- H), 7.30 (2H, d, $J = 8.6$, Ar- H); $^{13}\text{C}\{^1\text{H}\}$ NMR (100 MHz, CDCl_3) 25.0 ($\text{CH}_3\text{CH}(\text{OH})$), 55.3 ($\text{CH}_3\text{O-Ar}$), 69.9 ($\text{CH}(\text{OH})$), 113.8 (Ar), 126.7 (Ar), 138.1 (Ar), 158.9 (Ar); m/z (CI) 135.0809 (M-OH^+) (calculated: 135.1860); CAS number 3319-15-1.

**6.40.3. 1-(2,6-dimethylphenyl)ethan-1-ol**

(0.012 g, 3%, product was not separated from starting material) ^1H NMR (400 MHz, CDCl_3 , Me_4Si) 1.54 (3H, d, $J = 6.9$, $\text{CH}_3\text{CH}(\text{OH})$), 1.71 (1H, s, OH), 2.45 (6H, s, Ar- CH_3), 5.40 (1H, q, $J = 6.9$, $\text{CH}(\text{OH})$), (Ar- H overlapped with peaks for starting material); $^{13}\text{C}\{^1\text{H}\}$ NMR (100 MHz, CDCl_3) 20.7 (Ar- CH_3), 21.5 ($\text{CH}_3\text{CH}(\text{OH})$), 67.6 ($\text{CH}(\text{OH})$), 126.9 (Ar), 129.4 (Ar), 135.7 (Ar), 140.6 (Ar); m/z (CI) 133.0815 (M-OH^+) (calculated: 133.1017); CAS number 19447-06-4.

**6.40.4. 2-methyl-1-phenylpropan-1-ol**

(0.41 g, 92%) ^1H NMR (400 MHz, CDCl_3 , Me_4Si) 0.80 (3H, d, $J = 6.8$, CH_3), 1.00 (3H, d, $J = 6.6$, CH_3), 1.81 (1H, br m, OH), 1.96 (1H, octet, $J = 6.8$, $\text{CH}(\text{CH}_3)_2$), 4.36 (1H, dd, $J = 1.3$, $J = 6.8$, $\text{CH}(\text{OH})$), 7.24-7.37 (5H, m, Ar- H); $^{13}\text{C}\{^1\text{H}\}$ NMR (100 MHz, CDCl_3) 18.3 (CH_3), 19.0 (CH_3), 35.3 ($\text{CH}(\text{CH}_3)_2$), 80.0 ($\text{CH}(\text{OH})$), 126.6 (Ar), 127.4 (Ar), 128.2 (Ar), 143.7 (Ar); m/z (CI) 133.1015 (M-OH^+) (calculated: 133.1017); CAS number 611-69-8.

**6.41. General procedure for AH at AZ**

Each ligand (0.016 mmol) was weighed out into 4 ml sample vials. These were then put into a glove box and were dissolved in DCM (4 ml each). Then 0.5 ml samples (0.002 mmol) were taken out using an Eppendorf pipette and placed into 6 smaller sample vials for each ligand. The solvent was then removed using a Genevac.

$\text{Fe}_3(\text{CO})_{12}$ (approx. 1 mg (0.8-0.9 mg), 0.002 mmol) was weighed out into each of the 15 ligand sample vials in a glove box using an automatic weighing

machine. Then a solution of acetophenone (84 μ l) and KOH (9 mg) in methanol (6 ml) was prepared and 0.341 ml of this solution was added to each reaction (acetophenone, 0.04 mmol; KOH, 0.008 mmol; MeOH, 0.336 ml). The sample vials were then transferred into a clam shell. The clam shell was tightened and then removed from the glove box and put into the SPR (screening pressure reactor). The system was purged with nitrogen and then the nitrogen pressure was held for 10 minutes to check for any leaks. After this, the system was evacuated and refilled with hydrogen four times. The reaction was heated to 45 °C and then the pressure was increased to 100 bar and the shaker was started. The reaction was left for 16 hours at 45 °C, and then was cooled to 30 °C before stopping the shaking and releasing the hydrogen pressure. The system was then evacuated and refilled with nitrogen 4 times. The clam shell was disconnected from the SPR and put back into the glove box.

In the glove box, 70 μ l of each reaction were transferred into HPLC vials, then diluted up to 1 ml with methanol and submitted for analysis by SFC. Samples of acetophenone, racemic 1-phenylethanol and (*R*)-1-phenylethanol (1 mg/ml) were prepared for comparison.

6.42. General procedure for ATH at AZ

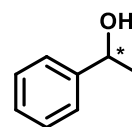
The ligands (0.5 - 2 mol%) were weighed out into sample vials and were placed into a glove box. $\text{Fe}_3(\text{CO})_{12}$ (approx. 1 mg, 0.5 - 2 mol%) was weighed into these using an automatic weighing machine. Isopropanol was added and the reactions were stirred at 60 °C for 30 minutes. Then a solution of base (12 mol%) in isopropanol was added and the reactions were stirred for a further 10 minutes. Then acetophenone was added and the reactions were stirred overnight. The reactions were cooled down and a sample from each reaction was placed into HPLC vials and diluted up to 1 ml with methanol for SFC analysis.

6.43. General procedure for ATH at University of Liverpool

The ligand and iron source were weighed out into an oven-dried reaction flask. Then the flask was connected to a Schlenk line and the air was removed and replaced with nitrogen at least 3 times. Dry isopropanol was added and the reaction was heated to the specified temperature for 30 minutes. Then a solution of base/isopropanol was added and the reaction was stirred for a further 10 minutes. Then the substrate was added and the reaction was stirred for the stated time, after which the solvent was removed on a rotary evaporator. If NMR analysis showed formation of product, the product was then extracted with ether, washed with water, dried with MgSO_4 , filtered and concentrated in order to remove the base before HPLC analysis.

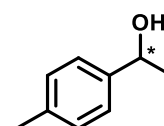
6.43.1. 1-phenylethanol

(33.5 mg, 91% yield, 40-55% ee) ^1H NMR (400 MHz, CDCl_3 , Me_4Si) 1.48 (3H, d, $J = 6.5$, CH_3), 2.05 (1H, br s, OH), 4.87 (1H, q, $J = 6.5$, $\text{CH}(\text{OH})$), 7.23-7.29 (1H, m, Ar-H), 7.30-7.38 (4H, m, Ar-H); $^{13}\text{C}\{^1\text{H}\}$ NMR (100 MHz, CDCl_3) 25.2 (CH_3), 70.4 ($\text{CH}(\text{OH})$), 125.4 (Ar), 127.5 (Ar), 128.5 (Ar), 145.9 (Ar); m/z (CI) 105.0702 (M-OH^+) (calculated: 105.0704).



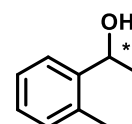
6.43.2. 1-(p-tolyl)ethan-1-ol

(96% conversion, 29% ee) ^1H NMR (400 MHz, CDCl_3 , Me_4Si) 1.47 (3H, d, $J = 6.1$, $\text{CH}(\text{OH})\text{CH}_3$), 1.92 (1H, br s, OH), 2.34 (3H, s, Ar- CH_3), 4.85 (1H, q, $J = 6.2$, $\text{CH}(\text{OH})$), 7.15 (2H, d, $J = 7.7$, Ar-H), 7.25 (2H, d, $J = 7.7$, Ar-H); $^{13}\text{C}\{^1\text{H}\}$ NMR (100 MHz, CDCl_3) 21.1 (Ar- CH_3), 25.1 ($\text{CH}(\text{CH}_3)\text{OH}$), 70.2 ($\text{CH}(\text{OH})$), 125.4 (Ar), 129.2 (Ar), 137.1 (Ar), 142.9 (Ar); m/z (CI) 119.0859 (M-OH^+) (calculated: 119.0861).



6.43.3. 1-(o-tolyl)ethan-1-ol

(>99% conversion, 68% ee) ^1H NMR (400 MHz, CDCl_3 , Me_4Si) 1.45 3H, d, $J = 6.5$, $\text{CH}(\text{CH}_3)$), 1.87 (1H, br s, OH), 2.33 (3H, s, Ar- CH_3), 5.11 (1H, q, $J = 6.4$, $\text{CH}(\text{OH})$), 7.12 (1H, d, $J = 7.1$, Ar-H), 7.16 (1H, td, $J = 1.3$, $J = 7.5$, Ar-H), 7.22 (1H, t, $J = 7.6$, Ar-H), 7.50 (1H, d, $J = 7.5$, Ar-H); $^{13}\text{C}\{^1\text{H}\}$ NMR (100 MHz, CDCl_3) 18.9 (Ar- CH_3), 23.9 ($\text{CH}(\text{CH}_3)\text{OH}$),

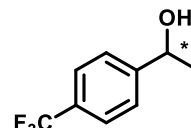


66.8 (CH(OH)), 124.5 (Ar), 126.4 (Ar), 130.4 (Ar), 134.2 (Ar), 143.9 (Ar); m/z (CI) 119.0855 (M-OH)⁺ (calculated: 119.0861).

6.43.4. 1-(4-(trifluoromethyl)phenyl)ethan-1-ol

(>99% conversion, 23% ee) ¹H NMR (400 MHz, CDCl₃, Me₄Si)

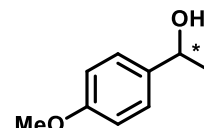
1.49 (3H, d, J = 6.7, CH₃), 2.19 (1H, br s, OH), 4.94 (1H, q, J = 6.5, CH(OH)), 7.47 (2H, d, J = 8.3, Ar-H), 7.59 (2H, d, J = 8.1, Ar-H); ¹³C{¹H} NMR (100 MHz, CDCl₃) 25.4 (CH₃), 69.8 (CH(OH)), 120.1 (Ar), 122.8 (Ar), 125.4 (q, J = 3.6, Ar), 125.6 (Ar), 129.6 (q, J = 32.3, CF₃), 149.7 (Ar); m/z (CI) 173.0571 (M-OH)⁺ (calculated: 173.0578).



6.43.5. 1-(4-methoxyphenyl)ethan-1-ol

(82% conversion, 35% ee) ¹H NMR (400 MHz, CDCl₃, Me₄Si)

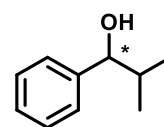
1.46 (3H, d, J = 6.4, CH(OH)CH₃), 2.01 (1H, br s, OH), 3.79 (3H, s, OCH₃), 4.83 (1H, q, J = 6.4, CH(OH)), 6.87 (2H, d, J = 8.3, Ar-H), 7.28 (2H, d, J = 8.8, Ar-H); ¹³C{¹H} NMR (100 MHz, CDCl₃) 25.0 (CH₃CH(OH)), 55.3 (CH₃O-Ar), 69.9 (CH(OH)), 113.8 (Ar), 126.7 (Ar), 138.1 (Ar), 158.9 (Ar); m/z (CI) 135.0810 (M-OH)⁺ (calculated: 135.1860).



6.43.6. 2-methyl-1-phenylpropan-1-ol

(98% conversion, 58% ee) 0.79 (3H, d, J = 6.9, CH₃), 0.99 (3H,

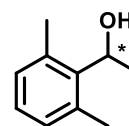
d, J = 6.9, CH₃), 1.88-2.01 (2H, m, CH(CH₃)₂ and OH), 4.34 (1H, d, J = 6.9, CH(OH)), 7.23-7.35 (5H, m, Ar-H); ¹³C{¹H} NMR (100 MHz, CDCl₃, Me₄Si) 18.3 (CH₃), 19.0 (CH₃), 35.3 (CH(CH₃)₂), 80.0 (CH(OH)), 126.6 (Ar), 127.4 (Ar), 128.2 (Ar), 143.7 (Ar); m/z (CI) 133.1015 (M-OH)⁺ (calculated: 133.1017).



6.43.7. 1-(2,6-dimethylphenyl)ethan-1-ol

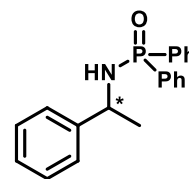
(6% conversion, 71% ee) ¹H NMR (400 MHz, CDCl₃, Me₄Si) 1.53

(3H, d, J = 6.6, CHCH₃), 2.44 (6H, s, Ar-CH₃), 5.39 (1H, q, J = 6.8, CH(OH)), (Ar-H overlapped with peaks for starting material); ¹³C{¹H} NMR (100 MHz, CDCl₃) 20.6 (Ar-CH₃), 21.5 (CH₃CH(OH)), 67.6 (CH(OH)), 126.9 (Ar), 129.4 (Ar), 135.7 (Ar), 140.6 (Ar); m/z (CI) 133.1011 (M-OH)⁺ (calculated: 133.1017).



6.43.8. *P,P*-diphenyl-*N*-(1-phenylethyl)phosphinic amide

(0.019 g, 20%) ^1H NMR (400 MHz, CDCl_3 , Me_4Si) 1.57 (3H, d, $J = 6.4$, CH_3), 3.21 (1H, br m, NH), 4.39 (1H, m, CHNH), 7.21-7.39 (7H, m, Ar- H), 7.39-7.52 (4H, m, Ar- H), 7.82 (2H, m, Ar- H), 7.91 (2H, m, Ar- H); $^{31}\text{P}\{^1\text{H}\}$ NMR (162 MHz, CDCl_3) 22.6 (s); $^{13}\text{C}\{^1\text{H}\}$ NMR (100 MHz, CDCl_3) 26.0 (d, $J = 3.3$, CH_3), 51.1 (s, CHNH), 125.9 (s, Ar), 127.1 (s, Ar), 128.4 (s, Ar), 128.5 (d, $J = 3.6$, Ar), 128.6 (m, Ar), 131.5 (Ar), 131.7-132.0 (m, Ar), 132.4 (Ar), 132.5 (Ar), 132.7 (Ar), 133.8 (Ar), 145.1 (d, $J = 6.7$, Ar); m/z (CI) 322.1355 ($\text{M}+\text{H}$) $^+$ (calculated: 322.1361).



Chapter 7. References

1. S. L. Yu, W. Y. Shen, Y. Y. Li, Z. R. Dong, Y. Q. Xu, Q. Li, J. N. Zhang and J. X. Gao, *Adv. Synth. Catal.*, 2012, **354**, 818-822.
2. Y. Y. Li, S. L. Yu, X. F. Wu, J. L. Xiao, W. Y. Shen, Z. R. Dong and J. X. Gao, *J. Am. Chem. Soc.*, 2014, **136**, 4031-4039.
3. G. P. Moss, *Pure Appl. Chem.*, 1996, **68**, 2193-2222.
4. B. Knoche and G. Blaschke, *J. Chromatogr. A*, 1994, **666**, 235-240.
5. A. K. Scott, *Drug Saf.*, 1993, **8**, 149-159.
6. R. Ciriminna, M. Lomeli-Rodriguez, P. Demma Cara, J. A. Lopez-Sanchez and M. Pagliaro, *Chem. Commun.*, 2014, **50**, 15288-15296.
7. I. Ali, V. K. Gupta, H. Y. Aboul-Enein, P. Singh and B. Sharma, *Chirality*, 2007, **19**, 453-463.
8. J. Clayden, N. Greeves and S. G. Warren, *Organic Chemistry*, Oxford University Press, Oxford; New York, 2012.
9. M. T. El Gihani and J. M. J. Williams, *Curr. Opin. Chem. Biol.*, 1999, **3**, 11-15.
10. R. Noyori, *Adv. Synth. Catal.*, 2003, **345**, 15-32.
11. G. Zassinovich, G. Mestroni and S. Gladiali, *Chem. Rev.*, 1992, **92**, 1051-1069.
12. J.-D. Huang, X.-P. Hu, Z.-C. Duan, Q.-H. Zeng, S.-B. Yu, J. Deng, D.-Y. Wang and Z. Zheng, *Org. Lett.*, 2006, **8**, 4367-4370.
13. J. G. de Vries, in *Selective Nanocatalysts and Nanoscience*, 2011, pp. 73-103.
14. M. J. Palmer and M. Wills, *Tetrahedron: Asymmetry*, 1999, **10**, 2045-2061.
15. S. Enthaler, B. Hagemann, G. Erre, K. Junge and M. Beller, *Chem. - Asian J.*, 2006, **1**, 598-604.
16. S. Gladiali and E. Alberico, *Chem. Soc. Rev.*, 2006, **35**, 226-236.
17. J. S. M. Samec, J.-E. Bäckvall, P. G. Andersson and P. Brandt, *Chem. Soc. Rev.*, 2006, **35**, 237-248.
18. R. Noyori, M. Koizumi, D. Ishii and T. Ohkuma, *Pure Appl. Chem.*, 2001, **73**, 227-232.
19. K. Matsumura, N. Arai, K. Hori, T. Saito, N. Sayo and T. Ohkuma, *J. Am. Chem. Soc.*, 2011, **133**, 10696-10699.
20. T. Ohkuma, M. Koizumi, K. Muniz, G. Hilt, C. Kabuto and R. Noyori, *J. Am. Chem. Soc.*, 2002, **124**, 6508-6509.
21. T. Ohkuma, C. A. Sandoval, R. Srinivasan, Q. Lin, Y. Wei, K. Muniz and R. Noyori, *J. Am. Chem. Soc.*, 2005, **127**, 8288-8289.
22. R. Noyori, M. Yamakawa and S. Hashiguchi, *J. Org. Chem.*, 2001, **66**, 7931-7944.
23. M. Palmer, T. Walsgrove and M. Wills, *J. Org. Chem.*, 1997, **62**, 5226-5228.
24. H. Matsunaga, T. Ishizuka and T. Kunieda, *Tetrahedron Lett.*, 2005, **46**, 3645-3648.
25. I. Bauer and H. J. Knolker, *Chem. Rev.*, 2015, **115**, 3170-3387.
26. L. C. M. Castro, H. Q. Li, J. B. Sortais and C. Darcel, *Green Chem.*, 2015, **17**, 2283-2303.
27. D. Wang and D. Astruc, *Chem. Rev.*, 2015, **115**, 6621-6686.
28. G. A. Filonenko, R. van Putten, E. J. M. Hensen and E. A. Pidko, *Chem. Soc. Rev.*, 2018, **47**, 1459-1483.
29. S. Enthaler, K. Junge and M. Beller, *Angew. Chem., Int. Ed.*, 2008, **47**, 3317-3321.
30. G. Sylvain and R. Jean-Luc, *ChemSusChem*, 2008, **1**, 505-509.
31. B. A. F. Le Bailly and S. P. Thomas, *RSC Adv.*, 2011, **1**, 1435-1445.
32. K. Junge, K. Schröder and M. Beller, *Chem. Commun.*, 2011, **47**, 4849-4859.
33. R. M. Bullock, *Science*, 2013, **342**, 1054.

34. A. C. Dlouhy and C. E. Outten, in *Met. Ions Life Sci.*, 2013, vol. 12, pp. 241-278.
35. J.-X. Gao, H. Zhang, X.-D. Yi, P.-P. Xu, C.-L. Tang, H.-L. Wan, K.-R. Tsai and T. Ikariya, *Chirality*, 2000, **12**, 383-388.
36. J. S. Chen, L. L. Chen, Y. Xing, G. Chen, W. Y. Shen, Z. R. Dong, Y. Y. Li and J. X. Gao, *Acta Chim. Sin.*, 2004, **62**, 1745-1750.
37. S. Enthaler, G. Erre, M. K. Tse, K. Junge and M. Beller, *Tetrahedron Lett.*, 2006, **47**, 8095-8099.
38. S. Enthaler, B. Spilker, G. Erre, K. Junge, M. K. Tse and M. Beller, *Tetrahedron*, 2008, **64**, 3867-3876.
39. H.-J. Knölker, E. Baum, H. Goesmann and R. Klauss, *Angew. Chem., Int. Ed.*, 1999, **38**, 2064-2066.
40. C. P. Casey and H. Guan, *J. Am. Chem. Soc.*, 2007, **129**, 5816-5817.
41. C. Sui-Seng, F. Freutel, A. J. Lough and R. H. Morris, *Angew. Chem., Int. Ed.*, 2008, **47**, 940-943.
42. N. Meyer, A. J. Lough and R. H. Morris, *Chem. - Eur. J.*, 2009, **15**, 5605-5610.
43. J. F. Sonnenberg, N. Coombs, P. A. Dube and R. H. Morris, *J. Am. Chem. Soc.*, 2012, **134**, 5893-5899.
44. D. E. Prokopchuk, J. F. Sonnenberg, N. Meyer, M. Zimmer-De Iuliis, A. J. Lough and R. H. Morris, *Organometallics*, 2012, **31**, 3056-3064.
45. A. Mikhailine, A. J. Lough and R. H. Morris, *J. Am. Chem. Soc.*, 2009, **131**, 1394-1395.
46. P. O. Lagaditis, A. J. Lough and R. H. Morris, *Inorg. Chem.*, 2010, **49**, 10057-10066.
47. P. E. Sues, A. J. Lough and R. H. Morris, *Organometallics*, 2011, **30**, 4418-4431.
48. A. A. Mikhailine and R. H. Morris, *Inorg. Chem.*, 2010, **49**, 11039-11044.
49. P. O. Lagaditis, A. J. Lough and R. H. Morris, *J. Am. Chem. Soc.*, 2011, **133**, 9662-9665.
50. A. A. Mikhailine, M. I. Maishan, A. J. Lough and R. H. Morris, *J. Am. Chem. Soc.*, 2012, **134**, 12266-12280.
51. W. Zuo, A. J. Lough, Y. F. Li and R. H. Morris, *Science*, 2013, **342**, 1080-1083.
52. R. Bigler, E. Otth and A. Mezzetti, *Organometallics*, 2014, **33**, 4086-4099.
53. R. Bigler and A. Mezzetti, *Org. Lett.*, 2014, **16**, 6460-6463.
54. R. Bigler, R. Huber and A. Mezzetti, *Angew. Chem.-Int. Edit.*, 2015, **54**, 5171-5174.
55. Y. Y. Li, S. L. Yu, W. Y. Shen and J. X. Gao, *Acc. Chem. Res.*, 2015, **48**, 2587-2598.
56. C. P. Casey and H. Guan, *J. Am. Chem. Soc.*, 2009, **131**, 2499-2507.
57. A. Berkessel, S. Reichau, A. von der Höh, N. Leconte and J.-M. Neudörfl, *Organometallics*, 2011, **30**, 3880-3887.
58. C. Sui-Seng, F. N. Haque, A. Hadzovic, A.-M. Pütz, V. Reuss, N. Meyer, A. J. Lough, M. Zimmer-De Iuliis and R. H. Morris, *Inorg. Chem.*, 2009, **48**, 735-743.
59. R. Langer, G. Leitius, Y. Ben-David and D. Milstein, *Angew. Chem.-Int. Edit.*, 2011, **50**, 2120-2124.
60. M. N. Hopkinson, C. Richter, M. Schedler and F. Glorius, *Nature*, 2014, **510**, 485-496.
61. K. Bowman-James, Macrocyclic Ligands, in *Encyclopedia of Inorganic Chemistry*, eds. R. B. King, R. H. Crabtree, C. M. Lukehart, D. A. Atwood and R. A. Scott, 2006, pp. 1-20.
62. F. J. Leeper, *Nat. Prod. Rep.*, 1989, **6**, 171-203.
63. P. W. Atkins, T. L. Overton, J. P. Rourke, M. T. Weller and F. A. Armstrong, *Shriver & Atkins' Inorganic Chemistry*, Oxford University Press, Oxford; New York, 5th edn., 2010.

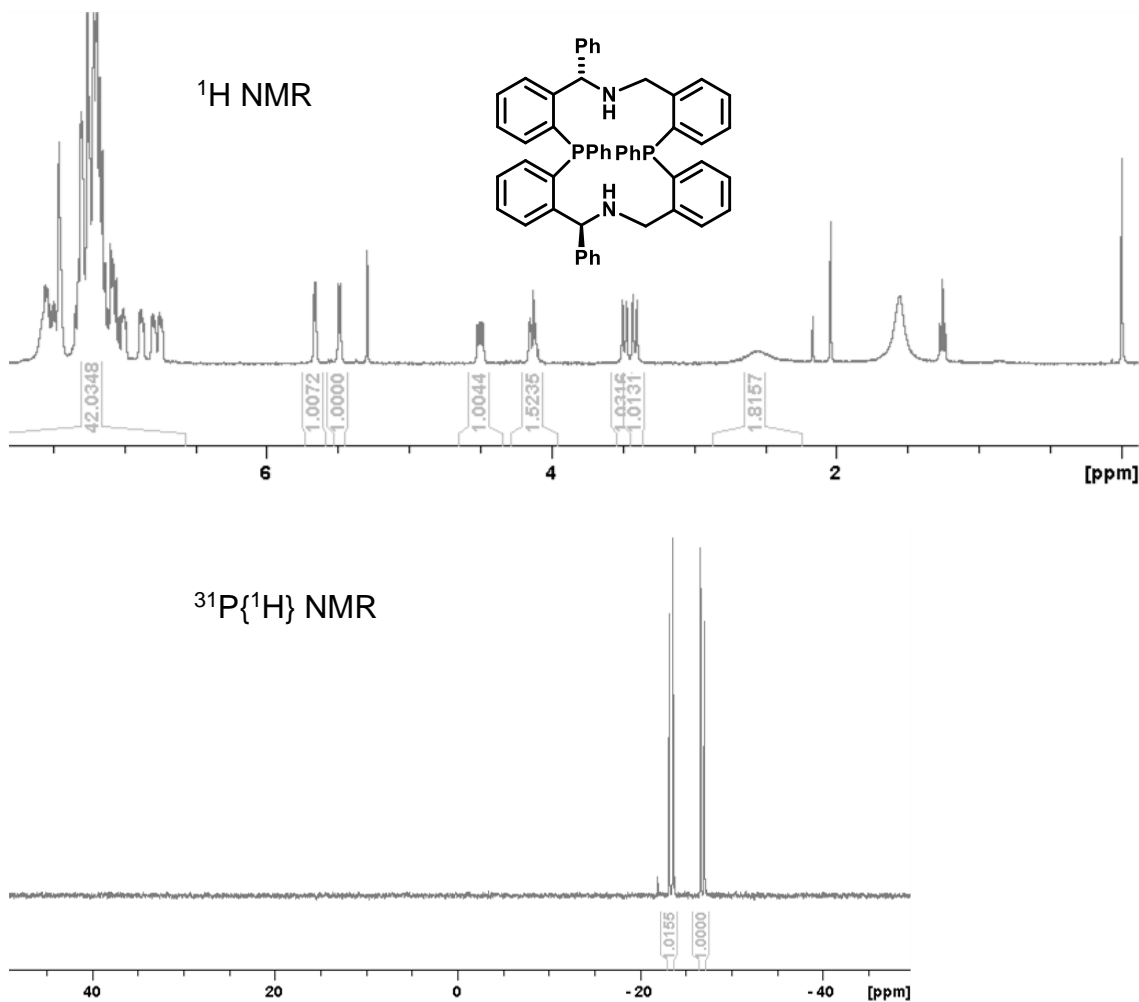
64. V. Martí-Centelles, M. D. Pandey, M. I. Burguete and S. V. Luis, *Chem. Rev.*, 2015, **115**, 8736-8834.
65. C. W. G. Ansell, M. K. Cooper, K. P. Dancey, P. A. Duckworth, K. Henrick, M. McPartlin and P. A. Tasker, *J. Chem. Soc., Chem. Commun.*, 1985, 439-441.
66. Y. Hamada, Y. Yamamoto and H. Shimizu, *J. Organomet. Chem.*, 1996, **510**, 1-6.
67. S. A. Burns, R. J. P. Corriu, V. Huynh and J. J. E. Moreau, *J. Organomet. Chem.*, 1987, **333**, 281-290.
68. V. Chandrasekhar, R. Boomishankar, R. Azhakar, K. Gopal, A. Steiner and S. Zacchini, *Eur. J. Inorg. Chem.*, 2005, **2005**, 1880-1885.
69. J. R. Ascenso, C. G. de Azevedo, A. R. Dias, M. T. Duarte, I. Eleutério, M. J. Ferreira, P. T. Gomes and A. M. Martins, *J. Organomet. Chem.*, 2001, **632**, 17-26.
70. N. Sewald, K. D. Hiller, M. Körner and M. Findeisen, *J. Org. Chem.*, 1998, **63**, 7263-7274.
71. R. K. Bagautdinova, L. K. Kibardina and M. A. Pudovik, *Russ. J. Gen. Chem.*, 2007, **77**, 1468-1469.
72. S. Djuric, J. Venit and P. Magnus, *Tetrahedron Lett.*, 1981, **22**, 1787-1790.
73. M. A. Alonso, J. A. Casares, P. Espinet, K. Soulantica, A. G. Orpen and H. Phetmung, *Inorg. Chem.*, 2003, **42**, 3856-3864.
74. D. Yu, L. Lu and Q. Shen, *Org. Lett.*, 2013, **15**, 940-943.
75. D. W. Slocum, T. K. Reinscheld, C. B. White, M. D. Timmons, P. A. Shelton, M. G. Slocum, R. D. Sandlin, E. G. Holland, D. Kusmic, J. A. Jennings, K. C. Tekin, Q. Nguyen, S. J. Bush, J. M. Keller and P. E. Whitley, *Organometallics*, 2013, **32**, 1674-1686.
76. H. Tsuge, T. Okano, S. Eguchi and H. Kimoto, *J. Chem. Soc., Perkin Trans. 1*, 1997, 1581-1586.
77. X. Hu, C. Bai, H. Dai, H. Chen and Z. Zheng, *J. Mol. Catal. A: Chem.*, 2004, **218**, 107-112.
78. H. Nie, G. Zhou, Q. Wang, W. Chen and S. Zhang, *Tetrahedron: Asymmetry*, 2013, **24**, 1567-1571.
79. J. J. Dannenberg, M. K. Levenberg and J. H. Richards, *Tetrahedron*, 1973, **29**, 1575-1584.
80. D. S. Trifan and R. Bacskai, *Tetrahedron Lett.*, 1960, **1**, 1-8.
81. M. T. Robak, M. A. Herbage and J. A. Ellman, *Chem. Rev.*, 2010, **110**, 3600-3740.
82. C. Rancurel, N. Daro, Oscar B. Borobia, E. Herdtweck and J.-P. Sutter, *Eur. J. Org. Chem.*, 2003, **2003**, 167-171.
83. A. K. Hoffmann and W. M. Thomas, *J. Am. Chem. Soc.*, 1959, **81**, 580-582.
84. E. F. Landvatter and T. B. Rauchfuss, *J. Chem. Soc., Chem. Commun.*, 1982, 1170-1171.
85. W. Winter, *Angew. Chem., Int. Ed. Engl.*, 1978, **17**, 947-948.
86. D. Hellwinkel and W. Krapp, *Chem. Ber.*, 1978, **111**, 13-41.
87. D. B. G. Williams, P. D. R. Kotze, A. C. Ferreira and C. W. Holzapfel, *J. Iran. Chem. Soc.*, 2011, **8**, 240-246.
88. L. B. Schenkel and J. A. Ellman, *Org. Lett.*, 2003, **5**, 545-548.
89. Z.-M. Zhang, P. Chen, W. Li, Y. Niu, X.-L. Zhao and J. Zhang, *Angew. Chem.*, 2014, **126**, 4439-4443.
90. P. Chen, X. Su, W. Zhou, Y. Xiao and J. Zhang, *Tetrahedron*, 2016, **72**, 2700-2706.
91. J.-C. Hierso, *Chem. Rev.*, 2014, **114**, 4838-4867.
92. K. Acharyya and P. S. Mukherjee, *Chem. - Eur. J.*, 2014, **20**, 1646-1657.
93. S. A. Cameron and S. Brooker, *Inorg. Chem.*, 2011, **50**, 3697-3706.
94. T. Takeshita, K. Sato and Y. Nakajima, *Dalton Trans.*, 2018, **47**, 17004-17010.
95. D. H. Busch and N. A. Stephenson, *Coord. Chem. Rev.*, 1990, **100**, 119-154.

96. A. A. Mikhailine, E. Kim, C. Dingels, A. J. Lough and R. H. Morris, *Inorg. Chem.*, 2008, **47**, 6587-6589.
97. G. Liu, D. A. Cogan and J. A. Ellman, *J. Am. Chem. Soc.*, 1997, **119**, 9913-9914.
98. V. Santes, E. Gómez, R. Santillan and N. Farfán, *Synthesis*, 2001, **2001**, 0235-0238.
99. Z. Yang, Z. Zhou, K. He, L. Wang, G. Zhao, Q. Zhou and C. Tang, *Tetrahedron: Asymmetry*, 2003, **14**, 3937-3941.
100. A. J. Arduengo, R. Krafczyk, R. Schmutzler, H. A. Craig, J. R. Goerlich, W. J. Marshall and M. Unverzagt, *Tetrahedron*, 1999, **55**, 14523-14534.
101. P. S. Reiss, M. A. Little, V. Santolini, S. Y. Chong, T. Hasell, K. E. Jelfs, M. E. Briggs and A. I. Cooper, *Chem. - Eur. J.*, 2016, **22**, 16547-16553.
102. A. D. Bain, in *Encyclopedia of Spectroscopy and Spectrometry*, ed. J. C. Lindon, Elsevier, Oxford, 1999, pp. 198-207.
103. J. F. Nixon and A. Pidcock, in *Annu. Rep. NMR Spectrosc.*, ed. E. F. Mooney, Academic Press, 1969, vol. 2, pp. 345-422.
104. K. M. Anderson and A. G. Orpen, *Chem. Commun.*, 2001, 2682-2683.
105. G. G. Christoph, P. Blum, W. C. Liu, A. Elia and D. W. Meek, *Inorg. Chem.*, 1979, **18**, 894-897.
106. E. Alberico, S. Möller, M. Horstmann, H.-J. Drexler and D. Heller, *Catalysts*, 2019, **9**, 582.
107. M. K. Cooper, P. A. Duckworth, T. W. Hambley, G. J. Organ, K. Henrick, M. McPartlin and A. Parekh, *J. Chem. Soc., Dalton Trans.*, 1989, 1067-1073.
108. T. L. Marxen, B. J. Johnson, P. V. Nilsson and L. H. Pignolet, *Inorg. Chem.*, 1984, **23**, 4663-4670.
109. P. E. Garrou, J. L. S. Curtis and G. E. Hartwell, *Inorg. Chem.*, 1976, **15**, 3094-3097.
110. I. O. Koshevoy, O. V. Sizova, S. P. Tunik, A. Lough and A. J. Poë, *Eur. J. Inorg. Chem.*, 2005, **2005**, 4516-4520.
111. P. S. Pregosin and R. W. Kunz, *³¹P and ¹³C NMR of Transition Metal Phosphine Complexes*, Springer Berlin Heidelberg, Berlin, Heidelberg, 1979.
112. J. Wassenaar, M. A. Siegler, A. L. Spek, B. de Bruin, J. N. H. Reek and J. I. van der Vlugt, *Inorg. Chem.*, 2010, **49**, 6495-6508.
113. A. Cagnolini, B. Ballard, H. P. Engelbrecht, T. L. Rold, C. Barnes, C. Cutler, T. J. Hoffman, R. Kannan, K. Katti and S. S. Jurisson, *Nucl. Med. Biol.*, 2011, **38**, 63-76.
114. D. W. Meek and T. J. Mazanec, *Acc. Chem. Res.*, 1981, **14**, 266-274.
115. F. H. Jardine, Rhodium: Inorganic & Coordination Chemistry, in *Encyclopedia of Inorganic and Bioinorganic Chemistry*, ed. R. A. Scott, 2011, pp. 1-30.
116. J.-X. Gao, X.-D. Yi, P.-P. Xu, C.-L. Tang, H.-L. Wan and T. Ikariya, *J. Organomet. Chem.*, 1999, **592**, 290-295.
117. J.-X. Gao, X.-D. Yi, P.-P. Xu, C.-L. Tang, H. Zhang, H.-L. Wan and T. Ikariya, *J. Mol. Catal. A: Chem.*, 2000, **159**, 3-9.
118. S. Burger, B. Therrien and G. Süß-Fink, *Helv. Chim. Acta*, 2005, **88**, 478-486.
119. S. Tanaka, C. Dubs, A. Inagaki and M. Akita, *Organometallics*, 2005, **24**, 163-184.
120. J. J. Gambaro, W. H. Hohman and D. W. Meek, *Inorg. Chem.*, 1989, **28**, 4154-4159.
121. R. Prabakaran and N. C. Fletcher, *Dalton Trans.*, 2003, 2558-2563.
122. J. A. Widegren and R. G. Finke, *J. Mol. Catal. A: Chem.*, 2003, **198**, 317-341.
123. R. S. Phatake, P. Patel and C. V. Ramana, *Org. Lett.*, 2016, **18**, 292-295.
124. R. Reingruber and S. Bräse, *Chem. Commun.*, 2008, 105-107.
125. P. Eisenberger, A. M. Bailey and C. M. Crudden, *J. Am. Chem. Soc.*, 2012, **134**, 17384-17387.

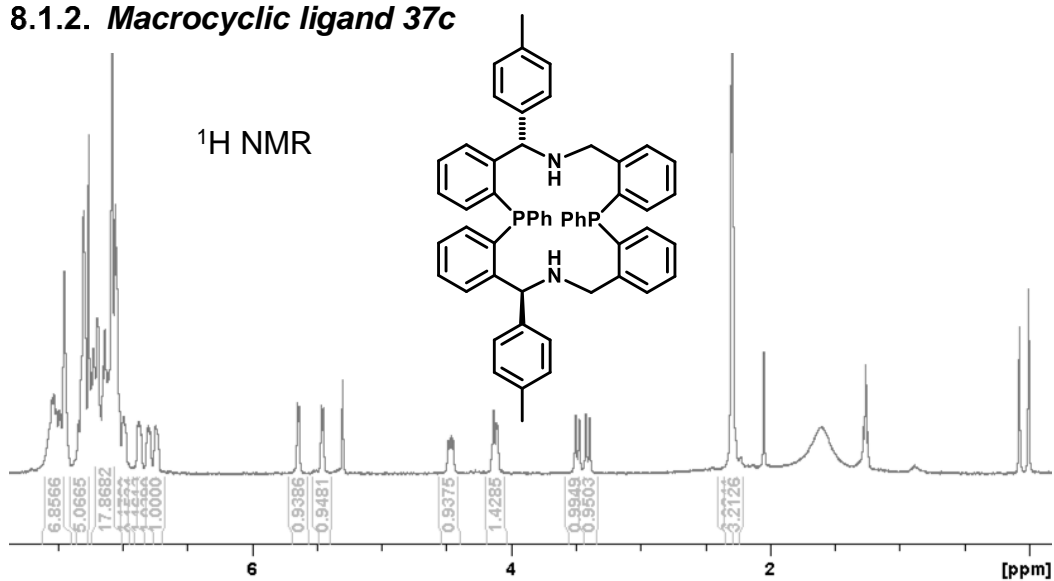
Chapter 8. Appendix

8.1. NMR spectra of ligands

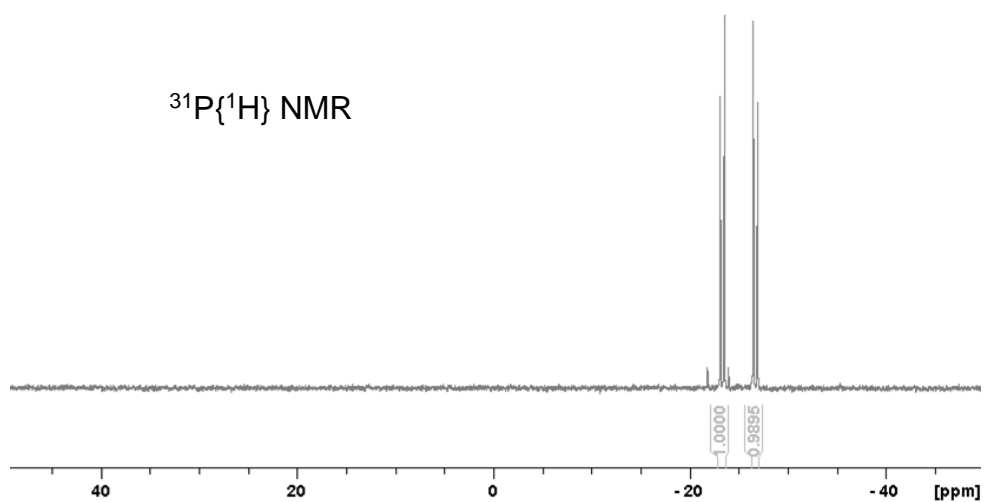
8.1.1. Macrocyclic ligand 37b



8.1.2. Macrocyclic ligand 37c

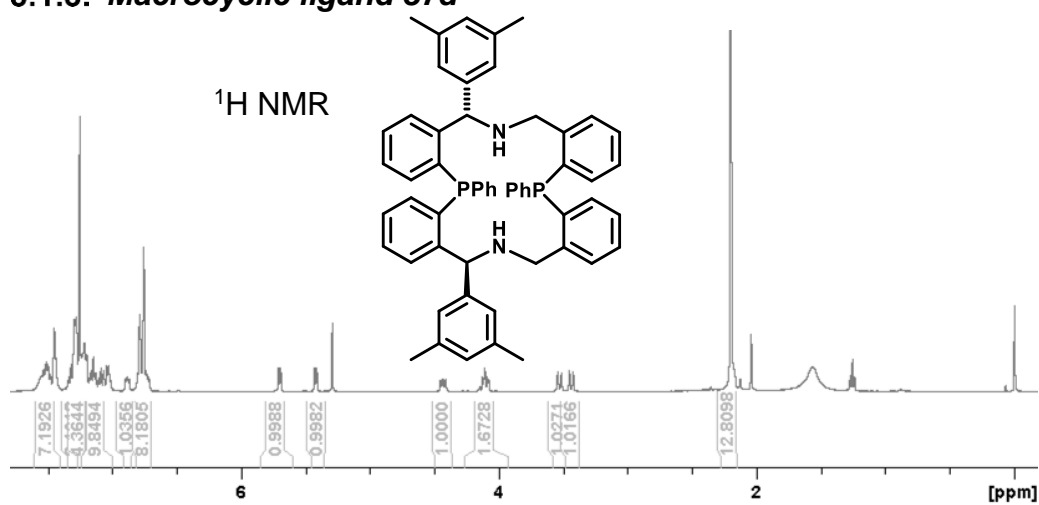


$^{31}\text{P}\{^1\text{H}\}$ NMR

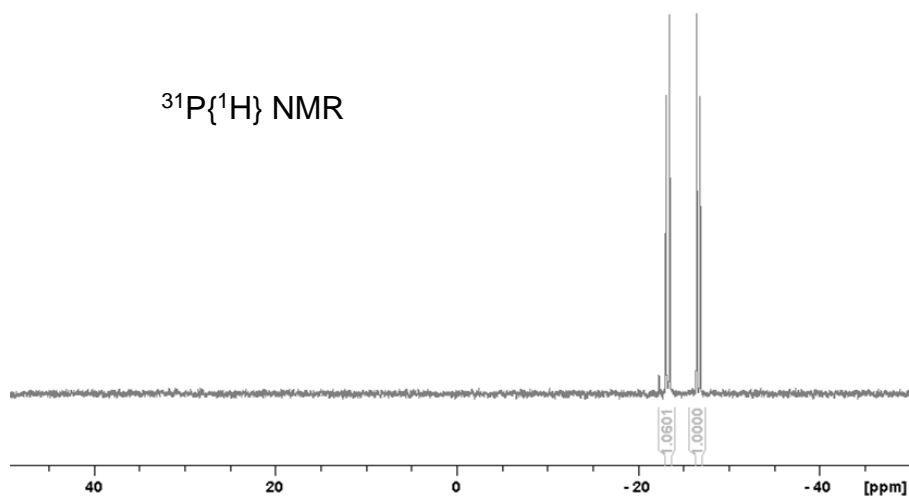


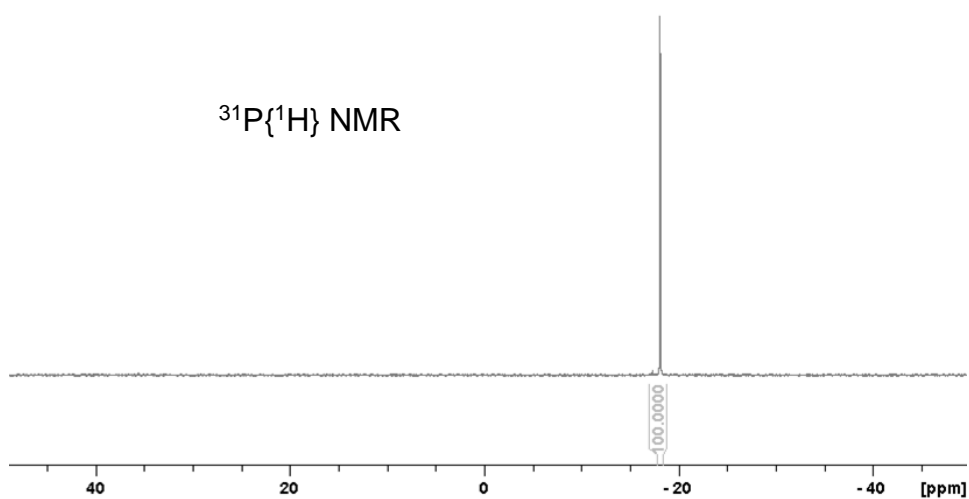
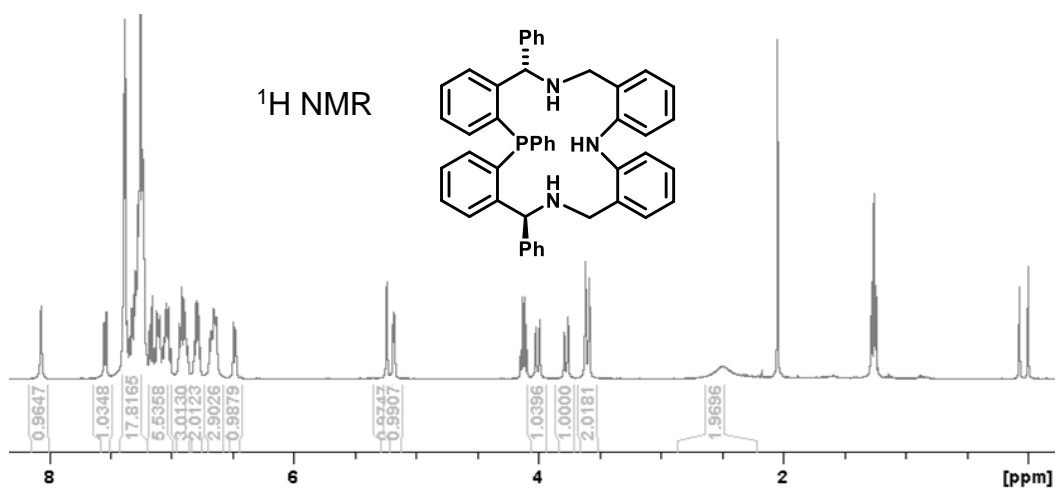
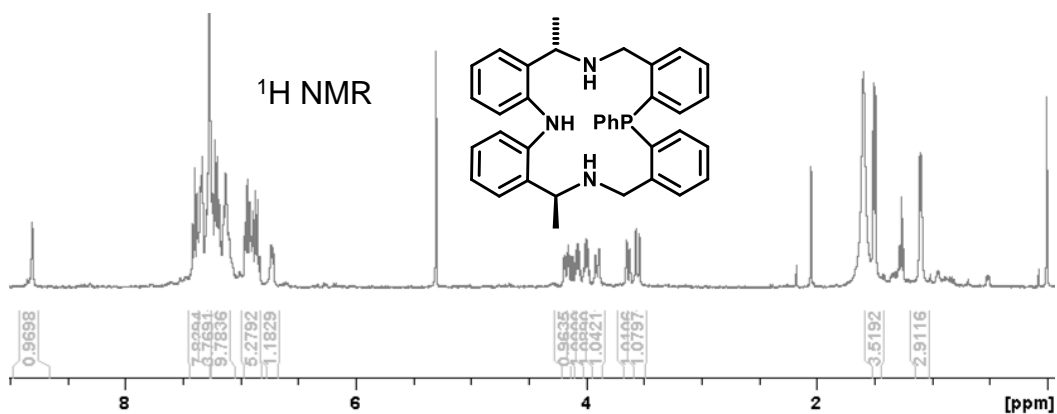
8.1.3. Macrocyclic ligand 37d

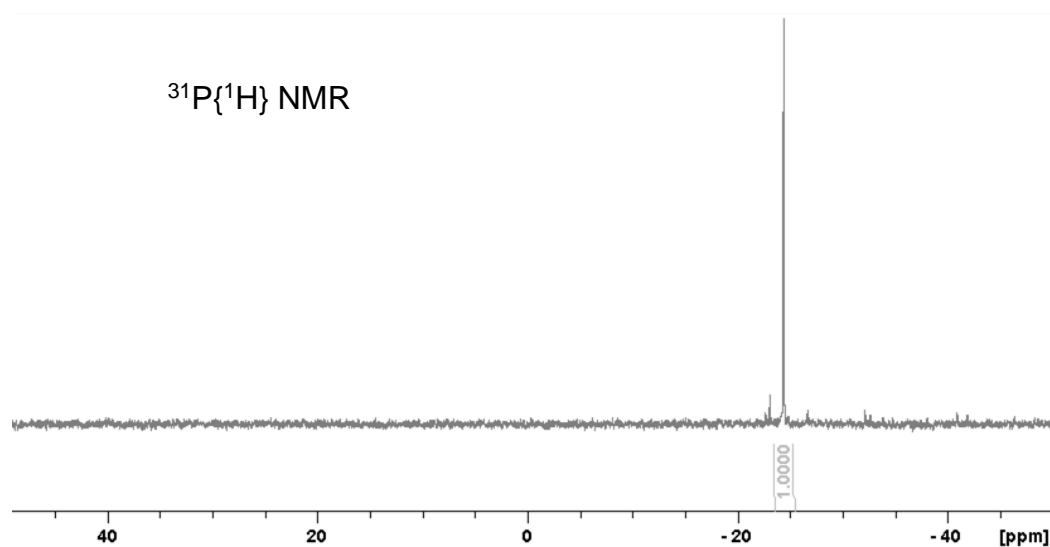
^1H NMR



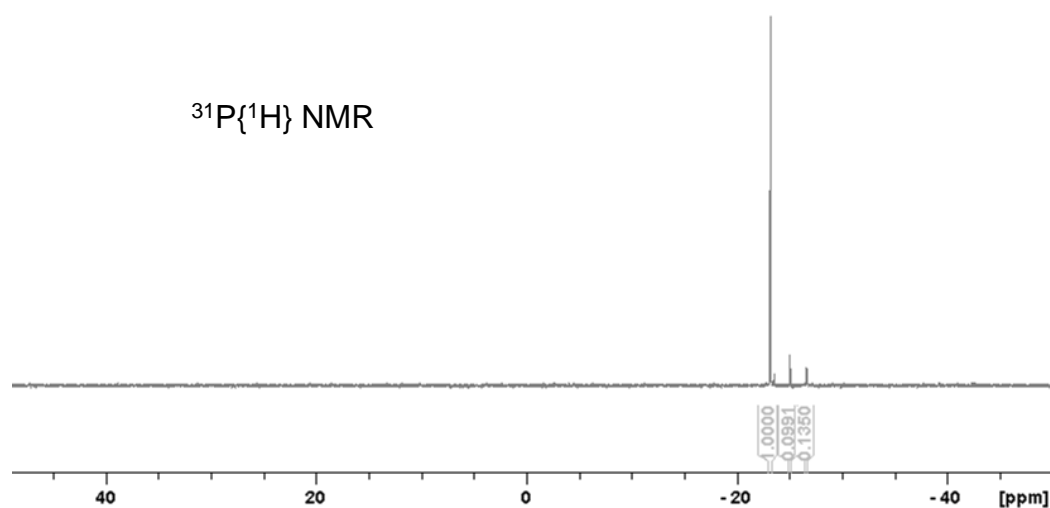
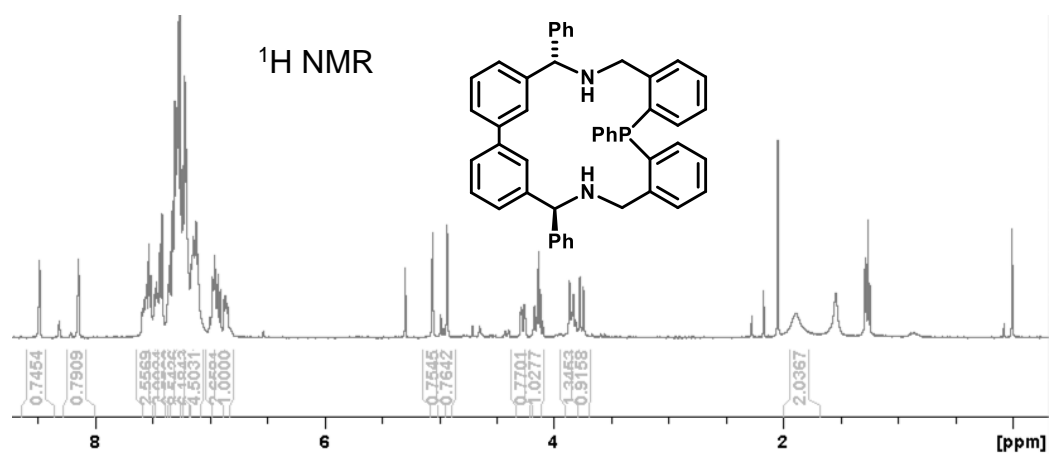
$^{31}\text{P}\{^1\text{H}\}$ NMR

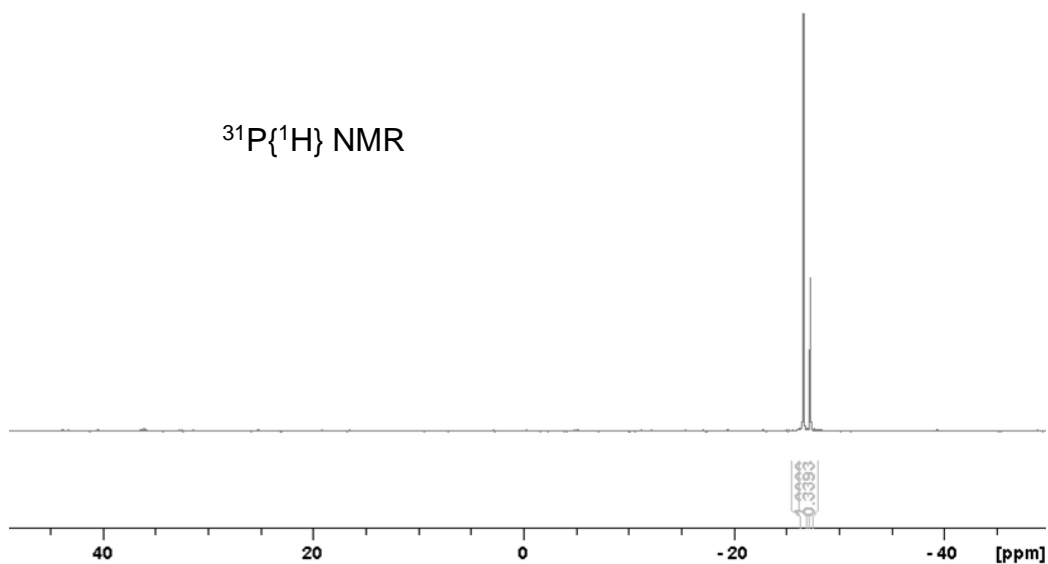
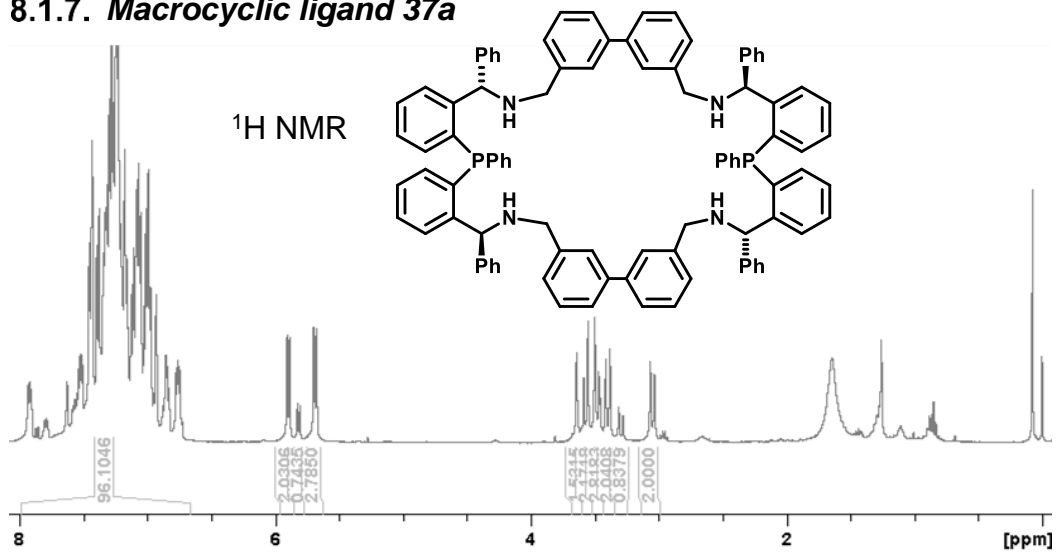
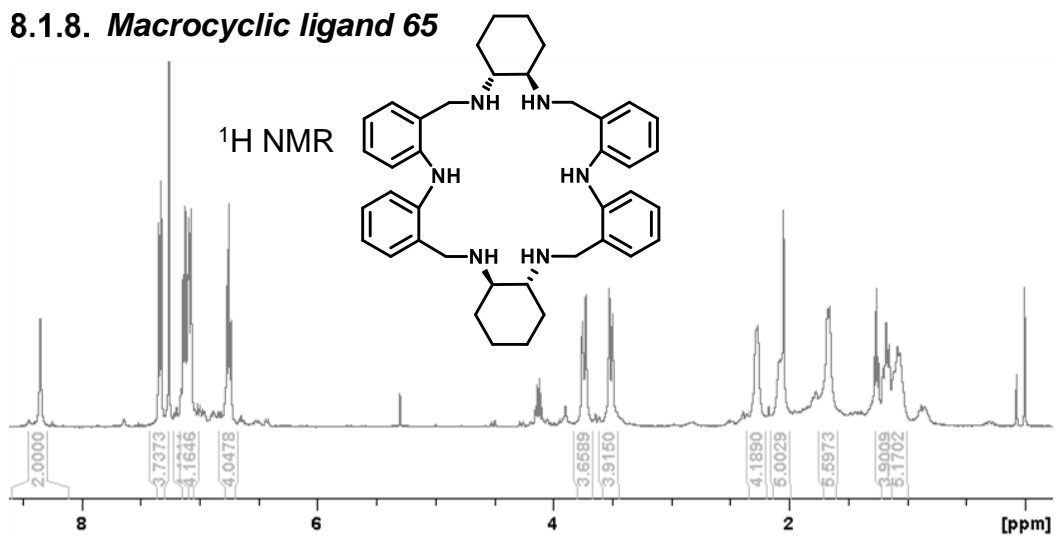


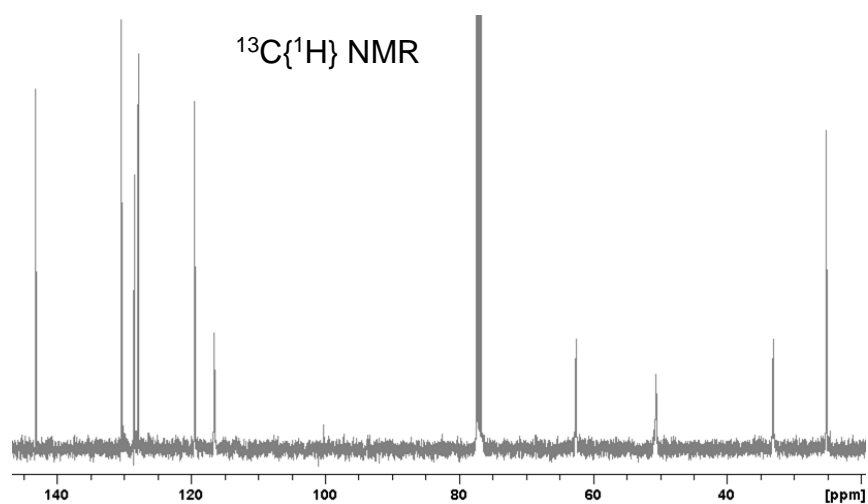
8.1.4. *Macrocyclic ligand 37e*8.1.5. *Macrocyclic ligand 64*



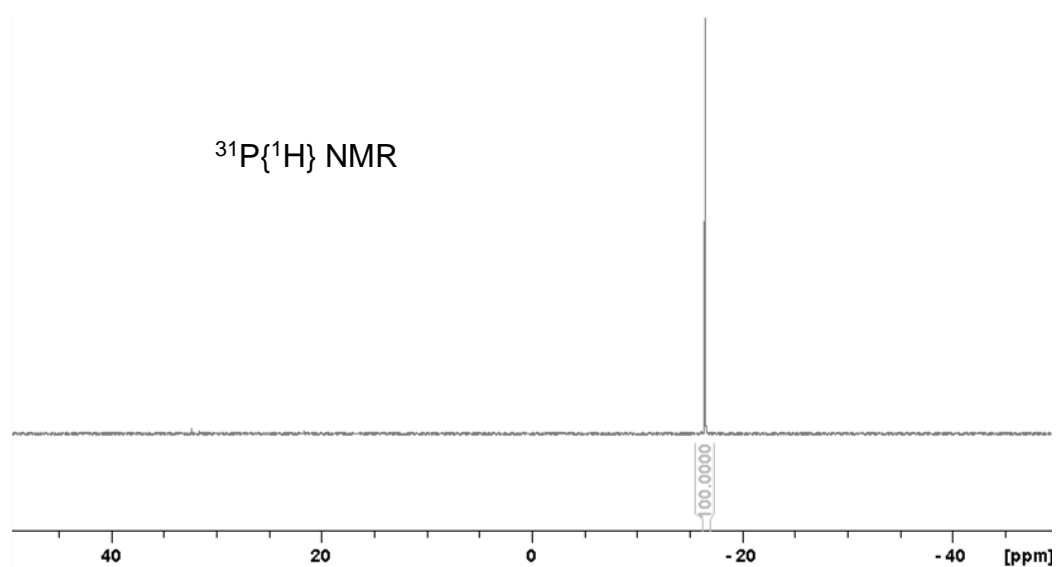
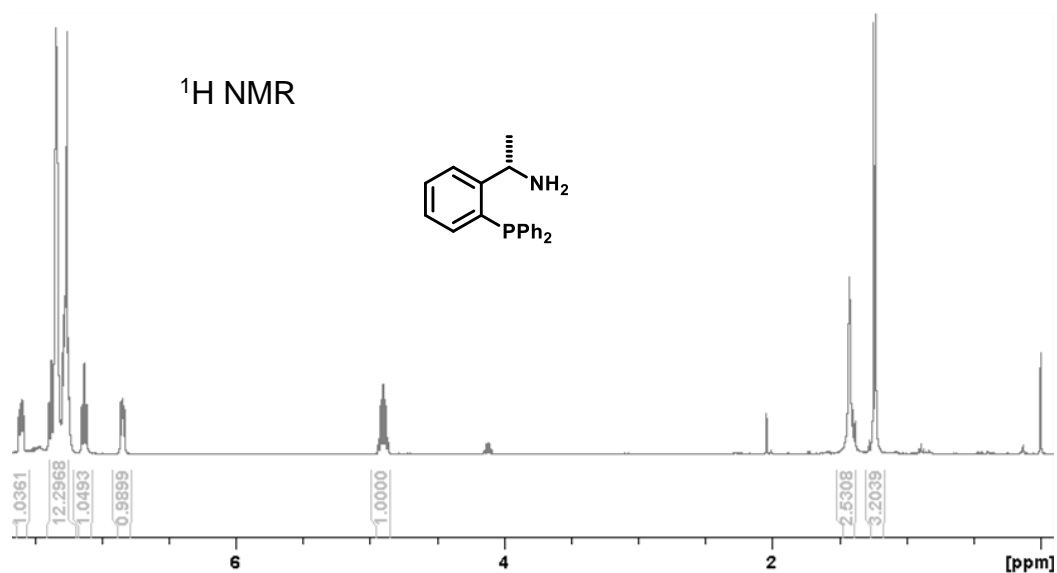
8.1.6. Macrocyclic ligand 63

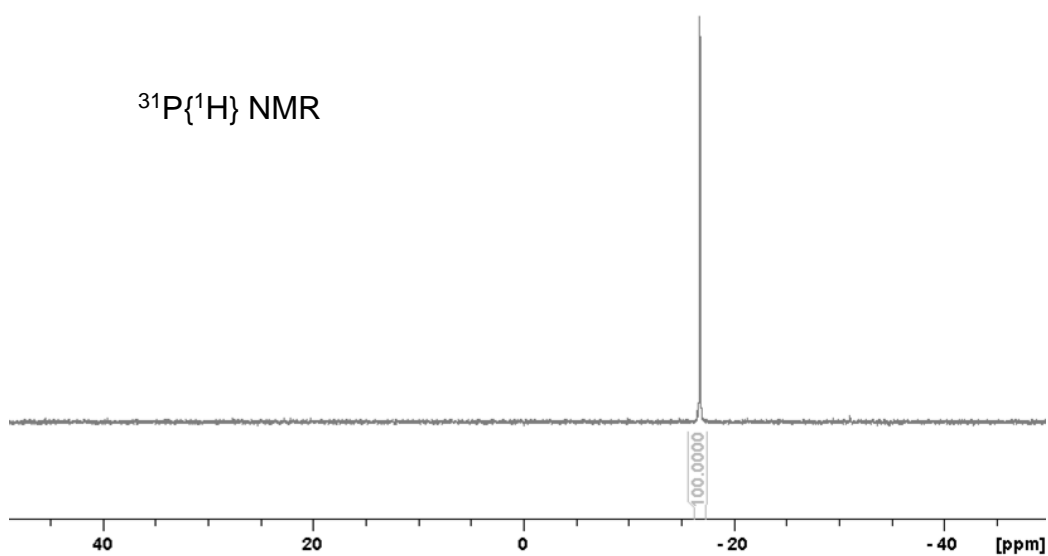
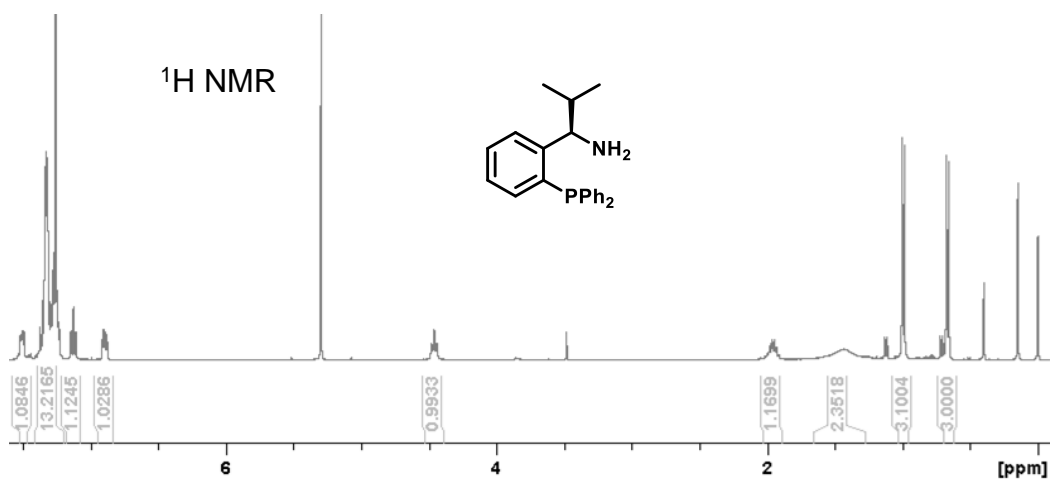
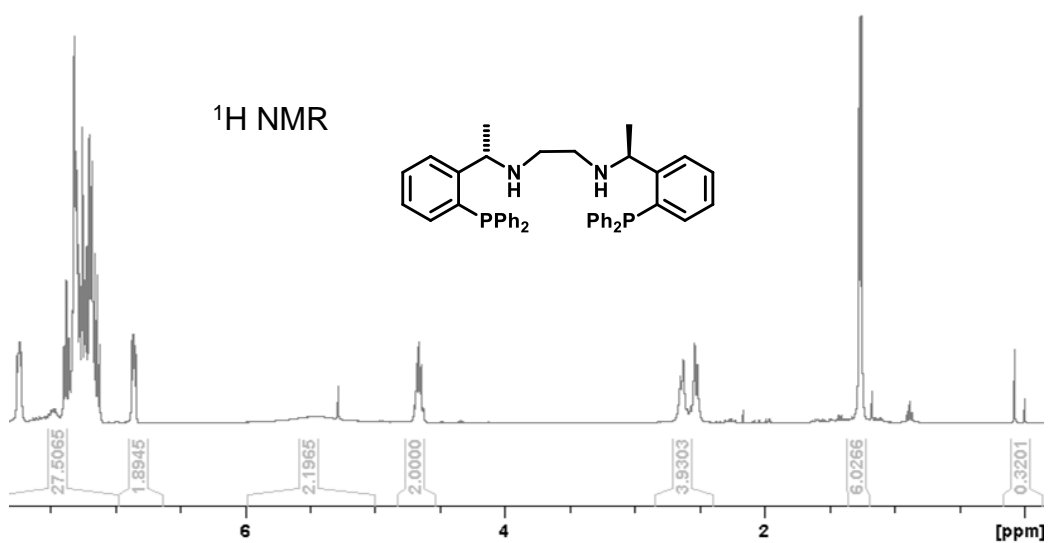


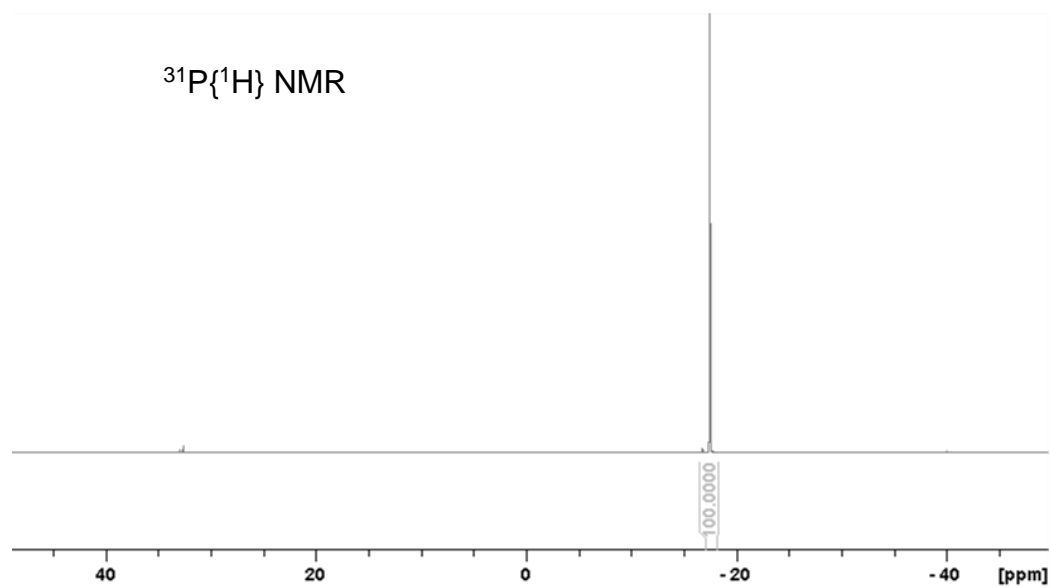
8.1.7. *Macrocyclic ligand 37a*8.1.8. *Macrocyclic ligand 65*



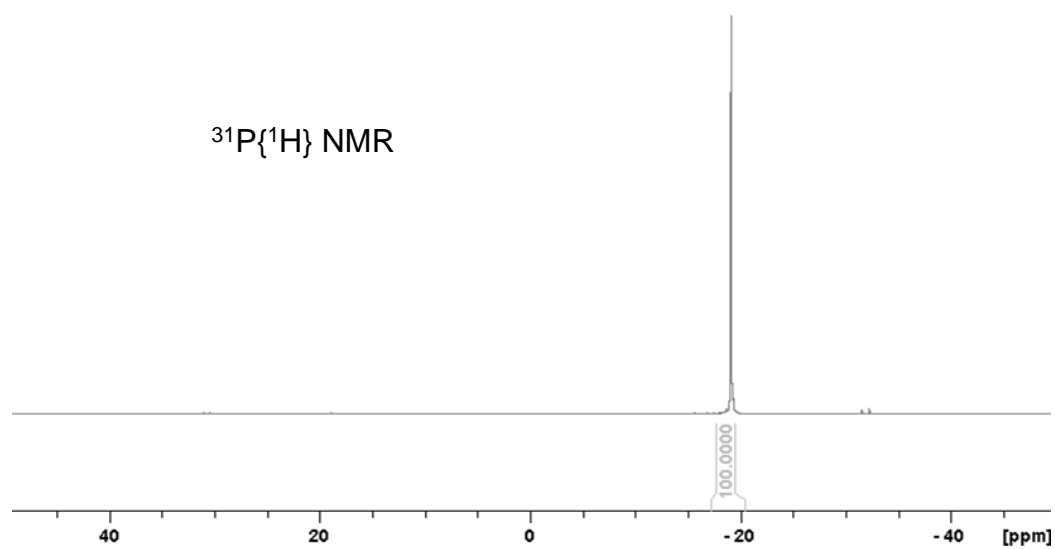
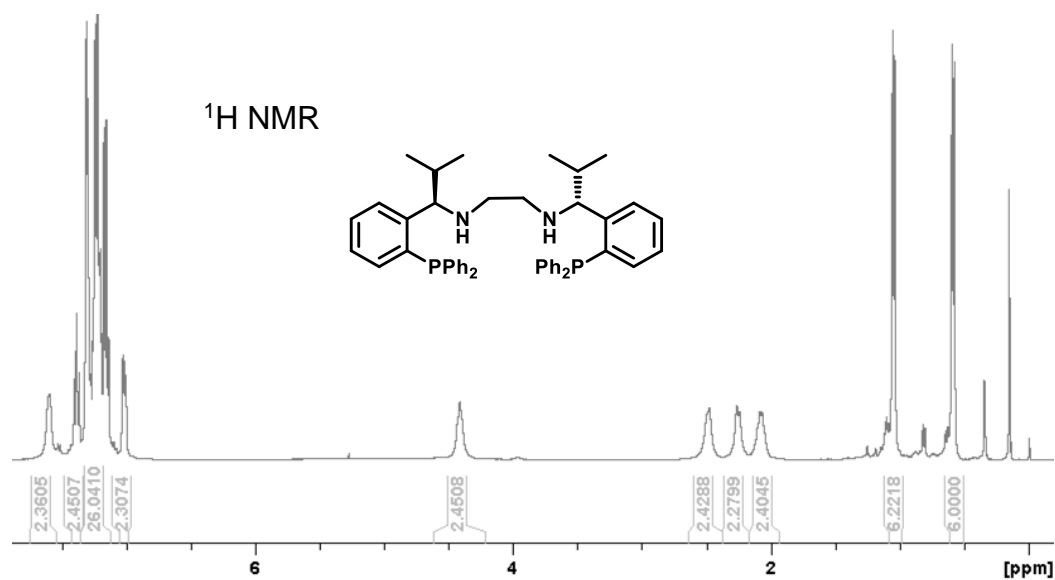
8.1.9. *PN ligand 81*

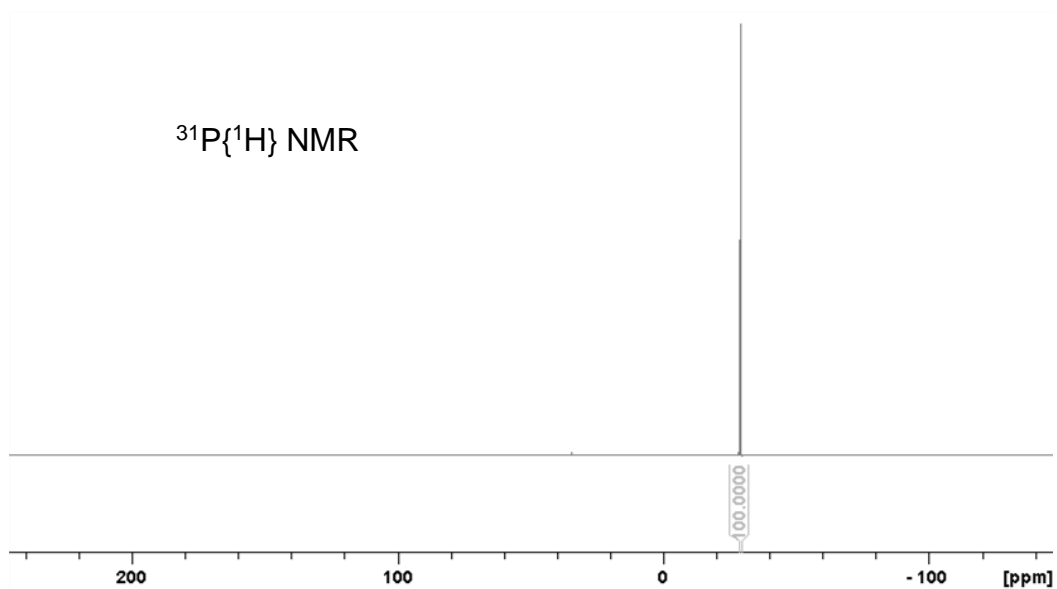
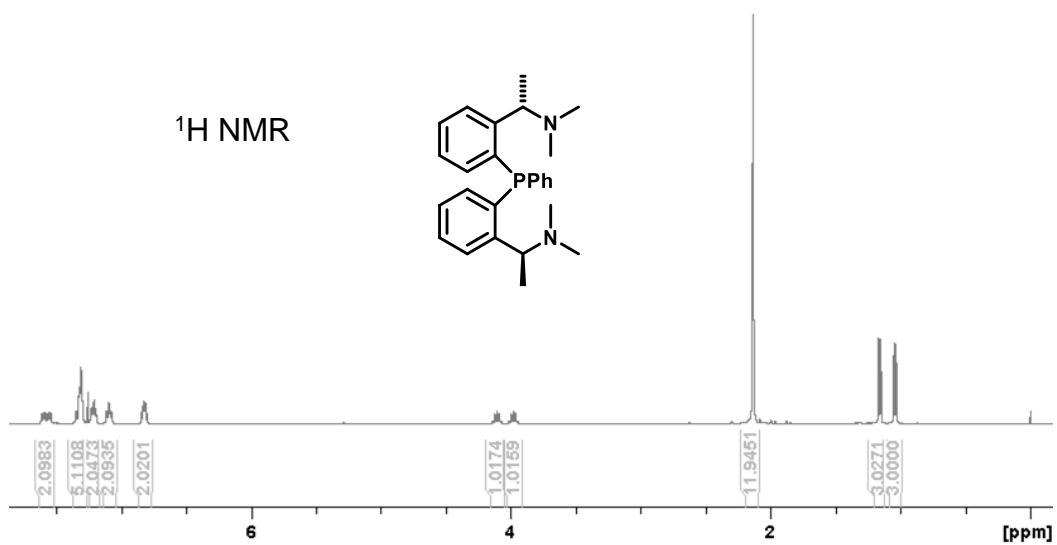
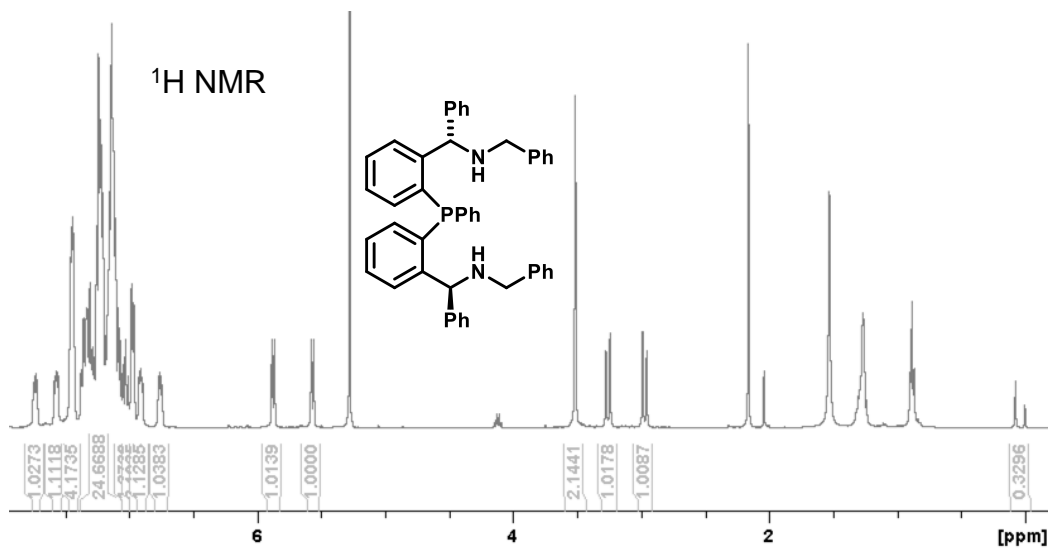


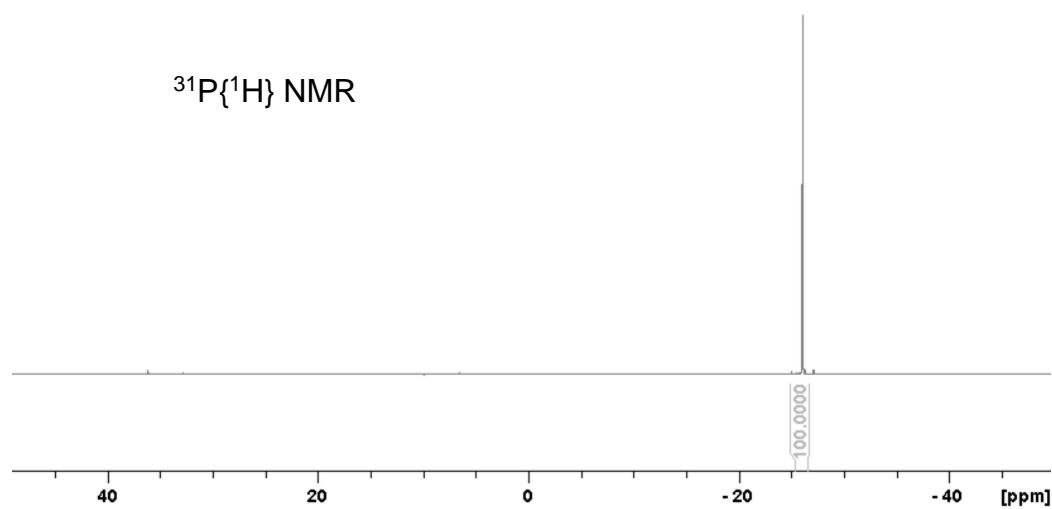
8.1.10. *PN ligand 85*8.1.11. *PNNP ligand 82*



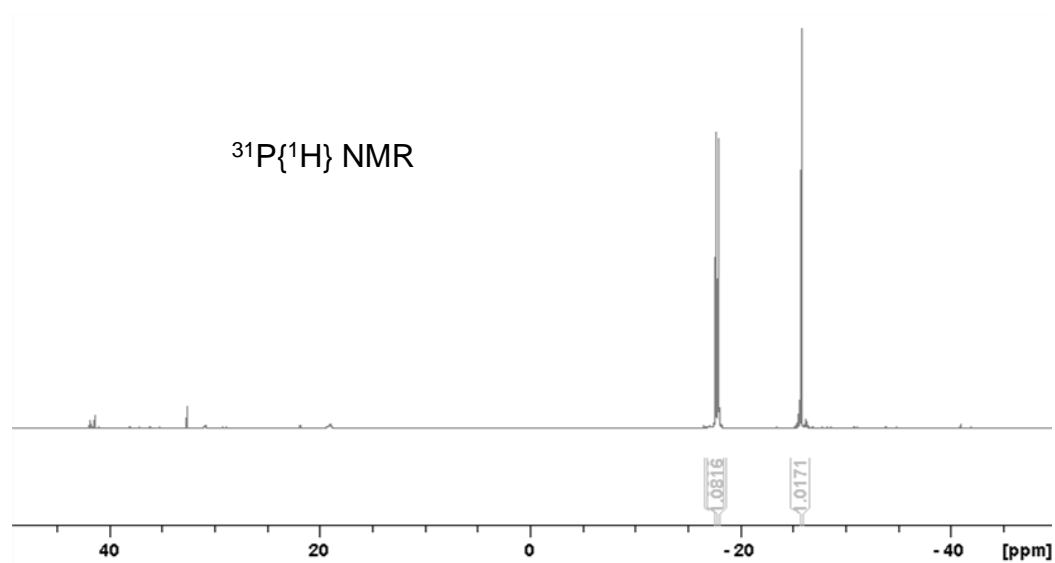
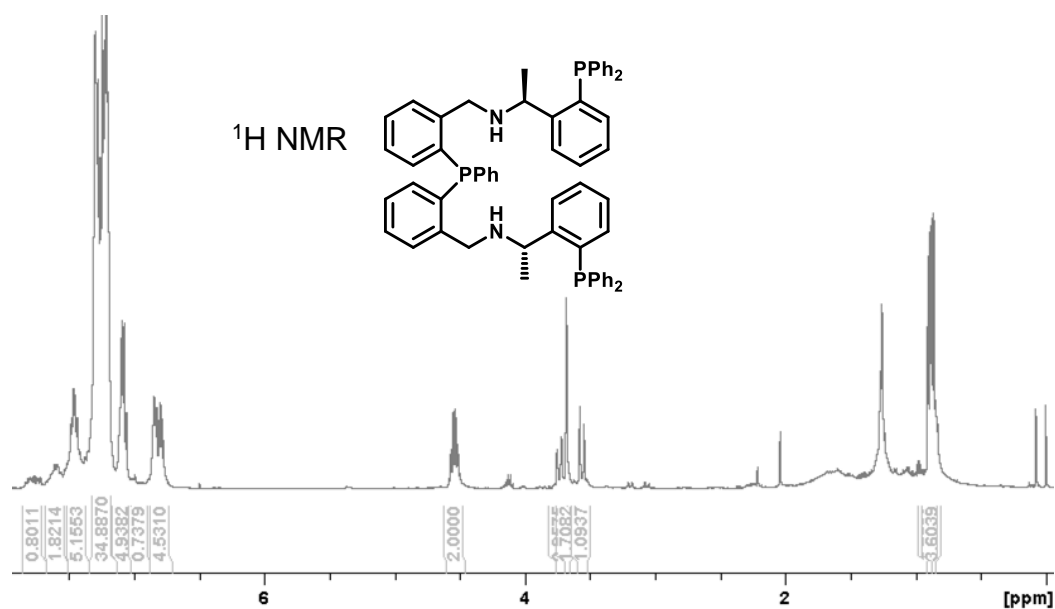
8.1.12. PNNP ligand 86



8.1.13. *PNP ligand 44*8.1.14. *PNP ligand 84*



8.1.15. *Pentadentate ligand 87*



8.2. Crystal structure data for 62

Crystal data and structure refinement:

_chemical_formula_moiety	'C52 H46 N2 P2, C H Cl3, 2(B F4)'
_chemical_formula_sum	'C52 H46 B3 Cl3 F8 N2 P2'
_chemical_formula_weight	1051.63
_space_group_crystal_system	'orthorhombic'
_space_group_name_H-M_alt	'P 21 21 21'
_cell_length_a	11.2657(7)
_cell_length_b	15.2832(8)
_cell_length_c	30.3398(17)
_cell_angle_alpha	90
_cell_angle_beta	90
_cell_angle_gamma	90
_cell_volume	5223.8(5)
_cell_formula_units_Z	4
_cell_measurement_temperature	296(2)
_exptl_absorpt_coefficient_mu	0.303
_exptl_crystal_density_diffn	1.337
_exptl_crystal_F_000	2160
_diffn_reflns_av_R_equivalents	0.0519
_diffn_reflns_av_unetI/netI	0.0528
_diffn_reflns_limit_h_max	13
_diffn_reflns_limit_h_min	-14
_diffn_reflns_limit_k_max	19
_diffn_reflns_limit_k_min	-18
_diffn_reflns_limit_l_max	37
_diffn_reflns_limit_l_min	-36
_diffn_reflns_number	53110
_diffn_reflns_theta_max	26.433
_diffn_reflns_theta_min	1.342
_diffn_radiation_type	MoK α
_diffn_radiation_wavelength	0.71073
_reflns_number_total	10641
_refine_ls_goodness_of_fit_ref	0.941
_refine_ls_number_parameters	631
_refine_ls_number_reflns	10641
_refine_ls_number_restraints	0

```

_refine_ls_R_factor_all      0.0634
_refine_ls_R_factor_gt      0.0473
_refine_ls_wR_factor_gt     0.1262
_refine_ls_wR_factor_ref     0.1395
REM Highest difference peak  0.837,  deepest hole -0.464

```

Fractional atomic coordinates:

```

loop_
  _atom_site_label
  _atom_site_type_symbol
  _atom_site_fract_x
  _atom_site_fract_y
  _atom_site_fract_z
  _atom_site_U_iso_or_equiv
  _atom_site_adp_type
  _atom_site_occupancy
  _atom_site_site_symmetry_order
  _atom_site_calc_flag
  _atom_site_refinement_flags_posn
  _atom_site_refinement_flags_adp
  _atom_site_refinement_flags_occupancy
  _atom_site_disorder_assembly
  _atom_site_disorder_group
P001 P 0.66260(9) 0.28720(6) 0.38481(3) 0.0203(2) Uani 1 1 d . . . . .
P002 P 0.61141(10) 0.55009(6) 0.35384(3) 0.0192(2) Uani 1 1 d . . . . .
Cl00 Cl 1.05869(15) 0.30756(13) 0.10311(5) 0.0694(5) Uani 1 1 d . . . . .
Cl1 Cl 0.88824(16) 0.44869(10) 0.09997(6) 0.0647(4) Uani 1 1 d . . . . .
Cl2 Cl 0.80992(16) 0.26904(11) 0.09658(6) 0.0668(5) Uani 1 1 d . . . . .
F006 F 0.3656(2) 0.41834(16) 0.38041(8) 0.0327(6) Uani 1 1 d . . . . .
F007 F 0.8077(2) 0.38476(16) 0.28384(8) 0.0347(6) Uani 1 1 d . . . . .
F008 F 0.8755(3) 0.33068(17) 0.21880(9) 0.0423(7) Uani 1 1 d . . . . .
F009 F 0.8496(3) 0.47639(17) 0.22741(10) 0.0462(8) Uani 1 1 d . . . . .
F00A F 0.2567(3) 0.3849(2) 0.31922(9) 0.0476(8) Uani 1 1 d . . . . .
F00B F 0.9973(3) 0.4073(2) 0.26464(10) 0.0500(8) Uani 1 1 d . . . . .
F00C F 0.2137(3) 0.32371(19) 0.38580(10) 0.0500(8) Uani 1 1 d . . . . .
N00D N 0.4919(3) 0.39137(19) 0.30111(10) 0.0206(7) Uani 1 1 d . . . . .
H00A H 0.5179 0.4099 0.3272 0.025 Uiso 1 1 calc R . . . .
H00B H 0.4132 0.3875 0.3028 0.025 Uiso 1 1 calc R . . . .
F00E F 0.1754(3) 0.4661(2) 0.37327(12) 0.0610(9) Uani 1 1 d . . . . .

```

N00F N 0.9370(3) 0.4096(2) 0.36321(11) 0.0242(8) Uani 1 1 d
 H00C H 1.0118 0.4279 0.3614 0.029 Uiso 1 1 calc R
 H00D H 0.9144 0.3931 0.3364 0.029 Uiso 1 1 calc R
 C00G C 0.7849(4) 0.2137(2) 0.36931(13) 0.0207(8) Uani 1 1 d
 C00H C 0.4962(4) 0.5943(2) 0.31748(13) 0.0187(8) Uani 1 1 d
 C00I C 0.3428(4) 0.7017(2) 0.30296(14) 0.0239(9) Uani 1 1 d
 H00I H 0.3028 0.7525 0.3110 0.029 Uiso 1 1 calc R
 C00J C 0.5229(4) 0.4608(2) 0.26659(12) 0.0182(8) Uani 1 1 d
 H00J H 0.6089 0.4704 0.2674 0.022 Uiso 1 1 calc R
 C00K C 0.8586(4) 0.5576(2) 0.34387(13) 0.0214(9) Uani 1 1 d
 C00L C 0.7496(4) 0.5949(2) 0.33172(12) 0.0193(8) Uani 1 1 d
 C00M C 0.4611(3) 0.5468(2) 0.27961(13) 0.0184(8) Uani 1 1 d
 C00N C 0.9029(4) 0.2464(2) 0.37036(13) 0.0214(9) Uani 1 1 d
 C00O C 0.7657(4) 0.1317(3) 0.35071(14) 0.0250(9) Uani 1 1 d
 H00O H 0.6895 0.1083 0.3506 0.030 Uiso 1 1 calc R
 C00P C 0.5313(4) 0.2246(2) 0.36816(13) 0.0205(8) Uani 1 1 d
 C00Q C 0.5730(4) 0.4331(2) 0.18754(14) 0.0254(9) Uani 1 1 d
 H00Q H 0.6492 0.4532 0.1936 0.030 Uiso 1 1 calc R
 C00R C 0.4852(4) 0.2377(2) 0.32550(13) 0.0203(8) Uani 1 1 d
 C00S C 0.8594(4) 0.4848(2) 0.37828(14) 0.0226(9) Uani 1 1 d
 H00S H 0.7782 0.4622 0.3799 0.027 Uiso 1 1 calc R
 C00T C 0.5405(4) 0.3017(2) 0.29327(13) 0.0226(9) Uani 1 1 d
 H00E H 0.6260 0.3022 0.2970 0.027 Uiso 1 1 calc R
 H00F H 0.5231 0.2836 0.2633 0.027 Uiso 1 1 calc R
 C00U C 0.9631(4) 0.5871(3) 0.32462(15) 0.0287(10) Uani 1 1 d
 H00U H 1.0350 0.5611 0.3320 0.034 Uiso 1 1 calc R
 C00V C 0.4904(4) 0.4277(2) 0.22110(13) 0.0217(9) Uani 1 1 d
 C00W C 0.4725(4) 0.1674(2) 0.39674(14) 0.0249(9) Uani 1 1 d
 H00W H 0.5017 0.1588 0.4251 0.030 Uiso 1 1 calc R
 C00X C 0.4362(4) 0.6713(2) 0.32834(14) 0.0242(9) Uani 1 1 d
 H00X H 0.4595 0.7028 0.3531 0.029 Uiso 1 1 calc R
 C00Y C 0.3096(4) 0.6565(2) 0.26594(14) 0.0247(9) Uani 1 1 d
 H00Y H 0.2473 0.6769 0.2486 0.030 Uiso 1 1 calc R
 C00Z C 0.3843(4) 0.1921(2) 0.31295(14) 0.0241(9) Uani 1 1 d
 H00Z H 0.3547 0.1996 0.2846 0.029 Uiso 1 1 calc R
 C010 C 0.9314(4) 0.3310(2) 0.39390(13) 0.0224(9) Uani 1 1 d
 H01A H 1.0072 0.3248 0.4088 0.027 Uiso 1 1 calc R
 H01B H 0.8714 0.3416 0.4162 0.027 Uiso 1 1 calc R

C011 C 0.5891(4) 0.6118(2) 0.40449(13) 0.0236(9) Uani 1 1 d
 C012 C 0.9939(4) 0.1989(3) 0.35112(14) 0.0257(9) Uani 1 1 d
 H012 H 1.0707 0.2212 0.3513 0.031 Uiso 1 1 calc R
 C013 C 0.9607(4) 0.6558(3) 0.29413(15) 0.0294(10) Uani 1 1 d
 H013 H 1.0310 0.6756 0.2816 0.035 Uiso 1 1 calc R
 C014 C 0.3696(4) 0.5795(2) 0.25415(13) 0.0227(9) Uani 1 1 d
 H014 H 0.3472 0.5499 0.2287 0.027 Uiso 1 1 calc R
 C015 C 0.8926(4) 0.5143(2) 0.42452(14) 0.0269(10) Uani 1 1 d
 C016 C 0.8580(4) 0.0845(2) 0.33245(15) 0.0295(10) Uani 1 1 d
 H016 H 0.8433 0.0294 0.3206 0.035 Uiso 1 1 calc R
 C017 C 0.3713(4) 0.1236(2) 0.38338(15) 0.0285(10) Uani 1 1 d
 H017 H 0.3332 0.0858 0.4028 0.034 Uiso 1 1 calc R
 C018 C 0.3264(4) 0.1355(2) 0.34154(15) 0.0272(10) Uani 1 1 d
 H018 H 0.2583 0.1060 0.3326 0.033 Uiso 1 1 calc R
 C019 C 0.7503(4) 0.6640(2) 0.30133(13) 0.0239(9) Uani 1 1 d
 H019 H 0.6789 0.6903 0.2935 0.029 Uiso 1 1 calc R
 C01A C 0.6686(4) 0.6750(3) 0.41990(14) 0.0279(9) Uani 1 1 d
 H01C H 0.7342 0.6904 0.4030 0.034 Uiso 1 1 calc R
 C01B C 0.3777(4) 0.3946(2) 0.21186(14) 0.0266(9) Uani 1 1 d
 H01D H 0.3218 0.3891 0.2342 0.032 Uiso 1 1 calc R
 C01C C 0.6542(4) 0.2849(3) 0.44465(13) 0.0256(9) Uani 1 1 d
 C01D C 0.9719(4) 0.1183(3) 0.33154(15) 0.0297(10) Uani 1 1 d
 H01E H 1.0330 0.0874 0.3180 0.036 Uiso 1 1 calc R
 C01E C 0.4914(5) 0.5892(3) 0.43048(15) 0.0340(11) Uani 1 1 d
 H01F H 0.4384 0.5467 0.4208 0.041 Uiso 1 1 calc R
 C01F C 0.8550(4) 0.6941(3) 0.28267(14) 0.0283(10) Uani 1 1 d
 H01G H 0.8536 0.7399 0.2625 0.034 Uiso 1 1 calc R
 C01G C 0.5427(5) 0.4089(3) 0.14494(15) 0.0368(12) Uani 1 1 d
 H01H H 0.5985 0.4136 0.1225 0.044 Uiso 1 1 calc R
 C01H C 0.9981(5) 0.5579(3) 0.43336(16) 0.0386(12) Uani 1 1 d
 H01I H 1.0506 0.5706 0.4106 0.046 Uiso 1 1 calc R
 C01I C 0.5692(4) 0.3399(3) 0.46411(15) 0.0338(11) Uani 1 1 d
 H01J H 0.5158 0.3700 0.4463 0.041 Uiso 1 1 calc R
 C01J C 0.3498(5) 0.3701(3) 0.16927(15) 0.0372(12) Uani 1 1 d
 H01K H 0.2747 0.3480 0.1632 0.045 Uiso 1 1 calc R
 C01K C 0.7329(4) 0.2407(3) 0.47161(14) 0.0335(11) Uani 1 1 d
 H01L H 0.7901 0.2043 0.4593 0.040 Uiso 1 1 calc R
 C01L C 0.8147(5) 0.4977(3) 0.45873(15) 0.0346(11) Uani 1 1 d

```

H01M H 0.7438 0.4685 0.4532 0.042 Uiso 1 1 calc R . . . .
C01M C 0.5639(5) 0.3501(4) 0.50939(17) 0.0423(13) Uani 1 1 d . . . .
H01N H 0.5075 0.3870 0.5219 0.051 Uiso 1 1 calc R . . . .
C01N C 0.6415(5) 0.3058(4) 0.53561(17) 0.0461(14) Uani 1 1 d . . . .
H01O H 0.6376 0.3124 0.5660 0.055 Uiso 1 1 calc R . . . .
C01O C 0.4312(5) 0.3780(3) 0.13570(15) 0.0385(13) Uani 1 1 d . . . .
H01P H 0.4108 0.3626 0.1070 0.046 Uiso 1 1 calc R . . . .
C01P C 0.6496(5) 0.7150(3) 0.46064(16) 0.0395(12) Uani 1 1 d . . . .
H01Q H 0.7035 0.7564 0.4709 0.047 Uiso 1 1 calc R . . . .
C01Q C 0.7267(5) 0.2506(4) 0.51726(16) 0.0462(13) Uani 1 1 d . . . .
H01R H 0.7792 0.2204 0.5354 0.055 Uiso 1 1 calc R . . . .
B01R B 0.8836(5) 0.4005(3) 0.24786(16) 0.0266(10) Uani 1 1 d . . . .
C01S C 0.4732(6) 0.6306(4) 0.47094(18) 0.0488(14) Uani 1 1 d . . . .
H01S H 0.4080 0.6159 0.4882 0.059 Uiso 1 1 calc R . . . .
C01T C 0.5535(6) 0.6942(3) 0.48549(17) 0.0478(14) Uani 1 1 d . . . .
H01T H 0.5410 0.7224 0.5123 0.057 Uiso 1 1 calc R . . . .
B01U B 0.2525(5) 0.3995(4) 0.3653(2) 0.0377(13) Uani 1 1 d . . . .
C01V C 1.0247(7) 0.5825(4) 0.4761(2) 0.0623(17) Uani 1 1 d . . . .
H01V H 1.0964 0.6103 0.4821 0.075 Uiso 1 1 calc R . . . .
C01W C 0.9458(8) 0.5662(4) 0.5100(2) 0.073(2) Uani 1 1 d . . . .
H01W H 0.9637 0.5838 0.5386 0.087 Uiso 1 1 calc R . . . .
C01X C 0.8418(7) 0.5243(3) 0.50138(18) 0.0578(18) Uani 1 1 d . . . .
H01X H 0.7885 0.5134 0.5242 0.069 Uiso 1 1 calc R . . . .
C01Y C 0.9157(5) 0.3415(4) 0.11793(18) 0.0505(14) Uani 1 1 d . . . .
H01Y H 0.9099 0.3405 0.1502 0.061 Uiso 1 1 calc R . . . .

```

anisotropic displacement parameters:

loop_

```

_atom_site_aniso_label
_atom_site_aniso_U_11
_atom_site_aniso_U_22
_atom_site_aniso_U_33
_atom_site_aniso_U_23
_atom_site_aniso_U_13
_atom_site_aniso_U_12
P001 0.0215(5) 0.0200(4) 0.0195(5) -0.0006(4) -0.0009(4) -0.0005(4)
P002 0.0219(5) 0.0174(4) 0.0182(5) -0.0021(4) -0.0011(4) -0.0001(4)
C100 0.0541(10) 0.0981(12) 0.0559(10) -0.0025(9) -0.0167(8) 0.0265(9)
C11 0.0674(10) 0.0542(8) 0.0723(11) -0.0109(7) -0.0151(9) 0.0091(8)

```

C12 0.0702(11) 0.0726(10) 0.0575(10) -0.0114(8) 0.0277(8) -0.0164(8)
 F006 0.0252(14) 0.0434(14) 0.0295(14) -0.0070(11) 0.0039(11) -0.0019(11)
 F007 0.0413(16) 0.0386(14) 0.0243(14) -0.0024(11) 0.0054(12) -0.0082(12)
 F008 0.0533(19) 0.0435(14) 0.0302(15) -0.0158(12) 0.0036(14) -0.0048(14)
 F009 0.059(2) 0.0349(13) 0.0445(17) 0.0128(12) -0.0116(15) -0.0109(14)
 F00A 0.0305(16) 0.076(2) 0.0362(16) 0.0070(15) -0.0017(13) -0.0013(15)
 F00B 0.0280(16) 0.072(2) 0.0502(19) -0.0158(16) -0.0058(14) -0.0002(15)
 F00C 0.0493(19) 0.0512(17) 0.0495(19) 0.0089(14) 0.0096(16) -0.0137(15)
 N00D 0.0292(19) 0.0166(15) 0.0158(17) 0.0010(13) 0.0000(15) 0.0022(14)
 F00E 0.0447(19) 0.0509(17) 0.087(3) -0.0080(17) 0.0087(18) 0.0124(16)
 N00F 0.032(2) 0.0203(16) 0.0201(18) -0.0021(13) 0.0023(16) 0.0002(15)
 C00G 0.023(2) 0.0211(18) 0.018(2) 0.0004(15) -0.0032(16) 0.0030(17)
 C00H 0.018(2) 0.0203(18) 0.018(2) 0.0022(15) 0.0023(16) -0.0012(16)
 C00I 0.024(2) 0.0182(17) 0.029(2) 0.0009(16) 0.0077(19) 0.0033(17)
 C00J 0.023(2) 0.0180(17) 0.0140(19) 0.0026(14) 0.0006(16) -0.0012(16)
 C00K 0.025(2) 0.0173(16) 0.022(2) -0.0018(15) 0.0004(17) -0.0023(16)
 C00L 0.027(2) 0.0156(17) 0.016(2) -0.0028(15) -0.0015(17) -0.0015(16)
 C00M 0.021(2) 0.0162(16) 0.018(2) 0.0012(15) 0.0041(16) -0.0035(16)
 C00N 0.025(2) 0.0209(18) 0.018(2) 0.0022(15) -0.0061(17) 0.0011(17)
 C00O 0.025(2) 0.0231(18) 0.026(2) 0.0004(17) -0.0035(19) 0.0011(17)
 C00P 0.024(2) 0.0172(17) 0.021(2) -0.0013(15) -0.0020(17) 0.0008(16)
 C00Q 0.035(3) 0.0180(18) 0.023(2) 0.0018(15) 0.0048(19) -0.0021(17)
 C00R 0.024(2) 0.0145(17) 0.022(2) -0.0011(15) 0.0019(17) 0.0027(15)
 C00S 0.019(2) 0.0198(17) 0.029(2) 0.0007(16) 0.0020(18) 0.0008(16)
 C00T 0.030(2) 0.0193(18) 0.018(2) -0.0019(15) -0.0017(17) 0.0046(17)
 C00U 0.025(2) 0.026(2) 0.034(3) 0.0003(18) 0.0001(19) -0.0016(18)
 C00V 0.031(2) 0.0146(17) 0.019(2) 0.0000(14) -0.0022(18) 0.0012(16)
 C00W 0.028(2) 0.0237(19) 0.023(2) 0.0036(16) -0.0024(18) 0.0008(18)
 C00X 0.028(2) 0.0206(18) 0.023(2) -0.0017(16) 0.0010(19) 0.0020(17)
 C00Y 0.022(2) 0.0233(19) 0.029(2) 0.0068(17) 0.0011(18) 0.0009(17)
 C00Z 0.027(2) 0.0220(18) 0.024(2) -0.0051(16) -0.0042(18) 0.0055(18)
 C010 0.026(2) 0.0205(18) 0.021(2) 0.0001(16) -0.0039(18) 0.0026(17)
 C011 0.030(2) 0.0215(18) 0.019(2) 0.0019(15) -0.0020(18) -0.0001(17)
 C012 0.022(2) 0.0252(19) 0.030(2) -0.0017(17) -0.0034(19) 0.0039(17)
 C013 0.028(2) 0.027(2) 0.033(3) 0.0026(18) 0.006(2) -0.0060(19)
 C014 0.028(2) 0.0216(18) 0.019(2) 0.0021(15) -0.0003(18) -0.0046(17)
 C015 0.038(3) 0.0187(17) 0.024(2) -0.0016(16) 0.002(2) 0.0049(18)
 C016 0.032(3) 0.0190(18) 0.037(3) -0.0048(17) -0.007(2) 0.0042(18)

C017 0.027(2) 0.0219(18) 0.037(3) 0.0026(17) 0.009(2) -0.0034(18)
 C018 0.020(2) 0.0205(18) 0.041(3) -0.0029(17) -0.003(2) 0.0001(17)
 C019 0.030(2) 0.0178(18) 0.024(2) 0.0012(16) -0.0013(19) 0.0018(17)
 C01A 0.035(3) 0.0261(19) 0.023(2) -0.0054(16) -0.001(2) 0.0020(19)
 C01B 0.033(2) 0.0230(18) 0.024(2) 0.0037(16) -0.0072(19) -0.0060(18)
 C01C 0.025(2) 0.030(2) 0.022(2) -0.0031(17) -0.0015(18) -0.0060(19)
 C01D 0.029(2) 0.026(2) 0.034(3) -0.0069(18) -0.003(2) 0.0055(19)
 C01E 0.039(3) 0.036(2) 0.027(3) -0.0033(19) 0.005(2) -0.005(2)
 C01F 0.037(3) 0.0192(17) 0.029(2) 0.0021(16) 0.001(2) -0.0036(18)
 C01G 0.059(3) 0.029(2) 0.022(2) 0.0004(19) 0.005(2) 0.001(2)
 C01H 0.046(3) 0.041(3) 0.029(3) -0.014(2) 0.002(2) -0.006(2)
 C01I 0.027(3) 0.046(3) 0.028(3) -0.004(2) 0.003(2) -0.007(2)
 C01J 0.060(3) 0.0219(19) 0.030(3) 0.0032(17) -0.018(2) -0.012(2)
 C01K 0.034(3) 0.049(3) 0.018(2) 0.001(2) -0.001(2) 0.000(2)
 C01L 0.043(3) 0.029(2) 0.032(3) 0.0074(19) 0.011(2) 0.004(2)
 C01M 0.035(3) 0.056(3) 0.037(3) -0.011(2) 0.007(2) -0.013(2)
 C01N 0.042(3) 0.071(3) 0.025(3) -0.005(2) 0.006(2) -0.021(3)
 C01O 0.074(4) 0.021(2) 0.021(2) -0.0002(17) -0.017(2) -0.008(2)
 C01P 0.052(3) 0.035(2) 0.031(3) -0.013(2) -0.010(2) 0.001(2)
 C01Q 0.040(3) 0.073(4) 0.026(3) 0.005(3) -0.005(2) -0.006(3)
 B01R 0.029(3) 0.027(2) 0.024(3) -0.0033(19) -0.001(2) -0.003(2)
 C01S 0.061(4) 0.053(3) 0.032(3) -0.006(2) 0.021(3) 0.000(3)
 C01T 0.073(4) 0.043(3) 0.028(3) -0.013(2) 0.002(3) 0.009(3)
 B01U 0.027(3) 0.044(3) 0.043(3) 0.001(3) 0.006(2) 0.004(3)
 C01V 0.085(5) 0.063(4) 0.040(3) -0.018(3) -0.005(3) -0.024(3)
 C01W 0.137(7) 0.050(3) 0.031(3) -0.013(3) 0.000(4) -0.020(4)
 C01X 0.104(6) 0.039(3) 0.031(3) 0.001(2) 0.023(3) 0.005(3)
 C01Y 0.053(4) 0.073(4) 0.026(3) -0.003(3) -0.001(2) 0.013(3)

bond lengths:

	P001 C01C 1.818(4) . ?
loop_	P002 C00H 1.832(4) . ?
_geom_bond_atom_site_label_1	P002 C00L 1.829(4) . ?
_geom_bond_atom_site_label_2	P002 C01I 1.820(4) . ?
_geom_bond_distance	Cl00 C01Y 1.751(6) . ?
_geom_bond_site_symmetry_2	Cl1 C01Y 1.754(6) . ?
_geom_bond_publ_flag	Cl2 C01Y 1.751(6) . ?
P001 C00G 1.839(4) . ?	F006 B01U 1.384(6) . ?
P001 C00P 1.833(4) . ?	F007 B01R 1.407(6) . ?

F008 B01R 1.387(5) . ?	C00R C00T 1.516(5) . ?
F009 B01R 1.371(6) . ?	C00R C00Z 1.387(6) . ?
F00A B01U 1.418(7) . ?	C00S H00S 0.9800 . ?
F00B B01R 1.383(6) . ?	C00S C015 1.520(6) . ?
F00C B01U 1.386(6) . ?	C00T H00E 0.9700 . ?
N00D H00A 0.8900 . ?	C00T H00F 0.9700 . ?
N00D H00B 0.8900 . ?	C00U H00U 0.9300 . ?
N00D C00J 1.532(5) . ?	C00U C013 1.400(6) . ?
N00D C00T 1.495(5) . ?	C00V C01B 1.394(6) . ?
F00E B01U 1.359(6) . ?	C00W H00W 0.9300 . ?
N00F H00C 0.8900 . ?	C00W C017 1.383(6) . ?
N00F H00D 0.8900 . ?	C00X H00X 0.9300 . ?
N00F C00S 1.515(5) . ?	C00Y H00Y 0.9300 . ?
N00F C010 1.522(5) . ?	C00Y C014 1.403(6) . ?
C00G C00N 1.420(6) . ?	C00Z H00Z 0.9300 . ?
C00G C00O 1.392(6) . ?	C00Z C018 1.389(6) . ?
C00H C00M 1.415(5) . ?	C010 H01A 0.9700 . ?
C00H C00X 1.397(5) . ?	C010 H01B 0.9700 . ?
C00I H00I 0.9300 . ?	C011 C01A 1.398(6) . ?
C00I C00X 1.384(6) . ?	C011 C01E 1.398(6) . ?
C00I C00Y 1.370(6) . ?	C012 H012 0.9300 . ?
C00J H00J 0.9800 . ?	C012 C01D 1.390(6) . ?
C00J C00M 1.539(5) . ?	C013 H013 0.9300 . ?
C00J C00V 1.515(5) . ?	C013 C01F 1.371(6) . ?
C00K C00L 1.403(6) . ?	C014 H014 0.9300 . ?
C00K C00S 1.525(5) . ?	C015 C01H 1.389(7) . ?
C00K C00U 1.389(6) . ?	C015 C01L 1.383(6) . ?
C00L C019 1.401(5) . ?	C016 H016 0.9300 . ?
C00M C014 1.382(6) . ?	C016 C01D 1.383(6) . ?
C00N C010 1.511(5) . ?	C017 H017 0.9300 . ?
C00N C012 1.385(6) . ?	C017 C018 1.378(6) . ?
C00O H00O 0.9300 . ?	C018 H018 0.9300 . ?
C00O C016 1.381(6) . ?	C019 H019 0.9300 . ?
C00P C00R 1.409(6) . ?	C019 C01F 1.387(6) . ?
C00P C00W 1.398(6) . ?	C01A H01C 0.9300 . ?
C00Q H00Q 0.9300 . ?	C01A C01P 1.395(6) . ?
C00Q C00V 1.382(6) . ?	C01B H01D 0.9300 . ?
C00Q C01G 1.387(6) . ?	C01B C01J 1.382(6) . ?

C01C C01I 1.404(6) . ?	_geom_angle_atom_site_label_2
C01C C01K 1.383(6) . ?	_geom_angle_atom_site_label_3
C01D H01E 0.9300 . ?	_geom_angle
C01E H01F 0.9300 . ?	_geom_angle_site_symmetry_1
C01E C01S 1.396(7) . ?	_geom_angle_site_symmetry_3
C01F H01G 0.9300 . ?	_geom_angle_publ_flag
C01G H01H 0.9300 . ?	C00P P001 C00G 102.42(17) . . ?
C01G C01O 1.371(7) . ?	C01C P001 C00G 106.42(19) . . ?
C01H H01I 0.9300 . ?	C01C P001 C00P 102.89(19) . . ?
C01H C01V 1.383(7) . ?	C00L P002 C00H 104.13(17) . . ?
C01I H01J 0.9300 . ?	C011 P002 C00H 102.68(18) . . ?
C01I C01M 1.384(7) . ?	C011 P002 C00L 103.47(18) . . ?
C01J H01K 0.9300 . ?	H00A N00D H00B 107.4 . . ?
C01J C01O 1.376(7) . ?	C00J N00D H00A 108.2 . . ?
C01K H01L 0.9300 . ?	C00J N00D H00B 108.2 . . ?
C01K C01Q 1.395(7) . ?	C00T N00D H00A 108.2 . . ?
C01L H01M 0.9300 . ?	C00T N00D H00B 108.2 . . ?
C01L C01X 1.390(7) . ?	C00T N00D C00J 116.3(3) . . ?
C01M H01N 0.9300 . ?	H00C N00F H00D 107.8 . . ?
C01M C01N 1.362(8) . ?	C00S N00F H00C 109.0 . . ?
C01N H01O 0.9300 . ?	C00S N00F H00D 109.0 . . ?
C01N C01Q 1.394(8) . ?	C00S N00F C01O 113.0(3) . . ?
C01O H01P 0.9300 . ?	C01O N00F H00C 109.0 . . ?
C01P H01Q 0.9300 . ?	C01O N00F H00D 109.0 . . ?
C01P C01T 1.357(8) . ?	C00N C00G P001 118.7(3) . . ?
C01Q H01R 0.9300 . ?	C00O C00G P001 122.5(3) . . ?
C01S H01S 0.9300 . ?	C00O C00G C00N 118.1(4) . . ?
C01S C01T 1.400(8) . ?	C00M C00H P002 119.9(3) . . ?
C01T H01T 0.9300 . ?	C00X C00H P002 120.7(3) . . ?
C01V H01V 0.9300 . ?	C00X C00H C00M 119.2(4) . . ?
C01V C01W 1.382(10) . ?	C00X C00I H00I 120.2 . . ?
C01W H01W 0.9300 . ?	C00Y C00I H00I 120.2 . . ?
C01W C01X 1.361(10) . ?	C00Y C00I C00X 119.6(4) . . ?
C01X H01X 0.9300 . ?	N00D C00J H00J 108.2 . . ?
C01Y H01Y 0.9800 . ?	N00D C00J C00M 108.2(3) . . ?
bond angles:	C00M C00J H00J 108.2 . . ?
loop_	C00V C00J N00D 109.6(3) . . ?
_geom_angle_atom_site_label_1	C00V C00J H00J 108.2 . . ?

C00V C00J C00M 114.2(3) . . ?	C00K C00U C013 120.3(4) . . ?
C00L C00K C00S 118.8(3) . . ?	C013 C00U H00U 119.8 . . ?
C00U C00K C00L 119.9(4) . . ?	C00Q C00V C00J 119.2(4) . . ?
C00U C00K C00S 121.3(4) . . ?	C00Q C00V C01B 119.1(4) . . ?
C00K C00L P002 119.7(3) . . ?	C01B C00V C00J 121.6(4) . . ?
C019 C00L P002 121.9(3) . . ?	C00P C00W H00W 119.6 . . ?
C019 C00L C00K 118.3(4) . . ?	C017 C00W C00P 120.8(4) . . ?
C00H C00M C00J 121.3(3) . . ?	C017 C00W H00W 119.6 . . ?
C014 C00M C00H 118.5(3) . . ?	C00H C00X H00X 119.4 . . ?
C014 C00M C00J 120.2(3) . . ?	C00I C00X C00H 121.3(4) . . ?
C00G C00N C010 120.7(4) . . ?	C00I C00X H00X 119.4 . . ?
C012 C00N C00G 119.9(4) . . ?	C00I C00Y H00Y 120.0 . . ?
C012 C00N C010 119.4(4) . . ?	C00I C00Y C014 120.0(4) . . ?
C00G C00O H00O 119.5 . . ?	C014 C00Y H00Y 120.0 . . ?
C016 C00O C00G 121.0(4) . . ?	C00R C00Z H00Z 119.1 . . ?
C016 C00O H00O 119.5 . . ?	C018 C00Z C00R 121.8(4) . . ?
C00R C00P P001 118.4(3) . . ?	C018 C00Z H00Z 119.1 . . ?
C00W C00P P001 122.6(3) . . ?	N00F C010 H01A 108.9 . . ?
C00W C00P C00R 119.0(4) . . ?	N00F C010 H01B 108.9 . . ?
C00V C00Q H00Q 119.8 . . ?	C00N C010 N00F 113.3(3) . . ?
C00V C00Q C01G 120.3(4) . . ?	C00N C010 H01A 108.9 . . ?
C01G C00Q H00Q 119.8 . . ?	C00N C010 H01B 108.9 . . ?
C00P C00R C00T 122.2(4) . . ?	H01A C010 H01B 107.7 . . ?
C00Z C00R C00P 118.8(4) . . ?	C01A C011 P002 123.5(3) . . ?
C00Z C00R C00T 118.9(4) . . ?	C01E C011 P002 117.2(3) . . ?
N00F C00S C00K 110.5(3) . . ?	C01E C011 C01A 119.1(4) . . ?
N00F C00S H00S 106.7 . . ?	C00N C012 H012 119.6 . . ?
N00F C00S C015 111.2(3) . . ?	C00N C012 C01D 120.8(4) . . ?
C00K C00S H00S 106.7 . . ?	C01D C012 H012 119.6 . . ?
C015 C00S C00K 114.7(3) . . ?	C00U C013 H013 119.9 . . ?
C015 C00S H00S 106.7 . . ?	C01F C013 C00U 120.3(4) . . ?
N00D C00T C00R 109.8(3) . . ?	C01F C013 H013 119.9 . . ?
N00D C00T H00E 109.7 . . ?	C00M C014 C00Y 121.3(4) . . ?
N00D C00T H00F 109.7 . . ?	C00M C014 H014 119.3 . . ?
C00R C00T H00E 109.7 . . ?	C00Y C014 H014 119.3 . . ?
C00R C00T H00F 109.7 . . ?	C01H C015 C00S 122.1(4) . . ?
H00E C00T H00F 108.2 . . ?	C01L C015 C00S 118.8(4) . . ?
C00K C00U H00U 119.8 . . ?	C01L C015 C01H 119.1(4) . . ?

C000 C016 H016 119.6 . . ?	C01M C01I H01J 119.5 . . ?
C000 C016 C01D 120.8(4) . . ?	C01B C01J H01K 119.4 . . ?
C01D C016 H016 119.6 . . ?	C010 C01J C01B 121.1(5) . . ?
C00W C017 H017 119.7 . . ?	C010 C01J H01K 119.4 . . ?
C00W C017 C018 120.6(4) . . ?	C01C C01K H01L 119.9 . . ?
C018 C017 H017 119.7 . . ?	C01C C01K C01Q 120.2(5) . . ?
C00Z C018 H018 120.5 . . ?	C01Q C01K H01L 119.9 . . ?
C017 C018 C00Z 119.0(4) . . ?	C015 C01L H01M 119.8 . . ?
C017 C018 H018 120.5 . . ?	C015 C01L C01X 120.4(5) . . ?
C00L C019 H019 119.2 . . ?	C01X C01L H01M 119.8 . . ?
C01F C019 C00L 121.5(4) . . ?	C01I C01M H01N 120.1 . . ?
C01F C019 H019 119.2 . . ?	C01N C01M C01I 119.7(5) . . ?
C011 C01A H01C 120.0 . . ?	C01N C01M H01N 120.1 . . ?
C01P C01A C011 120.0(5) . . ?	C01M C01N H01O 119.7 . . ?
C01P C01A H01C 120.0 . . ?	C01M C01N C01Q 120.6(5) . . ?
C00V C01B H01D 120.2 . . ?	C01Q C01N H01O 119.7 . . ?
C01J C01B C00V 119.6(4) . . ?	C01G C01O C01J 119.3(4) . . ?
C01J C01B H01D 120.2 . . ?	C01G C01O H01P 120.3 . . ?
C01I C01C P001 116.3(3) . . ?	C01J C01O H01P 120.3 . . ?
C01K C01C P001 124.5(3) . . ?	C01A C01P H01Q 119.6 . . ?
C01K C01C C01I 118.8(4) . . ?	C01T C01P C01A 120.8(5) . . ?
C012 C01D H01E 120.4 . . ?	C01T C01P H01Q 119.6 . . ?
C016 C01D C012 119.2(4) . . ?	C01K C01Q C01N 119.8(5) . . ?
C016 C01D H01E 120.4 . . ?	C01K C01Q H01R 120.1 . . ?
C011 C01E H01F 120.0 . . ?	C01N C01Q H01R 120.1 . . ?
C01S C01E C011 120.0(5) . . ?	F008 B01R F007 108.8(4) . . ?
C01S C01E H01F 120.0 . . ?	F009 B01R F007 109.0(4) . . ?
C013 C01F C019 119.6(4) . . ?	F009 B01R F008 110.2(4) . . ?
C013 C01F H01G 120.2 . . ?	F009 B01R F00B 111.2(4) . . ?
C019 C01F H01G 120.2 . . ?	F00B B01R F007 106.9(4) . . ?
C00Q C01G H01H 119.8 . . ?	F00B B01R F008 110.7(4) . . ?
C010 C01G C00Q 120.5(5) . . ?	C01E C01S H01S 120.1 . . ?
C010 C01G H01H 119.8 . . ?	C01E C01S C01T 119.8(5) . . ?
C015 C01H H01I 120.1 . . ?	C01T C01S H01S 120.1 . . ?
C01V C01H C015 119.8(5) . . ?	C01P C01T C01S 120.2(5) . . ?
C01V C01H H01I 120.1 . . ?	C01P C01T H01T 119.9 . . ?
C01C C01I H01J 119.5 . . ?	C01S C01T H01T 119.9 . . ?
C01M C01I C01C 121.0(5) . . ?	F006 B01U F00A 109.1(4) . . ?

F006 B01U F00C 108.4(4) . . ?
 F00C B01U F00A 108.7(4) . . ?
 F00E B01U F006 112.0(5) . . ?
 F00E B01U F00A 108.3(4) . . ?
 F00E B01U F00C 110.2(4) . . ?
 C01H C01V H01V 119.7 . . ?
 C01W C01V C01H 120.6(6) . . ?
 C01W C01V H01V 119.7 . . ?
 C01V C01W H01W 120.1 . . ?
 C01X C01W C01V 119.8(6) . . ?
 C01X C01W H01W 120.1 . . ?
 C01L C01X H01X 119.8 . . ?
 C01W C01X C01L 120.3(6) . . ?
 C01W C01X H01X 119.8 . . ?
 C100 C01Y C11 111.1(3) . . ?
 C100 C01Y H01Y 108.2 . . ?
 C11 C01Y H01Y 108.2 . . ?
 C12 C01Y C100 110.1(3) . . ?
 C12 C01Y C11 110.8(3) . . ?
 C12 C01Y H01Y 108.2 . . ?